CALIFORNIA ENERGY COMMISSION

Final Report Compilation for

Ventilation Energy Recovery Heat Pump Assessment

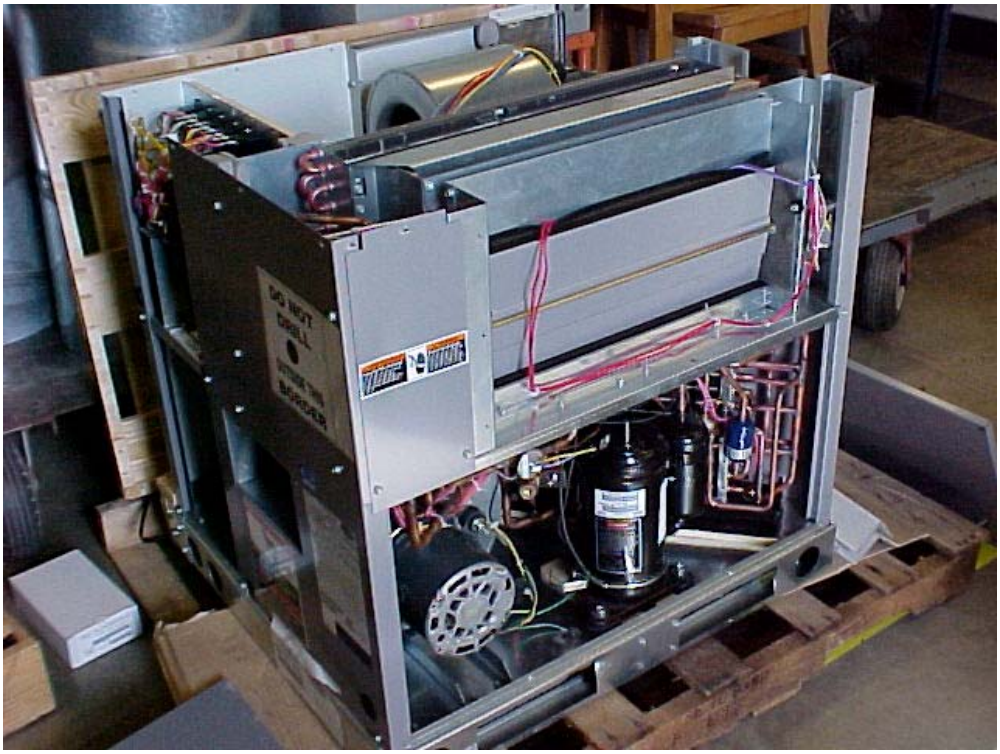

TECHNICAL REPORT

October 2003
P-500-03-096-A13

Gray Davis, *Governor*

CALIFORNIA ENERGY COMMISSION

Prepared By:
Architectural Energy Corporation
Vernon A. Smith
Boulder, CO

Purdue University
James Braun
West Layfayette, IN

CEC Contract No. 400-99-011

Prepared For:
Christopher Scruton
Contract Manager

Nancy Jenkins
PIER Buildings Program Manager

Terry Surles
PIER Program Director

Robert L. Therkelsen
Executive Director

Acknowledgements

Jim Braun and Kevin Mercer of Purdue University conducted this research. Todd Rossi and Doug Dietrich of Field Diagnostic Services, Inc. provided data collection services and field support.

Preface

The Public Interest Energy Research (PIER) Program supports public interest energy research and development that will help improve the quality of life in California by bringing environmentally safe, affordable, and reliable energy services and products to the marketplace.

The Program's final report and its attachments are intended to provide a complete record of the objectives, methods, findings and accomplishments of the Energy Efficient and Affordable Commercial and Residential Buildings Program. This attachment is a compilation of reports from Project 4.2, *Ventilation Energy Recovery Heat Pump Assessment*, providing supplemental information to the final report (Commission publication #P500-03-096). The reports, and particularly the attachments, are highly applicable to architects, designers, contractors, building owners and operators, manufacturers, researchers, and the energy efficiency community.

This document is one of 17 technical attachments to the final report, consolidating three research reports from Project 4.2:

- *Modeling and Testing Strategies for Evaluating Ventilation Load Reductions Technologies* (April 2001)
- *VSAT – Ventilation Strategy Assessment Tool* (Aug 2003)
- *Evaluation of Demand Controlled Ventilation, Heat Pump Technology, and Enthalpy Exchangers* (Aug 2003, rev)

The Buildings Program Area within the Public Interest Energy Research (PIER) Program produced this document as part of a multi-project programmatic contract (#400-99-011). The Buildings Program includes new and existing buildings in both the residential and the nonresidential sectors. The program seeks to decrease building energy use through research that will develop or improve energy-efficient technologies, strategies, tools, and building performance evaluation methods.

For the final report, other attachments or reports produced within this contract, or to obtain more information on the PIER Program, please visit www.energy.ca.gov/pier/buildings or contact the Commission's Publications Unit at 916-654-5200. The reports and attachments, as well as the individual research reports, are also available at www.archenergy.com.

Abstract

Project 4.2, ***Ventilation Energy Recovery Heat Pump Assessment***,

Purdue investigated application of a new heat pump application, called a "heat pump heat recovery" (HPHR) system. The heat pump in this case extracts heating or cooling energy from the exhaust air stream of an air handler or packaged air-conditioning unit and transfers it to pre-condition the incoming outside fresh air stream. In cooling season, it pre-cools the incoming air and in heating season it pre-heats it. The heat pump heat recovery (HPHR) system functioned properly during the field and laboratory testing. However, heating requirements are relatively low for California climates and therefore overall savings are dictated by cooling season performance.

- The HPHR system did not provide positive cost savings for most building type/climate combinations investigated using simulations.
- The HPHR system is an alternative to an economizer and so economizer savings are also lost when using this system. There are not sufficient hours of ambient temperatures above the breakeven point to yield overall positive savings with the HPHR system compared to a base case system with an economizer for the prototypical buildings in California climates.
- The HPHR system should not be considered for use in California, except in perhaps certain mountain areas with larger heating loads.

This document is a compilation of three technical reports from the research.

MODELING AND TESTING STRATEGIES FOR EVALUATING VENTILATION LOAD REDUCTION TECHNOLOLGIES

Deliverables 3.1.1a and 4.2.1a

Progress report submitted to:
Architectural Energy Corporation

For the Building Energy Efficiency Program
Sponsored by:
California Energy Commission

Submitted By:

Purdue University

Principal Investigator:	James Braun, Ph.D., P.E.
Research Assistants:	Kevin Mercer
	Tom Lawrence, P.E.

April 2001

Mechanical Engineering
1077 Ray W. Herrick Laboratories
West Lafayette, IN 47907-1077
(765) 496-6008
(765) 494-0787 (fax)

RAY W. HERRICK LABORATORIES
PURDUE ENGINEERING

TABLE OF CONTENTS

I. INTRODUCTION

A. Scope

The heating and cooling loads associated with ventilation can contribute significantly to the total energy requirements for a commercial space being conditioned. In recent years, several different approaches have been proposed to reduce ventilation loads including enthalpy exchangers, economizers, demand-control ventilation and ventilation heat recovery heat pumps. However, different technologies may be appropriate for different environments and buildings.

This project will focus on identifying appropriate applications and locations for ventilation load reduction technologies within the state of California. The performance of economizer, enthalpy exchanger, demand-controlled ventilation and heat recovery heat pump technologies will be compared for different types of buildings and locations. For demand-controlled ventilation, field sites are being established in coastal and inland sites in both northern and southern California. Three different building types are being considered with two nearly identical buildings for each location so that direct comparisons between the performance of fixed ventilation and demand-controlled ventilation can be made. Data from the field sites will be compared with simulation results in order to validate computer models. The models will then be used to evaluate the cost savings potential for this technology for other buildings and locations. In addition, the models will also consider economizer, enthalpy exchanger, and heat pump heat recovery technologies. The performance of all these technologies will be compared in terms of their cost effectiveness. As a further validation of the simulation results, an additional field will be established for testing the heat pump heat recovery unit.

B. Purpose of this Report

This progress report presents an overview of the modeling approach and input data to be used in evaluating the energy savings associated with each of the ventilation load reduction technologies. In addition, an overview of the preliminary test plan and field site monitoring setup for the heat pump heat recovery unit is given.

II. VENTILATION LOAD REDUCTION TECHNOLOGIES

A. Economizer

An economizer uses outside air to reduce or eliminate the mechanical cooling required to condition a building. This accessory usually includes an outside air damper, a relief damper, a return air damper, filters, an actuator and linkages. An economizer can be installed with any of the other three ventilation energy savings technologies that will be considered in this study. When the outdoor conditions are suitable, the outdoor air dampers switch from their minimum position (minimum ventilation air) to fully open. For a dry-bulb economizer, this switch point occurs when ambient air is less than a specified value. This switch point should be less than the switch point to return to minimum outside air in order to ensure stable control. The economizer switchover temperature may be significantly lower than the return air temperature (e.g., 10 F lower) in humid climates where latent ventilation loads are significant. However, in dry climates, the switchover temperature may be close to the return temperature (e.g., 75 F). An enthalpy (or wet-bulb) economizer compares the outside and return air enthalpies (or wet-bulb temperatures) in order to initiate or terminate economizer operation. In general, enthalpy economizers yield lower energy costs than dry-bulb economizers, but require a

humidity measurement. With either economizer, the outside air damper modulates the flow to maintain a mixed air temperature set point, and when this set point can no longer be achieved, the compressor is engaged (Howel et al., 1998).

B. Enthalpy Exchanger

A rotary air-to-air enthalpy exchanger, sometimes called a heat recovery wheel, is a revolving cylinder filled with an air permeable medium with a large internal surface area for contact with the air passing through it. Adjacent supply and exhaust streams each flow through half the exchanger in a counter-flow pattern as illustrated in Figure 1.

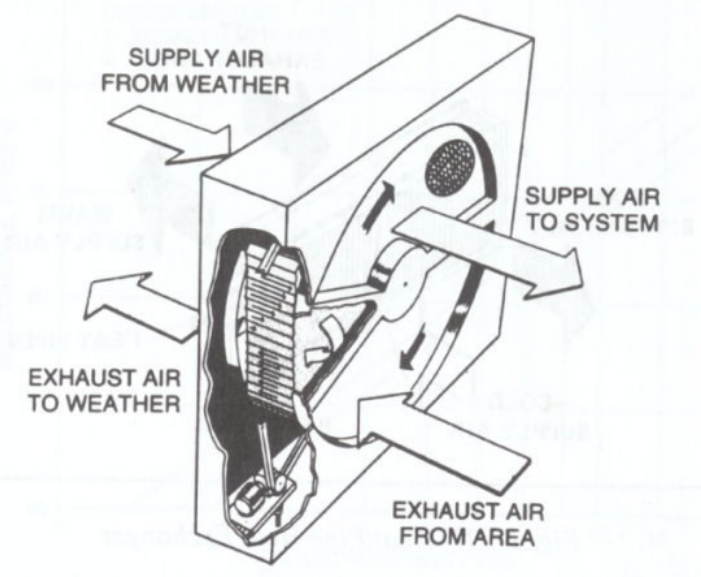

FIGURE 1. FLOW DIRECTION IN AN ENTHALPY EXCHANGER

Sensible heat is recovered as the medium picks up and stores heat from the hot airstream and gives it up to the cold airstream. Latent heat is transferred as the medium condenses moisture from the airstream having the higher humidity ratio, with a

simultaneous release of heat. The medium then releases the moisture through evaporation into the airstream with the lower humidity ratio. The enthalpy exchanger medium is fabricated from metal, mineral, or man-made materials and classified as providing either random flow or directionally oriented flow through their structures (Howel et al., 1998). An enthalpy exchanger works for both heating and cooling and can allow for 100% outside air.

C. Demand Controlled Ventilation

The energy requirements to heat or cool a building can be reduced by modulating ventilation air in response to the number of occupants in the building at any given time. This can be accomplished by controlling the ventilation air to maintain a specific CO_2 level within the building. This strategy is referred to as demand-controlled ventilation (DCV). Brandemuehl and Braun (1999) performed a simulation study for a number of different buildings and locations and showed that as much as 20% savings in electrical energy for cooling are possible with demand-controlled ventilation. The savings in heating energy associated with demand-controlled ventilation are generally much larger, but are strongly dependent upon the building type and occupancy schedule. Significantly greater savings are possible for buildings with highly variable occupancy schedules and relatively large internal gains. However, the overall cost effectiveness of DCV has not been evaluated and the savings have not been documented in the field.

D. Ventilation Heat Pump Heat Recovery

Carrier's Energy Recycler® accessory, available for 3 to 12.5 ton rooftop units, introduces a technique to help reduce the total load on the primary HVAC system by

outside air pre-treatment. Figure 2 illustrates operation of the Energy Recycler® using some example design cooling conditions. In the cooling season, the Energy Recycler® cools and possibly dehumidifies outside air entering the unit, allowing for larger quantities of outside air. The heat is rejected into the exhaust air from the building. The room air is used to cool the condenser coil and thus allows the condenser to operate at a lower temperature than the ambient. During heating season, the Energy Recycler® operates in reverse as a heat pump to extract heat from the exhaust air and pre-heat the outside air. The application of a ventilation heat pump heat recovery units leads to a lower load on the primary equipment. However, the unit requires energy and the overall economics are not known.

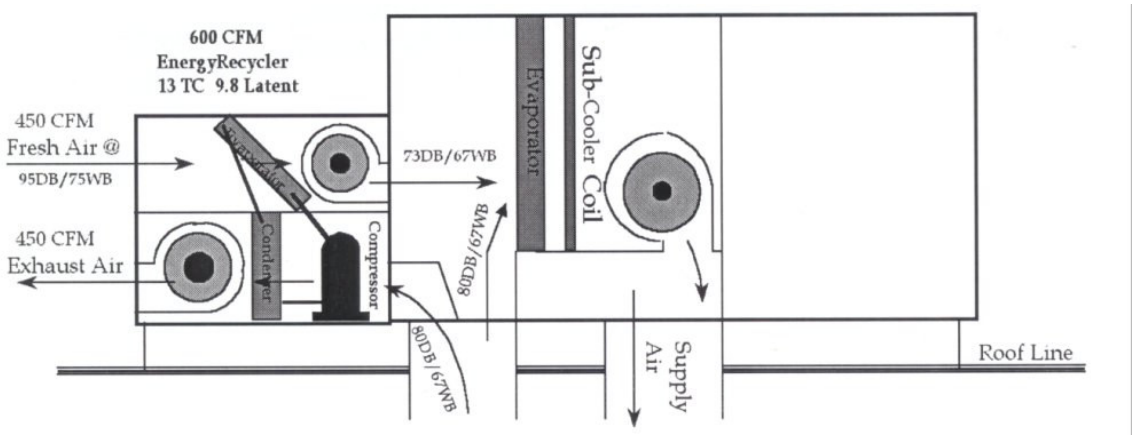

FIGURE 2. ENERGY RECYCLER® SCHEMATIC ATTACHED TO ROOFTOP UNIT

II. SIMULATION APPROACH

The simulations will be performed for a variety of small commercial building types that utilize packaged air conditioning and heating equipment. A computer simulation model is being developed for estimating the energy requirements and life cycle economic impact for the different ventilation load reduction technologies. The model is based upon the tool previously developed by Brandemuehl and Braun (1999). Figure 3 shows a flow diagram of the computer simulation model to be implemented for evaluating these different methods.

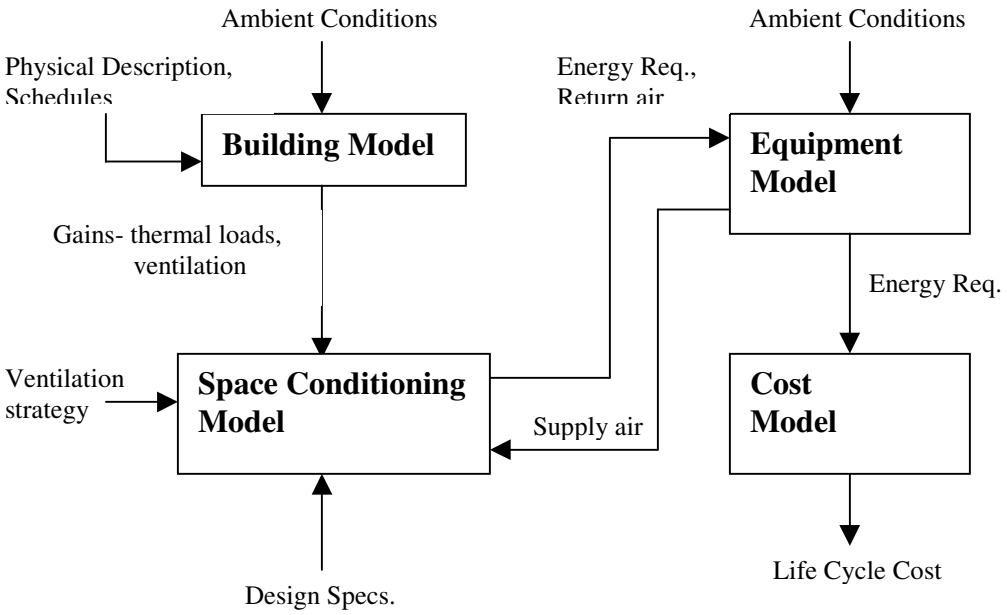

FIGURE 3. FLOW DIAGRAM OF MODELING APPROACH

The model will calculate hourly energy requirements for a particular building type and system type and then use this data to determine the total cost of HVAC operation. The building model will predict the thermal gains to or from the zone based upon transient heat transfer from outside walls and internal sources. The space-conditioning

model will solve mass and energy balances for the zone air and then determine return air conditions for the equipment model. The zone air humidity, dry-bulb temperature, and CO2 concentration will be calculated at each hour within the space conditioning model. The ventilation and return air will be mixed according to the ventilation technique being analyzed. The equipment model will use mixed air conditions and the sensible cooling requirement to determine the average supply air conditions. These entering mixed air conditions and supply air conditions will be determined iteratively using a nonlinear equation solver. The energy used by the equipment model will be calculated and used as an input in determining the life cycle cost for each system.

The cost model will incorporate current electricity rates in California and equipment costs to estimate the life cycle cost of the HVAC system for each ventilation control technique. From this economic data, comparisons can be made between all the different combinations of location and building type. The length of the economic analysis will be varied to reflect different potential decision makers.

The nonlinear equation solver to be used in this study is an HVAC building/ energy simulation program called TRNSYS (1996), developed by the Solar Energy Laboratory at the University of Wisconsin-Madison. TRNSYS is a transient systems simulation program with a modular structure. It recognizes a system description language in which the user specifies the components that constitute the system and the manner in which they are connected. The TRNSYS library includes many of the components commonly found in thermal energy systems, as well as component routines to handle input of weather data. The modular structure of TRNSYS gives the program tremendous flexibility and facilitates the addition to the program of mathematical models

that are not included in the standard TRNSYS library. An electronic simulation of the previously mentioned ventilation control strategies can thus be added to the TRNSYS library. With this computer simulation in place, several different combinations of location and building type can be simulated to evaluate the performance of all ventilation control strategies.

A. Building Model

The TYPE 56: "Multi-Zone Building" component from the TRNSYS library will be used for the building model. This component models the thermal behavior of a building having up to 25 thermal zones. This is a very detailed model of a building that is built up from individual descriptions of wall layers, windows, internal gain schedules, etc. The model solves individual transient conduction through walls and considers long-wave radiation exchanges within the space. Model inputs include separate hourly heating and cooling setpoints and the model outputs the required heating or cooling rates necessary to maintain the setpoints.

B. Space-Conditioning Model

The space-conditioning model determines return air conditions for the equipment model. The zone sensible heat gain or loss and the specified zone temperature setpoint determines the required average supply air temperature. Given the supply airflow rate and the supply air temperature, the thermal load requirements for the equipment model are determined by the mixed air conditions. These mixed air conditions depend on the ventilation control strategy implemented.

When the DCV control strategy is enabled, a minimum flow rate of ventilation air is determined that will keep the CO_2 concentration in the zone at or below a specified level (Brandemuehl and Braun, 1999). In the absence of DCV, ventilation percentages are based on design conditions for each specific building type from the ASHRAE Standard 62-1999. Table 1 shows the parameters used to estimate the minimum ventilation rates according to building type.

TABLE 1. ASHRAE MINIMUM VENTILATION REQUIREMENTS

Parameter	***Office***	***Retail***	***School***	***Restaurant***	***Hotel***	***Super-market***
Minimum Ventilation per Person, cfm	20	10*	15	20	15	15
Maximum Design Occupancy for minimum ventilation flow, P/1000 ft^2	7	20	50	70	30	8

*Retail store minimum ventilation is based upon an average of 0.25 cfm/ft^2 for upper and lower floors.

For known ventilation flow, zone temperature, and ambient conditions, steady-state mass and energy balances will be applied to the zone and air distribution system to determine average values over each timestep for the return and zone air CO_2 concentration and humidity ratio. These calculations will be based on a fully-mixed zone model, modified by an air exchange effectiveness to account for partial short-circuiting of the supply air to the ceiling return.

Within the TRNSYS environment, the space-conditioning model will be a custom TYPE component that will interact with the TYPE 56 model through inputs and outputs

C. Equipment Model

Packaged rooftop air conditioner with on/off controls will be simulated in this study. The model will use the return air and ambient air conditions to determine the average supply air conditions for the space-conditioning model. The analysis will

include air conditioners with gas furnaces and electric auxiliary heat. The supply fan will be on during all hours of occupancy, and the compressor or heater will cycle on and off as necessary to maintain the zone temperature at its set point. Models for a direct expansion air conditioner will taken from the ASHRAE Secondary Toolkit (Brandemuehl, et al., 1993) and adapted for this project. The secondary toolkit contains a library of subroutines and functions that have been debugged and documented. The direct expansion and heat pump models are based upon correlations used in DOE 2.1E. These models estimate capacity (cooling or heating) and power consumption as a function of mixed air and ambient conditions for typical devices. The outputs are scaled according to capacity and efficiency values that are specified for ARI rating conditions. Both high and moderate efficiency units will be considered in this study. For cooling, both sensible and total cooling capacities are determined. Iteration with the space-conditioning model is required, since the space humidity level is determined by the moisture removal rate of the equipment, which is affected by the mixed air humidity.

Models for a heat pump will also be taken from the ASHRAE Secondary Toolkit and adapted for modeling the heat pump heat recovery unit. Laboratory test data will be taken over a wide range of conditions and used to adjust coefficients of the model.

D. Cost Model

The cost model will consider utility and initial equipment costs to determine life-cycle costs (including inflation, alternative investments, taxes, financing, depreciation, maintenance, etc.). Utility rate information will be gathered for each location considered, including energy and demand rates. The life-cycle costs for different ventilation load technologies will be compared leading to an overall assessment.

III. SIMULATION INPUT DATA

A. Selected Locations

TMY2 (NREL, 1995) data for a number of locations in and near California will be used in the simulation studies. The National Renewable Energy Laboratory, NREL, has extracted data from the National Solar Research Data Base, NSRDB, for the years of 1961 to 1990 to produce the Typical Meteorological Year, or TMY weather data. TMY data is a set of hourly values of solar radiation and meteorological elements for a one-year period. It consists of months selected from individual years and concatenated to form a complete year. TMY2 data is a more recent version that was completed in March of 1994. Two minor errors that affected about 10% of the original TMY data stations were corrected in this version.

For this study, locations were selected from the available TMY2 data that are representative of diverse climates acrorss California. The selected cities are shown in Table 2.

TABLE 2. CALIFORNIA AND NEVADA CITIES FOR TRNSYS SIMULATIONS

City	Latitude Deg	Min	Longitude Deg	Min	Elev. (m)
Arcata	N40	59	W124	06	69
Bakersfield	N35	25	W119	03	150
Daggett	N34	52	W116	47	588
Fresno	N36	46	W119	43	100
Los Angeles	N33	56	W118	24	32
Sacramento	N38	31	W121	30	8
San Diego	N32	44	W117	10	9
San Francisco	N37	37	W122	23	5
Santa Maria	N34	54	W120	27	72
Reno, NV	N39	30	W119	47	1341
Las Vegas, NV	N36	05	W115	10	664

Arcata, San Francisco, Santa Maria, Los Angeles and San Diego are on the west coast of California proceeding from the north to south. These areas have very temperate

climates averaging around 80°F and 40 to 50% relative humidity during the summer season. During winter months, the mean temperature drops to the low 40's and perhaps on occasion the upper 30's. Sacramento, Fresno, Bakersfield, and Baggett are inland from the west coast, approximately in the middle of the state. These areas are much hotter in the summer season, especially Bakersfield and Baggett. Las Vegas and Reno, Nevada, were both chosen to represent the eastern border area of California. Las Vegas temperatures range from the 20's during the winter and above 100°F during the summer. Climates near Reno are in the high 90's during the summer and lower teens in the winter.

B. Buildings

Brandemuehl and Braun (1999) considered four different types of buildings in their study: office, large retail store, school, and sit-down restaurant. Descriptions for these buildings were obtained from prototypical descriptions of commercial buildings developed by Lawrence Berkeley National Laboratory (Huang and Franconi, 1995). Table 3 gives data to describe these buildings. The current study will expand upon the previous work in that the cost effectiveness of DCV and other ventilation load reduction technologies will be considered and compared.

Table 3: Prototypical Building Characteristics use by Brandemuehl and Braun (1999)

Characteristic	Office	Large Retail	School	Sit-Down Restrnt.
Floor area (ft^2)	6600	80,000	9,600	5250
Floors	1	2	2	1
Percent glass	15	15	18	15
Window R-value	1.6	1.7	1.7	1.5
Window shading coeff.	0.75	0.76	0.73	0.80
Wall R-value	5.6	4.8	5.7	4.9
Roof R-value	12.6	12.0	13.3	13.2
Wall material	Masonry	Masonry	Masonry	Masonry
Roof material	Built-up	Built-up	Built-up	Built-up
Weekday hours (hrs/day)	11	14	Varies	17
Weekend hours (hrs/day)	5	14	Varies	17
Equipment power (W/ft^2)	0.5	0.4	0.8	2.0
Lighting power (W/ft^2)	1.7	1.6	1.8	2.1

Four additional building types from the LBL report will be considered in the current study: small retail stores, hotels, supermarkets, and middle schools. Tables 4, 5, 6 and 7 give data that describe these buildings. All of the simulated buildings will utilize packaged air conditioning equipment with a natural gas electric heater. For supermarkets, both old and new buildings will be simulated. The construction of this building type has changed dramatically over the last 30 years. However, many older buildings still are in commission and could be retrofit with ventilation load reduction technologies.

The LBL study consulted the 1989 CBECS (EIA, 1992) to determine total floor area for each building type, vintage, and climatic zone, the percentages of floor area heated or cooled, and the total energy use of the building type. The building shell characteristics and schedules were derived from the LBL study; however, the LBL study derived the data from a previous study conducted by (Huang et al., 1990) along with updates from the 1989 CBECS.

In addition to the buildings from the LBL study, the field site buildings will also be simulated. Site-specific data necessary for simulating system performance is currently being gathered (see report on the Description of Field Sites for Deliverables 2.1.1a and 3.1.1a). Once all data has been gathered from the field sites, this information will serve to validate the computer simulation model before any HVAC simulations are conducted for other buildings and locations. For DCV, the field sites have been chosen with two nearly identical buildings for each site. This will allow some degree of side-by-side testing for comparison of fixed minimum ventilation and DCV. However, more importantly, the test data will be used for validating the models and the predicted savings. Then, the improved models can be used to evaluate savings for the other technologies and locations.

TABLE 4. CHARACTERISTICS OF A MODELED SMALL RETAIL STORE

	Parameters
FLOOR-AREA	
Building area (ft^2)	6400
Floors	1
SHELL	
Percent Glass	15
Window R-value	1.67
Window shading co-efficient	0.84
Wall R-value	4.83
Roof R-value	12.04
Wall material	masonry
Roof material	built-up
OCCUPANCY	
Occupancy (ft^2/pers)	1635
Weekday hours (hrs/day)	12
Weekend hours (hrs/day)	4
EQUIPMENT	
Power density (W/ft^2)	0.50
Full Eqp hours (hrs/yr)	3480
LIGHTING	
Power density (W/ft^2)	1.7
Full lighting hours (hrs/yr)	4412
SYSTEM AND PLANT CHARACTERISTICS	
System type	Packaged single-zone w/ economizer
Heating plant	Gas furnace
Cooling plant	Direct expansion

TABLE 5. CHARACTERISTICS OF MODELED HOTEL PROTOTYPES

	Large hotels	Small hotels (Motels)
FLOOR-AREA		
Building area (ft^2)	250000	12000
Floors	10	2
SHELL		
Percent Glass	35	21
Window R-value	1.67	1.71
Window shading co-efficient	0.74	0.76
Wall R-value	6.16	5.32
Roof R-value	14.00	13.16
Wall material	masonry	masonry
Roof material	built-up	shingle/ siding
OCCUPANCY		
Occupancy (ft^2/pers)	210	120
Weekday hours (hrs/day)	24	24
Weekend hours (hrs/day)	24	24
EQUIPMENT		
Power density (W/ft^2)	0.72	0.69
Full Eqp hours (hrs/yr)	2722	2826
LIGHTING		
Power density (W/ft^2)	1.18	1.06
Full lighting hours (hrs/yr)	5157	3443
SYSTEM AND PLANT CHARACTERISTICS		
System type	Packaged single-zone w/ economizer	Packaged single-zone w/ economizer
Heating plant	Gas furnace	Gas furnace
Cooling plant	Direct expansion	Direct expansion

TABLE 6. CHARACTERISTICS OF MODELED SUPER-MARKETS

	Supermarket	
	old	new
FLOOR-AREA		
Building area (ft^2)	21300	21300
Floors	1	1
SHELL		
Percent Glass	15	15
Window R-value	1.51	1.60
Window shading co-efficient	0.82	0.79
Wall R-value	3.3	5.8
Roof R-value	9.2	11.8
Wall material	masonry	masonry
Roof material	shingle/ siding	shingle/ siding
OCCUPANCY		
Occupancy (ft^2/pers)	227	227
Weekday hours (hrs/day)	18	18
Weekend hours (hrs/day)	18	18
EQUIPMENT		
Power density (W/ft^2)	1.20	1.20
Full Eqp hours (hrs/yr)	5168	5168
LIGHTING		
Power density (W/ft^2)	2.4	2.4
Full lighting hours (hrs/yr)	7816	7816
SYSTEM AND PLANT CHARACTERISTICS		
Numer of systems	5 (office, storage, deli, bakery, sales)	
System type	Constant-vol. single-zone	Variable-air vol. single-zone
Heating plant	Gas furnace	
Cooling plant	Direct expansion	

TABLE 7. CHARACTERISTICS OF MODELED MIDDLE SCHOOL PROTOTYPE

	Parameters
FLOOR-AREA	
Building area (ft^2)	136000
Floors	1
SHELL	
Percent Glass	6
Window R-value	1.39
Window shading co-efficient	0.85
Wall R-value	2.38
Roof R-value	7.56
Wall material	masonry
Roof material	metal surface
OCCUPANCY	
Occupancy (ft^2/pers)	2085
Weekday hours (hrs/day)	12
Weekend hours (hrs/day)	4
EQUIPMENT	
Power density (W/ft^2)	0.30
Full Eqp hours (hrs/yr)	6462
LIGHTING	
Power density (W/ft^2)	0.8
Full lighting hours (hrs/yr)	3638
SYSTEM AND PLANT CHARACTERISTICS	
System type	Packaged single-zone w/ economizer
Heating plant	Gas furnace
Cooling plant	Direct expansion

IV. TESTING

A. Overview

Two distinct types of testing will be conducted for the DCV and ventilation heat pump heat recovery projects. First of all, the Carrier heat pump heat recovery unit will be tested in the laboratory over a wide range of conditions to be encountered in the field. These data will be used to build performance maps for the unit that will be integrated in the simulation tool. Secondly, field tests will be performed for DCV and heat pump heat recovery. An overview of the data flow for the testing and evaluation phase of these projects is given in Figure 4.

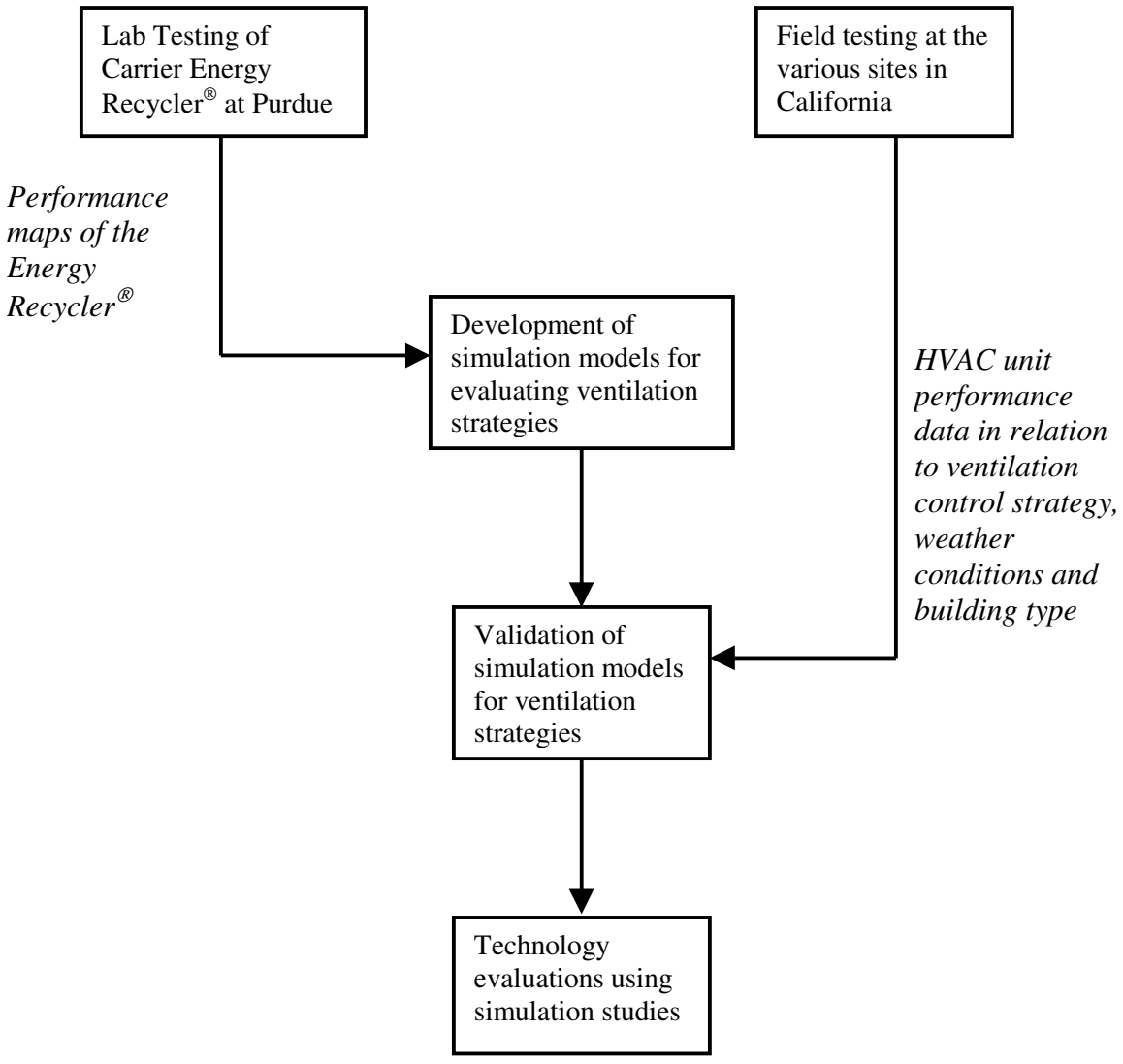

FIGURE 4. LAB AND FIELD TESTING DATA FLOW

B. Lab Testing of the Carrier Energy Recycler® Heat Pump

Project 4.2 is intended to demonstrate the savings potential for application of ventilation recovery heat pumps. This will be done primarily using simulation studies for various building and climate types found throughout California. To develop the simulation model, it is necessary to have accurate performance data for the ventilation recovery heat pump. Therefore, the first phase of Project 4.2 will focus on laboratory testing of a representative unit from Carrier. The environmental chambers at the Ray W. Herrick Laboratories will be used for this testing.

Carrier Corporation, as a sponsor of this program, has provided one of their Energy Recycler® units. This same unit will be used for both laboratory testing and field testing. The unit size was selected based on a field test site at a school that utilizes a Carrier 6-ton rooftop unit with gas heating. This unit was shipped to Purdue in late February of 2001. (See the photo in Figure 5.)

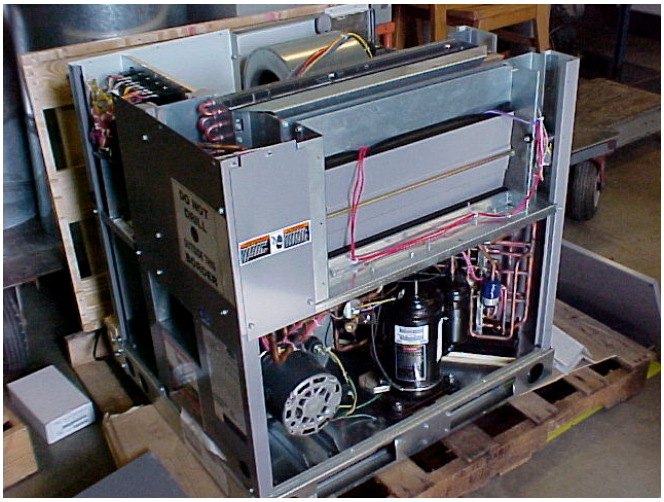

FIGURE 5. CARRIER ENERGY RECYCLER® HEAT PUMP AT HERRICK LAB
(SIDES REMOVED FOR CLARITY)

The ventilation heat pump is scheduled for testing at Herrick Laboratory beginning in May of 2001. The testing will result in a performance map of the unit that covers the complete expected operating envelope for the ambient and return air states. The expected range of the operating conditions for cooling and heating mode testing are given in Table 8. It is only necessary to vary humidity for the evaporator air stream (outside air for cooling mode and return air for heating mode) since performance is relatively independent of humidity when moisture is not condensed.

TABLE 8. OPERATING ENVELOPE FOR LAB TESTING OF THE CARRIER ENERGY RECYCLER® HEAT PUMP

Cooling Mode	
Ambient Temperature	50° to 120° F
Ambient Humidity	10% to 100%
Return Air Temperature	55° to 90° F
Return Air Humidity	Not varied
Heating Mode	
Ambient Temperature	-10° to 55° F
Ambient Humidity	Not varied
Return Air Temperature	50° to 80° F
Return Air Humidity	30% to 80%

The model will correlate sensible and total cooling capacity and power consumption as a function of the entering states and flow rates. The model will then be incorporated into the system model.

C. Field Testing

Field test data will be gathered at a total of 13 different sites in California: Twelve of the test sites are the ones being set up for joint evaluation of the demand controlled ventilation and the gathering of data for field evaluation of the fault detection and diagnostics algorithms. A detailed discussion of these sites and the test plan is included in the separate report: "Description of Field Test Sites".

The 13th site is for the heat pump heat recovery project. This site will be at one of the school districts (Woodland Joint Unified) where the modular schoolrooms are being monitored for DCV. The site selected is at the Junior High School for this district, and it has a 6-ton Carrier rooftop unit with gas heating.

The field testing for the ventilation recovery heat pump will involve two phases. The first phase, initiated in March 2001, was to install a Virtual Mechanic monitoring system on the existing rooftop unit at the California site. Performance data on this unit and the conditioned space will be collected for use in developing a baseline for the unit before installation of the Energy Recycler®. Once the laboratory testing is completed, the heat pump will be installed in the field and the second phase of the field testing initiated. It is anticipated that the field installation will occur during the July-August of 2001 time frame.

Table 9 gives a detailed list of the field test data for the Energy Recycler® as it will be set up for baseline data gathering. Additional sensors will be added when the Energy Recycler® is installed this summer. Detailed lists of test data for the other twelve field sites is contained in the Purdue report titled “Description of Field Test Sites”.

TABLE 9. DATA LIST FOR FIELD TESTING OF THE VENTILATION RECOVERY HEAT PUMP

Channel #	**Data Point**
SENSOR CHANNELS	
Power Transducer Channels	
1	Unit voltage, L1
2	Unit voltage, L2
3	Unit voltage, L3
4	Unit total current, L1
5	Not Used
6	Unit total current, L3
Other Analog Input Data	
7	SPARE - (Use later with heat pump)
8	SPARE - (Use later with heat pump)
9	SPARE - (Use later with heat pump)
10	SPARE - (Use later with heat pump)
11	SPARE - (Use later with heat pump)
12	SPARE - (Use later with heat pump)
13	SPARE - (Use later with heat pump)
14	SPARE - (Use later with heat pump)
15	Mixed air temperature
16	Return air temperature
17	Supply air temperature, before heater
18	Supply air temperature, after heater
19	Condenser inlet air temperature
20	Condenser outlet air temperature
21	Suction line temperature, rooftop unit
22	Discharge line temperature, rooftop unit
23	SPARE - (Use later with heat pump)
24	SPARE - (Use later with heat pump)
25	Evaporation temperature, rooftop unit
26	Condensation temperature, rooftop unit
27	Outdoor air temperature
28	Outdoor air humidity
29	Building zone temperature A
30	Building zone temperature B
31	Building zone temperature C
32	Building zone temperature D
CALCULATED DATA CHANNELS	
33-50	NOT USED
51-56	NOT USED

TABLE 9. DATA LIST FOR FIELD TESTING OF THE VENTILATION RECOVERY HEAT PUMP (CONT'D)

Channel	*Data Point*
57	superheat, stage 1
58	subcooling, stage 1
59	evaporating temperature, stage 1
60	condensing temperature, stage 1
61	condensing temperature over ambient (CT-AIC), stage 1
62	NOT USED
63	NOT USED
64	NOT USED
65	NOT USED
66	NOT USED
67	evaporator temperature difference (RA-SA)
68	NOT USED
69	NOT USED
70	unit power (kW)
71	unit KWh
72	unit MWh
73	compressor 1 power (kW)
74	compressor 1 KWh
75	compressor 1 MWh
76	compressor Vent Heat Pump Unit power (kW)
77	compressor Vent Heat Pump Unit KWh
78	compressor Vent Heat Pump Unit MWh
79	digital input 1, supply fan, run time (8 hours)
80	digital input 1, supply fan, run time (seconds)
81	digital input 2, cooling 1, run time (8 hours)
82	digital input 2, cooling 1, run time (seconds)
83	digital input 3, cooling Vent HP, run time (8 hours)
84	digital input 3, cooling Vent HP, run time (seconds)
85	digital input 4, heat 1, run time (8 hours)
86	digital input 4, heat 1, run time (seconds)
87	digital input 5, heat Vent Heat pump, run time (8 hours)
88	digital input 5, heat Vent Heat pump, run time (seconds)
89	digital input 6 run time (8 hours)
90	digital input 6 run time (seconds)
91	time since reset accumulators (8 hours)
92	time since reset accumulators (seconds)
93	up time (8 hours)
94	up time (seconds)
95	board temperature (F)
96	board battery voltage (V)

TABLE 9. DATA LIST FOR FIELD TESTING OF THE VENTILATION RECOVERY HEAT PUMP (CONT'D)

Digital Channels	
1	Supply fan contact (fan om / fan off)
2	Low voltage control signal for compressor main unit
3	Low voltage control signal for compressor, heat pump
4	Heating mode signal
5	
6	

VII. REFERENCES

ASHRAE. 1999. "ANSI/ASHRAE Standard 62-1999, "Ventilation for Acceptable Indoor Air Quality", Atlanta: American Society of Heating, Refrigerating and Air-Conditioning Engineers, Inc.

Brandemuehl, M.J., Gabel, S., and Andresen, I. 1993. HVAC2 Toolkit: Algorithms and Subroutines for Secondary HVAC System Energy Calculations. American Society of Heating, Refrigerating, and Air Conditioning Engineers, Inc., Atlanta, GA.

Brandemuehl, M., and Braun, J. 1999. "The Impact of Demand-Controlled and Economizer Ventilation Strategies on Energy Use in Buildings", Atlanta: American Society of Heating, Refrigerating and Air-Conditioning Engineers, Inc.

Carrier Corporation. 1999. "Product Data: 62AQ Energy$Recycler Energy Recovery Accessory For 3 to 12.5 Ton Rooftops", Form 62AQ-1PD. Syracuse, New York.

Energy Information Administration (EIA) 1992. "Commercial Building Energy Consumption and Expenditures", U.S. Department of Energy, Washington, D.C.

Howel, Ronald H., Sauer, Harry J., and Coad, William J. 1998. *Principles of Heating, Ventilating and Air Conditioning*, Atlanta: American Society of Heating, Refrigerating and Air-Conditioning Engineers, Inc.

Huang, Y.J., Akbari, H., Rainer, L., and Ritschard, R.L. 1990. "481 Prototypical Commercial Buildings for Twenty Urban Market Areas (Technical documentation of building loads data base developed for the GRI Cogeneration Market Assessment Model)", LBL Report 29798, Lawrence Berkley National Laboratory, Berkley CA.

Huang, Y.J., and Franconi, E. 1995. "Commercial Heating and Cooling Loads Component Analysis", LBL Report 37208, Lawrence Berkley National Laboratory, Berkley CA.

National Renewable Energy Laboratory (NREL) 1995. "User's Manual for TMY2s:
Typical Meteorological Years", U.S. Department of Energy. Golden, Colorado.

Solar Energy Laboratory (SEL) 1996. "TRNSYS: A Transient System Simulation Program User's Manual", University of Wisconsin. Madison, Wisconsin.

VSAT – Ventilation Strategy Assessment Tool

Submitted to

California Energy Commission

As Deliverables 3.1.2, 3.2.1, and 4.2.2

Prepared by

James E. Braun and Kevin Mercer
Purdue University

Revised August 2003

Table of Contents

SECTION 1: INTRODUCTION

This report describes a simulation tool (VSAT – Ventilation Strategy Assessment Tool) that estimates cost savings associated with different ventilation strategies for small commercial buildings. A set of prototypical buildings and equipment is part of the model. The tool is not meant for design or retrofit analysis of a specific building. It does provide a quick assessment of alternative ventilation technologies for common building types and specific locations with minimal input requirements.

Figure 1 shows a schematic of a small commercial building and HVAC system. The buildings currently considered within VSAT include a small office building, a sit-down restaurant, a retail store, a school class wing, a school auditorium, a school gymnasium, and a school library. All of these buildings are considered to be single zone with a slab on grade (no basement or crawl space). VSAT considers only packaged HVAC equipment, such as rooftop air conditioners with integrated cooling equipment, heating equipment, supply fan, and ventilation. Modifications to the ventilation system are the focus of the tool's evaluation. A basic ventilation system (shown within the box of Figure 1) consists of ambient supply, exhaust, and return ducts and dampers. The different ventilation strategies that are considered by VSAT are: 1) fixed ventilation rates with no economizer, 2) fixed ventilation rates with a differential enthalpy economizer, 3) demand-controlled ventilation with an economizer, 4) fixed ventilation rates with heat recovery using an enthalpy exchanger, 5) fixed ventilation rates with heat recovery using a heat pump, 6) night ventilation precooling, 7) night ventilation precooling with an economizer, and 8) night ventilation precooling with demand-control ventilation and an economizer. Details about these strategies are given in later sections.

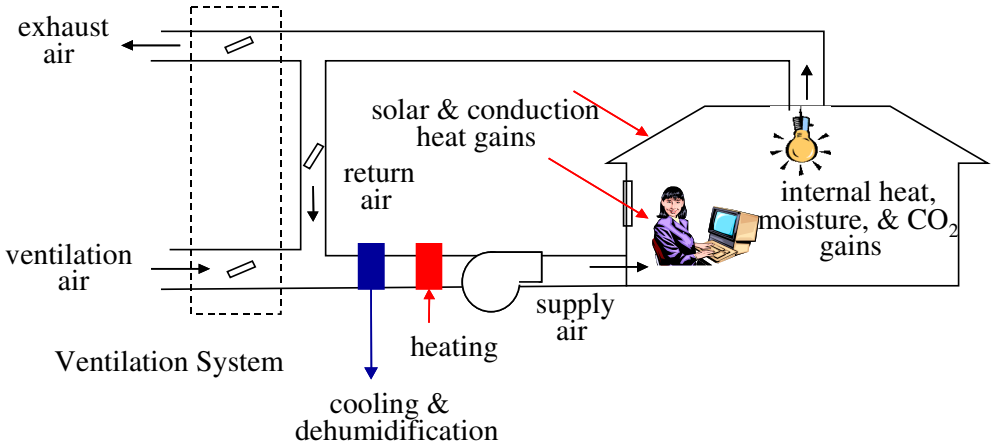

Figure 1. Schematic of a Small Commercial Building and HVAC System

VSAT is derived from a simulation tool that was developed by Braun and Brandemuehl (2002) called the Savings Estimator. It performs calculations for each hour of the year using fairly detailed models and TMY2 or California Climate Zone weather data. The goal in developing VSAT was to have a fast, robust simulation tool for comparison of ventilation options that could consider large parametric studies involving different systems and locations. Existing commercial simulation tools do not consider all of the ventilation options of interest

for this project.

Figure 2 shows an approximate flow diagram for the modeling approach used within VSAT. Given a physical building description, an occupancy schedule, and thermostat control strategy, the building model provides hourly estimates of the sensible cooling and heating requirements needed to keep the zone temperatures at cooling and heating setpoints. It involves calculation of transient heat transfer from the building structure and internal sources (e.g., lights, people, and equipment). The air distribution model solves energy and mass balances for the zone and air distribution system and determines mixed air conditions supplied to the equipment. The mixed air condition supplied to the primary HVAC equipment depends upon the ventilation strategy employed. The zone temperatures are outputs from the building model, whereas the zone and return air humidities and CO_2 concentrations are calculated by the air distribution model. The equipment model uses entering conditions and the sensible cooling requirement to determine the average supply air conditions. The entering and exit air conditions for the air distribution and equipment models are determined iteratively at each timestep of the simulation using a non-linear equation solver. Details of each of the component models are described in later sections.

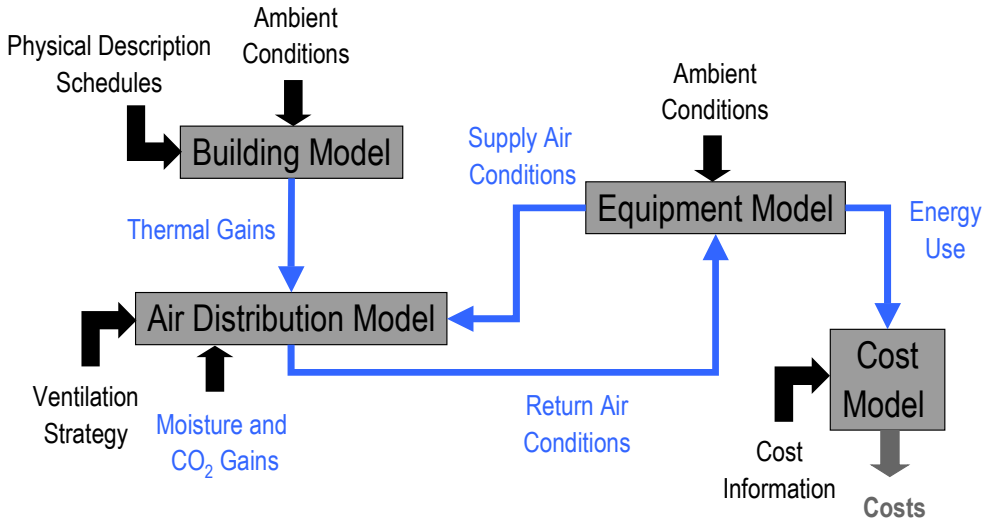

Figure 2. Schematic of VSAT Modeling Approach

SECTION 2: BUILDING MODEL

The space loads are based on the building physical characteristics, operating schedule, occupancy patterns, and space setpoints. The total sensible loads are calculated from an energy balance on the zone air for a given temperature setpoint with individual heat gains from walls, roof, floor, windows, internal gains, and infiltration. The following sections describe individual models for each of these elements and the overall strategy for estimating sensible cooling and heating requirements for the building.

2.1 Model Description

2.1.1 Exterior Walls and Roofs

Figure 3 shows the heat transfer rates and nomenclature associated with an external wall or roof (j^{th} wall). One-dimensional heat transfer is assumed. The symbols $\dot{Q}$ and T denote heat transfer rates and temperatures, respectively. The subscripts i and o refer to conditions at the inside and outside of the wall, respectively. The subscript c refers to convection, whereas r denotes radiation. The subscript s refers to conduction within the wall at the surface (inside or outside).

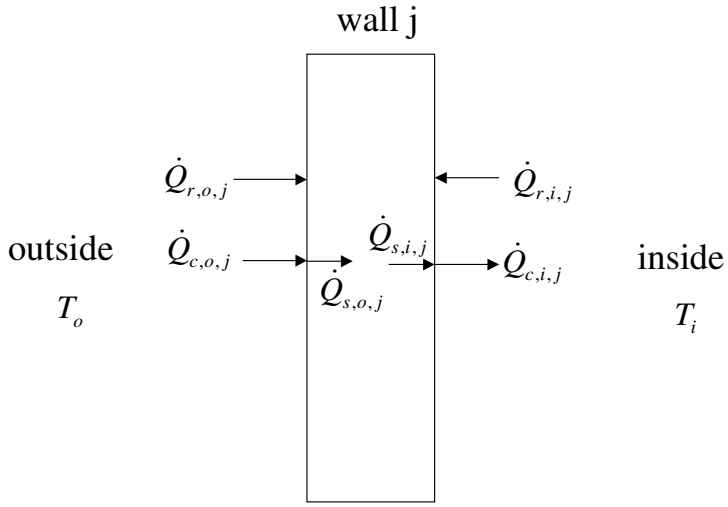

Figure 3. Heat transfer rates for an external wall

Radiation at the outside of the wall is due to solar (short-wave radiation) and long-wave radiation exchange with the sky and other surfaces. Long-wave radiation is assumed to occur between the wall surface and other surfaces that are at the ambient temperature (T_o). Furthermore, the radiation is linearized so that a radiation heat transfer coefficient is determined at a representative mean temperature. The long-wave radiation is combined with the convection using a combined convection and long-wave radiation heat transfer coefficient. With these assumptions, the effective outside convection (convection and long-wave radiation) and radiation (short-wave only) for wall j are calculated as

$$\dot{Q}_{c,o,j} = h_o A_j (T_o - T_{s,o,j}) \tag{2.1}$$

$$\dot{Q}_{r,o,j} = \alpha_o A_j I_{o,j} \tag{2.2}$$

where h_o is the outside heat transfer coefficient (convection and long-wave radiation), A is wall surface area, α_o is the absorptance for solar radiation of the outside surface, I_o is the instantaneous radiation incident upon the outside surface. The outside heat transfer coefficient and absorptance are assumed to be constant, independent of operating conditions (e.g., wind speed).

The conduction at the outside surface of the wall is equal to the sum of the convective and radiative gains. In order to simplify the transient heat transfer calculations, an equivalent outside air temperature is defined that would give the correct heat transfer rate in the absence of the solar radiation gains. This is commonly referred to as the sol-air temperature and is calculated as

$$T_{eq,o,j} = T_o + \frac{\alpha_o I_{o,j}}{h_o} \tag{2.3}$$

With this definition, the conduction heat transfer rate at the outside surface is

$$\dot{Q}_{s,o,j} = h_o A_j (T_{eq,o,j} - T_{s,o,j}) \tag{2.4}$$

A similar approach is followed for the inside surface: long-wave radiation is assumed to occur between each wall surface and other wall surfaces that are at the inside air temperature (T_i); long-wave radiation exchange with other surfaces is linearized so that a radiation heat transfer coefficient is determined at a representative mean temperature; long-wave radiation is combined with convection using a combined convection and long-wave radiation heat transfer coefficient; an equivalent inside air temperature is defined that would give the correct heat transfer rate in the absence of the internal radiation gains (from solar through windows and internal sources). With these assumptions, the conduction heat transfer rate at the inside wall surface is

$$\dot{Q}_{s,i,j} = h_i A_j (T_{eq,i,j} - T_{s,i,j}) \tag{2.5}$$

where

$$T_{eq,i,j} = T_i + \frac{\dot{q}_{g,r}}{h_i} \tag{2.6}$$

and where h_i is the inside heat transfer coefficient (convection and long-wave radiation) and $\dot{q}_{g,r}$ is the absorbed radiation flux due to internal sources and solar radiation transmitted through windows.

The transient heat transfer problem for a wall can be represented using an electrical analog. Figure 4 shows a simple two-node representation (two state variables) for a wall subjected to time-varying temperature boundary conditions. Outside and inside radiation gains are handled

with an equivalent air temperature. In this representation, R represents a thermal resistance and C is a thermal capacitance. The total thermal resistance ($R_1 + R_2 + R_3$) includes the thermal resistance between the outside air and the wall (combined convection and long-wave radiation), the conduction resistance within the wall and the thermal convection resistance between the wall and the building interior. The capacitors incorporate the total capacitance of the wall material. For this simple representation, the physical location of the nodes has a significant effect on the model predictions. Chaturvedi and Braun (2002) found that 2 or 3 nodes were sufficient to provide accurate transient predictions if the location of the nodes were optimized. For best results, the outside and inside resistances should include the air resistance and a portion of the material within the wall.

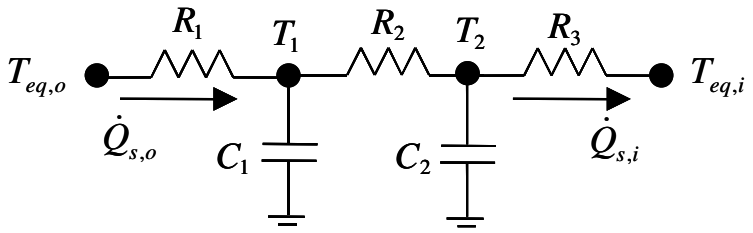

Figure 4. Thermal network representation of an external wall

The electrical circuit can easily be represented in state-space form as

$$\frac{d\vec{x}}{d\tau} = \hat{A}\vec{x} + \hat{B}\vec{u} \tag{2.7}$$

$$y = \vec{c}^{\,T}\vec{x} + \vec{d}^{\,T}\vec{u} \tag{2.8}$$

where $\vec{x}$ = vector of state variables
$\vec{u}$ = vector of inputs
y = output variable
$\hat{A}$ = constant coefficient matrix
$\hat{B}$ = constant coefficient matrix
$\vec{c}$ = constant coefficient vector
$\vec{d}$ = constant coefficient vector
τ = time

For a wall, the desired output variable is the rate of conduction heat transfer at the inside surface ($\dot{Q}_{s,i}$). The state vector contains temperatures of "nodes" within the structure of the wall, the input vector consists of the equivalent inside and outside air temperatures ($T_{eq,i}$ and $T_{eq,o}$), and coefficient matrices and vectors contain the physical characteristics of the wall (i.e., the R's and C's).

The state-space formulation could be solved at each timestep of a simulation. However, the computation can be significantly reduced if the state-space formulation is converted to a transfer function representation. Seem et al. (1989) presented a technique for determining an

equivalent transfer function representation from the state-space representation that involves the exact solution to the set of first-order differential equations with the inputs modeled as continuous, piecewise linear functions. This approach is used within VSAT for a one-hour timestep to determine a transfer function equation at the beginning of the simulation. After the transfer function has been developed, then the solution for the output at any time t is of the form

$$y(t) = \sum_{k=0}^{N_{state}} \vec{S}_k^T \cdot \vec{u}_{t-k\Delta\tau} - \sum_{k=1}^{N_{state}} e_k \cdot y(t - k\Delta\tau) \tag{2.9}$$

where N_{state} = number of state variables
$\vec{S}_k$ = vector containing transfer function coefficients for the input vector k timesteps prior to the current time t
e_k = transfer function coefficient for the zone sensible load for k timesteps prior to the current time t
$\Delta\tau$ = time step (one hour for VSAT)

At the beginning of the simulation, the vectors $\vec{S}_k$ for k = 0 to N_{state} are determined as

$$\begin{aligned} \vec{S}_0 &= \vec{c}\hat{R}_0\Gamma_2 + \vec{d} \\ \vec{S}_j &= \vec{c}\left[\hat{R}_{j-1}(\Gamma_1 - \Gamma_2) + \hat{R}_j\Gamma_2\right] + e_j\vec{d} \quad \text{for } 1 \le j \le (N_{state} - 1) \\ \vec{S}_{N_{state}} &= \vec{c}\hat{R}_{N_{state}-1}(\Gamma_1 - \Gamma_2) + e_{N_{state}}\vec{d} \end{aligned} \tag{2.10}$$

where

$$\begin{aligned} \Gamma_1 &= \hat{A}^{-1}\left(\Phi - \hat{I}\right)\hat{B} \\ \Gamma_2 &= \hat{A}^{-1}\left[\frac{\Gamma_1}{\Delta\tau} - \hat{B}\right] \end{aligned} \tag{2.11}$$

where $\hat{I}$ is the identity matrix, $\Delta\tau$ is the simulation time step (one hour for this study), and

$$\begin{aligned} \Phi &= e^{\hat{A}\Delta\tau} \\ e^{\hat{A}\Delta\tau} &= \hat{I} + \hat{A}\Delta\tau + \frac{\hat{A}^2(\Delta\tau)^2}{2!} + \frac{\hat{A}^3(\Delta\tau)^3}{3!} + \ldots + \frac{\hat{A}^n(\Delta\tau)^n}{n!} + \ldots \end{aligned} \tag{2.12}$$

Seem et al. (1989) presented an efficient algorithm for evaluating $e^{\hat{A}\Delta\tau}$ in equation 2.12 that is used within VSAT. The matrices $\hat{R}_j$ used in the determination of $\vec{S}_k$ and the e_j transfer function coefficients are determined recursively as

$$\begin{aligned}
&\hat{R}_0 = \hat{I} && e_1 = -\frac{Tr\left(\Phi\hat{R}_0\right)}{1} \\
&\hat{R}_1 = \Phi\hat{R}_0 + e_1\hat{I} && e_2 = -\frac{Tr\left(\Phi\hat{R}_1\right)}{2} \\
&\hat{R}_2 = \Phi\hat{R}_1 + e_2\hat{I} && e_3 = -\frac{Tr\left(\Phi\hat{R}_2\right)}{3} \\
&\vdots && \vdots \\
&\hat{R}_{N_{state}-1} = \Phi\hat{R}_{N_{state}-2} + e_{N_{state}-1}\hat{I} && e_{N_{state}} = -\frac{Tr\left(\Phi\hat{R}_{N_{state}-1}\right)}{N_{state}}
\end{aligned} \tag{2.13}$$

where Tr() is the trace of the matrix (the sum of the diagonal elements).

The transfer function representation gives the wall conduction at the inside surface for any wall j. The heat transfer to the inside air due to wall j is then

$$\dot{Q}_{i,j} = \dot{Q}_{s,i,j} + A_j\dot{q}_{g,r} \tag{2.14}$$

2.1.2 Floor Slabs

Slab on grade floors are modeled using a similar formulation as for exterior walls. However, the exterior of the floor is exposed to the ground so that there is no convection, solar radiation, or long-wave radiation. Furthermore, the predominant mechanism for heat loss or gain is heat transfer at the perimeter of the slab. The transfer function of equation 2.9 is used to determine the conduction heat transfer at the inside surface for floors. However, the bottom side of the floor is assumed to be adiabatic (infinite resistance for heat transfer between the outside floor surface and the ground). The primary mode for heat transfer to and from the ambient is through the perimeter of the slab. Perimeter heat transfer is assumed to be quasi-steady state from the ambient to the inside air across a resistance that is based upon the slab perimeter heat loss factor (ASHRAE, 2001). The combined heat transfer to the inside air from the floor is then

$$\dot{Q}_i = \dot{Q}_{s,i} + A\dot{q}_{g,r} + F_p \cdot P \cdot (T_o - T_i) \tag{2.15}$$

where F_p is the slab perimeter heat loss factor and P is the perimeter of the slab.

2.1.3 Interior Walls

An interior wall differs from an exterior wall in that the inside boundary conditions are experienced on both sides of the wall. The transfer function of equation 2.9 is used to determine the conduction heat transfer at the inside surfaces for interior walls with both boundary conditions given by equation 2.6. Interior walls are assumed to be symmetric with identical boundary conditions, so that the total heat transfer to the air from both surfaces is

$$\dot{Q}_i = 2 \cdot \left(\dot{Q}_{s,i} + A\dot{q}_{g,r}\right) \tag{2.16}$$

where A is the surface area for one face and $\dot{Q}_{s,i}$ is the conduction heat transfer rate for one surface of the wall.

Interior walls/furnishings are represented with a single node (capacitance) having a total surface area equal to twice the total floor area, a mass of 25 lbm/ft^2, and an average specific heat of 0.2 Btu/lbm-F.

2.1.4 Windows

Figure 5 shows the relevant heat transfer rates for the kth window. Windows are considered as quasi-steady-state elements that provide heat gains due to both solar transmission and conduction. Similar to walls, long-wave radiation is combined with convection using combined heat transfer coefficients at the inside and outside surfaces. Solar radiation passing through the window is partially absorbed and mostly transmitted. The overall absorptance and transmittance for solar radiation of the window are α and τ, respectively.

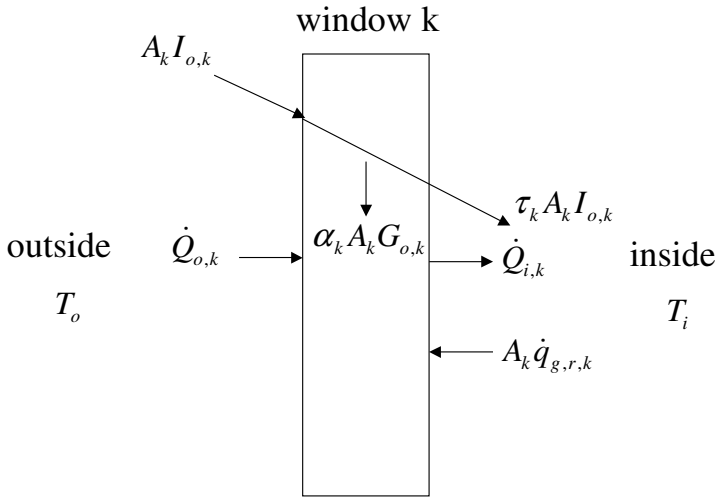

Figure 5. Heat transfer rates for a window

Assuming that the absorption of solar radiation occurs at the outside surface and absorption of internal radiative gains occurs at the inside surface, then the heat transfer rate by conduction through the glass is

$$\dot{Q}_{s,i,k} = U_k A_k (T_{eq,o,k} - T_{eq,o,k}) \tag{2.17}$$

where U is the overall unit conductance for the window. The equivalent inside and outside air temperatures ($T_{eq,i}$ and $T_{eq,o}$) are evaluated using equations 2.3 and 2.6, respectively. Then, the total heat gains through the window are

$$\dot{Q}_{win,k} = U_k A_k (T_{eq,o,k} - T_{eq,i,k}) + \tau_k \cdot A_k \cdot I_{o,k} + A_k \cdot \dot{q}_{g,r,k} \tag{2.18}$$

It is more common to have data for window shading coefficients than for window transmittances. The shading coefficient accounts for both solar transmission and solar absorption. In this formulation, the total heat gain to the air due to the window is given as

$$\dot{Q}_{win,k} = U_k A_k (T_o - T_{eq,i,k}) + SHGC_k \cdot A_k \cdot I_{o,k} + A_k \cdot \dot{q}_{g,r,k} \tag{2.19}$$

where *SHGC* is the solar heat gain coefficient defined as

$$SHGC = \tau + \frac{U\alpha}{h_o} \tag{2.20}$$

where h_o is the outside heat transfer coefficient (combined convection and long-wave radiation). Equations 2.18 and 2.19 are equivalent.

The shading coefficient is defined as

$$SC = \frac{SHGC}{SHGC_{ref}} \tag{2.21}$$

where $SHGC_{ref}$ is the solar heat gain coefficient for a single pane of double strength glass, which has a value of 0.87. In general, the shading coefficient can account for multiple glazings, different types of glazing materials, and indoor shading devices.

Using the definition of shading coefficient, equation 2.19 can be rewritten as

$$\dot{Q}_{win,k} = U_k A_k (T_o - T_{eq,i,k}) + SC \cdot SHGC_{ref} \cdot A_k \cdot I_{o,k} + A_k \cdot \dot{q}_{g,r,k} \tag{2.22}$$

The concept of a shading coefficient was developed for building models where the heat gains due to solar radiation are added directly to the air. In reality, solar transmission through windows leads to solar absorptance on other interior surfaces, whereas solar absorption in windows leads to increased convection to the air by the window. Although it is not strictly correct, VSAT uses the total solar gains determined with a shading coefficient and distributes them to other internal surfaces. With this approach, the window solar transmission and convection to the air are determined as

$$\dot{Q}_{t,k} = SC \cdot SHGC_{ref} \cdot A_k \cdot I_{o,k} \tag{2.23}$$

$$\dot{Q}_{i,k} = U_k A_k (T_o - T_{eq,i,k}) + A_k \cdot \dot{q}_{g,r,k} \tag{2.24}$$

VSAT assumes constant values for the shading coefficient and overall window unit conductance. Solar transmission through windows is distributed solely to the floor with a uniform heat flux.

2.1.5 Infiltration

Infiltration is a relatively small effect for commercial buildings and is modeled with a constant flow rate that is based upon a specified volumetric flow rate per unit floor area. The

default value is 0.05 cfm/ft^2, but can be changed. For a building with 10-foot ceiling height, this infiltration rate corresponds to 0.3 air changes per hour.

The sensible and latent heat gains due to infiltration are determined as

$$\dot{Q}_{\text{inf},s} = \dot{m}_{\text{inf}} C_{pm} (T_o - T_i) \tag{2.25}$$

$$\dot{Q}_{\text{inf},L} = \dot{m}_{\text{inf}} h_{fg} (\omega_o - \omega_i) \tag{2.26}$$

where C_{pm} is the moist air specific heat, h_{fg} is the heat of vaporization of water, ω_o is the humidity ratio of the outside air, and ω_i is the humidity ratio of the inside air.

2.1.7 Internal Gains

Internal gains due to lights, equipment, and people vary according to an occupancy schedule that is specified. The specific values of the heat gains and the proportion of gains from people that influence latent loads vary according to building type (see Prototypical Building Descriptions). For people and lights, 50% of the heat gains are assumed to be radiative and 50% convective. All the gains from equipment (e.g, computers) are assumed to be convective. The radiative internal gains are distributed with an even heat flux to all internal surfaces (including windows).

2.1.8 Zone Loads

At any time, the sensible cooling (+) or heating (-) required to keep the zone temperature at a specified setpoint is determined as

$$\dot{Q}_z = \sum_{j=1}^{walls} \dot{Q}_{i,j} + \sum_{k=1}^{windows} \dot{Q}_{i,k} + \dot{Q}_{g,c} + \dot{Q}_{s,\text{inf}} \tag{2.27}$$

where $\dot{Q}_{g,c}$ is the total convective heat gain due to lights, people, and equipment.

Separate temperature setpoints are specified for heating and cooling and the temperature can float in between with no required cooling or heating. In order to evaluate whether heating or cooling is required for a given time step, it is necessary to determine the zone temperature where the sensible cooling requirement for the equipment is equal to zero. In the absence of ventilation (unoccupied mode) then equation 2.27 would be solved inversely for the floating inside air temperature with $\dot{Q}_z$ set equal to zero. If the calculated zone temperature is less than the heating setpoint, then heating is required and equation 2.27 is evaluated using the heating setpoint. If the calculated zone temperature is greater than the cooling setpoint, then cooling is required and equation 2.27 is evaluated using the cooling setpoint. If the calculated temperature is between the setpoints, then the zone temperature is floating and the zone sensible cooling and heating requirement are zero. The case where the fans operate continuously with a ventilation load (unoccupied mode) is considered in section 4.

When there is a sensible cooling requirement, then the cooling equipment also provides latent cooling and it is necessary to know the latent loads for the zone. In this case, the zone latent gains are the sum of the latent gains due to people and due to infiltration.

2.1.9 Solar Radiation Processing

The weather data files used by VSAT contain hourly values of global horizontal radiation and direct normal radiation. The horizontal radiation is used for the roof, but it is necessary to calculate incident radiation on vertical surfaces for external walls. The total incident radiation for vertical surfaces is determined as

$$I_o = I_{DN} \sin(\theta_z) \cdot \cos(\gamma_s - \gamma) + \frac{I_D}{2} + \rho_g I_H \tag{2.28}$$

where I_{DN} is beam radiation that is measured normal to the line of sight to the sun, θ_z is the zenith angle, γ_s is the solar azimuth angle, γ is the surface azimuth angle, I_D is sky diffuse radiation, ρ_g is ground reflectance, and I_H is total radiation incident upon a horizontal surface. Zenith is the angle between the vertical and the line of site to the sun. Solar azimuth is the angle between the local meridian and the projection of the line of sight to the sun onto the horizontal plane. Zero solar azimuth is facing the equator, west is positive, while east is negative. The zenith and solar azimuth angle are calculated using relationships given in Duffie and Beckman (1980). The surface azimuth is the angle between the local meridian and the projection of the normal to the surface onto the horizontal plane (0 for south facing, -90 for east facing +90 for west facing, and +180 for north facing). The ground reflectance is assumed to have a constant value of 0.2, which is representative of summer conditions. The sky diffuse radiation is calculated from the

$$I_D = I_H - I_{DN} \cos(\theta_z) \tag{2.29}$$

2.2 Prototypical Building Descriptions

Seven different types of buildings are considered in VSAT: small office, school class wing, retail store, restaurant dining area, school gymnasium, school library, and school auditorium. Descriptions for these buildings were obtained from prototypical building descriptions of commercial building prototypes developed by Lawrence Berkeley National Laboratory (Huang, et al. 1990 & Huang, et al. 1995). These reports served as the primary sources for prototypical building data. However, additional information was obtained from DOE-2 input files used by the researchers for their studies.

Tables 1 - 7 contain information on the geometry, construction materials, and internal gains used in modeling the different buildings. Although not given in these tables, the walls, roofs and floors include inside air and outside air thermal resistances. The window R-value includes the effects of the window construction and inside and outside air resistances. Table 8 lists the properties of all construction materials and the air resistances. The geometry of each of the buildings is assumed to be rectangular with four sides and is specified with the following parameters: 1) floor area, 2) number of stories, 3) aspect ratio, 4) ratio of exterior perimeter to total perimeter, 5) wall height and 6) ratio of glass area to wall area. The aspect ratio is the ratio of the width to the length of the building. However, exterior perimeter and glass areas are assumed to be equally distributed on all sides of the building, giving equal exposure of exterior walls and windows to incident solar radiation. The four exterior walls face north, south, east, and west.

The user can specify occupancy schedules, but default values are based upon the original LBNL study. In the LBNL study, the occupancy was scaled relative to a daily average

maximum occupancy density (people per 1000 ft^2). In VSAT, the user can specify a peak design occupancy density (people per 1000 ft^2) that is used for determining fixed ventilation requirements (no DCV). This same design occupancy density is used as the scaling factor for the hourly occupancy schedules. As a result, the original LBNL occupancy schedules were rescaled using the default peak design occupancy densities.

The heat gains and CO_2 generation per person depend upon the type of building (and associated activity). Design internal gains for lights and equipment also depend upon the building and are scaled according to specified average daily minimum and maximum gain fractions. For all of the buildings, the lights and equipment are at their average maximum values whenever the building is occupied and are at their average minimum values at all other times.

Zone thermostat setpoints can be set for both occupied and unoccupied periods. The default occupied setpoints for cooling and heating are 75°F and 70°F, respectively. The default unoccupied setpoints for cooling (setup) and heating (setback) are 85°F and 60°F, respectively. The lights are assumed to come on one hour before people arrive and stay on one hour after they leave. The occupied and unoccupied setpoints follow this same schedule.

Table 1. Office Building Characteristics

Windows		
R-value, hr-ft^2-F/Btu	1.58	
Shading Coefficient	0.75	
Area ratio (window/wall)	0.15	
Exterior Wall Construction		
Layers	1" stone R-5.6 insulation R-0.89 airspace 5/8" gypsum	
Roof Construction		
Layers	Built-up roof (3/8") 4" lightweight concrete R-12.6 insulation R-0.92 airspace ½" acoustic tile	
Floor		
Layers	6" heavyweight concrete Carpet and pad	
Slab perimeter loss factor, Btu/h-ft-F	0.5	
General		
Floor area, ft^2	6600	
Wall height, ft	11	
Internal mass, lb/ft^2	25	
Number of stories	1	
Aspect Ratio	0.67	
Ratio of exterior perimeter to floor perimeter	1.0	
Design equipment gains, W/ft^2	0.5	
Design light gains, W/ft^2	1.7	
Ave. daily min. lights/equip. gain fraction	0.2	
Ave. daily max. lights/equip. gain fraction	0.9	
Sensible people gains, Btu/hr-person	250	
Latent people gains, Btu/hr-person	250	
CO_2 people generation, L/min-person	0.33	
Design occupancy for vent., people/1000 ft^2	7	
Design ventilation, cfm/person	20	
Average weekday peak occucpancy, ft^2/person	470	
Default average weekday occupancy schedule * Values given relative to average peak	Hours 1-7 8 9 10-16 17 18-24	Values 0.0 0.33 0.66 1.0 0.5 0.0
Default average weekend occupancy schedule * Values given relative to average peak	Hours 1-8 9 10-12 12-13 13-24	Values 0.0 0.15 0.2 0.15 0.0
Monthly occupancy scaling * relative to daily occupancy schedule	Month 1-12	Value 1.0

Table 2. Restaurant Dining Area Characteristics

Windows		
R-value, hr-ft^2-F/Btu	1.53	
Shading Coefficient	0.8	
Area ratio (window/wall)	0.15	
Exterior Wall Construction		
Layers	3" face brick ½" plywood R-4.9 insulation 5/8" gypsum	
Roof Construction		
Layers	Built-up roof (3/8") ¾" plywood R-13.2 insulation R-0.92 airspace ½" acoustic tile	
Floor		
Layers	4" heavyweight concrete Carpet and pad	
Slab perimeter loss factor, Btu/h-ft-F	0.5	
General		
Floor area, ft^2	5250	
Wall height, ft	10	
Internal mass, lb/ft^2	25	
Number of stories	1	
Aspect Ratio	1.0	
Ratio of exterior perimeter to floor perimeter	0.75	
Design equipment gains, W/ft^2	0.0	
Design light gains, W/ft^2	2.0	
Ave. daily min. lights/equip. gain fraction	0.2	
Ave. daily max. lights/equip. gain fraction	1.0	
Sensible people gains, Btu/hr-person	250	
Latent people gains, Btu/hr-person	275	
CO_2 people generation, L/min-person	0.35	
Design occupancy for vent., people/1000 ft^2	30	
Design ventilation, cfm/person	20	
Average weekday peak occucpancy, ft^2/person	50	
Default average weekday occupancy schedule * Values given relative to average peak	Hours 1-6 7-12 13-24	Values 0.0 0.2,0.3,0.1,0.05,0.2,0.5 0.5,0.4,0.2,0.05,0.1,0.4, 0.6,0.5,0.4,0.2,0.1,0.0
Default average weekend occupancy schedule * Values given relative to average peak	Hours 1-6 7-12 13-24	Values 0.0 0.3,0.4,0.5,0.2,0.2,0.3 0.5,0.5,0.5,0.35,0.25, 0.5,0.8,0.8,0.7,0.4,0.2, 0.0
Monthly occupancy scaling * relative to daily occupancy schedule	Month 1-5 6-8 9-12	Value 1.0 0.5 1.0

Table 3. Retail Store Characteristics

Windows		
R-value, hr-ft^2-F/Btu	1.5	
Shading Coefficient	0.76	
Area ratio (window/wall)	0.15	
Exterior Wall Construction		
Layers	8" lightweight concrete R-4.8 insulation R-0.89 airspace 5/8" gypsum	
Roof Construction		
Layers	Built-up roof (3/8") 1.25" lightweight concrete R-12 insulation R-0.92 airspace ½" acoustic tile	
Floor		
Layers	4" lightweight concrete Carpet and pad	
Slab perimeter loss factor, Btu/h-ft-F	0.5	
General		
Floor area, ft^2	80,000	
Wall height, ft	15	
Internal mass, lb/ft^2	25	
Number of stories	2	
Aspect Ratio	0.5	
Ratio of exterior perimeter to floor perimeter	1.0	
Design equipment gains, W/ft^2	0.4	
Design light gains, W/ft^2	1.6	
Ave. daily min. lights/equip. gain fraction	0.2	
Ave. daily max. lights/equip. gain fraction	0.9	
Sensible people gains, Btu/hr-person	250	
Latent people gains, Btu/hr-person	250	
CO_2 people generation, L/min-person	0.33	
Design occupancy for vent., people/1000 ft^2	25	
Design ventilation, cfm/person	15	
Average weekday peak occucpancy, ft^2/person	390	
Default average weekday occupancy schedule * Values given relative to average peak	Hours 1-7 8 9 10-20 21 22-24	Values 0.0 0.33 0.66 1.0 0.5 0.0
Default average weekend occupancy schedule * Values given relative to average peak	Hours 1-7 8 9 10-20 21 22-24	Values 0.0 0.33 0.66 1.0 0.5 0.0
Monthly occupancy scaling * relative to daily occupancy schedule	Month 1-12	Value 1.0

Table 4. School Class Wing Characteristics

Windows		
R-value, hr-ft^2-F/Btu	1.7	
Shading Coefficient	0.73	
Area ratio (window/wall)	0.18	
Exterior Wall Construction		
Layers	8" concrete block R-5.7 insulation 5/8" gypsum	
Roof Construction		
Layers	Built-up roof (3/8") ¾" plywood R-13.3 insulation R-0.92 airspace ½" acoustic tile	
Floor		
Layers	6" heavyweight concrete	
Slab perimeter loss factor, Btu/h-ft-F	0.5	
General		
Floor area, ft^2	9600	
Internal mass, lb/ft^2	25	
Wall height, ft	10	
Number of stories	2	
Aspect Ratio	0.5	
Ratio of exterior perimeter to floor perimeter	0.875	
Design equipment gains, W/ft^2	0.3	
Design light gains, W/ft^2	2.2	
Ave. daily min. lights/equip. gain fraction	0.1	
Ave. daily max. lights/equip. gain fraction	0.95	
Sensible people gains, Btu/hr-person	250	
Latent people gains, Btu/hr-person	200	
CO_2 people generation, L/min-person	0.3	
Design occupancy for vent., people/1000 ft^2	25	
Design ventilation, cfm/person	15	
Average weekday peak occucpancy, ft^2/person	50	
Default average weekday occupancy schedule * Values given relative to average peak	Hours 1-6 7 8-11 12-15 16 17 18 19-21 22-24	Values 0.0 0.1 0.9 0.8 0.45 0.15 0.05 0.33 0.0
Default average weekend occupancy schedule * Values given relative to average peak	Hours 1-9 10-13 14-24	Value 0.0 0.1 0.0
Monthly occupancy scaling * relative to daily occupancy schedule	Month 1-5 6-8 9-12	Value 1.0 0.5 1.0

Table 5. School Gymnasium Characteristics

Windows		
R-value, hr-ft^2-F/Btu	1.7	
Shading Coefficient	0.73	
Area ratio (window/wall)	0.18	
Exterior Wall Construction		
Layers	8" concrete block R-5.7 insulation 5/8" gypsum	
Roof Construction		
Layers	Built-up roof (3/8") ¾" plywood R-13.3 insulation R-0.92 airspace ½" acoustic tile	
Floor		
Layers	6" heavyweight concrete	
Slab perimeter loss factor, Btu/h-ft-F	0.5	
General		
Floor area, ft^2	7500	
Internal mass, lb/ft^2	25	
Wall height, ft	32	
Number of stories	1	
Aspect Ratio	0.86	
Ratio of exterior perimeter to floor perimeter	0.86	
Design equipment gains, W/ft^2	0.2	
Design light gains, W/ft^2	0.65	
Ave. daily min. lights/equip. gain fraction	0.0	
Ave. daily max. lights/equip. gain fraction	0.9	
Sensible people gains, Btu/hr-person	250	
Latent people gains, Btu/hr-person	550	
CO_2 people generation, L/min-person	0.55	
Design occupancy for vent., people/1000 ft^2	30	
Design ventilation, cfm/person	20	
Average weekday peak occucpancy, ft^2/person	180	
Default average weekday occupancy schedule * Values given relative to average peak	Hours 1-7 8-15 16-24	Value 0.0 1.0 0.0
Default average weekend occupancy schedule * Values given relative to average peak	Hours 1-24	Value 0.0
Monthly occupancy scaling * relative to daily occupancy schedule	Month 1-5 6-8 9-12	Value 1.0 0.1 1.0

Table 6. School Library Characteristics

Windows		
R-value, hr-ft^2-F/Btu	1.7	
Shading Coefficient	0.73	
Area ratio (window/wall)	0.18	
Exterior Wall Construction		
Layers	8” concrete block R-5.7 insulation 5/8” gypsum	
Roof Construction		
Layers	Built-up roof (3/8”) ¾” plywood R-13.3 insulation R-0.92 airspace ½” acoustic tile	
Floor		
Layers	6” heavyweight concrete	
Slab perimeter loss factor, Btu/h-ft-F	0.5	
General		
Floor area, ft^2	1500	
Internal mass, lb/ft^2	25	
Wall height, ft	10	
Number of stories	1	
Aspect Ratio	0.2	
Ratio of exterior perimeter to floor perimeter	0.75	
Design equipment gains, W/ft^2	0.4	
Design light gains, W/ft^2	1.5	
Ave. daily min. lights/equip. gain fraction	0.1	
Ave. daily max. lights/equip. gain fraction	0.95	
Sensible people gains, Btu/hr-person	250	
Latent people gains, Btu/hr-person	250	
CO_2 people generation, L/min-person	0.33	
Design occupancy for vent., people/1000 ft^2	20	
Design ventilation, cfm/person	15	
Average weekday peak occucpancy, ft^2/person	100	
Default average weekday occupancy schedule * Values given relative to average peak	Hours 1-6 7 8-11 12-15 16 17 18 19-21 22-24	Value 0.0 0.1 0.9 0.8 0.45 0.15 0.05 0.33 0.0
Default average weekend occupancy schedule * Values given relative to average peak	Hours 1-9 10-13 14-24	Value 0.0 0.1 0.0
Monthly occupancy scaling * relative to daily occupancy schedule	Month 1-5 6-8 9-12	Value 1.0 0.5 1.0

Table 7. School Auditorium Characteristics

Windows		
R-value, hr-ft^2-F/Btu	1.7	
Shading Coefficient	0.73	
Area ratio (window/wall)	0.18	
Exterior Wall Construction		
Layers	8" concrete block R-5.7 insulation 5/8" gypsum	
Roof Construction		
Layers	Built-up roof (3/8") ¾" plywood R-13.3 insulation R-0.92 airspace ½" acoustic tile	
Floor		
Layers	6" heavyweight concrete	
Slab perimeter loss factor, Btu/h-ft-F	0.5	
General		
Floor area, ft^2	6000	
Internal mass, lb/ft^2	25	
Wall height, ft	32	
Number of stories	1	
Aspect Ratio	0.64	
Ratio of exterior perimeter to floor perimeter	0.85	
Design equipment gains, W/ft^2	0.2	
Design light gains, W/ft^2	0.8	
Ave. daily min. lights/equip. gain fraction	0.0	
Ave. daily max. lights/equip. gain fraction	0.9	
Sensible people gains, Btu/hr-person	250	
Latent people gains, Btu/hr-person	200	
CO_2 people generation, L/min-person	0.3	
Design occupancy for vent., people/1000 ft^2	150	
Design ventilation, cfm/person	15	
Average weekday peak occucpancy, ft^2/person	100	
Default average weekday occupancy schedule * Values given relative to average peak	Hours 1-9 10-11 12 13-14 15-24	Values 0.0 0.75 0.2 0.75 0.0
Default average weekend occupancy schedule * Values given relative to average peak	Hours 1-24	Value 0.0
Monthly occupancy scaling * relative to daily occupancy schedule	Month 1-5 6-8 9-12	Value 1.0 0.1 1.0

Table 8. Construction Material Properties

	Conductivity (Btu/h*ft*F)	Density (lb/ft^3)	Specific Heat (Btu/lb*F)
stone	1.0416	140	0.20
light concrete	0.2083	80	0.20
heavy concrete	1.0417	140	0.20
built-up roof	0.0939	70	0.35
face brick	0.7576	130	0.22
acoustic tile	0.033	18	0.32
gypsum	0.0926	50	0.20
	Resistance ($h*ft^2*F/Btu$)		
3/4" plywood	0.93703		
1/2" plywood	0.62469		
carpet and pad	2.08		
inside air	0.67		
outside air	0.33		

2.3 Model Validation

The prototypical buildings were chosen to give representative building loads in order to determine if particular building types will benefit more or less from the ventilation strategies under examination. Absolute model predictions are not the goal but rather the impact of ventilation strategies on savings compared to a baseline. Even so, it is very important that the building load predictions have representative dynamics and absolute load levels. In order to validate predictions of VSAT, results have been compared with predictions of the TYPE 56 building model within TRNSYS (2000). This model has been validated with detailed measurements and through comparison with other accepted building load calculation programs.

The TYPE 56 is a very detailed model that is built up from individual descriptions of wall layers, windows, internal gains, schedules, etc. The user enters all pertinent information into a "front-end" program called *PRE-BID*. This program assimilates all the information into four different files that are used by the TYPE 56 component for generating the specific building loads and ultimately the total building load.

Two building prototypes were chosen as case studies to validate the building loads portion of VSAT. Identical construction properties, schedules, internal gains and weather data for each case study were entered into the TYPE 56 and VSAT models for comparison.

2.3.1 TYPE 56 and VSAT Building Model Assumptions

The TYPE 56 building type predicts the thermal behavior of a building having multiple zones. To determine zone heating and cooling requirements, an "energy rate" method is employed. The user specifies the zone setpoints for heating and cooling with any added setup

or setback control schedules. If the floating zone temperature is less than the heating setpoint, then heating is required or if the calculated zone temperature is greater than the cooling setpoint, then cooling is required. Otherwise, the zone temperature is floating and the zone sensible cooling and heating requirement are zero. Unlimited equipment capacity was assumed in the TYPE 56 for purposes of validating the building model in the VSAT.

Walls are modeled in the TYPE 56 using a transfer function method that is equivalent to the approach used in VSAT with a large number of resistors and capacitors. The primary differences between the building model in VSAT and the TYPE 56 are related to the way that solar and long-wave radiation are handled. The solar transmittance for windows is calculated as a function of window properties and solar incidence angle as opposed to the use of a constant shading coefficient employed within VSAT. The solar radiation that is transmitted through windows is distributed to all surfaces in the zone according to the following relation

$$f_j = \frac{\alpha_j \cdot A_j}{\sum_{j=1}^{surfaces} \alpha_j * A_j} \tag{2.30}$$

where f_j is the fraction of transmitted radiation that is absorbed on surface j, A_j is the area of surface j, α_j is the solar absorptance of surface j. In contrast, VSAT distributes all of the transmitted solar radiation to the floor with an even heat flux. It's difficult to say which approach is best, since both are simplifications and the actual solar distribution depends upon the specific geometry of the room and time.

Long-wave radiation exchange between surfaces within the zone is handled in the TYPE 56 using an effective zone surface temperature termed the star temperature. The zone air is coupled to the surface temperatures and star temperature through convective resistances. In contrast, VSAT uses a combined convective and radiative heat transfer coefficient that couples the surface temperatures to the zone air temperature. In both models, surfaces are assumed to be black with respect to long-wave radiation.

Long-wave radiation exchange between outside surfaces and the atmosphere is considered explicitly in the TYPE 56. Radiation occurs between the surface temperatures and an effective temperature that depends upon the surface orientation. The effective temperature is determined as

$$T_{r,o} = (1 - f_{sky}) * T_o + f_{sky} * T_{sky} \tag{2.31}$$

where f_{sky} is the view factor between the surface and the sky, T_o is the outside air temperature, and T_{sky} is a sky temperature that depends upon the air temperature and cloud cover. In contrast, VSAT uses a combined convective and radiative heat transfer coefficient, which is equivalent to assuming that the effective temperature for long-wave radiation is equal to the outside air temperature. In both models, surfaces are assumed to be black with respect to long-wave radiation.

2.3.2 Case Study Description

Two case study descriptions were simulated and compared in VSAT and TRNSYS. The

prototypical office and restaurant (see Tables 1 and 2) were both modeled in Madison, WI and San Diego, CA. Only sensible zone loads were considered, not including ventilation.

In VSAT, combined convective and radiation coefficients were utilized for the inside and outside air of 1.5 Btu/hr-ft^2-F and 3.0 Btu/hr-ft^2-F, respectively. Since long-wave radiation is handled explicitly in the TYPE 56, convective heat transfer coefficients need to be specified for the inside and outside air. Convective heat transfer coefficients that result in approximately the combined coefficients used in VSAT were found to be 1.25 Btu/hr-ft^2-F and 2.75 Btu/hr-ft^2-F and were used within the TYPE 56.

The TYPE 56 estimates U-Values for windows based upon the glass properties. For a single pane glass, the U-Value is about 1.0 Btu/hr-ft^2-F. In order to realize the specified overall R-values for the windows used in VSAT, the outside and inside convective heat transfer coefficients were set to 2.3 Btu/hr-ft^2-F and 6.8 Btu/hr-ft^2-F for windows within the TYPE 56.

In order to distribute transmitted solar radiation to the floor only, the solar absorptances of all inside walls were set to zero in the TYPE 56 and the floor solar absorptance was set equal to unity. Finally, the sky temperature used by the TYPE 56 was set equal to the ambient temperature.

2.3.3 Results for Constant Temperature Setpoints

As a first step, cooling and heating loads were evaluated for a constant temperature setpoint of 70°F (21.11°C). This eliminates any transients due to return from night setup and setback. Figure 6 shows hourly heating load comparisons for the office and restaurant over two days in January. VSAT predicts the correct transients and peak load. The relative differences are largest when the loads are smallest at night. Similar results are shown for two days of cooling load predictions in Figure 7.

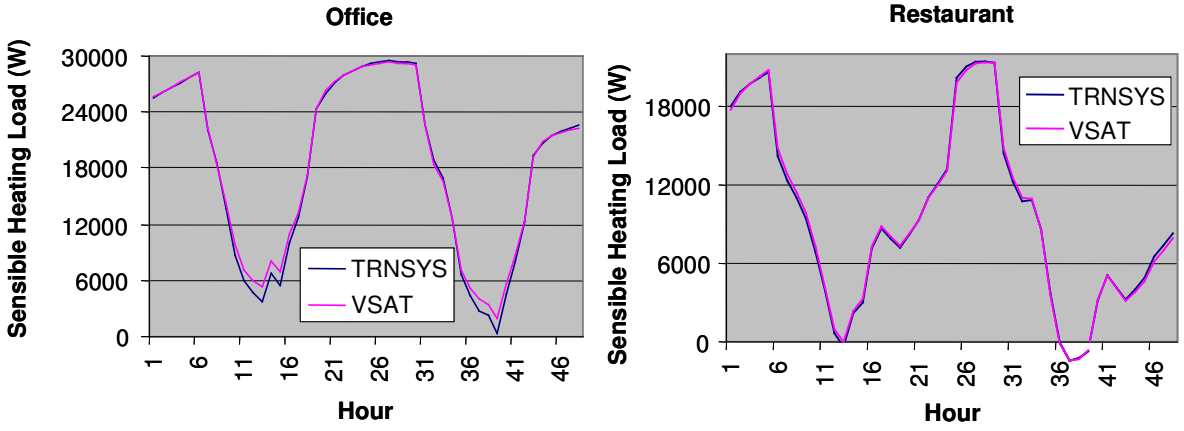

Figure 6. Hourly zone heating loads for constant setpoints (Jan. 9 – 10, Madison, WI)

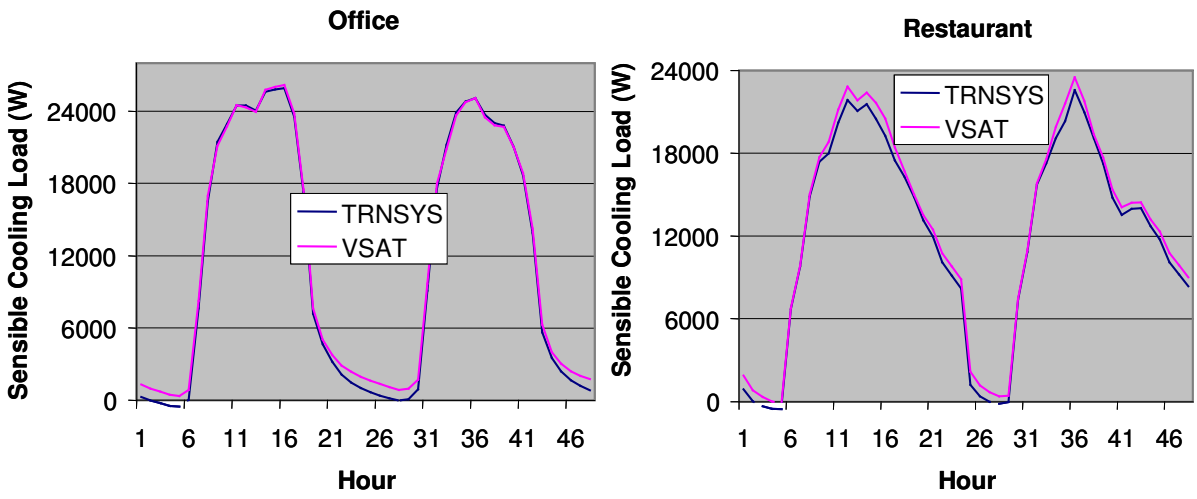

Figure 7. Hourly zone sensible cooling loads for constant setpoints (June 9– 10, San Diego, CA)

Figure 8 and Figure 9 give monthly comparisons for sensible heating and cooling loads. In general, VSAT tends to slightly underpredict heating loads and overpredict cooling loads. This may be due to differences in the manner in which solar radiation transmitted through windows is handle. Overall, the monthly loads are within 5%.

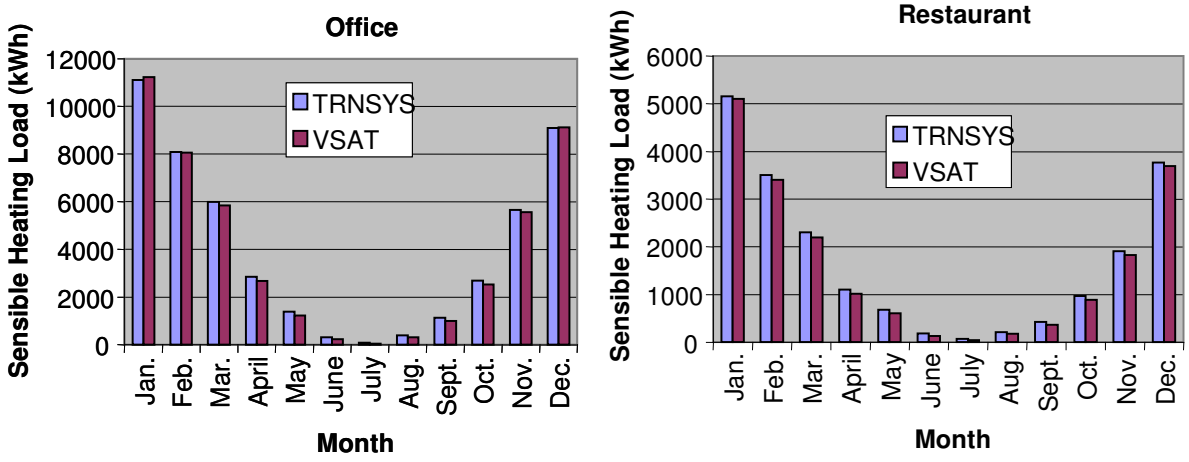

Figure 8. Monthly zone heating loads for constant setpoints (Madison, WI)

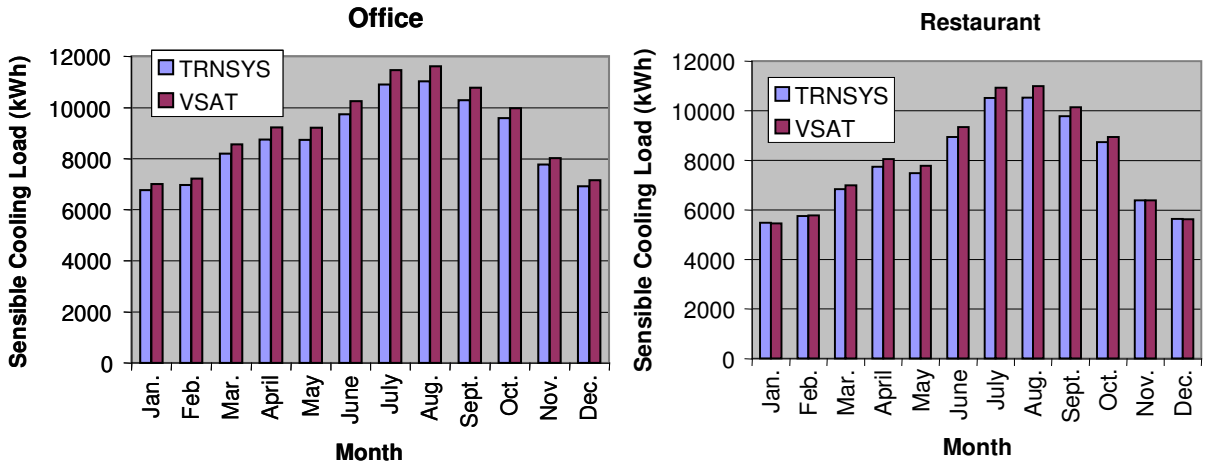

Figure 9. Monthly zone sensible cooling loads for constant setpoints (San Diego, CA)

2.3.4 Results for Night Setback/ Setup Control

The use of a night setback/setup thermostat results in significant dynamics at the start of the occupied period that are not encountered with constant setpoints. Results were generated using both the TYPE 56 and VSAT with night setup for cooling and night setback for heating. For cooling, the occupied period setpoint temperature was 75°F (23.89°C) and the unoccupied setpoint (night setup) temperature was 85°F (29.44°C). For heating, the occupied setpoint was 70°F (21.11°C) and the unoccupied setpoint (night setback) temperature was 60°F (15.56°C). Figure 10 shows sample hourly heat requirements and hourly average zone temperatures for the office in Madison. For both models, there is a large "spike" in the heating requirements when the setpoint returns to the occupied value at 7 am (one hour prior to occupancy). However, the spike is much larger for VSAT than for TRNSYS. This difference is due to differences in the way that zone temperature setpoint adjustsments are handled in the two models. VSAT models a true step change in the setpoint at 7 am, whereas TRNSYS assumes a linear variation in setpoint over the course of the hour from 7 am to 8 am. This difference is apparent in the zone temperature results in Figure 10. Similar results were obtained for the restaurant.

Figure 11 shows similar results for cooling in Madison. Once again, VSAT exaggerates the effect of return from night setup on the cooling loads because it assumes a pure step change in the temperature. Figure 11 also shows that both TRNSYS and VSAT predict similar floating temperatures during the setup (nighttime) period.

Figure 12 shows monthly heating and sensible cooling loads for the office in Madison with night setback/setup control. VSAT tends to overpredict the integrated loads by about 5%. This is partly due to the overprediction of loads at the onset of the return from night setback/setup.

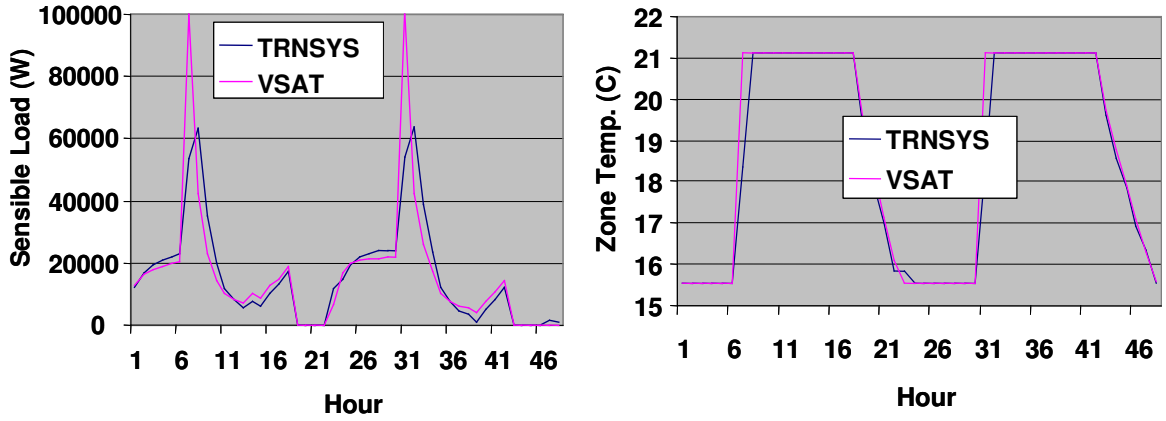

Figure 10. Hourly zone heating loads for the office with night setback (Jan. 9 – 10, Madison, WI)

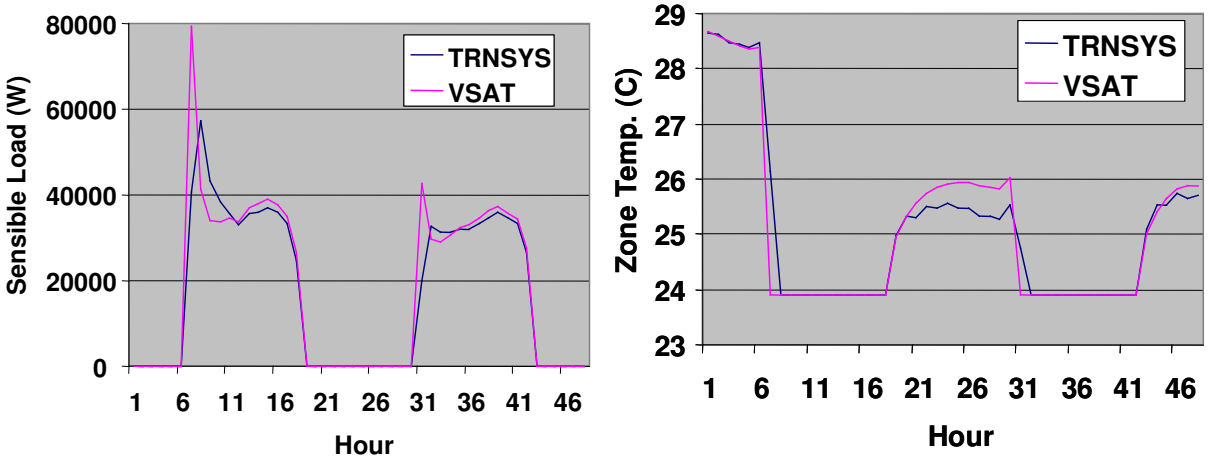

Figure 11. Hourly zone cooling loads for the office with night setup (June 9 – 10, Madison, WI)

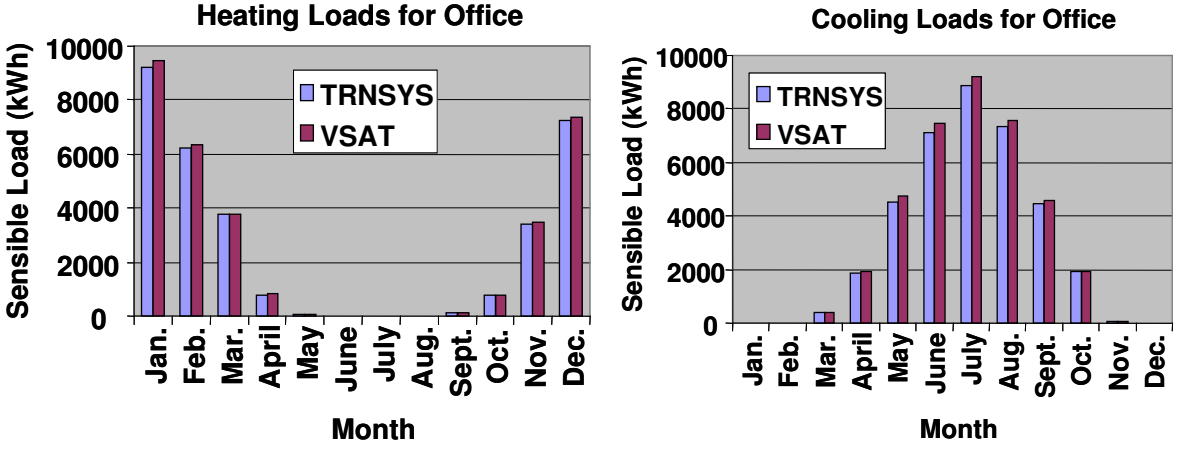

Figure 12. Monthly zone heating and sensible cooling loads for the office with night setup/setup (Madison, WI)

2.3.5 Conclusions

The TYPE 56 building component in TRNSYS is more detailed and accurate in predicting building loads than VSAT. However, for the purposes of comparing different ventilation techniques, this level of detail is not required. Except for return from night setback or setup, VSAT predicts very reasonable transients and overall load levels. Furthermore, VSAT is computationally much more efficient than the TYPE 56, which will facilitate large parametric studies involving many locations and system parameters. The issue of large peak loads at return from night setback or setup will be investigated and VSAT will be modified to predict more reasonable load requirements.

SECTION 3: HEATING AND COOLING EQUIPMENT MODELS

The primary cooling and heating are provided by unitary equipment incorporating a vapor compression air conditioner, a gas or electric heater, and a supply fan. In addition, rotary air-to-air enthalpy exchangers or heat pump heat recovery units can be used to reduce ventilation loads for the primary equipment. Figure 13 depicts a rooftop unit in combination with a heat pump heat recovery unit operating in cooling mode. Ventilation air is cooled and dehumidified by the heat recovery unit prior to mixing with return air from the zone. The mixed air is further cooled and dehumidified (when necessary) by the primary evaporator of the rooftop unit. Heat is rejected to the building exhaust air from the condenser of the recovery unit. The heat pump contains an exhaust fan. In addition, an optional supply fan is used if necessary to provide the proper ventilation air.

In heating mode, refrigerant flow within the heat pump is changed so that the exhaust air stream is cooled (the condenser becomes an evaporator) and heat is rejected to the ventilation air (the evaporator becomes a condenser). The preheated air is then mixed with return air. Although not shown in Figure 13, a gas or electric heater is located after the evaporator to provide additional heating of the supply air when necessary.

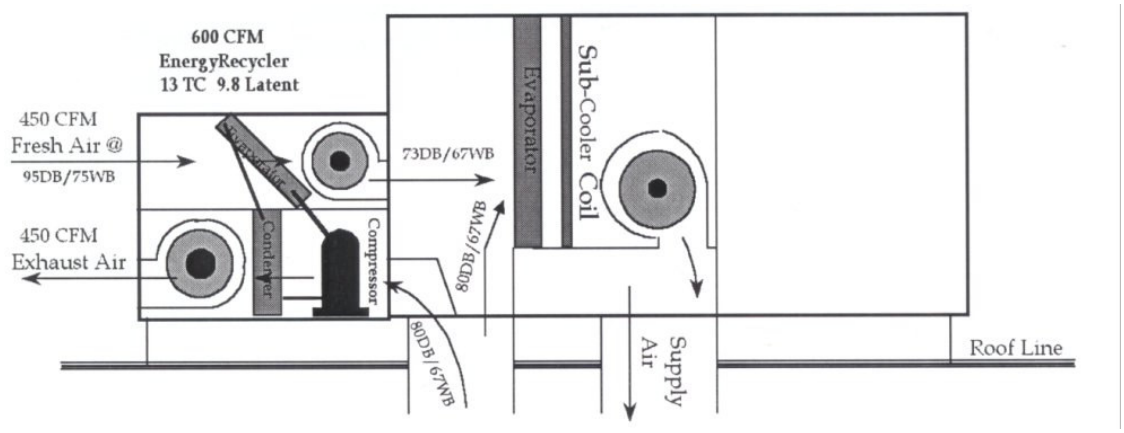

Figure 13. Rooftop air conditioner with heat pump heat recovery unit (cooling mode)

An alternative to heat pump heat recovery is an enthalpy exchanger. Figure 14 depicts a rotary air-to-air enthalpy exchanger considered in VSAT. The device consists of a revolving cylinder filled with an air-permeable medium having a large internal surface area that incorporates a desiccant material. Adjacent supply and exhaust air streams each flow through the exchanger in a counter-flow direction. Sensible heat is transferred as the wheel acquires heat from the hot air stream and releases it to the cold air stream. Moisture is adsorbed from the high humidity air stream to the desiccant material and desorbed into the low humidity air stream. In cooling mode, warm and moist ventilation air is cooled and dehumidified and exhaust air is warmed and humidified. In heating mode, cool and dry air is heated and humidified and exhaust air is cooled and dehumidified.

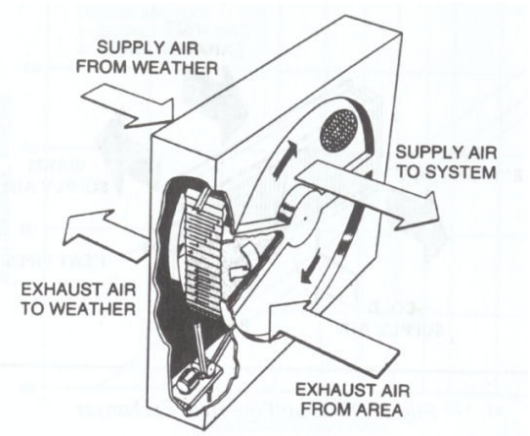

Figure 14. Rotary air-to-air enthalpy exchanger

This section describes the models used for the primary cooling, heating, and heat recovery equipment. Different efficiency equipment can be specified, since this may affect the economics of alternative ventilation strategies. Control strategies for this equipment, along with the description of ventilation control strategies are given in Section 4.

3.1 Vapor Compression System Modeling

Both the primary air conditioning and heat pump heat recovery units utilize a basic vapor compression cycle consisting of a compressor, evaporator coil, expansion valve and condenser coil. Both of these devices are modeled using an approach similar to that incorporated in ASHRAE's *HVAC Toolkit* (Brandemuehl et al., 1993). The model for the primary air conditioner utilizes prototypical performance characteristics, which are scaled according to the capacity requirements and efficiency at design conditions. The characteristics of the heat pump heat recovery unit are based upon measurements obtained from the manufacturer and from tests conducted at the Herrick Labs, which are also scaled for different applications.

3.1.1 Mathematical Description

Steady-State Capacity and COP

The total capacity (cooling or heating), $\dot{Q}_{cap}$, and coefficient of performance, COP, are calculated by applying correction factors to values specified at rating conditions. The correction factors include the effects of air temperature entering the condenser ($T_{c,i}$), evaporator entering wet bulb temperature ($T_{e,wb,i}$) or dry bulb temperature ($T_{e,i}$) and air flow rate ($\dot{m}$). For the case where moisture is removed from the air flowing over the evaporator, the capacity and COP are calculated using the following relations

$$\dot{Q}_{cap} = \dot{Q}_{cap,rat} \cdot f_{cap,t}(T_{e,wb,i}, T_{c,i}) \cdot f_{cap,m}(\dot{m}/\dot{m}_{rat}) \tag{3.1}$$

$$\frac{1}{COP_{cap}} = \frac{1}{COP_{rat}} \cdot f_{COP,t}(T_{e,wb,i}, T_{c,i}) \cdot f_{COP,m}(\dot{m}/\dot{m}_{rat}) \tag{3.2}$$

where $\dot{Q}_{cap}$ and COP_{cap} are the capacity and COP for the unit in steady state with the current operating conditions, $\dot{Q}_{cap,rat}$ and COP_{rat} are the capacity and COP at specified rating conditions, $f_{cap,t}$ is the capacity correction factor based on temperature, $f_{cap,m}$ is the capacity correction factor based on air mass flowrate, $f_{COP,t}$ is the COP correction factor based on temperature, and $f_{COP,m}$ is the COP correction factor based on air mass flowrate. The COP is defined as the ratio of the cooling or heating capacity to the power input. For the primary cooling equipment, the power includes both the compressor and condenser fan, but not the evaporator fan. For the heat pump heat recovery unit, the power includes only the compressor. For either type of equipment, the capacity (cooling or heating) does not include the effect of the supply air fan.

For the primary cooling equipment, the inlet wet bulb temperature to the evaporator is associated with the mixed air condition (mixture of outside and return air) and the inlet condenser temperature is the dry bulb ambient temperature (T_a). The air mass flow rate used within the correlations is the flow rate over the evaporator coil. The air flow rate for the condenser is assumed to be the value at the rating condition.

For the heat pump heat recovery unit, the air flow rate used within the correlations is the ventilation flow rate, which is assumed to be equal for the evaporator and condenser (ventilation and exhaust streams considered to have equal flow rates). For the heat pump recovery unit operating in a cooling mode, the inlet wet bulb to the evaporator is the ambient wet bulb temperature (T_{wb}) and the inlet condenser temperature is the return air temperature from the zone (T_z). During heating mode for the heat pump heat recovery unit, the inlet condenser air temperature is the ambient dry bulb temperature and the inlet condition to the evaporator is the state of air returning from the zone. Since the room air is relatively cool and dry, moisture is not generally condensed as the exhaust air flows over the heat pump evaporator. Therefore, the return air dry bulb temperature (T_z) is used in place of the wet bulb temperature for this case.

The correction factors are based upon correlations of the following form.

$$f_{cap,t}(T_{e,wb,i},T_{c,i}) = a_1 + b_1 \cdot T_{e,wb,i} + c_1 \cdot T_{e,wb,i}^2 + d_1 \cdot T_{c,i} + e_1 \cdot T_{c,i}^2 + f_1 \cdot T_{e,wb,i} \cdot T_{c,i} \tag{3.3}$$

$$f_{COP,t}(T_{e,wb,i},T_{c,i}) = a_2 + b_2 \cdot T_{e,wb,i} + c_2 \cdot T_{e,wb,i}^2 + d_2 \cdot T_{c,i} + e_2 \cdot T_{c,i}^2 + f_2 \cdot T_{e,wb,i} \cdot T_{c,i} \tag{3.4}$$

$$f_{cap,m}(\dot{m}/\dot{m}_{rat}) = a_3 + (\dot{m}/\dot{m}_{rat}) \cdot (b_3 + (\dot{m}/\dot{m}_{rat}) \cdot (c_3 + d_3(\dot{m}/\dot{m}_{rat}))) \tag{3.5}$$

$$f_{COP,m}(\dot{m}/\dot{m}_{rat}) = a_4 + (\dot{m}/\dot{m}_{rat}) \cdot (b_4 + (\dot{m}/\dot{m}_{rat}) \cdot (c_4 + d_4(\dot{m}/\dot{m}_{rat}))) \tag{3.6}$$

Different coefficients are used in equations 3.3 – 3.6 for three different cases: 1) primary cooling unit, 2) heat pump heat recovery operating in a cooling mode, and 3) heat pump heat recovery operating in heating mode. For the primary cooling, the coefficients are from the DOE 2.1E building simulation program. For the heat pump heat recovery unit, the coefficients were determined using performance data as described in a later section.

For cooling, the evaporator inlet air is not always humid enough to result in moisture condensation. In this case, unit performance depends upon inlet evaporator dry bulb rather than wet bulb temperature. However, the correlations developed in terms of wet bulb should

provide accurate predictions as long as the correct inlet dry bulb is used and the inlet humidity is set to a value where condensation just begins. This point represents the end of the range where the correlations apply (i.e., the correlation should apply at the point dehumidification begins to occur). Performance is independent of humidity for lower values. Therefore, if the moisture condensation is found not to occur (see section on sensible heat ratio), then the inlet humidity ratio is adjusted until the point where moisture condensation just beings (sensible heat ratio of one). The air inlet wet bulb temperature associated with the actual dry bulb temperature and this fictitious humidity is then used as the evaporator inlet condition for the capacity and COP correlations.

Sensible Heat Ratio

The model for cooling capacity allows determination of the leaving enthalpy using an energy balance, but not the leaving temperature or humidity. A model for moisture removal is utilized that incorporates the concept of a bypass factor (*BF*). The bypass factor approach considers two different air streams flowing across the evaporator. One air stream is in close proximity to the coil surface and exits the evaporator as saturated air at the effective temperature of the coil surface and the other air stream is away from the coil and assumed to remain at the entering air condition. Since the air close to the coil is allowed to come into equilibrium with the effective surface temperature at a saturated condition, then the effective surface temperature must be the dewpoint of inlet air. As a result, it is termed the apparatus dewpoint temperature, T_{adp}.

Mass and energy balances on both air streams give the following

$$\dot{m} = \dot{m}_{app} + \dot{m}_{byp} \tag{3.7}$$

$$\dot{m}\omega_{e,o} = \dot{m}_{app}\omega_{adp} + \dot{m}_{byp}\omega_{e,i} \tag{3.8}$$

$$\dot{m}h_{e,o} = \dot{m}_{app}h_{adp} + \dot{m}_{byp}h_{e,i} \tag{3.9}$$

where $\dot{m}$ is the total air mass flow rate, $\dot{m}_{app}$ is the air mass flow rate near the coil, $\dot{m}_{byp}$ is the air mass flow rate away from the coil (bypass), $h_{e,i}$ and $h_{e,o}$ are the evaporator inlet and outlet air enthalpy, and $\omega_{e,i}$ and $\omega_{e,o}$ are the evaporator inlet and outlet humidity ratio.

The bypass factor is defined as the ratio of the bypass flow to the total flow. With this definition and equations 3.7 – 3.9, the bypass factor can be related to the operating conditions according to

$$BF = \frac{\dot{m}_{byp}}{\dot{m}} = \frac{h_{e,o} - h_{adp}}{h_{e,i} - h_{adp}} = \frac{\omega_{e,o} - \omega_{adp}}{\omega_{e,i} - \omega_{adp}} \tag{3.10}$$

For a given bypass factor (*BF*), equation 3.10 indicates that on a psychrometric chart the outlet air state (h_{eo}, ω_{eo}) is on a straight line that connects the inlet state with the apparatus dewpoint. This is depicted in Figure 15. The larger the bypass factor the closer the outlet state is to the inlet state.

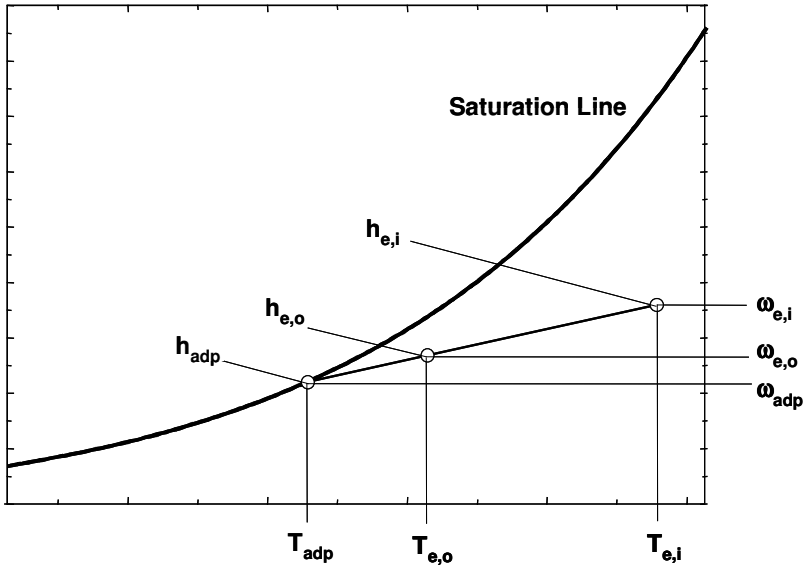

Figure 15. Psychrometric depiction of evaporator air process

The bypass factor can be determined from the heat transfer characteristics of a specific evaporator coil. The bypass factor is estimated from

$$BF = e^{-NTU} \tag{3.11}$$

$$NTU = \frac{UA}{\dot{m} \cdot C_{pm}} \approx \frac{NTU_{rated}}{(\dot{m}/\dot{m}_{rated})} \tag{3.12}$$

and where NTU is the number of transfer units, UA is the air-side conductance of the evaporator coil, C_{pm} *is the* specific heat of moist air, and NTU_{rated} is the value of NTU at the rated flow rate. The right-hand form of equation 3.12 employs the assumption that the conductance does not change with air flow rate. NTU_{rated} can be determined from rated performance since the bypass factor can be determined from entering and leaving conditions. Then, the bypass factor is estimated as a function of air flow using equations 3.11 and 3.12.

The outlet air enthalpy for the evaporator operating at steady state is first determined using an energy balance with the known entering enthalpy and the cooling capacity determined as described in the previous section. For a given bypass factor and inlet and outlet enthalpy, the saturated air enthalpy corresponding to the apparatus dewpoint is determined from equation 3.10 as

$$h_{adp} = h_{e,i} - \frac{h_{e,i} - h_{e,o}}{1 - BF} \tag{3.13}$$

The apparatus dewpoint temperature and saturated humidity ratio are determined using psychrometric relationships for a relative humidity of 100% and an air enthalpy of h_{adp}. Then,

the outlet air humidity ratio is determined from equation 3.10 as

$$\omega_{e,o} = BF \cdot \omega_{e,i} + (1 - BF) \cdot \omega_{adp} \tag{3.14}$$

Since the outlet state lies on the locus of point connecting the inlet and apparatus dewpoint conditions (see Figure 15), the sensible heat ratio (*SHR*) can be determined as

$$SHR = \frac{h(T_{e,i}, \omega_{adp}) - h_{adp}}{h_{e,i} - h_{adp}} \tag{3.15}$$

where *SHR* is the ratio of the sensible cooling capacity to the total cooling capacity.

If the calculated value of *SHR* is greater then unity, then moisture condensation does not occur and *SHR* is unity. In this case, the inlet humidity ratio is adjusted until the point where *SHR* = 1. The air inlet wet bulb temperature associated with the actual dry bulb temperature and this fictitious humidity is then used as the evaporator inlet condition for the capacity and COP correlations given in the previous section.

Compressor Power Consumption

When there is a cooling requirement for the primary equipment, the compressor(s) and condenser fan(s) cycle on and off to maintain the zone temperature at the cooling setpoint. VSAT utilizes one-hour timesteps and yet the equipment must generally cycle on and off at smaller time intervals. The fraction of the hour that the equipment must operate in order to meet the load is assumed to be equal to the part-load ratio (*PLR*), which is the ratio of the average hourly equipment cooling requirement ($\dot{Q}_c$) to the steady-state capacity ($\dot{Q}_{cap}$) of the equipment or

$$PLR = \frac{\dot{Q}_c}{\dot{Q}_{cap}} \tag{3.16}$$

There are energy losses associated with cycling primarily due to the loss of the pressure differential between the condenser and evaporator when the unit shuts down. The compressor must re-establish the steady-state evaporator and condenser pressures to achieve the steady-state capacity whenever the unit turns on. These pressures equilibrate very quickly after the unit is shut down. The effect of cycling on power consumption is considered through the use of a part-load factor (*PLF*). For any given hour, the average power consumption of the compressor and condenser fan are calculated as

$$\dot{W}_c = PLF \cdot \frac{\dot{Q}_{cap}}{COP_{cap}} \tag{3.17}$$

where *PLF* is ratio of the average power to the full-load power consumption. *PLF* is determined in terms of *PLR* using the following correlation from DOE 2.1E.

$$PLF = a_5 + PLR \cdot (b_5 + PLR \cdot (c_5 + d_5 \cdot PLR)) \quad (3.18)$$

For the heat pump heat recycler, both the ventilation (optional) and exhaust fans operate continuously during the occupied period and do not cycle with the compressor. As a result, the correlations presented for COP_{cap} only include the compressor. For this equipment, the compressor power is determined with equation 3.17.

3.1.2 Prototypical Rooftop Air Conditioner Characteristics

The correlations for the primary rooftop cooling equipment were taken from DOE 2.1E. In VSAT, the rated cooling capacity in equation 3.1 is determined based upon the peak cooling requirements associated with the building, ventilation system, and location (see sizing section). The rated flow rate is 450 cfm/ton. The user can choose between three different rated COPs corresponding to EERs of 8, 10, 12. The default is an EER of 12. The actual evaporator air flow rate when the unit is operating can be set by the user, but the default is 350 cfm/ton.

Figure 16 shows the variation in the temperature-dependent capacity and COP correction factors as a function of condenser air inlet temperature and evaporator air inlet wet bulb temperature for the prototypical rooftop air conditioner. The values were determined with equations 3.3 and 3.4 using the coefficients given in Table 9. The cooling capacity and COP vary by about a factor of two over the range of interest. The maximum capacity and COP (minimum $f_{COP,t}$) occur at a low condenser inlet temperature and high evaporator inlet wet bulb temperature.

Figure 17 shows the mass flow rate-dependent capacity and COP correction factors as a function of the ratio of the supply air flow rate to the rated flow rate. The values were determined with equations 3.5 and 3.6 using the coefficients given in Table 10. Over the range of interest, the impact of supply air flow on COP is relatively small. The COP decreases by only about 5% when the flow is 50% of the design flow. The sensitivity of cooling capacity to changes in flow rate is greater than for COP and the effect becomes more important at low flow rates.

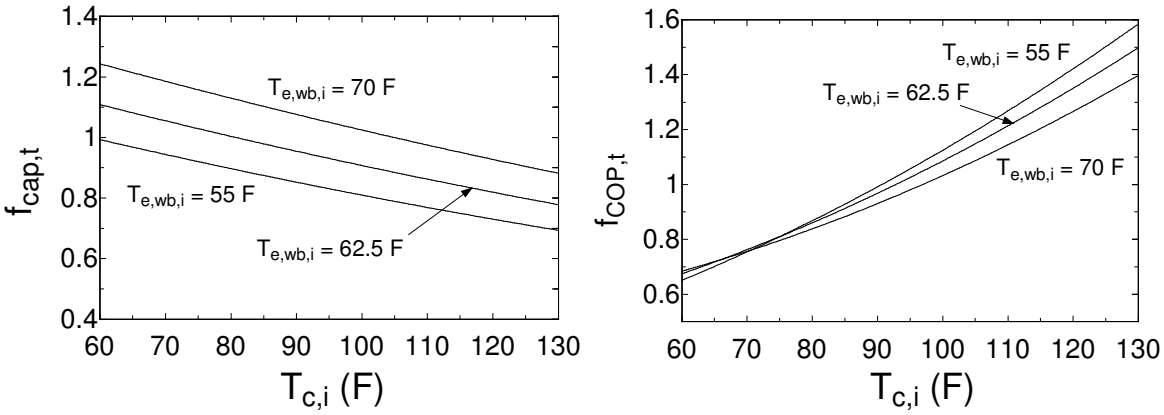

Figure 16. Temperature-dependent capacity and COP correction factors for prototypical rooftop air conditioner

Table 9: Coefficients of temperature-dependent capacity and COP correction factor correlations for the prototypical rooftop air conditioner

Coefficient	Value	Units
a_1	0.8740302	-
b_1	-0.0011416	F^{-1}
c_1	0.0001711	F^{-2}
d_1	-0.0029570	F^{-1}
e_1	0.0000102	F^{-2}
f_1	-0.0000592	F^{-2}
a_2	-1.0639310	-
b_2	0.0306584	F^{-1}
c_2	-0.0001269	F^{-2}
d_2	0.0154213	F^{-1}
e_2	0.0000497	F^{-2}
f_2	-0.0002096	F^{-2}

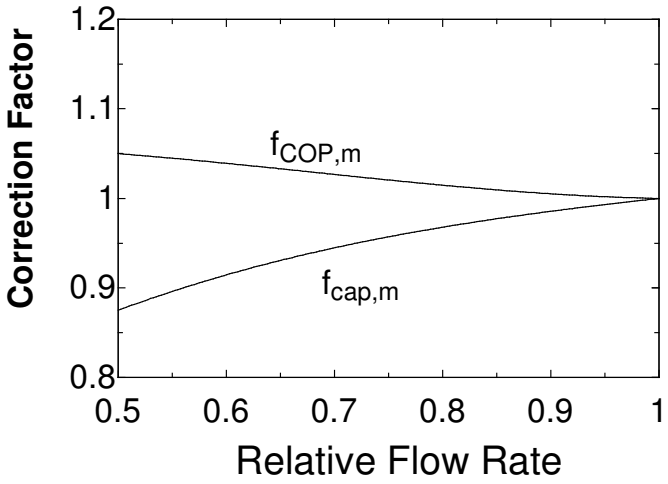

Figure 17. Flow rate-dependent capacity and COP correction factors for prototypical rooftop air conditioner

Table 10: Coefficients of mass flow rate-dependent capacity and COP correction factor correlations for the prototypical rooftop air conditioner

Coefficient	Value
a_3	0.4727859
b_3	1.2433414
c_3	-1.0387055
d_3	0.3225781
a_4	1.0079484
b_4	0.3454413
c_4	-0.6922891
d_4	0.3388994

Figure 18 shows *PLF* as a function of *PLR* determined using the correlation of equation

3.18 with coefficients given in Table 11. Also shown in this plot is a line for constant COP (*PLF* = *PLR*). The impact of cycling on power consumption is relatively small for part-load ratios greater than about 30%. The deviation from constant COP becomes very significant below a *PLR* of 0.2.

Table 11: Coefficients of part-load factor correlations

Coefficient	Value
a_5	0.2012301
b_5	-0.0312175
c_5	1.9504979
d_5	-1.1205105

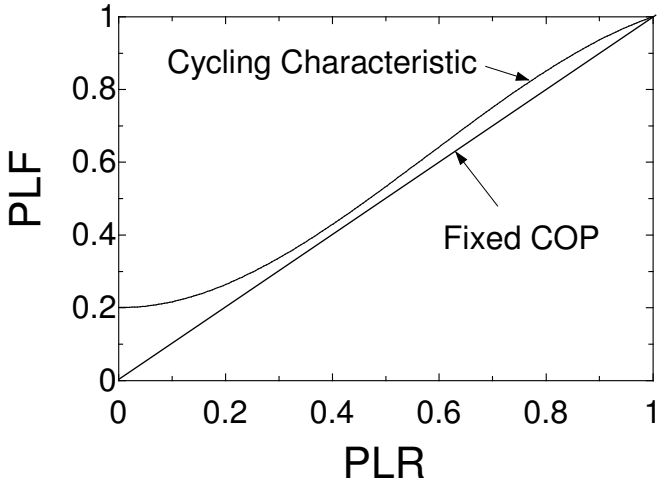

Figure 18. Part-load factor correlation

The user can specify a sensible heat ratio (*SHR*) at the rating condition. This value is used along with the rated flow rate per unit cooling capacity (cfm/ton) and the rated operating conditions to determine the rated bypass factor (*BF*) and *NTU*. The bypass factor is then corrected for the actual flow rate using equations 3.11 and 3.12. Standard ARI rating conditions are assumed: condenser inlet temperature of 95 F, evaporator inlet temperature of 80 F, and evaporator inlet wet bulb temperature of 67 F. The default value for the rated *SHR* is 0.75. For the prototypical unit with these specifications, the rated bypass factor is 0.261 and the rated *NTU* is 1.35.

3.1.3 Heat Pump Heat Recovery Unit (Energy Recycler®)

The heat pump heat recovery unit is modeled using a very similar approach as for the primary air conditioner except that equation 3.2 is replaced with

$$COP_{cap} = COP_{rat} \cdot f_{COP,t}(T_{e,wb,i}, T_{c,i}) \cdot f_{COP,m}(\dot{m} / \dot{m}_{rat}) \tag{3.19}$$

This form resulted in better correlation of data. Coefficients of equations 3.3 - 3.6 were determined using manufacturer's data and tests conducted at the Herrick Labs. The laboratory tests provided data beyond the range available from the manufacturer. The rating conditions for the heat pump were taken from suggested rating points given in the manufacturer's data for both cooling and heating modes (Carrier, 1999).

Cooling Mode

For the unit considered, the rated air supply flow rate for cooling mode is 533 cfm/ton (1000 cfm rated supply air divided by 22.5 MBtu/hr gross cooling capacity). Rated air conditions are 75°F condenser air inlet dry bulb temperature, 95°F evaporator air inlet dry bulb temperature and 75°F evaporator air inlet wet bulb temperature. For the unit tested at this rating point, the total capacity is 22.5 MBtu/hr, COP is 4.515 and SHR is 0.902. The Energy Recycler is not available at different EERs, thus only one performance characteristic is available for analysis. The coil heat transfer units (NTUs) parameter at the rated condition is 1.08 and the rated bypass factor is 0.34.

Figure 19 shows the variation of temperature dependent correction factors for total cooling capacity and COP as a function of condenser air inlet temperature and evaporator air inlet wet bulb temperature. The correction factors were determined from equations 3.3 and 3.4 using the coefficients in Table 12.

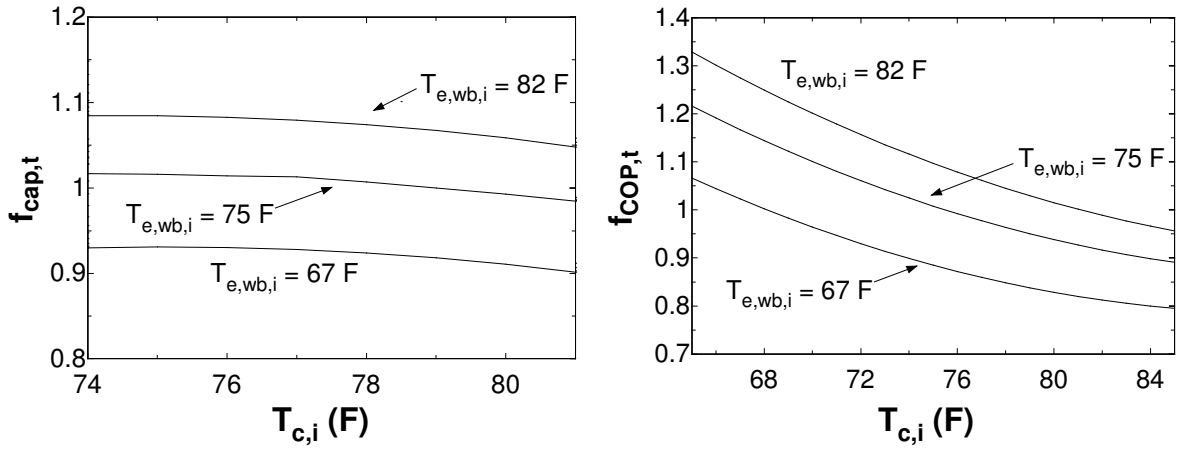

Figure 19. Temperature-dependent capacity and COP correction factors for heat pump heat recovery unit – cooling mode

Table 12: Coefficients of temperature-dependent capacity and COP correction factor correlations for the heat pump heat recovery unit – cooling mode

Coefficient	Value	Units
a_1	-6.758	-
b_1	0.0946	F^{-1}
c_1	-0.000223	F^{-2}
d_1	0.09721	F^{-1}
e_1	-0.0003967	F^{-2}
f_1	-0.0005549	F^{-2}
a_2	0.8402	-
b_2	0.06599	F^{-1}
c_2	-0.0001786	F^{-2}
d_2	-0.0592	F^{-1}
e_2	0.0004547	F^{-2}
f_2	-0.0003368	F^{-2}

Figure 20 shows the variation of mass dependent correction factors for total cooling capacity and COP as a function of the flow rate relative to the rated flow rate. The correction factors were determined from equations 3.5 and 3.6 using the coefficients in Table 13. The impact of flow rate on performance is much more significant than for the primary air conditioner because both condenser and evaporator flow rate change (not just evaporator flow rate).

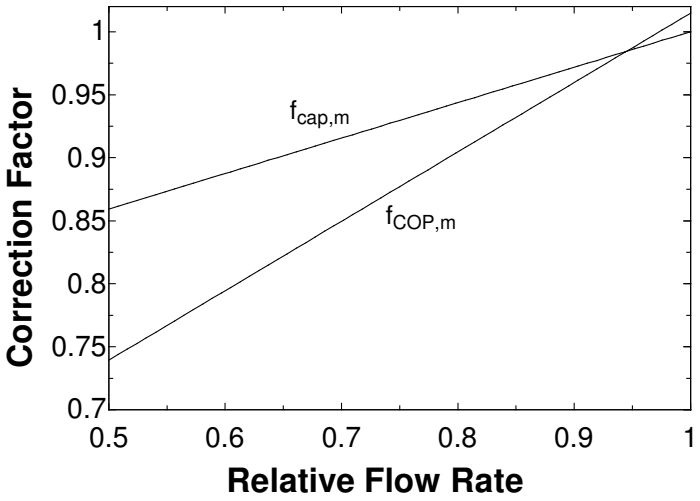

Figure 20. Flow rate-dependent capacity and COP correction factors for heat pump heat recovery unit – cooling mode

Table 13: Coefficients of mass flow rate-dependent capacity and COP correction factor correlations for heat pump heat recovery unit – cooling mode

Coefficient	Value
a_3	0.7187
b_3	0.2813
c_3	0.0
d_3	0.0
a_4	0.4639
b_4	0.5509
c_4	0.0
d_4	0.0

Heating Mode

For the unit considered, the rated air supply flow rate for heating mode is 540 cfm/ton (1000 cfm rated supply air divided by 22.2 MBtu/hr gross heating capacity). Rated air conditions are 70°F evaporator air inlet temperature and 33°F condenser air inlet temperature. The total capacity is 22.2 MBtu/hr and COP is 7.425 at this rating point.

Figure 21 shows the variation of the temperature dependent correction factors for total heating capacity and COP as a function of evaporator (return) air inlet temperature and condenser air inlet temperature. The correction factors were determined from equations 3.3 and 3.4 using the coefficients in Table 14. Total heating capacity and COP increase as the evaporator inlet temperature increases and condenser inlet temperature decreases. The maximum capacity for heating is thus experienced at higher air evaporating temperatures and lower condenser inlet temperatures.

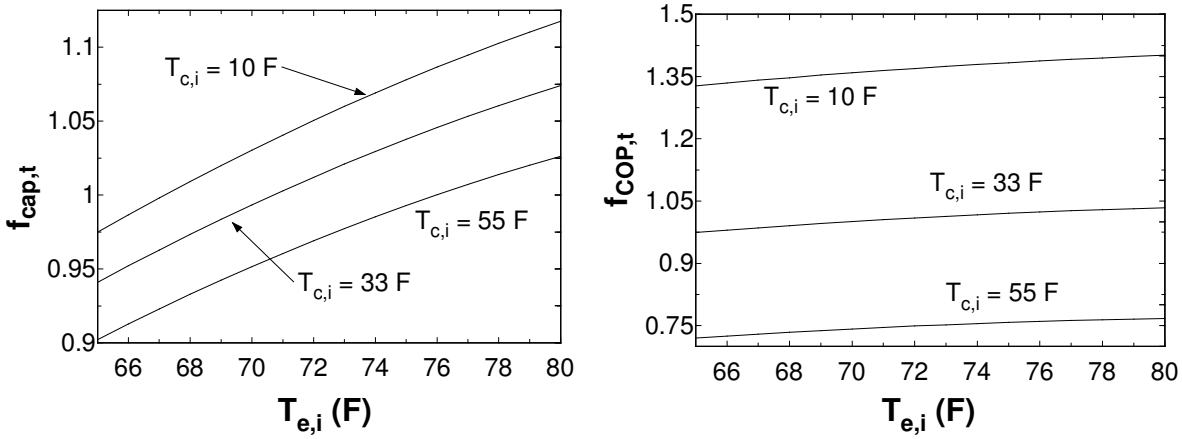

Figure 21. Temperature-dependent capacity and COP correction factors for heat pump heat recovery unit – heating mode

Table 14: Coefficients of temperature-dependent capacity and COP correction factor correlations for the heat pump heat recovery unit – heating mode

Coefficient	Value	Units
a_1	-0.4831	-
b_1	0.0006157	F^{-1}
c_1	-0.000006376	F^{-2}
d_1	0.03305	F^{-1}
e_1	-0.0001604	F^{-2}
f_1	-0.0000279	F^{-2}
a_2	0.4873	-
b_2	-0.01648	F^{-1}
c_2	0.00008504	F^{-2}
d_2	0.02423	F^{-1}
e_2	-0.0001307	F^{-2}
f_2	-0.00003938	F^{-2}

Figure 22 shows the variation of mass dependent correction factors for total heating capacity and COP as a function of the relative flow rate. The correction factors were determined from equations 3.5 and 3.6 using the Energy Recycler coefficients in Table 15.

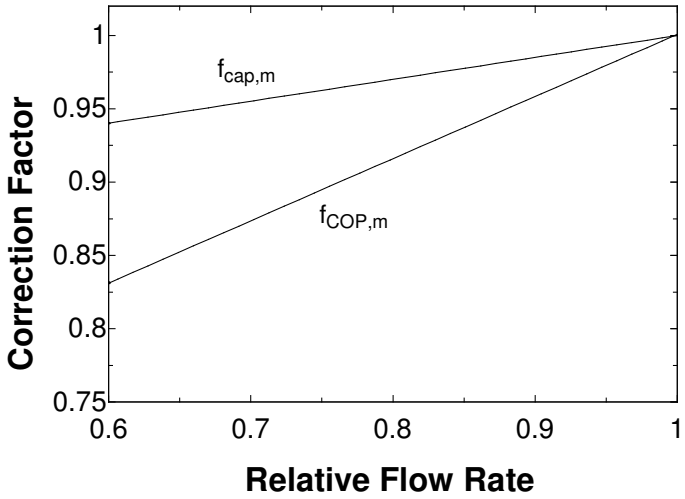

Figure 22. Flow rate-dependent capacity and COP correction factors for heat pump heat recovery unit – heating mode

Table 15: Coefficients of mass flow rate-dependent capacity and COP correction factor correlations for heat pump heat recovery unit – heating mode

Coefficient	Value
a_3	0.8505
b_3	.1495
c_3	0.0
d_3	0.0
a_4	0.5768
b_4	0.424
c_4	0.0
d_4	0.0

3.2 Primary Heater

The primary heater incorporated within the rooftop unit can be either gas or electric. For electric heat, the power consumption at any time is assumed to be equal to the heating requirement for any hour. For a gas heater, gas costs are based upon the primary fuel energy consumption integrated over the billing period (therms). For any time, the rate of primary fuel energy consumption is calculated as

$$\dot{Q}_F = \frac{\dot{Q}_h}{\eta_F} \tag{3.20}$$

where $\dot{Q}_h$ is the heating requirement for the heating and η_f is the heater efficiency. The efficiency is assumed to be constant. The user can choose between three different efficiencies of 0.65, 0.80, and 0.95. The default efficiency is 0.95

3.3 Enthalpy Exchanger

3.3.1 Mathematical Description

The model for enthalpy exchangers that is incorporated within VSAT was developed by Stiesch et al. (1995) and Klein et al. (1990). Both of these studies incorporate the use of temperature, humidity, and enthalpy effectiveness defined as

$$\varepsilon_T = \frac{T_v - T_a}{T_z - T_a} \tag{3.21}$$

$$\varepsilon_\omega = \frac{\omega_v - \omega_a}{\omega_z - \omega_a} \tag{3.22}$$

$$\varepsilon_h = \frac{h_v - h_a}{h_z - h_a} \tag{3.23}$$

where ε is effectiveness, T is temperature, ω is humidity ratio, h is enthalpy, and the subscripts a, v, and z refer to conditions associated with the ambient air, ventilation air leaving the enthalpy exchanger, and return air from the zone, respectively.

For known values of effectiveness, equations 3.21 – 3.23 are used to estimate ventilation stream conditions in terms of ambient and zone air conditions. As the effectiveness values go to one, the ventilation temperature, humidity, and enthalpy approach the conditions of the return air. In general, the effectiveness increases as the speed of the wheel increases for given air flow rates.

Klein et al. (1990) used detailed numerical studies and found that for balanced flow rates, a Lewis number of one, and at high rotation speeds, the temperature, humidity, and enthalpy effectiveness for enthalpy exchangers are equal and can be estimated in terms of the number of transfer units as

$$\varepsilon_T = \varepsilon_\omega = \varepsilon_h = \frac{NTU}{NTU + 2} \tag{3.24}$$

where NTU is defined as

$$NTU = \frac{hA_s}{\dot{m}_{vent} C_{pm}} \tag{3.25}$$

and h is the heat transfer coefficient and A_s is the total surface area of the exchanger.

Stiesch et al. (1995) correlated temperature and enthalpy effectiveness as a function of rotation speeds, where the results were generated from detailed simulations. The correlations are of the form

$$\varepsilon_T = \frac{NTU}{NTU + 2} \cdot (1 - \exp[a_T \cdot \Gamma^2 + b_T \cdot \Gamma]) \tag{3.26}$$

$$\varepsilon_h = \frac{NTU}{NTU + 2} \cdot (1 - \exp[a_h \cdot \Gamma^3 + b_h \cdot \Gamma^2 + c_h \cdot \Gamma]) \tag{3.27}$$

where the *a, b,* and *c* coefficients are empirical factors that depend upon ambient temperature and Γ is a dimensionless rotation speed defined as

$$\Gamma = \frac{M_m / \dot{m}_{vent}}{t_r} \tag{3.28}$$

and where t_r is the time required for one exchanger rotation, M_m is the mass of the dry matrix, and $\dot{m}_{vent}$ is the ventilation flow rate.

Equations 3.26 and 3.27 tend to approach the limiting case result of equation 3.24 for dimensionless rotation speeds greater than about 3. Well-designed enthalpy exchangers would tend to operate at higher speeds. However, it may be necessary to operate at lower

speeds to maintain a fixed ventilation supply air temperature under feedback control conditions.

Feedback control of the wheel speed is initiated under two situations: 1) the ambient air temperature is below 55 F and the ventilation stream outlet air temperature rises above 55 F or 2) the exhaust stream outlet air temperature falls below a freeze setpoint. The control logic incorporated in VSAT is based upon typical practice (Semco, 2002).

If the ambient temperature is below 55 F and the ventilation stream outlet air temperature falls would rise above 55 F (at full speed), then the wheel speed is modulated below the maximum speed to maintain an outlet temperature of 55 F. This limits preheating of the ventilation stream under conditions where cooling may be required. The temperature effectiveness necessary to achieve this condition is calculated as

$$\varepsilon_{T,vent,sp} = \frac{T_{vent,sp} - T_a}{T_z - T_a} \tag{3.29}$$

where $T_{vent,sp}$ is the setpoint temperature (55 F) for the ventilation supply air. Under low ambient conditions, the ventilation temperature is below 55 F and the wheel operates at full speed.

At low ambient temperatures, water vapor removed from the exhaust stream may condense and freeze. Reducing the speed reduces the effectiveness of the enthalpy exchanger and increases the matrix temperature within the exhaust speed. Freeze protection is initiated in VSAT when the exhaust temperature falls below a specified freeze protection limit. In this case, the exhaust temperature is set equal to the freeze protection limit and the temperature effectiveness necessary to achieve this condition is calculated as

$$\varepsilon_{T,freeze} = \frac{T_z - T_{freeze}}{T_z - T_a} \tag{3.30}$$

where T_{freeze} is the freeze protection limit for the exhaust temperature.

For either feedback control case, the dimensionless rotation speed necessary to achieve the required effectiveness given by equation 3.29 or 3.30 is determined from equation 3.26 using the required temperature effectiveness. Then, the ventilation stream enthalpy is evaluated using equations 3.27 and 3.23.

A frost set point is specified based on winter ambient and zone design conditions as discussed by Semco (2002) and Stiesch (1995). Figure 23 depicts the process on a psychrometric chart. Point A1 represents a low ambient temperature condition, whereas points Z1 and Z2 represent zone conditions with high and low humidities, respectively. For an enthalpy exchanger operating at full speed, the ventilation and exhaust air streams follow processes that are approximately on these lines. For process line Z2-A1, the exhaust air process line never crosses the saturation line and therefore moisture would not condense. However, for process line Z1-A1, moisture condenses at point Z1a for a wheel operating at full speed. In this case, the frost setpoint should be set a temperature greater than the temperature at Z1a.

The frost set point is determined by first estimating the point where the enthalpy exchanger process line (e.g., one Z1-A1) crosses the saturation line (e.g., point Z1a) assuming 1) an

ambient condition of 90% relative humidity at the lowest temperature occurring during the year and 2) a zone condition of 35% relative humidity at the heating setpoint. The crossing point is determined numerically and then a 2 C safety factor is added to the result

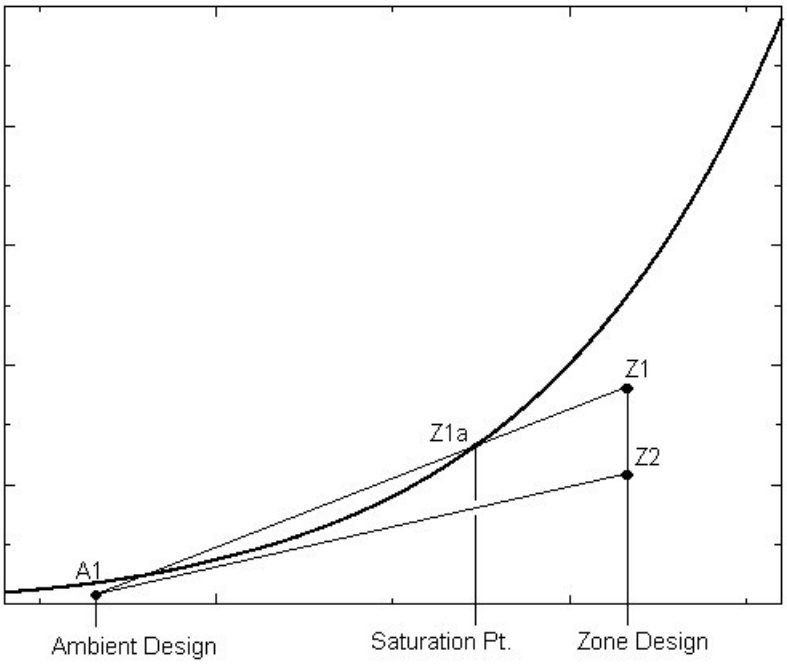

Figure 23. Frost set point determination

.

3.3.2 Prototypical Exchanger Descriptions

The specific correlations developed by Stiesch et al. (1995) were obtained using data from a commercial enthalpy exchanger (Carnes 1989) having a medium constructed of aluminum foil of thickness 0.025 mm coated with a thin, uniform layer of polymer desiccant. The medium has a counter-flow design and is constructed by coiling smooth and corrugated aluminum sheets to produce small triangular air passages. The equivalent hydraulic diameter of the triangular air passages is approximately 1.7 mm and the medium has a length in the direction of flow of 0.2 m. The diameter of the wheel is 1.23 m and the idealized rotational speed is approximately 15 rpm.

The manufacturer gives effectiveness as a function of air face velocity for their designs. At a face velocity of 650 fpm, the effectiveness for heat and mass transfer is about 0.75. From equation 3.24, this results in an NTU of about 6. These values are assumed for the prototypical enthalpy exchanger.

The effectiveness is constant unless the feedback control is initiated as described in the previous subsection. If this occurs, then the empirical factors determined by Stiesch et al. (1995) are used in equations 3.26 and 3.27. These are:

$$a_T = a_{T_1} + \frac{a_{T_2}}{NTU\, a_{T_3}} \tag{3.31}$$

$$b_T = b_{T_1} + \frac{b_{T_2}}{NTU^{b_{T_3}}} \tag{3.32}$$

$$a_h = a_{h_1} + a_{h_2} \cdot NTU + a_{h_3} \cdot NTU^2 \tag{3.33}$$

$$b_h = b_{h_1} + b_{h_2} \cdot NTU + b_{h_3} \cdot NTU^2 \tag{3.34}$$

$$c_h = c_{h_1} + \frac{c_{h_2}}{NTU^{0.8}} \tag{3.35}$$

where

$$a_{T_1} = 0.002259 - 1.376\times10^{-3} \cdot T_a - 6.91\times10^{-6} \cdot T_a^2$$
$$a_{T_2} = 0.09084 - 3.263\times10^{-4} \cdot T_a + 7.4\times10^{-6} \cdot T_a^2$$
$$a_{T_3} = 0.7388 - 0.01994 \cdot T_a - 3.829\times10^{-4} \cdot T_a^2$$
$$b_{T_1} = -1.007 + 0.0093 \cdot T_a + 2.778\times10^{-4} \cdot T_a^2$$
$$b_{T_2} = -1.533 + 0.02287 \cdot T_a - 2.356\times10^{-4} \cdot T_a^2$$
$$b_{T_3} = 1.111 - 2.667\times10^{-3} \cdot T_a - 1.378\times10^{-4} \cdot T_a^2$$
$$a_{h_1} = 3.381\times10^{-3} - 9.679\times10^{-4} \cdot T_a \qquad \text{for } T_a \le 0°C$$
$$a_{h_1} = 3.381\times10^{-3} - 4.127\times10^{-5} \cdot T_a \qquad \text{for } T_a > 0°C$$
$$a_{h_2} = 5.088\times10^{-4} + 4.89\times10^{-6} \cdot T_a$$
$$a_{h_3} = 5.298\times10^{-6} - 7.652\times10^{-7} \cdot T_a$$
$$b_{h_1} = 6.237\times10^{-3} + 8.827\times10^{-3} \cdot T_a - 6.042\times10^{-4} \cdot T_a^2$$
$$b_{h_2} = -0.02133 + 1.323\times10^{-4} \cdot T_a$$
$$b_{h_3} = 4.908\times10^{-4} + 6.46\times10^{-6} \cdot T_a$$
$$c_{h_1} = -0.4087 + 0.00253 \cdot T_a + 3.34\times10^{-4} \cdot T_a^2$$
$$c_{h_2} = -1.449 + 0.02337 \cdot T_a - 5.578\times10^{-4} \cdot T_a^2$$

SECTION 4: AIR DISTRIBUTION SYSTEM AND CONTROLS

The air distribution system includes ducts, fans, dampers, and controls. A supply fan integrated with the primary cooling/heating equipment provides the flow rate to the zone. A return fan is not considered. The ventilation heat pump heat recovery unit utilizes an exhaust fan and an optional ventilation fan. The ventilation fan is only necessary if the required ventilation flow rate cannot be provided using the primary supply fan. During the occupied period, the fan(s) operate(s) continuously and provide a constant flow rate of air to the zone, while the equipment cycles on and off as necessary to maintain the zone temperature setpoint. During the unoccupied period, the fan(s) cycle(s) on and off with the equipment, but the airflow rate is constant when the system is on.

There are separate heating and cooling setpoints for the zone. If the zone temperature falls between these setpoints, then the temperature is "floating" and no heating or cooling is required. If the zone temperature falls below the heating setpoint, then the heating required to maintain the zone at this temperature is calculated as the zone heating load. The total equipment heating load includes an additional load associated with ventilation. If the zone temperature rises above the cooling setpoint, then the cooling required to maintain the zone at this temperature is calculated as the sensible zone cooling load. The total equipment cooling load includes additional loads associated with ventilation and latent gains within the zone.

When installed, the ventilation heat pump heat recovery unit is only enabled during occupied hours. During unoccupied hours, the primary air conditioner and heater must meet the cooling and heating requirements. In addition, the heat pump will only operate in cooling mode when the ambient temperature is above 68 F.

The enthalpy exchanger operates when the primary fan is on and the ambient temperature is less than 55 F or greater than the return air temperature. When the ambient temperature is between 55 F and the return air temperature, it is assumed that a cooling requirement exists and it is better to bring in cooler ambient air. When the ambient temperature is below 55 F, then a feedback controller adjusts the speed to maintain a ventilation supply air temperature of 55 F. When the ambient temperature is above the return air temperature, then wheel operates at maximum speed.

There are four ventilation control strategies considered in VSAT: fixed ventilation, demand-controlled ventilation, economizer, and night ventilation precooling. When a heat recovery heat exchanger or heat pump is employed within the ventilation stream, then fixed ventilation is assumed. Demand-controlled ventilation is considered both with and without an economizer. Night ventilation is considered with and without an economizer and with and without demand-controlled ventilation.

This section describes modeling of the air distribution components and controls and calculation of the equipment heating and cooling loads.

4.1 Ventilation Flow

4.1.1 Fixed Ventilation

In the absence of demand-controlled ventilation and during occupied mode, the minimum ventilation flow rate is a fixed value and is determined using ASHRAE Standard 62-1999 based upon the design occupancy. Table 1 - Table 7 include ventilation requirements and design occupancies for the prototypical buildings considered in VSAT. Note that in many

cases, the average occupancy levels are much lower than the design occupancies used to determine minimum ventilation flow requirements. During unoccupied mode, the minimum ventilation flow is zero and the damper is closed.

4.1.2 Demand-Controlled Ventilation

When demand-controlled ventilation is enabled, a minimum flow rate of ventilation air is determined that will keep the CO_2 concentration in the zone at or below a specified level. The minimum flow rate is calculated assuming a quasi-steady state mass balance on the air within the zone and the ducts, fully-mixed zone air, and a constant ventilation effectiveness that accounts for short-circuiting of ventilation air within the supply to the return duct. With these assumptions, the minimum ventilation flow rate is

$$\dot{m}_{vent,\min} = \min\left(\frac{\dot{C}_{CO_2,gen}}{\eta_v \cdot \left(C_{CO_2,set} - C_{CO_2,amb}\right)}, \dot{m}_{\sup} \right) \tag{4.1}$$

where $\dot{C}_{CO_2,gen}$ is the rate of CO_2 generation within the zone, $C_{CO_2,set}$ is the setpoint for CO_2 concentration in the zone, $C_{CO_2,amb}$ is the ambient CO_2 concentration, and η_v is the ventilation efficiency. The ventilation efficiency is a measure of how effectively the ventilation air removes pollutants from the zone. The default value is 0.85. The user can set values for the zone setpoint and ambient CO_2 concentrations. The default values are 1000 ppm and 350 ppm, respectively.

The CO_2 generation rate is the product of the generation rate per person and the number of occupants at any given time. Table 1 - Table 7 include generation rates per person and default occupancy information for the prototypical buildings considered in VSAT.

4.1.3 Economizer

At any given time, the ventilation flow can be greater than the minimum due to economizer operation. VSAT considers a differential enthalpy economizer. The differential enthalpy economizer is engaged whenever the enthalpy of the ambient air is less than the enthalpy of the air in the return duct and the zone requires cooling.

In economizer mode, the ventilation flow rate is modulated between the minimum and maximum (wide open) values to maintain a specified setpoint for the mixed air temperature supplied to the primary equipment. The default mixed air setpoint is 55 F. During the occupied mode, the economizer will cycle on and off as necessary to maintain the zone temperature setpoint. However, during unoccupied mode, both the economizer and the fan cycle on and off together to maintain the zone temperature. In either case, the average hourly ventilation flow rate when the economizer is enabled is determined as

$$\dot{m}_{vent} = \min\left(\max\left(\dot{m}_{vent,\min}, \dot{m}_{vent,mix}\right), \dot{m}_{vent,z}, \dot{m}_{\sup}\right) \tag{4.2}$$

where $\dot{m}_{vent,mix}$ is the ventilation flow rate necessary to give a mixed air temperature equal to its setpoint and $\dot{m}_{vent,z}$ is the ventilation flow rate that keeps the zone temperature at its setpoint. This logic simulates a perfect economizer controller that requires a call for 1st stage

cooling to enable the economizer (and fan during unoccupied mode) and uses damper modulation to maintain a mixed air temperature setpoint.

With the economizer enabled, the ventilation flow rate necessary to maintain the zone temperature at its setpoint is

$$\dot{m}_{vent,z} = \frac{\dot{Q}_{z,c} + \dot{W}_{fan,s}}{C_{pm}\left(T_{z,c} - T_a\right)} \tag{4.3}$$

where $\dot{Q}_{z,c}$ is the zone sensible cooling load, $T_{z,c}$ is the zone temperature setpoint for cooling, and $\dot{W}_{fan,s}$ is the power associated with the primary supply fan.

4.1.4 Night Ventilation Precooling

Whenever the ambient temperature drops below the zone temperature, the ambient air can be used to precool the zone and reduce cooling loads during the next day. However, the next day savings associated with operating the ventilation system at night should be sufficient to offset the cost of operating the fan. In addition, the ambient humidity should be low enough to avoid increased latent loads during the next day and the ambient temperature should be high enough so as to avoid additional heating requirements after occupancy. With these issues in mind, the rules in Table 16 are employed to enable precooling.

Table 16. Rules for Enabling Ventilation Precooling

Rule	Description
$(T_z - T_a) > \Delta T_{on}$	The ambient temperature (T_a) must be less than the zone temperature (T_z) by a threshold (ΔT_{on}) chosen to balance fan operating costs with next day savings.
$T_a > 50^{\circ}F$	The ambient temperature must be greater than 50 ˚F to avoid conditions where heating might be required the next day.
$T_{a,dp} < 55^{\circ}F$	The ambient dew point ($T_{a,dp}$) must be less than 55 ˚F to avoid conditions where the latent load might increase the next day.
$\Delta t_{occ} < 6$ hours	The time to occupancy (Δt_{occ}) must be less than 6 hours to achieve good storage efficiency.
$N_{heat} > 24$ hours	The number of hours (N_{heat}) since the last call for heating should be greater than 24 hours to lock out precooling in the heating season

When night ventilation precooling is enabled, mechanical cooling is disabled and the ventilation system operates with 100% outside air to precool the zone with a setpoint of 67 ºF. Once the zone temperature reaches 67 ºF, the fan cycles to maintain this setpoint. Just prior to the occupied period, the setpoint for ventilation precooling is raised to 69 ºF. Once the occupied period begins, there are separate setpoints associated cooling provided by the economizer (1st stage cooling) and the packaged air conditioner (2nd stage cooling). The 1st and 2nd stage setpoints are 69 ºF and 75 ºF, respectively. Once the occupied period ends, the zone temperature setpoint is raised to 80 ºF.

The threshold for the zone/ambient temperature difference is determined based upon trading off nighttime fan energy and daytime compressor energy saved. When ventilation precooling is enabled, mechanical cooling is disabled and the zone temperature setpoint is set at 67 F. The damper is fully open and the ventilation flow rate is equal to the primary supply air flow rate. The fan cycles, as necessary, to maintain the zone setpoint. At this point, the temperature difference required to achieve savings is estimated from equation 2.7 as

$$\Delta T_{on} = \frac{\dot{W}_{fan}}{\rho_a c_{pa} \dot{V}_{fan}} \cdot \left(\frac{COP_{nv,occ}}{\eta_s} \cdot \frac{\overline{R}_{unocc}}{\overline{R}_{occ}} + 1 \right) \tag{4.4}$$

Figure 24 shows the breakeven temperature difference as a function of the ratio of unoccupied to occupied energy rates and the ratio of fan power to volumetric flow rate for a storage efficiency of 0.8 and an occupied period COP of 3. For typical values, the threshold varies between about 1 F and 10 F. The breakeven point increases with fan power (i.e., pressure drop) for a given flow rate since the cost of providing a given quantity of precooling increases. The fan power typically varies between about 0.4 and 0.7 W/cfm. The threshold also increases as the ratio between occupied and unoccupied energy rates decreases. Lower occupied period energy costs reduce the savings associated with precooling leading to a larger threshold. For similar reasons, the threshold increases with increasing occupied period COP. For packaged air conditioning equipment, the COP varies between about 2 and 4. Finally, the threshold increases with decreasing storage efficiency as less of the precooling results in cooling load reductions during the occupied period. Storage efficiencies vary between about 0.5 and 0.9.

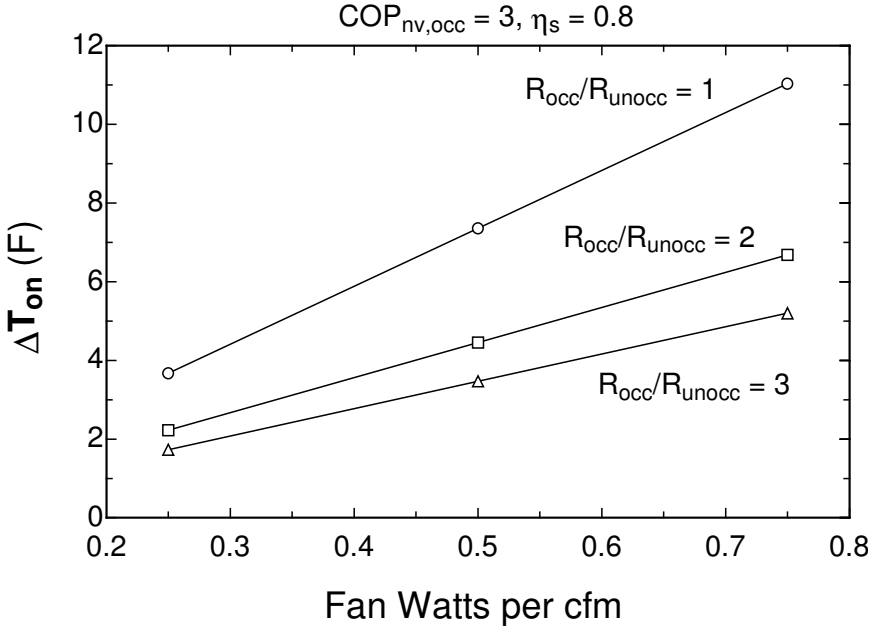

Figure 24. Night Ventilation Breakeven Threshold

4.2 Mixed Air Conditions

The mixed air conditions entering the primary air conditioner and heater are determined from mass and energy balances for adiabatic mixing according to

$$\omega_{mix} = \frac{\dot{m}_{vent}}{\dot{m}_{\sup}} \omega_v + \left(1 - \frac{\dot{m}_{vent}}{\dot{m}_{\sup}}\right) \omega_z \tag{4.4}$$

$$h_{mix} = \frac{\dot{m}_{vent}}{\dot{m}_{\sup}} h_v + \left(1 - \frac{\dot{m}_{vent}}{\dot{m}_{\sup}}\right) h_z \tag{4.5}$$

where ω is humidity ratio, h is air enthalpy, and the subscripts z and v refer to zone return and ventilation air conditions, respectively. For a system with a heat recovery heat exchanger or heat pump, ω_v and h_v are the conditions exiting the device within the ventilation stream. Otherwise, these properties are evaluated at ambient humidity conditions. The mixed air temperature is evaluated with psychrometric property routines in terms of the mixed air humidity and enthalpy or

$$T_{mix} = T\left(h_{mix}, \omega_{mix}\right) \tag{4.6}$$

4.3 Equipment Heating Requirements

If the zone requires heating to maintain the temperature at the heating setpoint, then the furnace and/or heat pump heat recovery unit must operate to meet the zone requirements and any additional load associated with ventilation. The furnace and heat pump provide only sensible heating (no humidification). If a heat pump heat recovery unit is employed, then it has the first priority for heating (i.e., 1st stage heating) during occupied mode. During unoccupied mode, the heat pump unit does not operate.

4.3.1 Heat Pump Heat Recovery Unit

From an energy balance on the air within the zone and distribution system, the heating load for the heat pump during occupied mode is

$$\dot{Q}_{hphr,h} = \min\left(\dot{Q}_{z,h} + \dot{m}_{vent} C_{pm} (T_{z,h} - T_a) - \dot{W}_{fan,s} - \dot{W}_{fan,v}, \dot{Q}_{hphr,h,cap}\right) \tag{4.7}$$

where $\dot{Q}_{z,h}$ is the zone heating load, $\dot{m}_{vent}$ is the ventilation flow rate, $T_{z,h}$ is the zone heating temperature setpoint, $\dot{W}_{fan,s}$ is the power associated with the primary supply fan, $\dot{W}_{fan,v}$ is the power associated with the optional ventilation fan for the heat pump, and $\dot{Q}_{hphr,h,cap}$ is the heating capacity associated with the heat pump.

4.3.2 Primary Heater

The heating requirement for the primary heater is

$$\dot{Q}_h = \dot{Q}_{z,h} + \dot{m}_{vent} C_{pm} (T_{z,h} - T_v) - \dot{W}_{fan,s} \tag{4.8}$$

where T_v is the temperature of the ventilation air that is mixed with return air. For a system with a heat recovery heat exchanger or heat pump, T_v is the temperature exiting the device within the ventilation stream. Otherwise, T_v is equal to the ambient temperature.

4.4 Equipment Cooling Requirements

The first priority for cooling (1st stage cooling) is the economizer if it is installed and enabled. If the economizer can meet the sensible zone cooling requirement, then the primary air conditioner does not operate. If a heat pump heat recovery unit is installed, then an economizer is not employed and the heat pump is the first priority for cooling during occupied mode. During unoccupied mode, the heat pump unit does not operate.

4.4.1 Heat Pump Heat Recovery Unit

The sensible cooling requirement for the heat pump is

$$\dot{Q}_{hphr,s,c} = \min\left(\dot{Q}_{s,T}, SHR \cdot \dot{Q}_{hphr,c,cap}\right) \tag{4.9}$$

where $\dot{Q}_{hphr,c,cap}$ is the cooling capacity of the heat pump, *SHR* is the heat pump sensible heat ratio, and $\dot{Q}_{s,T}$ is the total sensible load determined as

$$\dot{Q}_{s,T} = \dot{Q}_{z,c} + \dot{m}_{vent} C_{pm} (T_a - T_{z,c}) + \dot{W}_{fan,s} + \dot{W}_{fan,v} \tag{4.10}$$

where $\dot{Q}_{z,c}$ is the zone sensible cooling load. The cooling capacity and *SHR* are evaluated using the ambient and zone return air conditions as inlet conditions for the evaporator and condenser.

The total cooling requirement for the heat pump is

$$\dot{Q}_{hphr,c} = \frac{\dot{Q}_{hphr,s,c}}{SHR} \tag{4.11}$$

4.4.2 Primary Air Conditioner

The sensible cooling requirement for the primary air conditioner is

$$\dot{Q}_{ac,s,c} = \min\left(\dot{Q}_{s,T}, SHR \cdot \dot{Q}_{ac,c,cap}\right) \tag{4.12}$$

where $\dot{Q}_{ac,c,cap}$ is the cooling capacity of the air conditioner, SHR is the air conditioner sensible heat ratio, and $\dot{Q}_{s,T}$ is the total sensible load determined as

$$\dot{Q}_{s,T} = \dot{Q}_{z,c} + \dot{m}_{vent} C_{pm} (T_v - T_{z,c}) + \dot{W}_{fan,s} \tag{4.13}$$

where T_v is the temperature of the ventilation air that is mixed with return air. For a system with a heat recovery heat exchanger or heat pump, T_v is the temperature exiting the device within the ventilation stream. Otherwise, T_v is equal to the ambient temperature.

The cooling capacity and *SHR* are evaluated using the mixed air conditions as described in Section 3. When an economizer is not enabled, the mixed air condition depends on both ventilation and zone return air conditions according to equations 4.4 and 4.5. However, the return air humidity depends on the exit humidity from the air conditioner, which in turn depends on the mixed air condition. A quasi-steady state mass balance for humidity within the air distribution system is used along with an iterative solution to determine the zone and mixed air states and equipment performance. The zone return air humidity ratio must satisfy equations 4.4, 4.5, 4.12, 4.13 and the following equations.

$$(1 - SHR) \cdot \dot{Q}_{ac,c} = \dot{Q}_{p,L} + \dot{m}_{\inf} (\omega_a - \omega_z) h_{fg} + \dot{m}_{vent} (\omega_v - \omega_z) h_{fg} \tag{4.14}$$

$$\dot{Q}_{ac,c} = \frac{\dot{Q}_{ac,s,c}}{SHR} \tag{4.15}$$

where $\dot{Q}_{ac,c}$ is the total equipment cooling requirement, $\dot{Q}_{p,L}$ is the latent load associated with people in the zone, $\dot{m}_{\inf}$ is the infiltration flow rate, ω_a is the ambient humidity ratio, and h_{fg} is the heat of vaporization of water.

4.5 Supply, Ventilation, and Exhaust Fans

Only single-speed air distribution fans are considered in VSAT. For systems without a heat pump heat recovery unit or enthalpy exchanger, only a single supply fan is used for each primary air conditioner. The heat pump heat recovery unit incorporates a fan for the exhaust stream and has an optional fan for the ventilation stream. Enthalpy exchangers typically employ both ventilation and exhaust stream fans to ensure effective purging. For each fan, the fan power is scaled with the volumetric flow according to

$$\dot{W}_{fan,on} = w_f \cdot \dot{V}_{on} \tag{4.16}$$

where $\dot{W}_{fan,on}$ is fan power at steady state, w_f is fan power per unit of volume flow and $\dot{V}_{on}$ is the volumetric flow rate when the fan is operating. The user can specify values for w_f. For the primary supply fans, the default value for w_f is 0.5 W/cfm. For the ventilation and exhaust fans, the default value for w_f is 0.25 W/cfm.

During occupied mode, any of the air distribution fans operate continuously. However, during unoccupied mode, the fans cycle with the heater or primary air conditioner and/or economizer. In this case, the average hourly fan power is calculated as

$$\dot{W}_{fan} = PLR \cdot \dot{W}_{fan,on} \tag{4.17}$$

where *PLR* is the ratio of the average hourly heating or cooling requirement to the heat or cooling capacity. When heating or mechanical cooling is required, then the *PLR* is determined as outlined in Section 3. When cooling is required and the economizer can meet the cooling requirements, then *PLR* is determined as

$$PLR = \frac{\dot{Q}_{z,c}}{\dot{m}_{\sup} C_{pm} (T_{z,c} - T_{mix,econ})} \tag{4.18}$$

where $T_{mix,econ}$ is the mixed air setpoint temperature for the economizer.

4.6 Zone Controls – Call for Heating or Cooling

The first step in evaluating whether heating or cooling is required is to determine the zone temperature if the equipment were off. During unoccupied mode, the supply air fan is off when there is no heating and cooling requirement. In this case, the floating zone temperature is determined by setting $\dot{Q}_z$ to zero in equation 2.27 and solving for the zone temperature. During occupied mode, the fan(s) operate(s) continuously so that ventilation loads and fan energy influence the floating zone temperature. In this case, the zone temperature is determined that satisfies the following equation.

$$\dot{Q}_z + \dot{W}_{fan,s} + \dot{W}_{fan,v} + \dot{m}_{vent} C_{pm} (T_a - T_z) = 0 \tag{4.19}$$

SECTION 5: WEATHER DATA, SIZING, AND COSTS

5.1 Weather Data

VSAT contains typical meteorological year (TMY2) weather data for 239 US locations and California Climate Zone data for 16 representative zones within California. The data include hourly values of ambient temperature, horizontal radiation, and direct normal radiation. In addition, the user can specify the ambient CO_2 level. The default value is 350 ppm.

The California Climate Zones are shown in Figure 25 and the representative cities for each climate zone (CZ) are given in Table 17. The climate zones are based on energy use, temperature, weather and other factors. They are basically a geographic area that has similar climatic characteristics. The California Energy Commission originally developed weather data for each climate zone by using unmodified (but error-screened) data for a representative city and weather year (representative months from various years). The Energy Commission analyzed weather data from weather stations selected for (1) reliability of data, (2) currency of data, (3) proximity to population centers, and (4) non-duplication of stations within a climate zone.

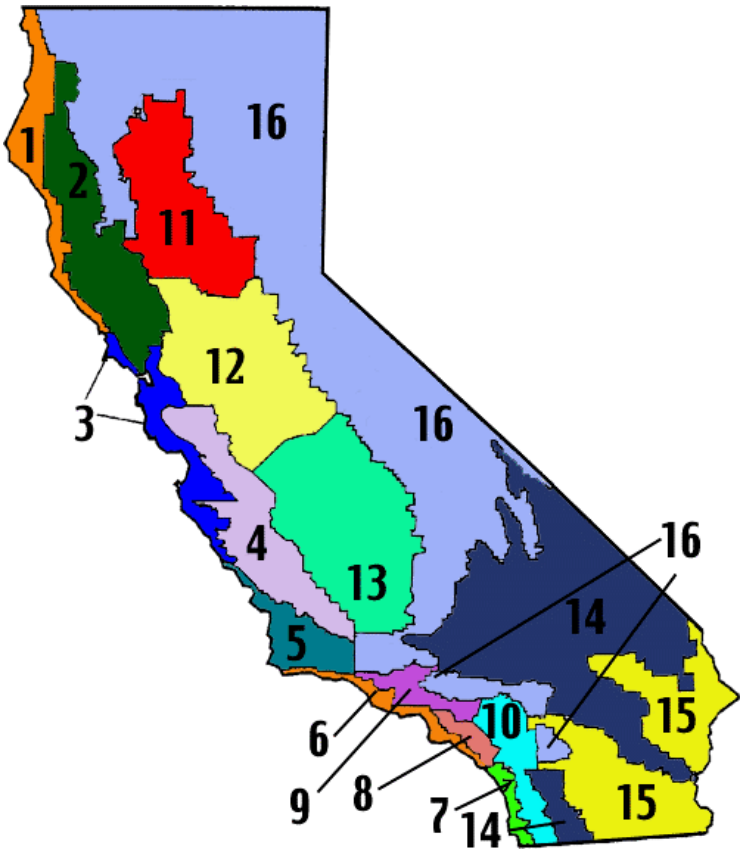

Figure 25. California Climate Zones

Table 17. Cities associated with California Climate Zones

CZ 1: Arcata	CZ 5: Santa Maria	CZ 9: Pasadena	CZ13: Fresno
CZ 2: Santa Rosa	CZ 6: Los Angeles	CZ10: Riverside	CZ14: China Lake
CZ 3: Oakland	CZ 7: San Diego	CZ11: Red Bluff	CZ15: El Centro
CZ 4: Sunnyvale	CZ 8: El Toro	CZ12: Sacramento	CZ16: Mount Shasta

There are two sets of Climate Zone data included in VSAT, the original and a massaged set. In the massage data, the dry bulb temp has been modified in an effort to give the file a better "average" across the entire zone. Because only dry bulb was adjusted, the humidity conditions are affected and therefore the massaged files are not preferred.

5.2 Equipment Sizing

The heating and cooling equipment are automatically sized for a given building and location. The primary heating and cooling equipment are sized assuming no ventilation heat recovery (enthalpy exchanger or heat pump), no economizer, fixed ventilation, and constant zone temperature setpoints (no night setup or setback). The peak sensible heating and cooling requirements are first determined by calculating the hourly zone and ventilation loads throughout the heating and cooling seasons. The heating capacity is set at 1.4 times the peak sensible heating load.

For cooling, the required equipment cooling capacity depends upon the latent load, which depends on ambient and zone humidities and the zone internal latent gains. The required capacity is determined iteratively using the ambient conditions and zone latent gains associated with the peak sensible cooling requirement along with the equipment and air distribution models. The cooling equipment is then oversized by 10%.

The supply air flow rate is determined based upon a specified flow per unit cooling capacity with a default of 350 cfm/ton. The supply fan power is based upon a specified fan power per unit flow rate with a default of 0.5 W/cfm.

The number of rooftop units employed for a given application will influence the economics of the different ventilation strategies. Individual rooftop units require separate enthalpy exchangers, heat pump heat recovery units, economizers, or controllers (demand-controlled ventilation or night ventilation precooling). It will be assumed that rooftop units are available in sizes of 3.5, 5, 7.5, 10, 15, and 20 ton cooling capacities. For a given application and location, the number of individual rooftop units will be based upon the using fewest possible number of units necessary to realize a cooling capacity that is greater than, but within 10% of the target equipment cooling capacity.

The diameter of individual enthalpy exchangers will be scaled so as to achieve a flow velocity of 650 fpm. At this velocity, the exchanger has a constant effectiveness for heat and mass transfer of 0.75 when operated at normal speed.

The heat pump heat recovery unit cooling capacity will be scaled to achieve a flow per unit cooling capacity of 533 cfm/ton based upon the rated cooling capacity and the ventilation flow requirements.

5.3 Costs

VSAT is set up to calculate the simple payback period associated with different ventilation strategies. The alternatives are compared with a base case that has fixed ventilation with no

economizer or other ventilation strategy. For any alternative k, the simple payback period is calculated as

$$N_{pb} = \frac{C_k}{S_k} \tag{5.1}$$

where S_k is the annual savings in utility costs associated with the ventilation strategy as compared with the base case and C_k is the installed cost associated with implementing the ventilation strategy.

The annual utility costs associated with operating the HVAC system are calculated according to

$$C_{HVAC} = \sum_{m=1}^{m=12} \left\{ \begin{array}{c} r_{d,on,m} \cdot \dot{W}_{peak,on,m} + r_{d,mid,m} \cdot \dot{W}_{peak,mid,m} + r_{d,off,m} \cdot \dot{W}_{peak,off,m} \\ + \sum_{i=1}^{N_m} \left(r_{e,i,m} \cdot W_{i,m} + r_{g,i,m} \cdot G_{i,m} \right) \end{array} \right\} \tag{5.2}$$

where m is the month, i is the hour, N_m is the number of hours in month m, and for each month m: $r_{d,on,m}$, $r_{d,mid,m}$ and $r_{d,off,m}$ are the utility rates for electricity demand during the on-peak, mid-peak and off-peak periods ($/kW) and $\dot{W}_{peak,on,m}$, $\dot{W}_{peak,mid,m}$ and $\dot{W}_{peak,off,m}$ are the peak power consumption for the HVAC equipment during the on-peak, mid-peak and off-peak periods; and for each hour i of month m: r_e is the utility rate for electricity usage ($/kWh), W is the electricity usage (kWh), r_g is the utility rate for natural gas usage ($/therm), G is the gas usage (therm).

The electricity costs include both energy ($/kWh) and demand charges ($/kW) for on-peak, off-peak, and mid-peak periods. Gas energy usage does not vary with time of the day. However, the user can enter different electric and gas rates for summer and winter periods.

The default rates and periods incorporated in VSAT are given in Table 18, Table 19, and Table 20. The default electric utility rates incorporated in VSAT are based upon Pacific, Gas and Electric Company (PG&E) Schedule E-19. The default natural gas rates are based on PG&E Schedule G-NR1.

Table 18. Default time periods for utility rates

PG&E			
Summer:	May 1 - Oct. 31	Winter:	Nov. 1 - April 30
On-Peak	12:00 - 6:00, M - F	On-Peak	N/A
Mid-Peak	8:30 AM - 12:00 &	Mid-Peak	8:30 AM - 9:30 PM, M - F
	6:00 PM - 9:30 PM, M - F		
Off-Peak	9:30 PM - 8:30 AM, all week	Off-Peak	9:30 PM - 8:30 AM, all week

Table 19. Default natural gas rates in VSAT

PG&E Schedule G-NR1, CA Climate Zones 1, 2, 3, 4, 11, 12, 13, 1	
Summer Season	$0.67355
Winter Season	$0.74220

Table 20: Default electric rates in VSAT

PG&E Schedule E-19, CA Climate Zones 1, 2, 3, 4, 5, 11, 12, 13			
Energy Charge - $/kWh			
Summer Season	On-Peak	$0.08773	
	Mid-Peak	$0.05810	
	Off-Peak	$0.05059	
Winter Season	On-Peak	N/A	
	Mid-Peak	$0.06392	
	Off-Peak	$0.05038	
Time Related Demand Charge - $kW			
Summer Season	On-Peak	$13.35	
	Mid-Peak	$3.70	
	Off-Peak	$2.55	
Winter Season	On-Peak	N/A	
	Mid-Peak	$3.65	
	Off-Peak	$2.55	

SECTION 6: SAMPLE RESULTS AND COMPARISONS WITH ENERGY-10

6.1 Sample Results

Figure 26 shows sample hourly results for the Base Case (night setup with no economizer) and with Night Ventilation Precooling for the school class wing within early summer in Climate Zone 10 obtained using the default VSAT utility rates (PG&E E-19 and GNR-1). Night ventilation precooling is enabled during the unoccupied mode when the ambient temperature is sufficiently cooler than the zone temperature. For this example, this occurs during the hour from 11-12:00 pm and continues until the occupied mode begins at 5 am. Prior to occupancy the zone temperature is cooled to around 20˚C. At occupancy, the economizer keeps the zone temperature at a lower economizer setpoint until 8 am when the temperature begins to rise. The temperature reaches the setpoint for mechancial cooling at 11:00 am.

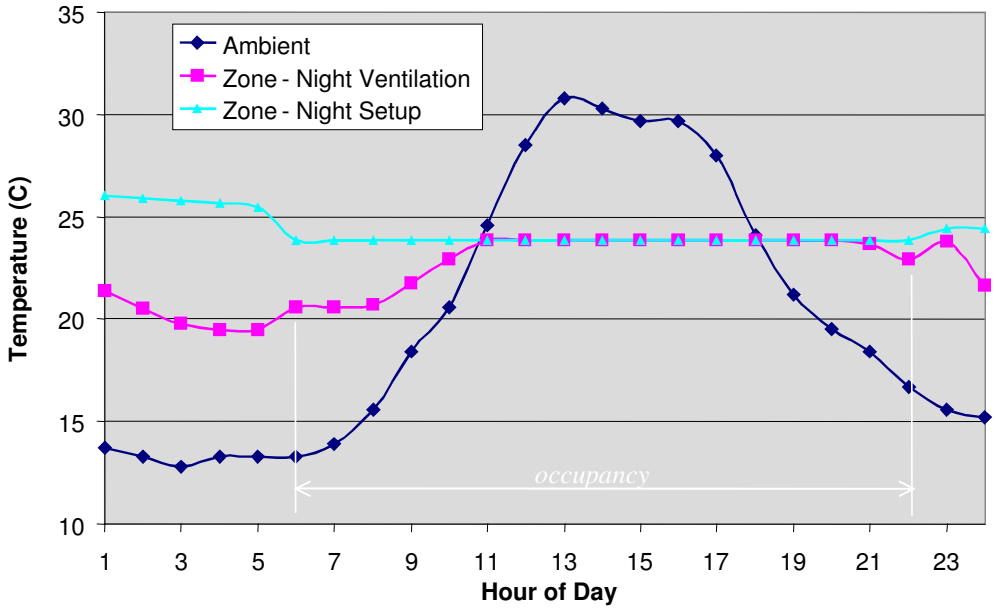

Figure 26. Sample hourly results night ventilation precooling and the base case (class school wing during early summer in Rialto, California).

Figure 27 shows hourly fan and compressor power comparisons for the situation considered for Figure 26. Additional fan energy is utilized during the early morning hours with night ventilation precooling, but this leads to a reduction in compressor energy over much of the day. Part of the savings is due to the low zone setpoint for the economizer, which acts to maintain a cool building thermal mass during the morning hours. For the night ventilation control, mechanical cooling is not needed until 11 am. Clearly, the night ventilation control requires significantly less compressor energy and has slightly lower peak electrical demand at the expense of additional fan energy.

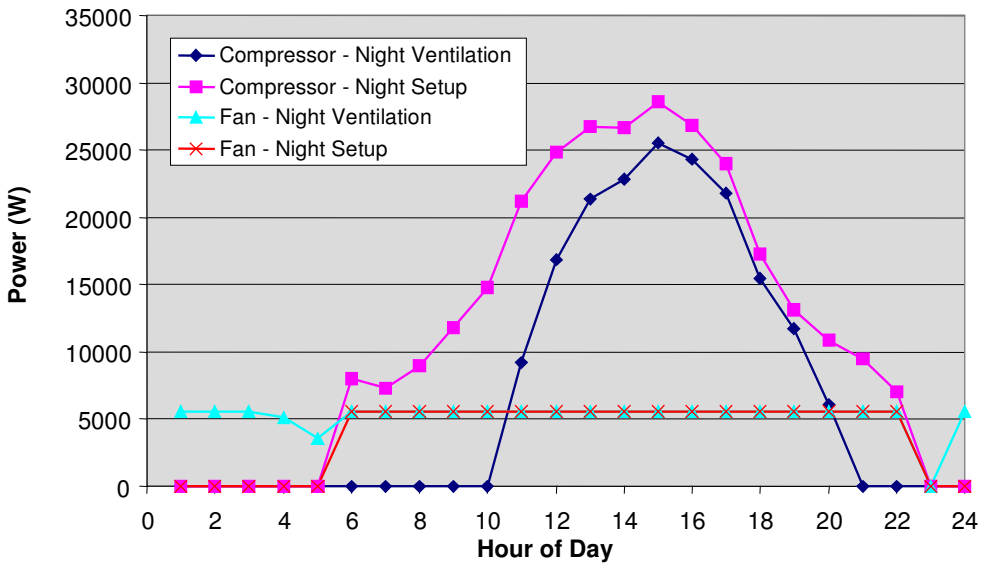

Figure 27: Simulated hourly power for night ventilation precooling and the base case (class school wing during early summer in California Climate Zone 10).

Figure 28 gives annual electrical energy usage for the class school wing in California Climate Zone 10 for three ventilation strategies: 1) a base case with a night setup thermostat, 2) case 1 with the addition of a differential enthalpy-based economizer, and 3) case 2 with the addition of the night ventilation precooling algorithm. Compared to the base case, the economizer results in a savings in compressor energy of 17.4%. The combined compressor and fan savings are about 11.1%. Compared to the economizer, the addition of the night ventilation algorithm leads to an additional savings of about 14.0% in compressor energy. However, the fan energy increases by about 14.2%, and because the compressor energy is the major consumption, the energy saved in compressor is more than the additional comsumption by fan, the combined savings about 2.6% is achieved compared to the economizer only.

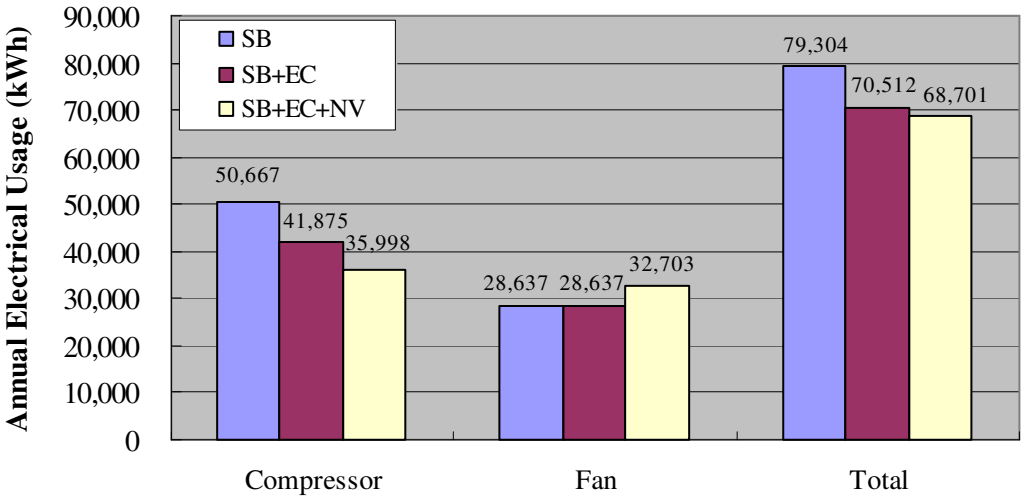

Figure 28: Simulated electrical energy usage for different ventilation strategies (class school wing in California Climate Zone 10).

6.2 Comparisons with Energy-10

Energy-10 is a conceptual design tool for low-energy buildings developed under sponsorship of the U.S. Department of Energy (DOE). The program performs transient, hour-by-hour load calculations for small commercial and residential buildings and allows comparisons of different energy savings strategies. The underlying methods used in Energy-10 are very similar to those used in VSAT. However, VSAT focuses on energy savings due to different ventilation strategies, whereas Energy-10 considers more conventional design changes such as day-lighting, air leakage control, glazing, shading, economizer, thermal mass, passive solar heating and high efficiency equipment. More information on Energy-10 can be found at www.sbicouncil.org or from the user manual.

Since Energy-10 is an accepted tool for analysis of small commercial building, it was chosen for benchmarking predictions of VSAT for a base case system with a night setup/setback thermostat and no economizer. The office-building prototype was chosen for this case study and comparisons of monthly equipment loads and energy consumptions were performed in two locations, Madison, WI, and Atlanta, GA.

There are some basic differences in the modeling approaches in Energy-10 and VSAT that had to be considered. VSAT neglects the effects of cycling on furnace efficiency, whereas Energy-10 includes a significant penalty for cycling. For the purposes of comparison, the part-load effects of furnace cycling were not included in the Energy-10 results. However, part-load effects for the air conditioning equipment were included for both models.

A window in Energy-10 is characterized with a rough-frame opening dimension(the hole left by the framers), a glazing type, and a frame type. The U-value is calculated from the dimensions and the U-values of the glass and frame. In VSAT, the window U-value is simply a given value in the building description and no frame is assumed. Solar transmittances and shading coefficients are also inputs in VSAT, whereas these values are calculated from a windows library in Energy-10. For comparison purposes, a window assembly was built in Energy-10 that had an effective U-value and transmittance very similar to that in VSAT.

Energy-10 weather files are constructed using the 1994 and 1995 updated TMY2 weather

files. This update is based on 30 years of data, rather than 20 years, and incorporates new and improved solar radiation information from the 1992 National Solar Radiation Data Base. The weather data in VSAT used for comparison purposes is TMY data.

The prototypical office was modeled in both Madison and Atlanta. The air-conditioner and furnace equipment models assumed a rated EER of 11 and efficiency of 85%, respectively. In VSAT, the supply fan power was assumed to be 0.5 W/cfm. This value corresponds to a fan efficiency of 11.78% and 0.5 inches H_2O system static pressure as entered in Energy-10. Infiltration was neglected for both models. The occupied zone set point for cooling was 23.89°C with a night setup to 29.44°C. The occupied zone set point for heating was 21.11°C with a night setback to 15.56°C.

Table 21 gives equipment sizing determined by VSAT for Madison and Atlanta. These equipment sizes were specified in Energy-10.

Table 21: Equipment Sizing Results from VSAT

	Office - Madison, WI	Office - Atlanta, GA
AC Rated Total Cap., Btu/h	210180	210260
AC Rated Sens. Cap., Btu/h	153064	162822
Furnace Rated Cap., Btu/h	252924	148583
Total Air Flow, cfm	6130	6133
Ventilation Air Flow, cfm	924	924
Office Floor Area, ft^2	6600	6600

Figures 29 – 31 give monthly electricity for the condensing units (compressors and condenser fans), furnace gas input, and supply fan power for both VSAT and Energy-10 in Atlanta, GA. Figures 32 – 34 give similar results for Madison, WI. The trends and absolute magnitudes are very similar for predictions obtained with VSAT and Energy-10. In general, VSAT tends to give slightly higher condensing unit energy and lower gas input energy than Energy-10. Tables 22 and 23 gives tabulated results along with percentage differences between Energy-10 and VSAT for Atlanta and Madison.

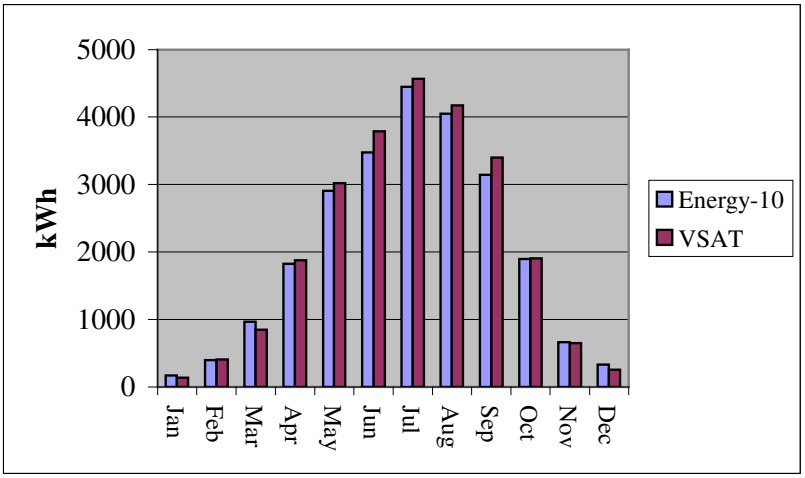

Figure 29. Monthly Electrical Consumption for Cooling – Atlanta, GA

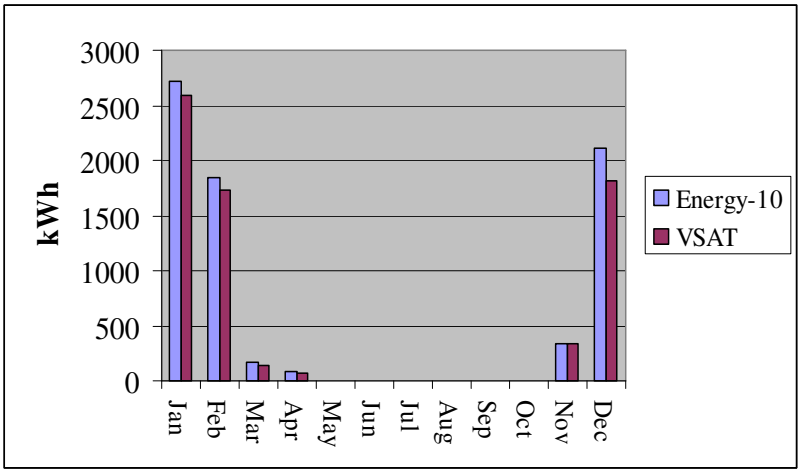

Figure 30. Monthly Furnace Gas Input – Atlanta, GA

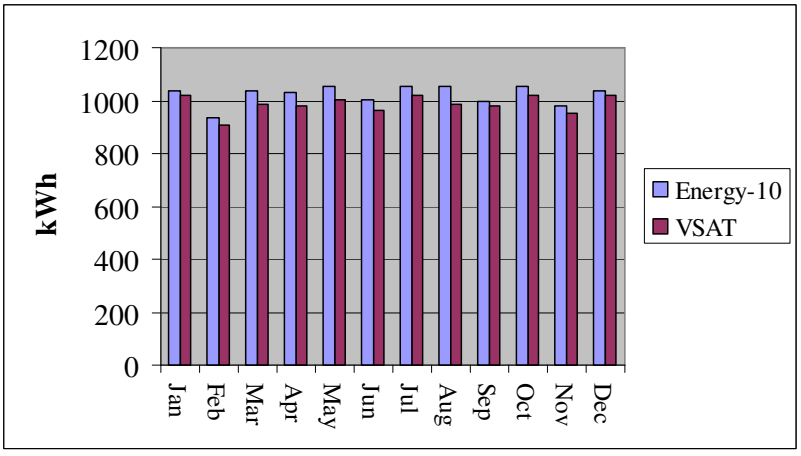

Figure 31. Monthly Supply Fan Power Consumption – Atlanta, GA

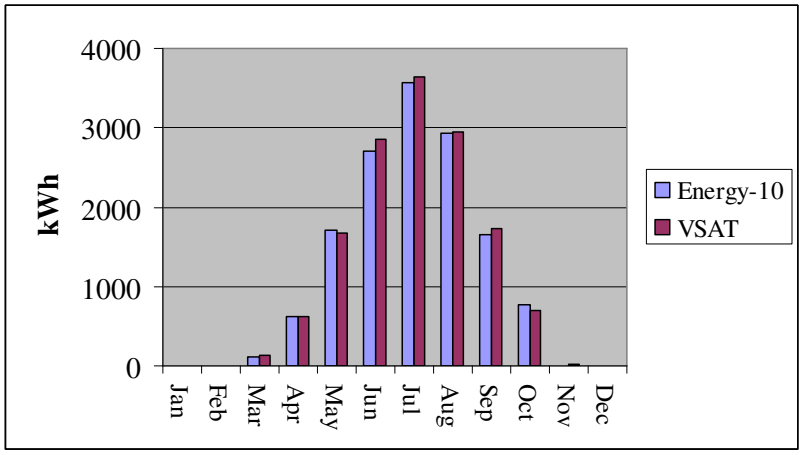

Figure 32. Monthly Electrical Consumption for Cooling –Madison, WI

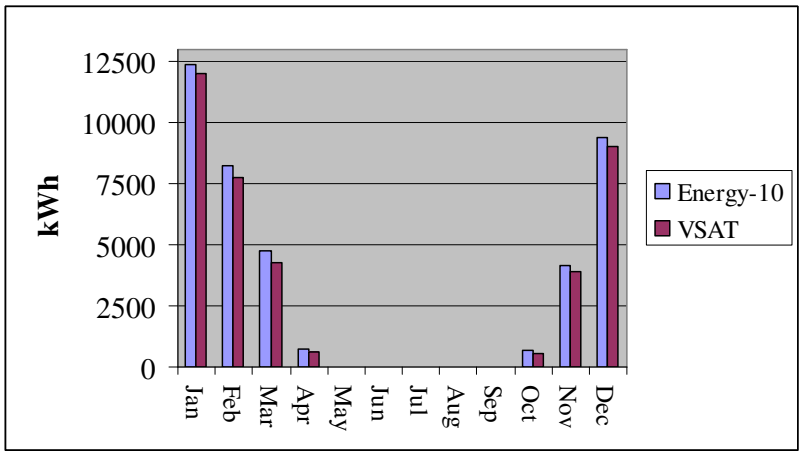

Figure 33. Monthly Furnace Gas Input – Madison, WI

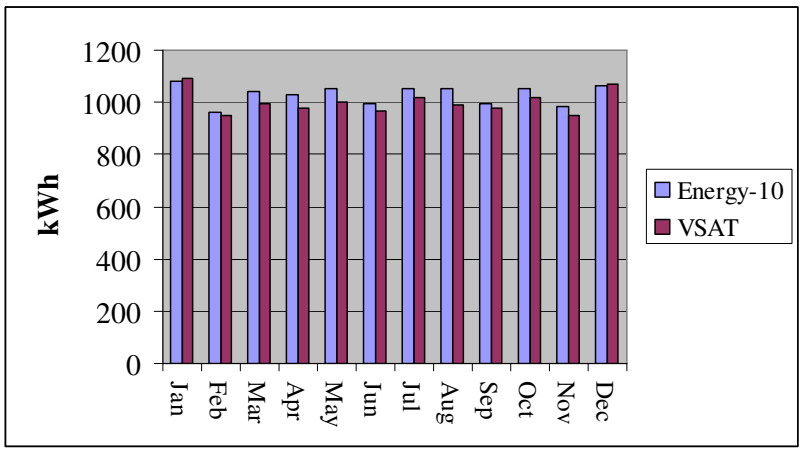

Figure 34. Monthly Supply Fan Power Consumption – Madison, WI

Table 22: VSAT and Energy-10 Results – Atlanta, GA

	AC kWhr		Furnace kWhr		Fan kWhr	
Month	Energy-10	VSAT	Energy-10	VSAT	Energy-10	VSAT
Jan	168	139	2712	2589	1038	1020
Feb	397	407	1851	1738	937	909
Mar	968	849	171	142	1037	987
Apr	1828	1878	78	74	1031	981
May	2905	3021	0	0	1053	1003
Jun	3474	3790	0	0	1000	966
Jul	4448	4570	0	0	1054	1018
Aug	4050	4173	0	0	1054	987
Sep	3144	3398	0	0	999	981
Oct	1898	1905	0	0	1053	1018
Nov	662	650	332	345	982	951
Dec	330	258	2118	1815	1037	1018
Yr	24272	25038	7262	6703	12275	11839
	AC error	3.06%	Furnace error	-8.35%	Fan error	-3.68%

Table 23: VSAT and Energy-10 Results – Madison, WI

	AC kWhr		Furnace kWhr		Fan kWhr	
Month	Energy-10	VSAT	Energy-10	VSAT	Energy-10	VSAT
Jan	0	0	12378	12018	1082	1092
Feb	5	0	8247	7779	960	948
Mar	110	128	4779	4264	1039	994
Apr	622	618	711	622	1030	981
May	1716	1664	11	12	1053	1002
Jun	2705	2852	0	0	998	966
Jul	3561	3636	0	0	1054	1018
Aug	2934	2943	0	0	1053	987
Sep	1650	1728	0	18	998	981
Oct	766	687	694	523	1053	1018
Nov	2	20	4178	3927	982	951
Dec	0	0	9414	9023	1065	1070
Yr	14070	14276	40412	38186	12367	12008
	AC error	1.44%	Furnace error	-5.83%	Fan error	-2.99%

SECTION 7: REFERENCES

ASHRAE. 2000. *ASHRAE Handbook: HVAC Systems and Equipment*, Atlanta: American Society of Heating, Refrigerating and Air-Conditioning Engineers, Inc.

ASHRAE. 1999. "ANSI/ASHRAE Standard 62-1999, "Ventilation for Acceptable Indoor Air Quality", Atlanta: American Society of Heating, Refrigerating and Air-Conditioning Engineers, Inc.

ASHRAE. 1993. *ASHRAE Handbook: Fundamentals*, Atlanta: American Society of Heating, Refrigerating and Air-Conditioning Engineers, Inc.

Brandemuehl, M.J. and Braun, J.E., "The Impact of Demand-Controlled and Economizer Ventilation Strategies on Energy Use in Buildings, ASHRAE Transactions, Vol. 105, Pt. 2, pp. 39-50, 1999.

Brandemuehl, M.J., Gabel, S., and Andresen, I. 1993. *HVAC2 Toolkit: Algorithms and Subroutines for Secondary HVAC System Energy Calculations*. American Society of Heating, Refrigerating, and Air Conditioning Engineers, Inc., Atlanta, GA.

Braun, J.E. and Brandemuehl, M.J. 2002. *Savings Estimator Technical Reference Manual.*

Carrier Corporation. 1999. "Product Data: 62AQ Energy$Recycler Energy Recovery Accessory For 3 to 12.5 Ton Rooftops", Form 62AQ-1PD. Syracuse, New York.

Carnes Company. 1989. "Energy Recovery Wheel Design Manual," Verona, WI.

Chaturvedi, N. and Braun, J.E. "An Inverse Gray-Box Model for Transient Building Load Prediction," International Journal of Heating, Ventilating, Air-Conditioning and Refrigeration Research, Vol. 8, No. 1, pp. 73-100, 2002.

Duffie, J.A. and Beckman, W.A., Solar Engineering of Thermal Processes, Wiley—Interscience, 1980.

DOE-2. 1982. Engineer's Manual, Version 2.1A. Lawrence Berkeley Laboratory and Los Alamos National Laboratory.

Huang, Y.J., Akbari, H., Rainer, L., and Ritschard, R.L. 1990. *481 Prototypical Commercial Buildings for Twenty Urban Market Areas (Technical documentation of building loads data base developed for the GRI Cogeneration Market Assessment Model)*. LBL Report 29798, Lawrence Berkley National Laboratory, Berkley CA.

Huang, Y.J., and E. Franconi. 1995. *Commercial Heating and Cooling Loads Component Analysis.* LBNL Report 38970, Lawrence Berkeley National Laboratory, Berkeley, CA.

Kays, W.M., and M.E. Crawford. 1980. *Convective Heat and Mass Transfer.* New York: McGraw-Hill.

Klein, H., Klein, S.A., and Mitchell, J.W., 1990, "Analysis of regenerative enthalpy exchangers," International *Journal of Heat and Mass Transfer*, Vol. 33, No.4, pp. 735-744.

Maclaine-cross, I.L. 1974. *A Theory of Combined Heat and Mass Transfer in Regenerators.* Ph.D. Thesis in Mechanical Engineering, Monash University, Australia.

Seem, J.E., Klein, S.A., Beckman, W.A., and Mitchell, J.W., 1989, "Transfer functions for efficient calculations of multi dimensional heat transfer," *Journal of Heat Transfer-Transactions of the ASME*, Vol. 111, No.1, pp. 5-12.

Stiesch, G., S.A. Klein, J.W. Mitchell. 1995. *Performance of Rotary Heat and Mass Exchangers.* HVAC&R Research 1(4): 308-324.

TRNSYS. 2000. *TRNSYS Users Guide: A Transient Simulation Program.* Solar Energy Laboratory, University of Wisconsin-Madison.

EVALUATION OF DEMAND CONTROLLED VENTILATION, HEAT PUMP HEAT RECOVERY AND ENTHALPY EXCHANGERS

Submitted to

California Energy Commission

As a Final Report for Deliverables 3.1.6b and 4.2.6a

Prepared by

James E. Braun, Kevin Mercer, and Tom Lawrence
Purdue University

August 2003

ACKNOWLEDGEMENTS

The research that resulted in this document was part of the "Energy Efficient and Affordable Small Commercial and Residential Buildings Research Program", which was a Public Interest Energy Research Program (PIER) sponsored by the California Energy Commission (CEC). We are extremely grateful for the funding from the CEC through PIER. Several organizations and people were involved in the project described in this final report and deserve our many thanks. Chris Scruton of the CEC was very enthusiastic throughout this project and provided valuable insight and encouragement. Vern Smith and Erin Coats of Architectural Energy Corporation (AEC) provided excellent overall project management for the numerous projects within this large program. Todd Rossi and Doug Dietrich of Field Diagnostic Services, Inc. (FDSI) and Lanny Ross of Newport Design Consultants (NDS) were essential in setting up and maintaining the field sites. Martin Nankin of FDSI provided monitoring equipment at cost for this project. Bob Sundberg of Honeywell, Inc. arranged the donation of Honeywell equipment and was an enthusiastic supporter of the research. Adrienne Thomle and Bill Bray at Honeywell, Inc. made sure that equipment was delivered to the field sites and provided replacement equipment and troubleshooting when necessary. We also had excellent support from the organizations that own and/or operate buildings at the field sites. Individual contributors include Jim Landberg for the Woodland schools, Tadashi Nakadegawa for the Oakland schools, Tony Spata and Mike Godlove for McDonalds, and Mike Sheldon, Paul Hamann, Gordon Pellegrinetti, and Tim Schmid for Walgreens.

EXECUTIVE SUMMARY

The overall objective of the work described in this report was to provide an economic assessment of three alternative ventilation strategies for small commercial buildings in the state of California. The three alternative technologies considered were demand-controlled ventilation (DCV), enthalpy exchanger heat recovery (HXHR), and heat pump heat recovery (HPHR). These three technologies were compared with a base case incorporating fixed ventilation with a differential enthalpy economizer.

The primary evaluation approach involved the use of detailed simulations to estimate operating costs and economic payback periods. A simulation tool, termed the **V**entilation **S**trategy **A**ssessment **T**ool (VSAT), was developed to estimate cost savings associated with the three different ventilation strategies for a set of prototypical buildings and equipment. The buildings considered within VSAT cover a wide range of occupancy schedules and include a small office building, a sit-down restaurant, a retail store, a school class wing, a school auditorium, a school gymnasium, and a school library.

Field sites were also established for the DCV and heat pump heat recovery systems. The goals of the field testing were to verify savings and identify practical problems associated with these technologies. Several field sites were established for DCV that would allow side-by-side testing for different building types in different climates. A single field site was established for the heat pump heat recovery unit in order to verify the performance of the unit.

The simulation study considered both retrofit and new building designs. In both cases, demand-controlled ventilation coupled with an economizer (DCV+EC) was found to give the largest cost savings and best economics relative to an economizer only system for the different prototypical buildings and systems evaluated in the California climate zones. DCV reduces ventilation requirements and loads whenever the economizer is not enabled and the occupancy is less than the peak design value typically used to establish fixed ventilation rates according to ASHRAE Standard 62-1999. Lower ventilation loads lead to lower equipment loads, energy usage and peak electrical demand.

Figure A shows sample payback periods for DCV+EC compared to the base case for a retrofit analysis. The greatest cost savings and lowest payback periods occur for buildings that have low average occupancy relative to their peak occupancy, such as auditoriums, gyms and retail stores. From a climate perspective, the greatest savings and lowest payback periods occur in extreme climates (either hot or cold). The mild coastal climates have smaller savings and longer payback periods. In most cases, the payback period associated with DCV+EC was less than 2 years.

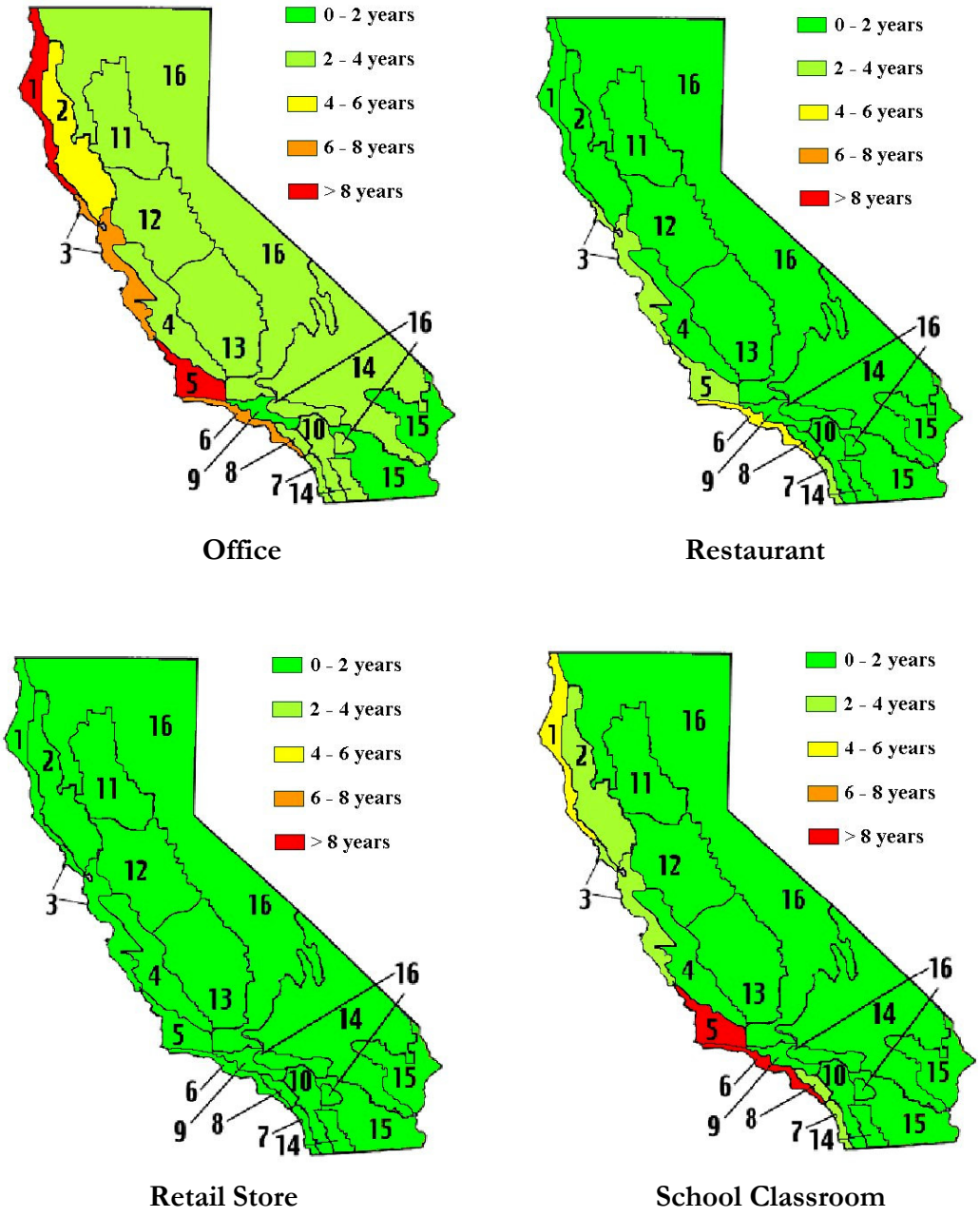

Figure A. Sample Payback Periods for DCV + EC in a Retrofit Application

The heat pump heat recovery (HPHR) system did not provide positive cost savings for many situations investigated for California climates. Heating requirements are relatively low for California climates and therefore overall savings are dictated by cooling season performance. The cooling COP of the HPHR system must be high enough to overcome additional cycling losses from the primary air conditioner compressor, additional fan power associated with the exhaust and/or ventilation fan, additional cooling requirements due to a higher latent removal and a lower operating COP for the primary air conditioner compressor because of a colder mixed air temperature. In addition, the HPHR system is an alternative to an economizer and so economizer savings are also lost when utilizing

this system. There are not sufficient hours of ambient temperatures above the breakeven points to yield overall positive savings with the HPHR system compared to a base case system with an economizer for the prototypical buildings in California climates.

The breakeven ambient temperatures for positive savings with the HXHR system are much lower than for the HPHR system because energy recovery (and reduced ventilation load) does not require additional compressor power. The primary penalty is associated with increased fan power due to an additional exhaust fan. In addition, as with the HPHR system, the HXHR system is an alternative to an economizer. Therefore, economizer savings are also lost when utilizing this system. Although positive savings were realized for a number of different buildings and climate zones, the HXHR system had greater operating costs than the DCV system for all cases considered. Furthermore, the initial cost for an HXHR system is higher than a DCV system and also requires higher maintenance costs. Payback for the enthalpy exchanger was found to be greater than 7 years for most all areas of California, except for some building types in climate zone 15.

The payback periods presented in Figure A were calculated assuming a retrofit application. The use of an enthalpy exchanger or heat pump heat recovery unit would lead to a smaller design load for the HVAC equipment which impacts the overall economics. This effect was also considered through simulation. Figures B and C show cumulative rates of return for two different buildings in CACZ 15 as a function of year after the retrofit. The rate of return is the total savings in costs (including a reduction in primary equipment costs) divided by the cost of the ventilation strategy and expressed as a percent. The simple payback period occurs at the point where the rate of return becomes positive. The enthalpy exchanger results in an immediate rate of return (immediate payback) due to RTU equipment cost savings. Although the rates return for the DCV+EC start out negative (due to the initial investment), they surpass the enthalpy exchanger rates of return within a short time period. In general, the rates of return are higher in hotter climates and for the buildings having higher peak occupancy (e.g, the retail store versus the office). Rates of return for both the HXHR and HPHR systems were negative in the moderate climates, but economics for DCV+EC were still positive. In general, the HPHR system is not competitive with the other technologies.

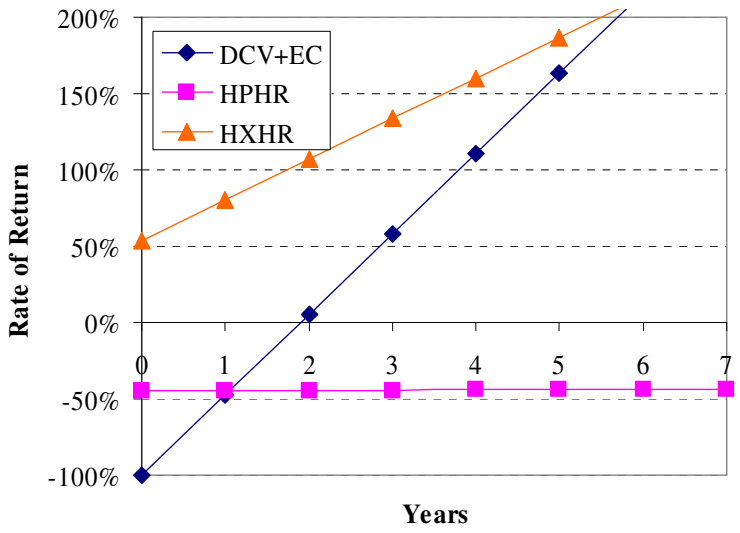

Figure B. Cumulative Rate of Return for New Office Building Design in CACZ 15

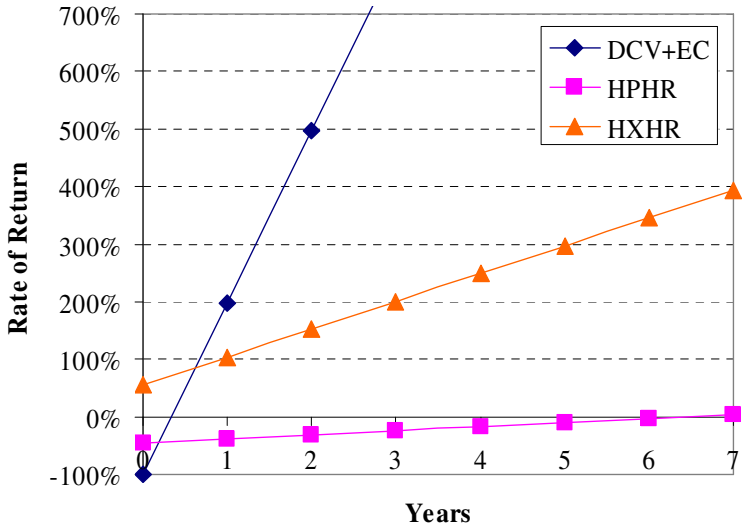

Figure C. Cumulative Rate of Return for New Retail Store in CACZ 15

The different ventilation strategies also have some different effects on comfort conditions due to variations in humidity conditions. For humid climates (outside of California), the alternative ventilation strategies provide lower zone humidity levels than a conventional system during the cooling season. DCV typically provides the lowest zone humidities, followed by the HXHR system, and then the HPHR system.

The savings and trends determined through simulation for DCV were verified through field testing in a number of sites. Field sites were established for three different building types in two different climate zones within California. The building types are: 1)

McDonalds PlayPlace® areas, 2) modular school rooms, and 3) Walgreens drug stores. In each case, nearly duplicate test buildings were identified in both coastal and inland climate areas. For cooling, greater energy and cost savings were achieved at the McDonalds PlayPlaces and Walgreens than for the modular schoolrooms. Primarily, this is because these buildings have more variability in their occupancy than the schoolrooms. The largest energy and cost savings were achieved at the Walgreens in Rialto, followed by the Bradshaw McDonalds PlayPlaces. The Rialto Walgreens appears to have the lowest occupancy and is located in a relatively hot climate with relatively large ventilation loads. The Bradshaw McDonalds PlacePlace appears to have the lowest average occupancy level compared to the other McDonalds PlacePlaces. This site is located in Sacramento and has larger ventilation and total cooling loads than the bay area McDonalds. The payback period for the Rialto Walgreens is less than a year and is between 3 and 6 years for the McDonalds PlayPlaces.

There were no substantial cooling season savings for the modular school rooms. The occupancy for the schools is relatively high with relatively small variability. The school sites are also on timers or controllable thermostats that mean the HVAC units only operate during the normal school day. The schools are also generally unoccupied during the heaviest load portion of the cooling season. Furthermore, the results imply that the average metabolic rate of the students may be higher than the value used in ASHRAE Standard 62-1999 to establish a fixed ventilation rate. In fact, the DCV control resulted in lower CO_2 concentrations than for fixed ventilation rate at the modular schoolroom sites in Sacramento.

A single field site was established for the heat pump heat recovery unit for school in Woodland, CA. The field data confirmed that the steady-state performance of the heat pump in the field is very close to the performance determined in the laboratory and published by the manufacturer for both cooling and heating modes. Furthermore, the model implemented within VSAT for the heat pump accurately predicts capacity and compressor power when compared to recorded field data for steady-state conditions.

For most all locations throughout the state of California, demand-controlled ventilation with an economizer is the recommended ventilation strategy. An enthalpy exchanger is viable in many situations, but DCV was found to have better overall economics for retrofit applications. Heat pump heat recovery is not recommended for California. This technology would make more sense in cold climates where heating costs are more significant. The savings potential for all ventilation strategies is greater in cold climates where heating dominates.

TABLE OF CONTENTS

I. INTRODUCTION

This report describes an assessment of three competing ventilation strategies for reducing ventilation loads in small commercial buildings located in California that utilize packaged equipment. Figure 1 illustrates a typical HVAC system application for small commercial buildings that was considered. A single packaged unit (e.g., a rooftop unit) serves a single zone and incorporates a direct expansion air conditioner, gas or electric heater, a supply fan, and a ventilation system.

The ventilation and exhaust air streams are outlined in Figure 1 to depict the portion of the system where alternative ventilation strategies are employed. The three alternative technologies considered were demand-controlled ventilation, enthalpy exchangers, and heat pump heat recovery. These three technologies were compared with a base case incorporating fixed ventilation with a differential enthalpy economizer.

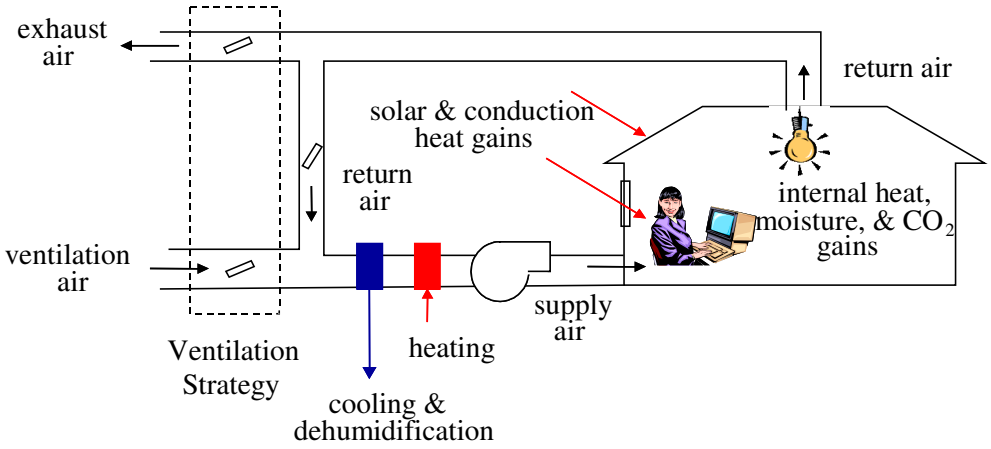

Figure 1. Small Commercial HVAC System

Base Case Ventilation Strategy

The base case ventilation system employs a controllable ventilation and exhaust (and possibly return) damper and a differential enthalpy economizer. The minimum ventilation air flowrate is determined from ASHRAE Standard 62-1999 based upon a design occupancy. The economizer is enabled whenever the ambient enthalpy is less than the return air enthalpy and there is a call for cooling. Under economizer operation, the dampers are controlled to maintain a mixed air temperature set point (e.g., 55 F). With a controllable return damper, this control strategy leads to the use of 100% outside air at many ambient conditions when cooling is required.

Demand-Controlled Ventilation (DCV)

Demand-controlled ventilation involves adjusting the outdoor air ventilation flowrates to maintain a fixed set point for indoor carbon dioxide (CO_2) concentration. The sensor can be placed in the zone or in the return duct. In this study, DCV was considered in combination with an enthalpy economizer. In effect, the minimum ventilation flowrate is determined by the DCV control and the economizer acts to override this minimum and provide additional ventilation flow and a load reduction. During the cooling season, DCV reduces the cooling requirements for the primary equipment whenever there is a call

for cooling and the ambient enthalpy is greater than the return air enthalpy. During the heating season, DCV reduces the heating requirements for the primary equipment whenever there is a call for heating and the ambient enthalpy is less than the return air enthalpy. Greater ventilation loads and therefore greater savings opportunities for DCV occur in more extreme climates (hot or cold).

Enthalpy Exchanger Heat Recovery (HXHR)

Figure 2 depicts a typical rotary air-to-air enthalpy exchanger. This device is composed of a revolving cylinder filled with an air-permeable medium having a large internal surface area that transfers both heat and moisture between two air streams. The media is typically fabricated from metal, mineral or polymer materials. The heat and moisture transfer occur between the ventilation and exhaust air streams shown in Figure 2. In the cooling season, an enthalpy wheel can precool and dehumidify the ventilation air reducing the load on the primary air conditioning equipment. In the heating season, the ventilation air is typically preheated and humdified. Greater potential for heat recovery occurs in more extreme climates (hot or cold) because of larger temperature and humidity differences between the ventilation and exhaust air streams. Systems with enthalpy exchangers do not typically incorporate controllable dampers and economizers capable of 100% outside air. The ventilation flow is fixed based upon requirements determined using ASHRAE 62-1999. The wheel is usually controlled based upon the ambient temperature. The wheel rotates when the ambient temperature is either above the return air temperature (cooling) or below a temperature where cooling is not expected (e.g., 55 F). Enthalpy exchangers require an additional exhaust fan to overcome the additional pressure drop associated with flow through the heat exchanger media.

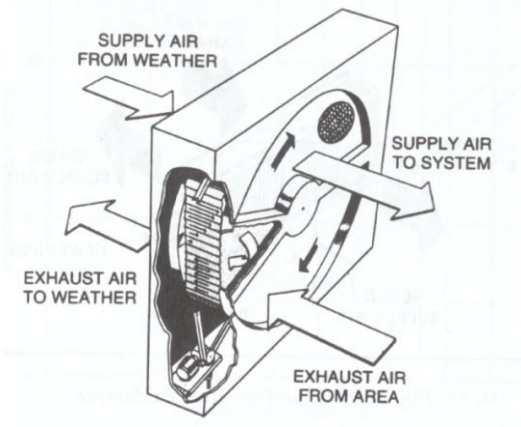

Figure 2. Enthalpy Exchanger (HXHR)

Heat Pump Heat Recovery (HPHR)

Figure 3 shows a heat pump operating between the ventilation and exhaust air streams to recover energy. During the cooling season, the heat pump cools and possibly dehumidifies the ventilation air and rejects heat to the exhaust stream. During the heating season, the heat pump operates in reverse to extract heat from the exhaust air and preheat the outside air. The advantage of this type of system is that the heat pump operates under very favorable conditions as compared with a heat pump having the ambient as a source

(heating) or sink (cooling). The COP of the heat pump for heating improves as the ambient gets colder. Similarly, the COP for cooling improves as the ambient gets hotter. Therefore, the savings opportunities for heat pump heat recovery are better in more extreme (hot or cold) climates.

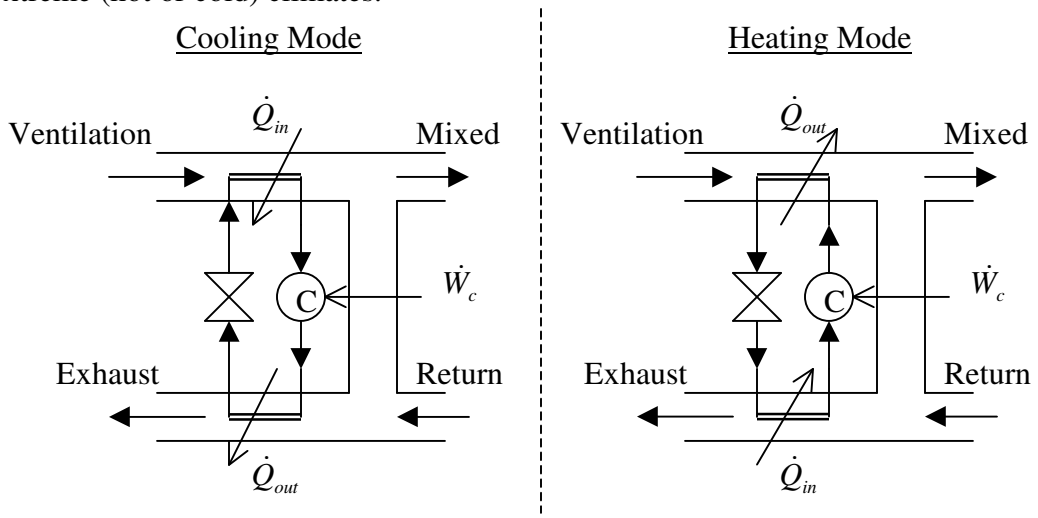

Figure 3. Heat Pump Heat Recovery (HPHR)

Literature Review

Emmerich (2001) performed an extensive literature review for DCV that is a valuable resource in understanding the development and application of DCV technology. With respect to evaluation of energy savings associated with DCV, there have been a number of simulation and field studies. Simulation studies were performed by Knoespel et al. (1991), Haghighat et al. (1993), Carpenter (1996), and Brandemuehl and Braun (1999). These studies demonstrated significant savings associated with the implementation of DCV for both small and large commercial buildings. The largest savings occur for buildings with highly variable occupancy, such as auditoriums and in more extreme climates (hot or cold) where ventilation loads are a larger fraction of the total loads. It is extremely important to use an economizer in conjunction with DCV so as not to lose any free cooling poetenail. For commercial buildings, the percent savings are greater for DCV during the heating season than the cooling season. Also, relative savings are greater for VAV systems than for CAV systems.

Field studies for DCV have been performed by Janssen et al. (1982), Gabel et al. (1986), Donnini et al. (1991), and Zamboni et al. (1991). The savings determined from field results have generally been consistant with the simulation results. The energy savings are significant and greater savings occur for buildings with highly variable occupancies, such as auditoriums. In some cases, the maximum occupancy was a small percentage of the design occupancy used to determine the fixed ventilation rates and the zone CO_2 concentrations never reached the set point. In these situations, infiltration and air leakage through the damper were sufficient to satisfy the ventilation requirements. In some cases, there were some occupant complaints of increased odor during DCV control.

Enthalpy exchangers were initially developed for commercial HVAC applications in the late 1970s. However, assessment of this technology has only recently appeared within the literature. Stiesch et al. (1995), Rengarajan et al. (1996), and Shirey et al. (1996)

evaluated enthalpy exchangers through simulation and found the technology to be economically viable. Greater potential was found for cooling in warm and humid climates. One of the significant factors affecting performance is pressure drop associated with air flow through the media. The additional fan power associated with application of this technology is significant.

Very few studies have been performed to evaluate the application of heat pumps for heat recovery in ventilation systems. Fehrm et al. (2002) estimated that for residential systems in Sweden and Germany, the use of heat pump heat recovery in a forced ventilation system would reduce energy consumption and peak demand by about 20% when compared to a conventional gas-fired boiler system.

Objective

Although individual case studies have been performed for DCV, enthalpy exchanger and heat pump heat recovery systems, the overall economics of these technologies have not been fully evaluated and compared. These are competing technologies and would not be implemented together. The overall objective of the work described in this report is to provide an economic assessment of these alternative ventilation strategies for a range of small commercial buildings in the state of California.

Assessment Approach

The primary approach for assessing the ventilation strategies was to perform detailed simulations to estimate operating costs, economic payback periods and rate of return. A simulation tool, termed the **V**entilation **S**trategy **A**ssessment **T**ool (VSAT) was developed to estimate cost savings associated with different ventilation strategies for small commercial buildings. A set of prototypical buildings and equipment is also part of the model. The tool is not meant for design or retrofit analysis of a specific building, but to provide a quick assessment of alternative ventilation technologies for common building types and specific locations with minimal user input requirements. The goal in developing VSAT was to have a fast, robust simulation tool for comparison of ventilation options that could consider large parametric studies involving different systems and locations. Existing commercial simulation tools do not consider all of the ventilation options of interest for this project.

The buildings considered within VSAT include a small office building, sit-down restaurant, retail store, school class wing, school auditorium, school gymnasium, and school library. All of these buildings are considered to be single zone with a slab on grade (no basement or crawl space). VSAT considers only packaged HVAC equipment, such as rooftop air conditioners with integrated cooling equipment, heating equipment, supply fan, and ventilation. Modifications to the ventilation system are the focus of the tool's evaluation.

Field sites were also established for the DCV and heat pump heat recovery systems. The goals of the field testing were to verify savings and to identify practical problems associated with these technologies. Several field sites were established for DCV that would allow side-by-side testing for different building types in different climates. A single field site was established for the heat pump heat recovery unit in order to verify the performance of the unit.

II. SIMULATION DESCRIPTION

Braun and Mercer (2003a) provide a detailed description of the models employed within VSAT along with validation results. The tool is based upon a program developed by Brandemuehl and Braun (2002). Figure 4 shows an approximate flow diagram for the modeling approach. Given a physical building description, an occupancy schedule, and thermostat control strategy, the building model provides hourly estimates of the sensible cooling and heating requirements needed to keep the zone temperatures at cooling and heating set points. This involves calculation of transient heat transfer from the building structure and internal sources (e.g., lights, people, and equipment). The air distribution model solves energy and mass balances for the zone and air distribution system and determines mixed air conditions supplied to the equipment. The mixed air condition supplied to the primary HVAC equipment depends upon the ventilation strategy employed. The zone temperatures are outputs from the building model, whereas the zone and return air humidities and CO_2 concentrations are calculated by the air distribution model. The equipment model uses entering conditions and the sensible cooling requirement to determine the average supply air conditions. The entering and exit air conditions for the air distribution and equipment models are determined iteratively at each timestep of the simulation using a non-linear equation solver. The economic model predicts hourly operating cost for each system employing a different ventilation strategy based on electrical and gas rate structures. Payback is calculated from annual results with respect to the base case strategy.

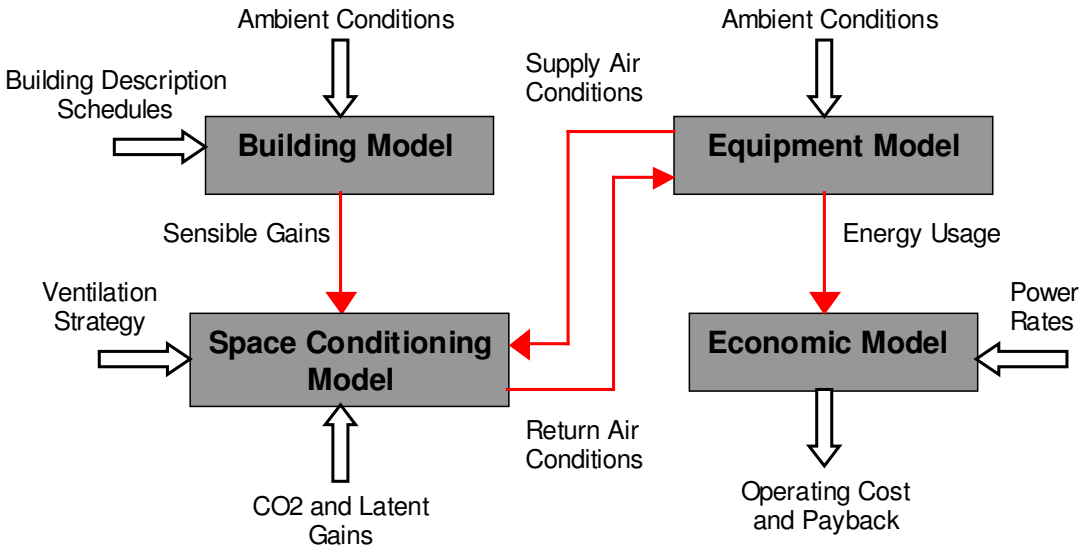

Figure 4. Diagram of VSAT Modeling Approach

Component Modeling Approaches

The building model involves detailed calculations that consider transient conduction through walls using transfer function representations. Predictions of the model compare well with other detailed models from the literature with substantially faster calculation speeds (Braun and Mercer, 2003a).

The space conditioning model follows the approach employed by Brandemuehl and Braun (1999) and employs the use of quasi-steady-state mass and energy balances on the air within the zone and air distribution system. A fixed ventilation effectiveness is employed for the zone to consider short-circuiting of supply air to the return duct. The DCV control is assumed to be ideal: the model determines the minimum ventilation air necessary to maintain the CO_2 set point. The base case and DCV systems employ a differential enthalpy economizer.

Both the primary air conditioning and heat pump heat recovery units are modeled using an approach similar to that incorporated in ASHRAE's *HVAC Toolkit* (Brandemuehl et al., 2000). The model for the primary air conditioner utilizes prototypical performance characteristics, which are scaled according to the capacity requirements and efficiency at design conditions. The characteristics of the heat pump heat recovery unit are based upon measurements obtained from the manufacturer and from tests conducted at the Herrick Labs, which are also scaled for different applications. Braun and Mercer (2002) describe the laboratory testing and development of the heat pump model.

The ventilation heat pump heat recovery unit is only enabled during occupied hours. During unoccupied hours, the primary air conditioner and heater must meet the cooling and heating requirements. In addition, the heat pump will only operate in cooling mode when the ambient temperature is above 68 F. When the heat pump is enabled, it provides the 1st stage for cooling or heating with the 2nd stage provided by the primary air conditioner or heater.

The enthalpy exchanger is modeled using an approach developed by Stiesch et al. (1995). This component model predicts temperature, humidity and enthalpy effectiveness based on a dimensionless wheel speed and media NTU. The enthalpy exchanger operates when the primary fan is on and the ambient temperature is less than 55 F or greater than the return air temperature. When the ambient temperature is between 55 F and the return air temperature, it is assumed that a cooling requirement exists and it is better to bring in cooler ambient air. When the ambient temperature is below 55 F, then a feedback controller adjusts the speed to maintain a ventilation supply air temperature of 55 F. When the ambient temperature is above the return air temperature, then the wheel operates at maximum speed. Feedback control of wheel speed is also initiated under conditions where water vapor in the exhaust stream would condense and freeze. A frost set point is specified based on winter ambient and zone design conditions as discussed by Stiesch (1995).

The primary supply fan operates at a fixed speed and is modeled assuming a constant fan/motor efficiency and overall pressure loss. An additional exhaust fan is included for systems utilizing a heat pump heat recovery unit or enthalpy exchanger.

VSAT was validated by comparing annual equipment loads and power consumptions for similar case studies in Energy-10 (Balcomb, 2002) and TRNSYS (2002). Energy-10 is a design tool developed for the U.S. Department of Energy (DOE) to analyze residential and small commercial buildings. TRNSYS is a complex transient system simulation program that incorporates a detailed building load model (Type-56 multi-zone building component). Neither of these tools incorporates the ventilation strategies considered in this study. Therefore, VSAT was validated for a base case employing the conventional ventilation strategies. In general, the VSAT predictions were within about

5% of the hourly, monthly, and annual predictions from TRNSYS and Energy-10 (Braun and Mercer, 2003a).

Modeling Parameters

The default parameters in VSAT were employed for the simulation results (medium efficiency equipment index with rated air conditioner EER of 9.5 and gas furnace efficiency of 0.75, supply fan power of 0.4 W/cfm, ventilation effectiveness of 0.85, and 350 ppm ambient air CO_2 concentration). The DCV system utilizes a set point for CO_2 concentration in the zone of 1000 ppm. With an 85% ventilation effectiveness, this leads to a return air CO_2 set point of approximately 900 ppm. The exhaust fan power for the enthalpy exchanger and heat pump is 0.5 W/cfm for each unit. Appendix A contains detailed descriptions of the prototypical buildings that are employed within VSAT.

Weather Data

VSAT includes weather data for the California climate zones shown in Figure 5. The representative cities for each climate zone (CZ) are given in Table 1. The climate zones are based on energy use, temperature, weather and other factors. They are basically a geographic area that has similar climatic characteristics. The California Energy Commission (CEC) originally developed weather data for each climate zone by using unmodified (but error-screened) data for a representative city and weather year (representative months from various years). The CEC analyzed weather data from weather stations selected for (1) reliability of data, (2) currency of data, (3) proximity to population centers, and (4) non-duplication of stations within a climate zone. There are two sets of climate zone data included in VSAT, the original and a massaged set. In the massage data, the dry bulb temperature has been modified in an effort to give the file a better "average" across the entire zone. However, because only dry bulb was adjusted, the humidity conditions are affected and therefore, the massaged files are not preferred. The original data set was used for the results presented in this report.

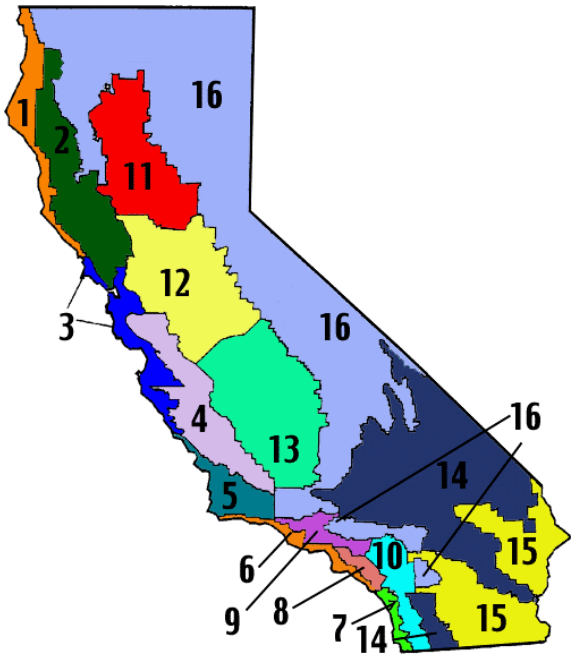

Figure 5. California Climate Zones

Table 1. Cities Associated with California Climate Zones

CZ 1: Arcata	CZ 5: Santa Maria	CZ 9: Pasadena	CZ13: Fresno
CZ 2: Santa Rosa	CZ 6: Los Angeles	CZ10: Riverside	CZ14: China Lake
CZ 3: Oakland	CZ 7: San Diego	CZ11: Red Bluff	CZ15: El Centro
CZ 4: Sunnyvale	CZ 8: El Toro	CZ12: Sacramento	CZ16: Mount Shasta

Economic Analysis

Operating costs associated with each ventilation strategy are calculated based on annual electric power and/or gas consumption by the HVAC equipment. Percent savings for each ventilation strategy are assessed by comparing annual operating costs to the base case. For retrofit applications, simple payback period is used to compare technologies. However, for new buildings, a cumulative rate of return is the performance indice used for comparisons.

The annual operating costs for an HVAC system within VSAT are calculated assuming a three tiered utility rate structure of on-peak, mid-peak and off-peak rates. These costs are calculated according to

$$C_k = \sum_{m=1}^{m=12} \left\{ \begin{array}{c} r_{d,on,m} \cdot \dot{W}_{peak,on,m} + r_{d,mid,m} \cdot \dot{W}_{peak,mid,m} + r_{d,off,m} \cdot \dot{W}_{peak,off,m} \\ + \sum_{i=1}^{N_m} \left(r_{e,i,m} \cdot W_{i,m} + r_{g,i,m} \cdot G_{i,m} \right) \end{array} \right\} \quad (1)$$

where subscript k denotes the HVAC system associated with a particular ventilation strategy k, m is the month and i is the hour of the year. N_m is the number of hours within month m. For each month m, $r_{d,on,m}$, $r_{d,mid,m}$ and $r_{d,off,m}$ correspond to the utility rates for

electricity demand during the on-peak, mid-peak and off-peak time periods ($/kW). Peak power consumption for the HVAC equipment during the on-peak, mid-peak and off-peak periods is represented as $\dot{W}_{peak,on,m}$, $\dot{W}_{peak,mid,m}$ and $\dot{W}_{peak,off,m}$, respectively. For each hour i of month m, r_e is the utility rate associated with electricity usage ($/kWh), W corresponds to the amount of electricity consumed (kWh), r_g is the utility rate associated with natural gas usage ($/therm) and G represents the amount of gas consumed (therm).

Annual electricity costs include both energy ($/kWh) and demand charges ($/kW). Gas energy usage costs do not vary with time of the day. However, the user may enter different electric and gas rates for summer and winter periods. The user may also adjust the start month for the summer and winter periods and the times of day associated with on-peak, mid-peak and off-peak periods.

Each ventilation strategy is compared with an assumed base case of fixed ventilation incorporating a setup/ setback thermostat and differential enthalpy economizer. Annual operating cost savings (S_k) for each ventilation strategy k, when compared to the base case, are calculated according to

$$S_k = C_{BASE.CASE} - C_k \tag{2}$$

Annual operating cost percent savings ($\%S_k$) for each ventilation strategy k are calculated according to

$$\%S_k = \left\{1 - \frac{C_k}{C_{BASE.CASE}}\right\} \cdot 100\% \tag{3}$$

For retrofit analysis, the economics of the different technologies only depend upon the initial costs of the equipment and the energy cost savings. In this case, simple yearly payback (N_{pb}) for each ventilation strategy k is calculated according to

$$N_{pb} = \frac{I_k}{S_k} \tag{4}$$

where I_k is the first cost, including installation and any equipment, associated with implementing ventilation strategy k. If annual operating cost savings for any ventilation strategy are negative, implying the base case is less expensive to operate, payback is not calculated.

For new buildings, additional cost savings can be realized for the enthalpy exchanger and heat pump through reductions in the size of the primary heating and cooling equipment. In this case, payback periods are not a very good performance indice for comparison and rate of return was employed instead. The cumulative rate of return (RR_k) for each ventilation strategy k is calculated according to

$$RR_k = \left(\frac{QS_k - I_k + (N_{cum} \cdot S_k)}{I_k}\right) \cdot 100\% \tag{5}$$

where QS_k is the savings in equipment cost ($) due to primary RTU downsizing compared the base case and N_{cum} represents the number of years (cumulative years) used in calculating the rate of return. The HXHR and HPHR systems require smaller primary RTUs because of energy recovery in the ventilation streams. However, the DCV requires the same equipment capacity as the base case (QS_k =$0) because the system must be able to handle the design ventilation requirement at design conditions.

All utility rates used for economic results assume secondary, firm service (electricity constantly supplied) and a monthly electric demand less than 500 kW. Typical utility rate information was obtained for small commercial service in each of the California climate zones and implemented within VSAT. Table 2 summarizes the utility rates that were considered for each climate zone. Pacific Gas and Electricity (PGE), Southern California Edison (SCE), Southern California Gas (SCG) and San Diego Gas and Electricity (SDGE) are the major utility suppliers in California. The utility rates of each supplier differ depending upon time-of-use. Table 3 shows the time-of-use associated with each utility provider. The cities associated with climate zones 10 (Riverside) and 15 (El Centro) are served by local energy companies. However, for the electric rate structure within VSAT, Southern California Edison was assumed for both climate zones 10 and 15 because the majority of CZ 10 and approximately half of CZ 15 is territory within the service area of Southern California Edison. Southern California Gas Company was also assumed for most all the southern California climate zones except CZ 07, which is serviced by San Diego Gas and Electricity.

For summer electricity consumption, the demand charge for Pacific Gas and Electricity is higher, almost twice that of Southern California Edison; while Pacific Gas and Electricity's energy charge is low, only half of Southern California Edison's energy charge. For Pacific Gas and Electric, the ratio of on-peak to off-peak demand charges is greater than 5, whereas Southern California Edison does not charge demand fees during off-peak times. For energy charges, both companies have on-peak to off-peak ratios of about 2. San Diego's time-of-use energy charge ratio is much lower.

Table 2. Utility Rates in California

CZ	Representative City	Service Provider	Time of Use	Summer Season	Winter Season
1	Arcata		*Demand Charge- $/kW*		
2	Santa Rosa		On Peak	$13.35	N/A
3	Oakland	Pacific Gas	Mid Peak	$3.70	$3.65
4	Sunnyvale	And	Off Peak	$2.55	$2.55
5	Santa Maria	Electricity	*Energy Charge - $/kWh*		
11	Red Bluff	(Schedules E-19	On Peak	0.0877	N/A
12	Sacramento	and G-NR1)	Mid Peak	0.0581	0.0639
13	Fresno		Off Peak	0.0506	0.0504
			Gas Charge - $/therm		
				$0.6736	$0.7422
6	Los Angeles		*Demand Charge- $/kW*		
8	El Toro	Southern	On Peak	$7.75	$0.00
9	Pasadena	California Edison	Mid Peak	$2.45	$0.00
10	Riverside	(Schedule TOU-	Off Peak	$0.00	$0.00
14	China Lake	GS-2) and	*Energy Charge - $/kWh*		
15	El Centro	Southern	On Peak	0.2960	N/A
16	Mount Shasta	California Gas	Mid Peak	0.1176	0.1296
		(Schedule GN-10)	Off Peak	0.0942	0.0942
			Gas Charge - $/therm		
				$0.7079	$0.7079
7	San Diego		*Demand Charge- $/kW*		
			On Peak	$10.42	$4.83
		San Diego Gas	Mid Peak	N/A	N/A
		and Electricity	Off Peak	N/A	N/A
		(Schedules AL-	*Energy Charge - $/kWh*		
		TOU and EECC	On Peak	$0.1163	$0.1151
		and GN-3)	Mid Peak	$0.0895	$0.0894
			Off Peak	$0.0884	$0.0884
			Gas Charge - $/therm		
				$0.6524	$0.7497

Table 3. Time-Of-Use for California Utility Companies

PGE			
Summer:	May 1 - Oct. 31	Winter:	Nov. 1 - April 30
On-Peak	12:00 - 6:00, M - F	On-Peak	N/A
Mid-Peak	8:00 AM - 12:00 &	Mid-Peak	8:00 AM - 9:00 PM, M - F
	6:00 PM - 9:00 PM, M - F		
Off-Peak	9:00 PM - 8:00 AM, all week	Off-Peak	9:00 PM - 8:00 AM, all week
SCE			
Summer:	June 1 - Sept. 30	Winter:	Oct. 1 - May 31
On-Peak	12:00 - 6:00, M - F	On-Peak	N/A
Mid-Peak	8:00 AM - 12:00 &	Mid-Peak	8:00 AM - 9:00 PM, M - F
	6:00 PM - 11:00 PM, M - F		
Off-Peak	11:00 PM - 8:00 AM, all week	Off-Peak	9:00 PM - 8:00 AM, all week
SDGE - Electric Rate			
Summer:	May 1 - Sept. 30	Winter:	Oct. 1 - April 30
On-Peak	11:00 - 6:00, M - F	On-Peak	5:00 - 8:00, M - F
Mid-Peak	6:00 AM - 11:00 &	Mid-Peak	6:00 AM - 5:00 PM &
	6:00 PM - 10:00 PM, M - F		8:00 PM - 10:00 PM, M - F
Off-Peak	10:00 PM - 6:00 AM, all week	Off-Peak	10:00 PM - 6:00 AM, all week
SDGE - Gas Rate			
Summer:	April 1 - Nov. 30	Winter:	Dec. 1 - March 31
SCG			
Summer:	April 1 - Nov. 30	Winter:	Dec. 1 - March 31

First costs for demand controlled ventilation, the heat pump and enthalpy exchanger were obtained from personal contact with representatives from each specific equipment manufacturer. The first costs included equipment and installation costs associated with each ventilation strategy.

For DCV, the number of rooftop units employed for a particular HVAC system must be known in order to determine the associated first costs. It is difficult to ascertain how many DCV controllers, or rooftop units are necessary for a given application. This situation is very sensitive to the dynamics of the duct runs, availability of space and actual number of RTUs that may or may not accommodate the specific building. The economic analysis assumed that RTUs are available in sizes of 5, 7.5, 10, 15 and 20 ton cooling capacities. For a simulated prototypical building and location, the number of individual RTUs was determined based upon utilizing the fewest possible number of units necessary to realize a cooling capacity that was within a target range of 5% of the sized equipment cooling capacity. First costs for DCV included a DCV logic controller, zone CO_2 sensor and 4 hours time for installation. These costs combined were estimated at $900 per RTU within VSAT.

The heat pump first costs were based on the actual equipment, installation, controls and thermostat costs. Based on correspondence with manufacturer's representatives, $5 per/cfm ventilation air was assumed for calculating a generalized first cost of the heat pump.

The enthalpy exchanger first costs include the same elements as for the heat pump, however, $2 per/cfm ventilation air is assumed. Enthalpy exchangers do not require as many components as a heat pump and are easier to manufacture, therefore the equipment cost is lower.

A value of $1000 per ton was assumed for installed costs of RTUs in calculating the equipment cost savings for new building applications. Savings in primary heater costs were not considered.

III. SIMULATION RESULTS

Sample Hourly Results

Systems with DCV generally have higher zone CO_2 concentrations because of lower ventilation rates. Figure 6 and Figure 7 show example weekday hourly CO_2 levels for the different ventilation strategies when applied to the restaurant and office building prototypes. These example days were simulated on July 19 in CZ 15. The zone CO_2 levels track the occupancy schedules and are identical for the base case, HPHR and HXHR cases because the ventilation rates are identical. The CO_2 levels for the base case can be lower than the HXHR and HPHR levels when the economizer operates, however, economizer operation did not occur on this particular day. The CO_2 levels are higher for the DCV+EC strategy due to lower ventilation rates. For the restaurant, the CO_2 concentrations were at the set point for a large portion of the occupied period. However, the set point was not reached for the office on this day. For the office, the average occupancy was low enough that infiltration (0.05 cfm/ft^2) provided sufficient fresh air to keep CO_2 levels in the zone below 1000 ppm. If infiltration did not exist, then an outdoor air fraction of about 0.06 would be necessary, on average, during the occupied period to maintain the zone CO_2 concentration at 1000 ppm in the office.

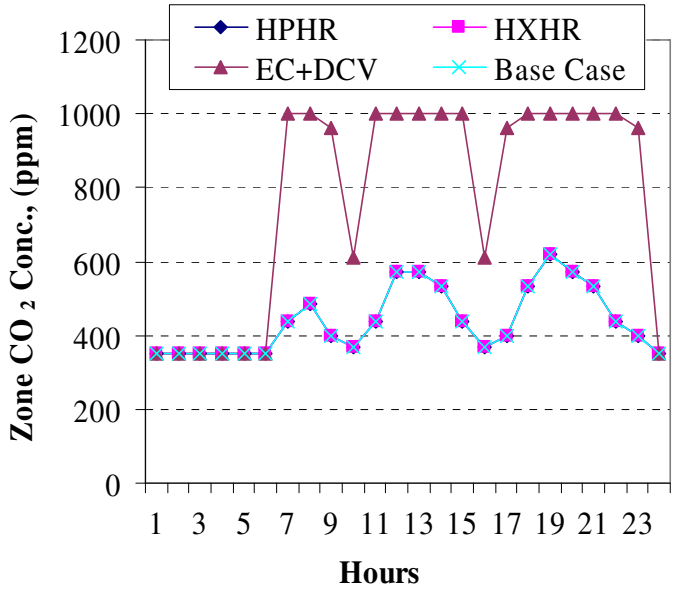

Figure 6. Hourly Zone CO_2 Concentration – Restaurant

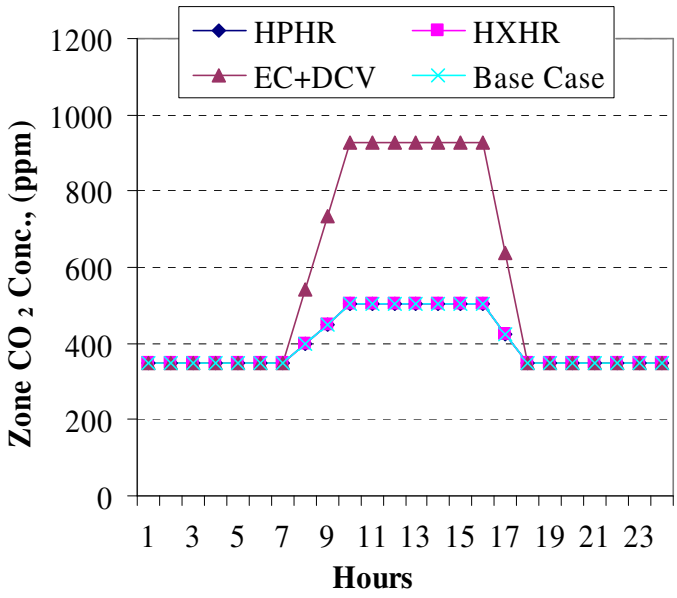

Figure 7. Hourly Zone CO_2 Concentration - Office

The different systems also lead to different humidity levels in the zone. Both the heat pump and enthalpy exchanger can remove moisture from the ventilation stream during the cooling season. The use of DCV can also lead to lower moisture levels when the ambient air is more humid than the zone air. Figure 8 and Figure 9 show sample hourly relative humidities for the restaurant in CZ 06 and the office in CZ 15 during summer.

For the more humid CZ 06, DCV plus economizer gave the lowest humidity levels except during economizer operation (e.g., morning hours for the restaurant). Also, the enthalpy exchanger had greater moisture removal from the ventilation air than the heat pump during occupied mode for CZ 06.

The heat pump and base case gave the lowest humidity levels in CZ 15 because this is a dry climate and the ventilation did not introduce an additional latent load. The heat pump did not dehumidify the air on this day and therefore the relative humidity in the zone was the same for the HPHR and base case case systems. The enthalpy exchanger actually transferred moisture from the exhaust stream and humidified the ventilation air. Thus, zone relative humidities for the enthalpy exchanger were higher than the base case for CZ 15. DCV+EC leads to lower outside air and therefore humidity levels in the zone were higher than for to the other ventilation strategies in this dry climate.

Clearly, the impact of the ventilation technology on zone humidity levels is very dependent on the climate. Both DCV and the HXHR systems provide higher humidity levels in dry climates and lower humidity levels in more humd climates than the base case. Both of these trends are good. The HPHR system provides lower humidity levels in humid climates and the same humidity levels in dry climates as the base case.

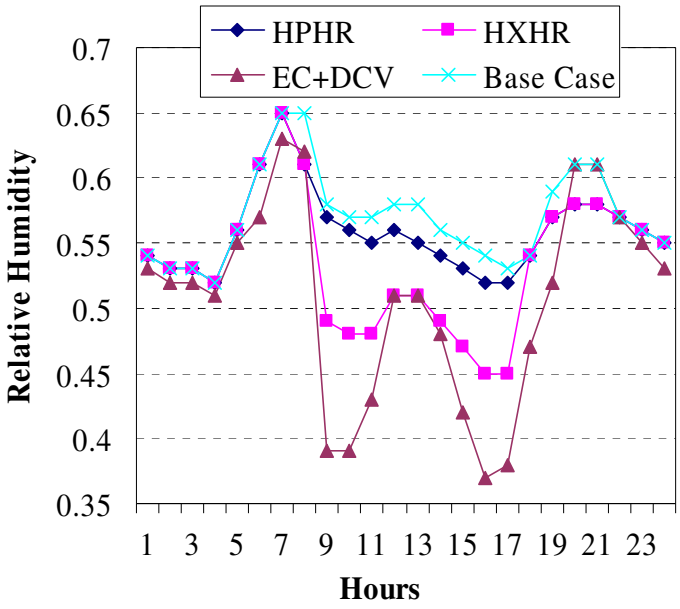

Figure 8. Relative Humidity – Restaurant, CZ06, June 20

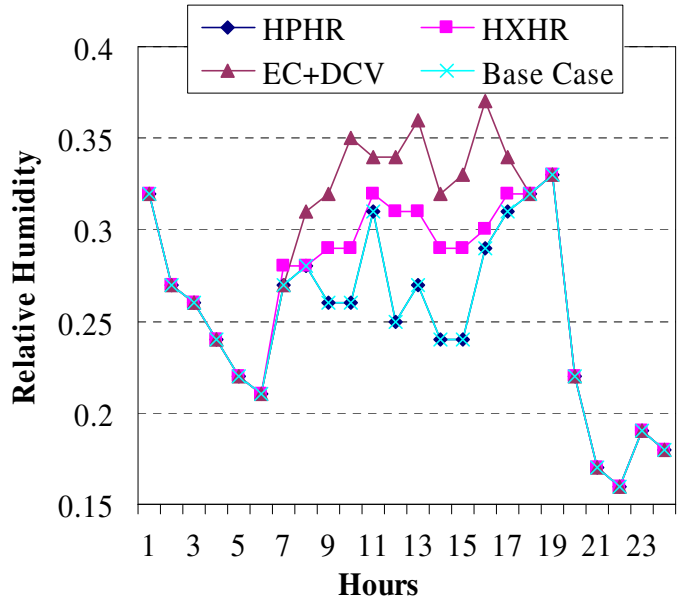

Figure 9. Relative Humidity – Office, CZ15, June 20

Implementation of any particular ventilation strategy should reduce the load and power consumption associated with the primary air conditioner. However, for the HPHR system, this power reduction is at the expense of power usage associated with the HPHR compressor. For both the HPHR and HXHR systems, an additional exhaust fan is also required to provide proper exhaust air flowrates for heat and mass exchange. The wheel medium and extra heat exchanger typically add 0.5 to 0.9 inches H_2O of pressure drop that must be overcome. The total fan power consumption of the heat pump or enthalpy

exchanger plays a significant role in determining if either of these ventilation strategies is competitive when compared to the base case.

Figure 10 shows an example of hourly power consumption for the restaurant. The fan power for the heat pump and enthalpy exchanger is notably increased over the fan power for the base case and DCV+EC strategies. The "compressor power" includes power usage for the primary AC compressor and condenser fan and the HPHR compressor (for HPHR case). Although the total AC and heat pump compressor power input is slightly less than the compressor power for the base case, it is not sufficient to offset the increase in fan power at any time of the day for this example. However, for the HXHR system, the decrease in AC compressor power does overcome the additional power required for the exhaust fan.

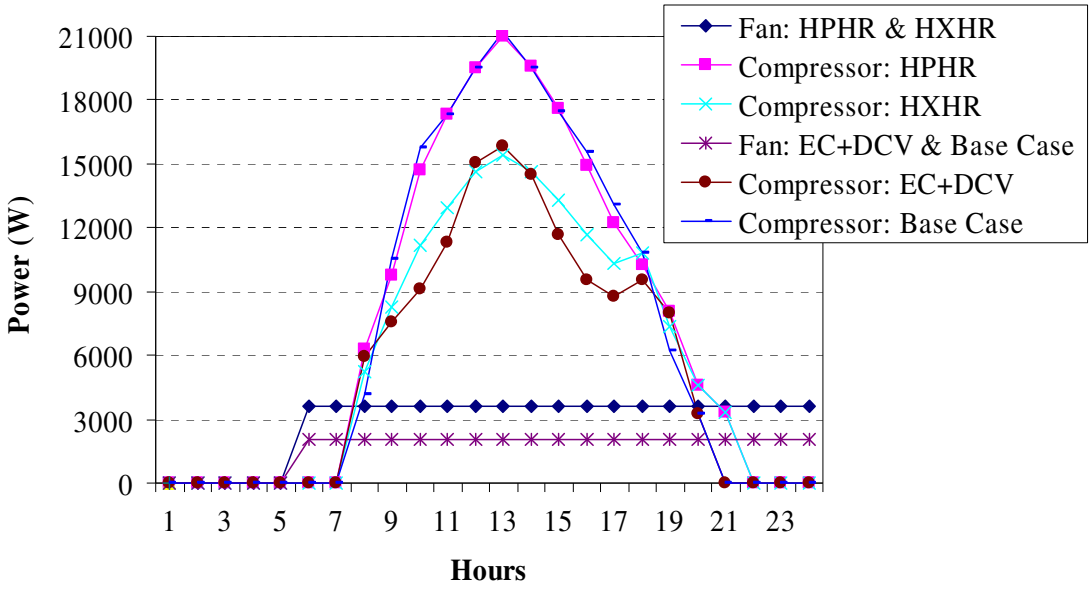

Figure 10. Equipment Power Consumption – Restaurant, CZ06, June 20

Each ventilation strategy also reduces primary energy consumption associated with heating. However, for the HPHR and HXHR systems, these reductions are offset by increases in electric power consumption. Figure 11 shows example hourly gas consumption for each of the strategies for the restaurant on January 20 in CZ 16. Figure 12 shows the corresponding electrical power consumption associated with each strategy and the base case for the same day. For this example day, all of the strategies result in reduced gas consumption when compared with the base case. However, the DCV+EC strategy results in the lowest gas consumption and there is no penalty associated with increased power requirements. From Figure 12, the power for the HPHR system is considerably higher than the power for the base case due to the additional compressor and fan. The power for the HXHR system is also greater than the base case because of the additional fan requirement.

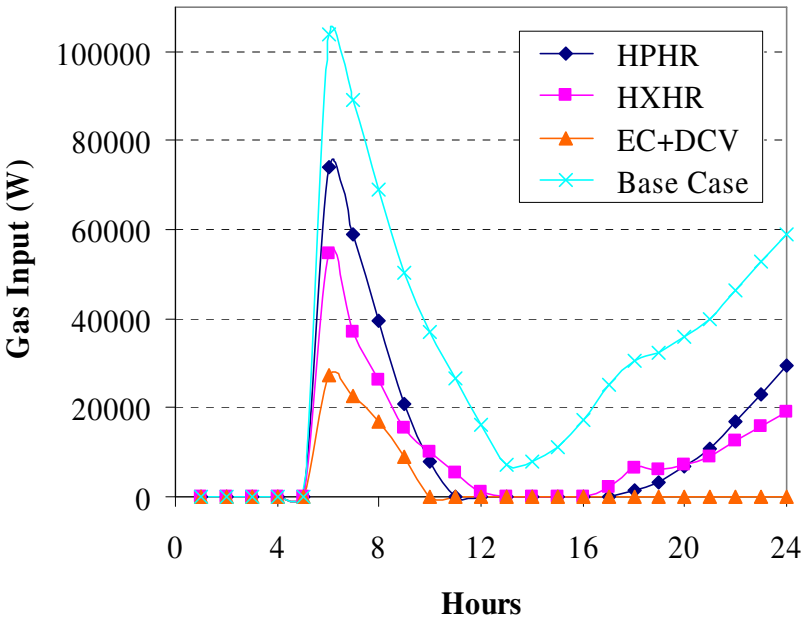

Figure 11. Furnace Gas Input – Restaurant, CZ16, Jan. 20

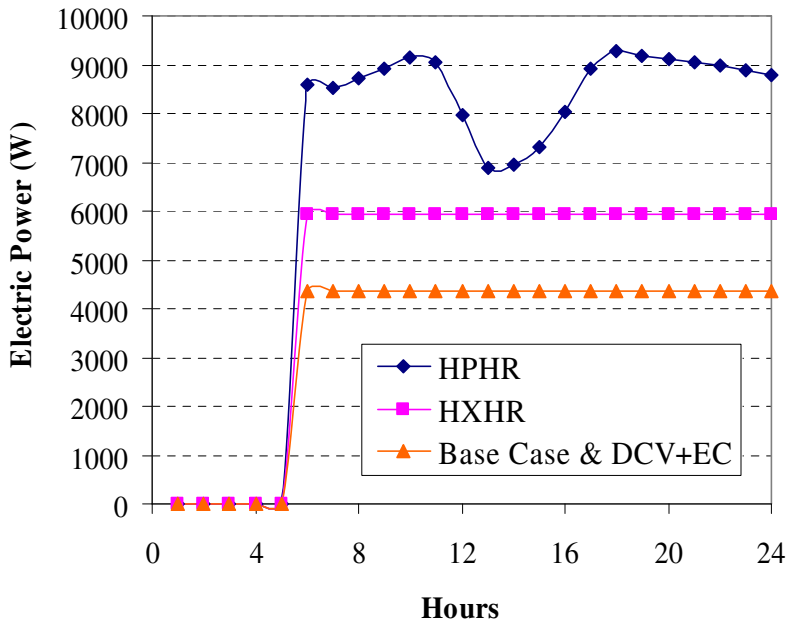

Figure 12. Electric Power Input – Restaurant, CZ16, Jan. 20

Figure 13 shows the daily operating cost for this example day for each ventilation strategy. All of the strategies result in some overall savings for this day when compared to the base case. However, HPHR savings are very small. As ambient temperatures get

colder and occupied periods last longer, the heat pump performs much better and approaches the performance of the enthalpy exchanger. CZ 16 requires the most heating when compared to all other climate zones within California. Since California is a mild climate, the savings potential of the HPHR technology is not very significant when compared to the savings potential in other colder areas of the United States. This consequence will be further investigated in a later section.

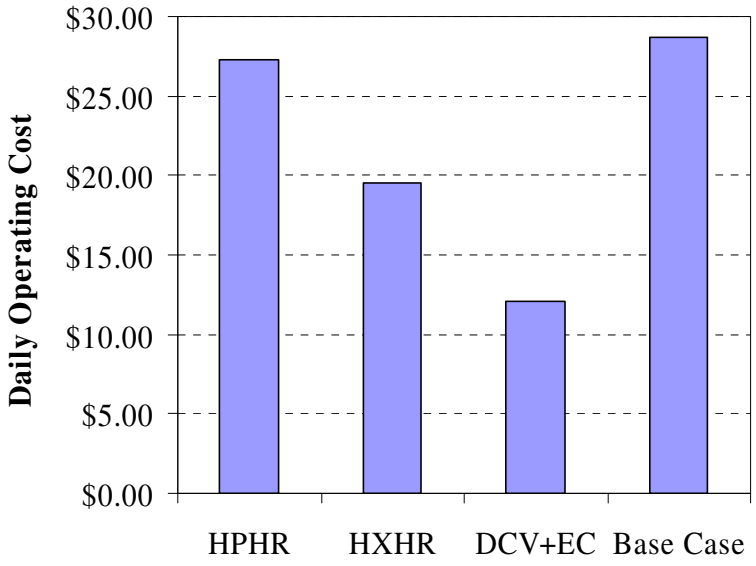

Figure 13. Daily Restaurant Operating Costs, CZ16, Jan. 20

Annual Operating Cost Savings

The cost savings associated with demand-controlled ventilation and an economizer (DCV+EC), heat pump heat recovery (HPHR) and the enthalpy exchanger (HXHR) were compared on a percent savings basis relative to the assumed base case (fixed ventilation with a differential economizer). Appendix B gives annual energy usage and costs for the base case applied to the seven prototypical buildings in the 16 California climate zones. The percent savings were calculated according to

$$Y = \left[1 - \frac{X.vent.strategy}{X.base.case}\right] * 100\% \tag{5}$$

where; Y = relative percent savings

$X.vent.strategy$ = quantity under consideration for the specific ventilation strategy (DCV+EC, HXHR, or HPHR)

$X.base.case$ = quantity under consideration for the base case

Table 4 through Table 10 give percent savings for each of the strategies applied to all prototypical buildings in all climate zones assuming a retrofit application. Four quantities are compared for each building type: total electrical energy costs, electric demand costs,

gas costs and total equipment operating costs. Negative savings imply that the strategy had greater costs than the base case.

The greatest savings potential for all the building types is associated with demand-controlled ventilation with an economizer. For DCV+EC, the ventilation load is directly related to the occupancy schedule. For most buildings, the average occupancies are much lower than the design occupancy used to determine fixed ventilation rates. The total cost savings for DCV+EC ranged from about 1% to 48%, whereas the electrical demand savings were between 1% and 52%. The greatest savings for DCV+EC among the building types occurred for the school auditorium and school gym. Both of these building types have intermittent occupancy schedules and average occupancies that are a small fraction of the peak design occupancy. The heating load for DCV is practically eliminated for several building types where internal gains tend to balance other heat losses from the building. Even greater overall DCV+EC cost savings would be expected in climates that have significantly greater heating loads than occur for California.

The enthalpy exchanger was the next most effective ventilation strategy for the cases considered. The percent savings in gas costs are significant in most cases. However, gas costs are relatively low for these climates and therefore these savings have a relatively small impact on total savings. In most cases, the electrical energy costs are higher for the HXHR system than for the base case due to two effects: 1) increased fan energy and 2) loss of significant free cooling opportunities without an economizer. However, there are significant demand cost savings in many cases. The greatest electrical energy and demand cost savings occur for buildings and locations that have the highest ventilation loads. Positive total cost savings occurred for the central and eastern portions of the state for the restaurant, retail store, auditorium and gym. These regions have the most extreme ambient temperatures and these buildings have the highest peak occupant densities. With high ambient temperatures, there is less opportunity for economizer operation and better opportunities for heat recovery. Both of these effects tend to increase savings associated with the HXHR system.

The trends for the heat pump heat recovery system are similar to the HXHR system, but the overall performance is worse. The savings in gas consumption are actually greater than those for the HXHR, but at the expense of increased electrical usage for heating. In almost every situation, the HPHR system had greater overall operating costs than the base case. In general, the cooling COP for the HPHR unit increases with ambient wet bulb temperature whereas the heating COP increases with decreasing ambient temperature. The performance of the HPHR unit needs to be “good enough” so that primary equipment savings offset increases in electrical energy due to the HPHR compressor and exhaust fan. Overall cooling savings only occur at very high ambient wet bulb temperatures. For heating, positive savings can be at relatively moderate ambient temperatures. However, the California climate zones are all relatively moderate and any savings associated with heating are not sufficient to offset increases in cooling season costs.

Table 4. Office Savings Comparisons

	Demand Controlled Ventilation + EC				**Heat Pump Heat Recovery**				**Enthalpy Exchanger**			
	Elec. Energy, %	Elec. Dmd, %	Gas, %	Total, %	Elec. Energy, %	Elec. Dmd, %	Gas, %	Total, %	Elec. Energy, %	Elec. Dmd, %	Gas, %	Total, %
CACZ01	-0.9	7.6	54.1	9.2	-66.7	-11.1	29.8	-22.5	-65.0	-8.4	20.0	-21.2
CACZ02	3.6	6.6	50.0	7.7	-20.6	-3.3	29.8	-7.8	-18.1	1.1	24.8	-4.5
CACZ03	2.3	8.4	56.8	7.5	-37.0	-5.7	36.4	-15.5	-35.7	1.6	22.7	-10.8
CACZ04	8.0	13.7	53.6	12.5	-20.0	-2.7	34.4	-8.4	-15.9	6.1	25.6	-1.9
CACZ05	0.4	2.6	50.0	2.7	-31.6	-2.0	36.5	-12.1	-30.2	2.7	24.3	-8.9
CACZ06	5.0	13.8	66.7	6.6	-23.5	-2.8	50.0	-20.1	-21.9	6.3	25.0	-17.4
CACZ07	5.6	6.1	66.7	5.9	-24.9	-10.4	55.6	-20.6	-22.4	-2.9	33.3	-16.7
CACZ08	6.9	14.6	51.6	8.3	-16.2	-1.6	38.7	-13.6	-12.3	8.1	22.6	-9.0
CACZ09	7.1	15.5	70.0	8.6	-14.9	0.6	55.0	-12.2	-10.9	9.3	40.0	-7.5
CACZ10	6.9	11.0	45.2	7.9	-12.4	0.9	30.6	-10.0	-9.0	6.2	21.0	-6.4
CACZ11	3.8	2.3	50.0	5.0	-14.9	-2.0	29.4	-5.7	-12.2	1.3	24.4	-3.0
CACZ12	6.0	10.0	51.2	10.0	-16.7	-2.5	27.7	-6.9	-13.3	2.3	23.9	-3.0
CACZ13	6.7	9.5	51.8	9.4	-11.3	-1.4	28.9	-4.8	-7.8	3.7	24.7	-0.6
CACZ14	3.0	7.4	43.5	5.1	-9.8	1.3	23.1	-6.9	-7.8	5.4	25.4	-4.6
CACZ15	8.4	11.8	54.5	9.0	-4.3	1.2	40.9	-3.5	-0.3	7.3	31.8	0.7
CACZ16	3.7	7.2	44.4	10.8	-22.6	-0.9	23.5	-11.7	-18.2	5.1	24.9	-7.6

Table 5. Restaurant Savings Comparisons

	Demand Controlled Ventilation + EC				**Heat Pump Heat Recovery**				**Enthalpy Exchanger**			
	Elec. Energy, %	Elec. Dmd, %	Gas, %	Total, %	Elec. Energy, %	Elec. Dmd, %	Gas, %	Total, %	Elec. Energy, %	Elec. Dmd, %	Gas, %	Total, %
CACZ01	-21.3	1.4	99.9	35.0	-139.1	-19.8	90.8	-0.8	-89.4	-13.3	43.7	-6.4
CACZ02	3.4	10.3	99.4	24.1	-41.6	-2.8	83.3	-0.8	-26.4	8.4	56.2	4.8
CACZ03	-5.3	9.2	100.0	17.9	-64.3	-7.9	92.1	-11.3	-50.4	6.6	47.1	-5.7
CACZ04	5.9	21.1	99.9	23.4	-37.1	-1.7	86.1	-6.3	-24.4	16.6	56.6	4.9
CACZ05	-8.7	3.4	100.0	12.3	-58.7	-2.4	88.0	-9.3	-47.5	5.9	53.0	-5.9
CACZ06	0.0	20.6	100.0	8.0	-42.7	-6.2	94.8	-30.4	-36.9	13.2	42.4	-25.4
CACZ07	2.6	15.2	100.0	10.2	-44.9	-12.7	93.3	-30.3	-37.1	4.3	51.3	-22.3
CACZ08	6.9	21.4	100.0	12.8	-31.0	-1.9	91.0	-21.8	-21.8	17.4	54.5	-13.0
CACZ09	9.2	22.1	100.0	13.8	-25.1	0.1	92.0	-17.9	-16.0	19.0	58.7	-8.7
CACZ10	10.6	22.2	100.0	16.3	-20.2	4.2	86.5	-12.1	-11.0	18.6	61.1	-3.8
CACZ11	8.1	11.7	99.3	22.7	-27.6	2.0	84.4	1.3	-14.9	12.8	57.6	7.6
CACZ12	8.1	15.3	99.7	24.2	-31.6	-2.2	85.7	-1.8	-18.3	11.4	56.5	5.7
CACZ13	12.2	18.6	99.8	22.9	-20.1	0.4	84.9	-1.4	-8.8	14.0	58.8	7.6
CACZ14	9.6	16.5	98.4	20.1	-18.4	7.8	74.1	-5.3	-6.7	19.5	64.3	4.1
CACZ15	18.4	25.4	100.0	20.2	-5.3	5.7	87.5	-2.9	5.4	22.2	65.9	8.0
CACZ16	3.5	16.6	95.1	35.8	-54.4	2.5	70.9	-5.9	-28.7	14.3	62.3	6.7

Table 6. Retail Store Savings Comparisons

	Demand Controlled Ventilation + EC				**Heat Pump Heat Recovery**				**Enthalpy Exchanger**			
	Elec. Energy, %	Elec. Dmd, %	Gas, %	Total, %	Elec. Energy, %	Elec. Dmd, %	Gas, %	Total, %	Elec. Energy, %	Elec. Dmd, %	Gas, %	Total, %
CACZ01	-17.8	11.5	100.0	23.4	-97.3	-19.3	88.2	-15.4	-76.3	-12.0	56.0	-13.3
CACZ02	6.9	18.7	100.0	22.2	-34.1	-2.5	80.0	-6.4	-23.8	9.9	66.3	2.6
CACZ03	-2.2	19.0	100.0	16.6	-53.3	-8.7	88.8	-18.3	-47.2	6.8	61.7	-8.8
CACZ04	9.0	31.8	100.0	25.7	-31.4	-2.6	82.0	-10.5	-22.0	16.2	69.2	3.1
CACZ05	-6.4	11.7	100.0	8.8	-48.4	-3.0	82.4	-16.2	-44.7	5.4	70.0	-10.5
CACZ06	1.4	31.0	100.0	6.7	-34.4	-6.6	93.0	-29.1	-31.7	12.4	73.6	-24.2
CACZ07	4.4	21.3	100.0	9.7	-38.5	-11.9	93.6	-30.4	-33.6	4.9	85.6	-22.4
CACZ08	8.8	33.4	100.0	13.4	-27.0	-2.3	86.7	-22.1	-19.5	17.7	74.6	-13.0
CACZ09	11.0	35.7	100.0	15.2	-23.7	0.7	93.2	-19.4	-15.2	19.6	85.9	-9.4
CACZ10	14.2	31.1	100.0	17.8	-17.4	3.1	81.4	-13.1	-9.0	17.8	74.9	-4.1
CACZ11	11.1	12.5	100.0	19.3	-23.2	1.7	82.5	-2.3	-12.6	12.9	65.5	6.3
CACZ12	11.3	23.9	100.0	24.2	-26.8	-1.0	82.9	-5.8	-16.5	12.2	66.1	4.0
CACZ13	16.3	28.1	100.0	26.0	-16.8	-0.2	81.7	-4.1	-6.6	13.9	67.7	6.9
CACZ14	12.4	18.1	99.7	18.6	-14.8	7.5	70.9	-6.7	-5.4	18.9	70.7	2.3
CACZ15	22.6	35.7	100.0	24.3	-4.8	5.3	85.4	-3.4	5.8	21.6	86.7	7.8
CACZ16	5.9	23.7	99.1	32.2	-46.1	0.4	70.6	-10.0	-26.8	13.6	65.5	2.2

Table 7. School Library Savings Comparisons

	Demand Controlled Ventilation + EC				**Heat Pump Heat Recovery**				**Enthalpy Exchanger**			
	Elec. Energy, %	Elec. Dmd, %	Gas, %	Total, %	Elec. Energy, %	Elec. Dmd, %	Gas, %	Total, %	Elec. Energy, %	Elec. Dmd, %	Gas, %	Total, %
CACZ01	-5.8	4.3	75.8	17.1	-78.4	-15.7	63.0	-14.3	-63.7	-10.2	28.5	-14.8
CACZ02	3.1	6.5	74.0	11.4	-26.5	-2.9	55.3	-6.0	-19.9	4.1	36.0	-1.7
CACZ03	-1.0	9.3	82.9	10.3	-46.4	-5.9	62.9	-15.2	-41.9	4.9	31.4	-9.0
CACZ04	5.9	14.9	82.7	14.6	-25.5	-2.6	58.0	-8.7	-18.7	10.2	38.3	0.3
CACZ05	-3.3	-0.1	88.1	2.0	-38.8	-2.6	61.9	-13.3	-36.4	3.3	42.9	-9.6
CACZ06	1.3	17.2	100.0	4.4	-33.1	-2.1	75.0	-27.6	-30.8	10.5	50.0	-23.7
CACZ07	3.7	8.5	100.0	5.5	-34.0	-10.5	80.0	-26.8	-30.5	0.6	60.0	-21.2
CACZ08	5.5	16.6	94.1	8.0	-22.0	-2.3	64.7	-18.2	-16.6	11.3	47.1	-11.7
CACZ09	5.8	17.4	100.0	8.2	-20.2	0.3	76.9	-16.4	-14.4	12.2	53.8	-9.8
CACZ10	7.4	13.0	90.0	9.3	-15.1	0.3	56.7	-11.9	-9.9	9.0	46.7	-6.4
CACZ11	4.8	4.4	66.3	9.6	-18.1	-0.9	53.6	-3.4	-12.1	4.2	33.1	0.0
CACZ12	5.9	11.0	71.4	13.4	-22.1	-1.5	55.7	-5.5	-15.3	6.2	34.3	-0.3
CACZ13	8.0	10.6	73.2	12.6	-13.5	-1.6	56.3	-3.9	-7.0	7.0	34.8	2.3
CACZ14	4.3	8.4	70.3	8.6	-11.6	0.8	46.2	-6.5	-7.1	6.2	41.4	-2.5
CACZ15	10.0	13.7	88.9	10.7	-5.3	1.4	66.7	-4.3	0.5	8.9	55.6	1.7
CACZ16	3.5	11.7	56.1	17.7	-31.6	-1.6	41.9	-9.2	-20.3	6.6	35.5	-2.7

Table 8. School Gym Savings Comparisons

	Demand Controlled Ventilation + EC				**Heat Pump Heat Recovery**				**Enthalpy Exchanger**			
	Elec. Energy, %	Elec. Dmd, %	Gas, %	Total, %	Elec. Energy, %	Elec. Dmd, %	Gas, %	Total, %	Elec. Energy, %	Elec. Dmd, %	Gas, %	Total, %
CACZ01	-11.5	1.7	59.8	24.8	-166.1	-38.3	66.8	-8.7	-89.3	-21.1	15.2	-13.7
CACZ02	8.3	13.6	59.2	19.4	-32.4	-5.7	58.0	-2.2	-16.6	6.4	23.2	3.6
CACZ03	2.3	16.8	66.7	21.2	-56.5	-11.0	69.7	-8.4	-38.0	5.1	17.6	-1.8
CACZ04	14.2	27.2	65.3	27.6	-29.2	-4.7	62.4	-4.4	-14.5	15.5	22.5	8.6
CACZ05	-0.4	12.2	73.0	14.8	-44.3	-4.9	68.2	-7.3	-33.4	4.3	19.9	-3.0
CACZ06	8.8	28.3	88.2	16.3	-29.6	-2.5	80.3	-19.2	-23.4	11.0	22.2	-13.6
CACZ07	11.8	26.3	94.4	19.4	-27.5	-4.3	88.7	-15.8	-19.1	16.0	31.5	-4.6
CACZ08	14.3	30.7	79.8	20.1	-18.4	-3.6	71.1	-12.3	-8.7	16.8	24.3	-1.7
CACZ09	13.5	29.5	84.2	19.0	-14.8	0.1	76.3	-9.1	-6.2	17.3	33.8	0.3
CACZ10	14.4	25.7	75.9	18.8	-11.8	-0.4	65.6	-6.9	-3.6	14.5	28.5	1.4
CACZ11	8.6	8.6	53.5	14.3	-20.2	-0.3	52.5	0.7	-9.2	9.6	23.1	5.9
CACZ12	11.8	19.8	57.5	22.2	-23.0	-2.8	57.0	-1.2	-10.2	9.4	23.1	5.5
CACZ13	13.0	19.9	58.4	20.9	-14.2	-3.1	57.4	-1.6	-3.8	10.5	23.0	6.9
CACZ14	9.9	20.2	60.6	16.8	-11.3	3.0	50.3	-2.5	-3.2	12.9	32.0	3.3
CACZ15	15.3	28.2	86.1	18.0	-2.5	2.8	77.0	-1.0	5.3	17.7	41.0	7.6
CACZ16	9.5	24.1	48.5	26.1	-41.5	-2.1	41.6	-4.6	-18.6	11.8	27.7	3.6

Table 9. School Classroom Wing Savings Comparisons

	Demand Controlled Ventilation + EC				**Heat Pump Heat Recovery**				**Enthalpy Exchanger**			
	Elec. Energy, %	Elec. Dmd, %	Gas, %	Total, %	Elec. Energy, %	Elec. Dmd, %	Gas, %	Total, %	Elec. Energy, %	Elec. Dmd, %	Gas, %	Total, %
CACZ01	-3.7	3.9	99.3	7.4	-88.1	-13.9	81.3	-30.2	-88.2	-13.0	74.6	-30.0
CACZ02	4.0	6.5	95.7	9.0	-32.5	-4.0	76.1	-11.8	-29.4	3.4	78.7	-6.2
CACZ03	-0.3	8.2	99.0	6.5	-57.2	-7.4	84.0	-23.7	-57.1	2.9	77.0	-17.3
CACZ04	6.0	11.1	99.3	10.4	-33.2	-3.8	84.6	-14.2	-28.8	10.7	85.3	-3.9
CACZ05	-2.3	1.6	100.0	1.0	-49.5	-2.6	89.2	-19.5	-50.2	2.9	92.3	-16.5
CACZ06	-0.2	14.6	100.0	2.1	-45.6	-0.9	100.0	-38.6	-44.0	12.0	75.0	-35.2
CACZ07	3.4	11.9	100.0	5.8	-41.8	-9.1	100.0	-32.5	-39.0	3.7	100.0	-26.8
CACZ08	5.7	15.2	100.0	7.3	-27.6	-2.9	95.8	-23.6	-23.0	13.6	95.8	-17.2
CACZ09	6.5	17.6	100.0	8.3	-26.8	1.0	100.0	-22.4	-21.4	16.6	100.0	-15.4
CACZ10	8.6	14.0	100.0	9.8	-19.4	0.9	87.5	-16.0	-14.5	13.1	92.2	-10.1
CACZ11	6.7	7.7	93.7	10.8	-21.9	-1.2	76.4	-6.9	-17.1	4.9	74.5	-1.7
CACZ12	6.8	9.3	97.3	11.1	-26.4	-3.6	75.9	-10.5	-21.5	5.1	76.5	-3.7
CACZ13	9.5	10.1	98.1	11.7	-16.8	-3.0	77.0	-7.5	-11.0	7.4	78.2	0.6
CACZ14	7.2	12.6	93.3	10.7	-13.8	3.2	66.7	-8.9	-9.6	10.3	80.5	-3.9
CACZ15	13.1	17.4	100.0	13.7	-6.2	2.2	100.0	-5.1	1.2	14.1	100.0	2.8
CACZ16	3.9	11.9	84.9	18.7	-36.6	-2.4	65.3	-14.3	-27.4	7.6	71.3	-5.4

Table 10. School Auditorium Savings Comparisons

	Demand Controlled Ventilation + EC				**Heat Pump Heat Recovery**				**Enthalpy Exchanger**			
	Elec. Energy, %	Elec. Dmd, %	Gas, %	Total, %	Elec. Energy, %	Elec. Dmd, %	Gas, %	Total, %	Elec. Energy, %	Elec. Dmd, %	Gas, %	Total, %
CACZ01	-1.7	-1.3	88.7	45.3	-233.9	-126.5	90.9	-28.4	-111.1	-54.9	11.2	-28.3
CACZ02	20.9	41.7	86.2	45.8	-53.2	-6.6	81.2	0.3	-22.2	17.8	20.1	10.9
CACZ03	3.7	32.7	91.5	40.6	-117.7	-22.0	92.4	-12.3	-68.6	4.6	11.2	-4.6
CACZ04	24.2	51.7	90.1	51.0	-48.9	-7.0	88.3	-3.8	-20.6	22.4	14.0	13.3
CACZ05	7.0	35.1	93.6	36.6	-76.6	-11.2	93.7	-11.1	-52.9	9.8	6.8	-1.4
CACZ06	13.7	46.4	98.7	30.1	-51.0	-1.9	98.3	-24.7	-37.5	16.8	3.6	-17.8
CACZ07	21.4	46.9	99.7	37.1	-40.6	-4.5	99.7	-16.7	-27.2	19.8	3.7	-4.3
CACZ08	28.4	52.3	96.4	38.6	-24.2	-2.0	96.2	-12.1	-9.6	25.0	6.0	1.6
CACZ09	26.6	52.2	97.7	36.7	-17.0	2.1	96.4	-7.2	-4.6	27.0	10.4	5.1
CACZ10	30.1	49.5	96.2	38.2	-13.0	4.7	95.4	-3.7	0.3	26.5	9.2	7.9
CACZ11	21.7	37.1	82.8	39.9	-30.3	0.1	75.9	3.6	-8.8	20.9	21.8	14.1
CACZ12	23.6	43.3	85.5	45.0	-34.9	-4.5	80.7	1.0	-11.9	18.6	20.0	12.0
CACZ13	26.7	43.9	86.3	43.4	-19.8	-1.6	81.7	1.6	-1.3	21.3	19.4	15.1
CACZ14	26.1	45.7	87.2	37.9	-17.7	9.9	76.1	-0.1	0.7	27.9	26.3	10.2
CACZ15	33.4	52.9	98.2	38.0	0.9	8.4	97.6	3.2	13.5	32.0	11.0	17.4
CACZ16	21.8	43.2	76.7	48.3	-75.3	1.0	62.3	-4.1	-27.5	19.5	30.6	5.7

Payback Periods

Yearly payback periods associated with the ventilation strategies are highly dependent upon first costs. Section II describes the assumptions used to estimate first costs for the different technologies. All payback periods assume a retrofit application. DCV requires the lowest first costs because of lower installation time and equipment costs, followed by the enthalpy exchanger and then the heat pump heat recovery unit.

Table 11 shows payback periods for all building types and locations throughout California for DCV+EC.

Figure 14 shows the payback periods on a California map for four of the buildings covering the range of results. The payback periods associated with DCV are very attractive for most all applications throughout California. As expected, the lowest payback periods occur in the more extreme climates and for buildings with a lower ratio of average to peak occupancy. The payback periods are significantly higher in the coastal climates because of significantly lower cooling and heating requirements and greater economizer opportunities. Therefore, less opportunity for savings with DCV control exists. The payback periods are also significantly higher for the office, restaurant, library, and classroom because of higher average occupancy.

Table 11. Payback Periods for DCV + EC (years)

	Office	Restaurant	Retail Store	Library	Gym	Classroom	Auditorium
CACZ01	8.0	1.4	0.6	6.8	1.0	5.2	0.4
CACZ02	5.0	0.5	0.6	9.6	1.2	2.3	0.5
CACZ03	6.8	2.1	1.0	7.6	1.6	4.0	0.6
CACZ04	3.0	1.1	0.6	7.4	0.8	1.8	0.4
CACZ05	17.9	2.9	1.8	39.5	2.2	24.2	0.7
CACZ06	6.0	4.0	1.7	13.9	2.0	9.0	0.9
CACZ07	3.9	3.4	1.5	13.1	1.9	3.9	0.8
CACZ08	3.7	0.9	0.9	11.7	1.2	2.1	0.7
CACZ09	1.6	1.4	0.8	9.8	1.0	1.6	0.6
CACZ10	3.4	1.1	0.6	8.3	1.0	1.4	0.6
CACZ11	3.1	1.0	0.7	9.2	1.3	1.6	0.5
CACZ12	3.2	1.0	0.6	7.0	0.8	1.6	0.4
CACZ13	2.9	0.8	0.5	6.3	0.8	1.3	0.4
CACZ14	2.5	0.8	0.6	8.2	1.0	1.2	0.5
CACZ15	1.9	0.6	0.3	4.4	0.9	0.9	0.4
CACZ16	3.5	0.6	0.4	2.8	0.9	1.0	0.4

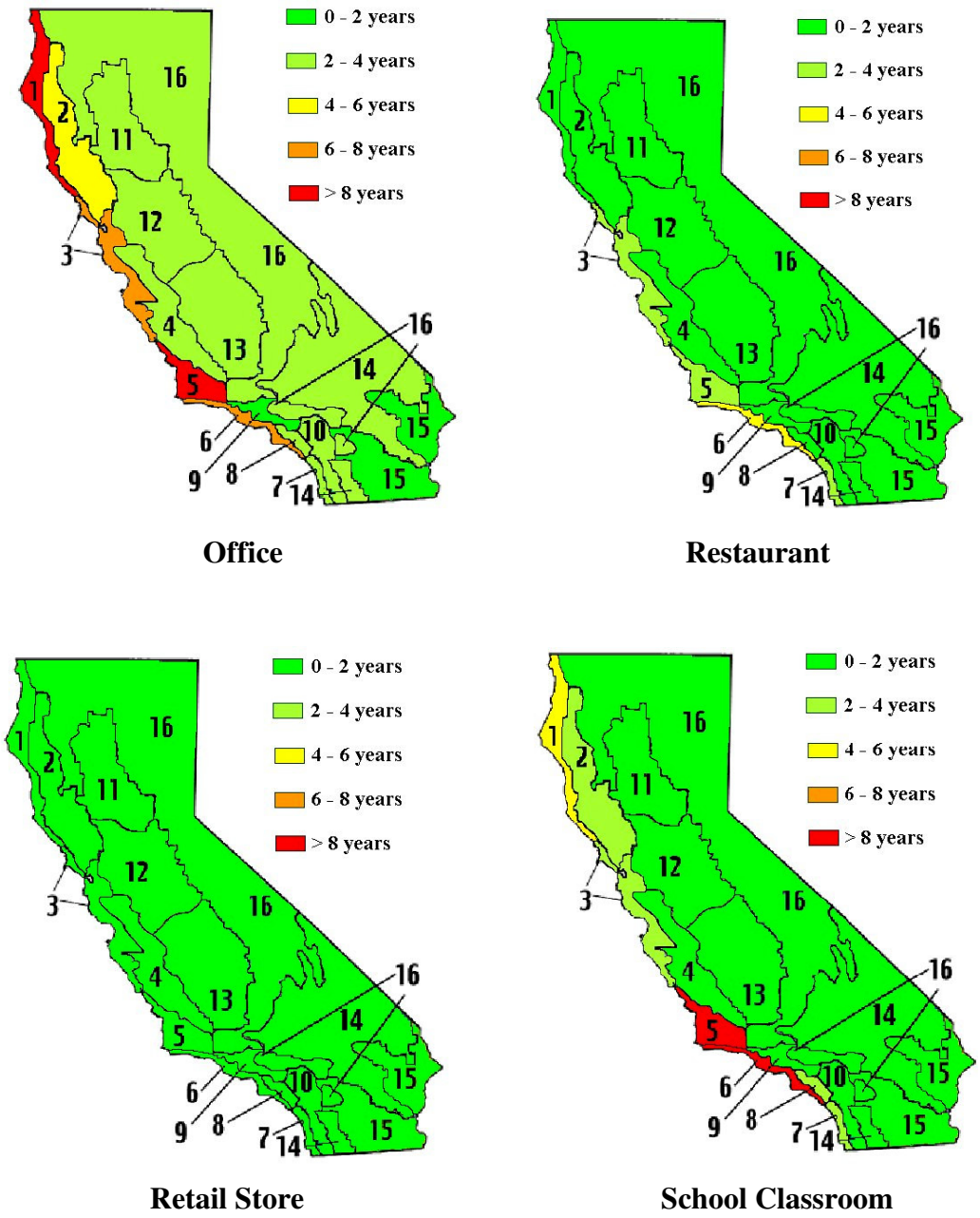

Figure 14. Sample Payback Periods for DCV + EC

Table 12 shows payback periods for enthalpy exchangers as a retrofit in all the building types and locations throughout California. Figure 15 shows results for four of the buildings superimposed on a map. Paybacks for the enthalpy exchanger are typically greater than 7 years for most areas of California, except for some building types in climate zone 15. The payback periods were determined assuming that the primary equipment was not resized with the addition of the enthalpy exchanger (i.e., it's a retrofit). The paybacks would be lower for new installations where the primary cooling and heating equipment were downsized in response to lower ventilation loads.

Table 12. Payback Periods for Enthalpy Exchangers (years)

	Office	Restaurant	Retail Store	Library	Gym	Classroom	Auditorium
CACZ01	-	-	-	-	-	-	-
CACZ02	-	19.0	36.5	-	31.7	-	21.8
CACZ03	-	-	-	-	-	-	-
CACZ04	-	17.6	28.9	-	12.4	-	17.0
CACZ05	-	-	-	-	-	-	-
CACZ06	-	-	-	-	-	-	-
CACZ07	-	-	-	-	-	-	-
CACZ08	-	-	-	-	-	-	-
CACZ09	-	-	-	-	-	-	-
CACZ10	-	-	-	-	-	-	27.9
CACZ11	-	10.1	12.6	-	15.2	-	13.4
CACZ12	-	14.5	20.5	-	17.0	-	16.9
CACZ13	-	8.9	10.0	17.6	11.8	-	11.2
CACZ14	-	13.9	25.1	-	25.1	-	18.4
CACZ15	23.8	4.9	5.0	13.6	7.3	12.0	7.0
CACZ16	-	11.1	38.3	-	32.3	-	46.7

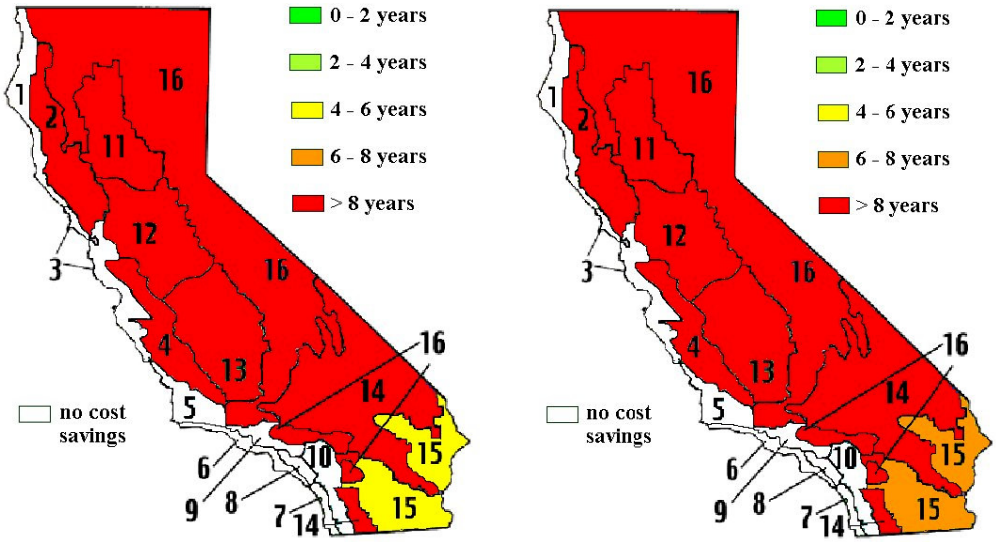

Figure 15. Sample Payback Periods for Enthalpy Exchangers

The heat pump heat recovery system does not provide cost savings for many locations in California. Furthermore, for the locations where savings do occur the payback periods are not reasonable. Figure 16 shows the best case results for this technology. In addition to smaller savings, first costs for the heat pump are significantly higher than for the other two ventilation strategies. Savings only occur with very extreme ambient conditions.

The paybacks would be somewhat smaller for new installations than for retrofits because the primary air conditioning and heating equipment could be downsized. However, it is not expected that it could be competitive with an enthalpy exchanger or DCV for new installations in California.

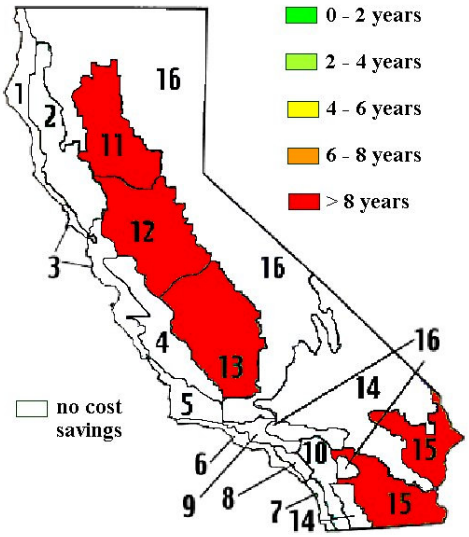

Figure 16. Sample Payback Periods for Heat Pump Heat Recovery

Impact of Occupancy

The savings associated with each ventilation strategy are strongly dependent upon the peak occupant density and average occupancy schedules. The peak occupant density is important because it establishes the fixed ventilation requirement for the base case, HPHR, and HXHR systems. The average occupancy is important for DCV because ventilation varies indirectly with occupancy. For the default simulations, the occupancy schedules and peak occupant densities were assumed based on the LBNL study (Huang, et al. 1990 & Huang, et al. 1995). Average hourly occupancy values were assumed in relation to a daily average maximum occupant density (people per 1000 ft^2).

Figure 17, Figure 18 and Figure 19 show savings potential for three different peak occupant densities (7, 30, and 150 people per 1000 ft^2) as a function of average occupancy relative to the peak for the three ventilation strategies for the office building prototype in CZ 15. Percent savings decrease as the average-to-peak occupancy ratio increases for all three ventilation strategies. The average occupancy was assumed to be constant for all occupied hours of the day and days of the year. For DCV, as the relative occupancy approaches the peak value, the opportunity for modulating the outside air damper in response to zone CO_2 diminishes. At 100% peak occupancy, DCV does not modulate the damper below the fixed ventilation requirement and the savings are zero. The savings for DCV also increase with peak occupant density. This is because the ventilation load associated with the base case having fixed ventilation increases with occupant density due to an increase in the required ventilation rate. Thus, there is a greater opportunity for reducing the ventilation load.

The heat pump and enthalpy exchanger systems exhibit similar trends. The energy recovery opportunites are greater for the higher ventilation rates associated with the

higher peak occupancies. For a given peak occupancy, the sensitivity of savings to average occupancy is less than for the DCV case. The primary impact of average occupancy on operating costs for the base case, heat pump, and enthalpy exhanger systems is due to increased internal gains. At lower internal gains associated with lower average occupancy, the ventilation cooling load is a larger fraction of the total cooling load and the relative savings for energy recovery increase.

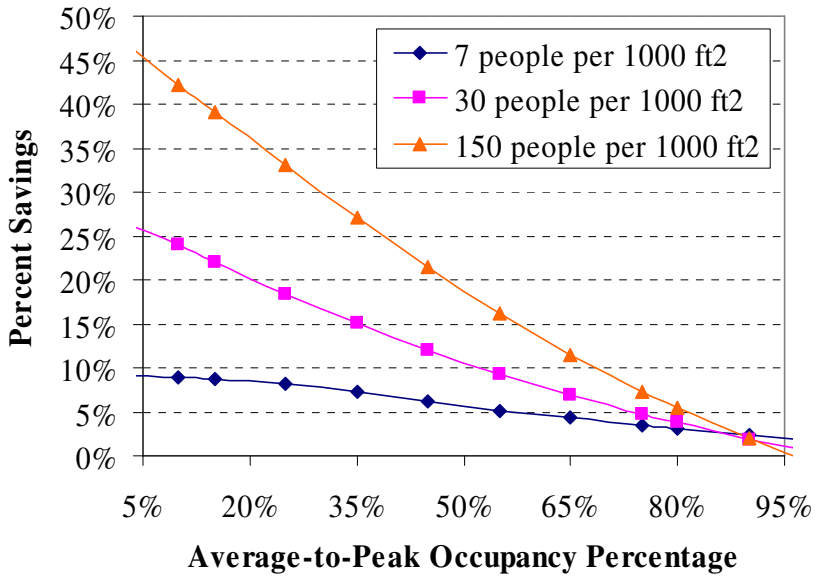

Figure 17. DCV+EC Percent Savings vs. Average-to-Peak Occupancy Percentage for Office in CZ 15

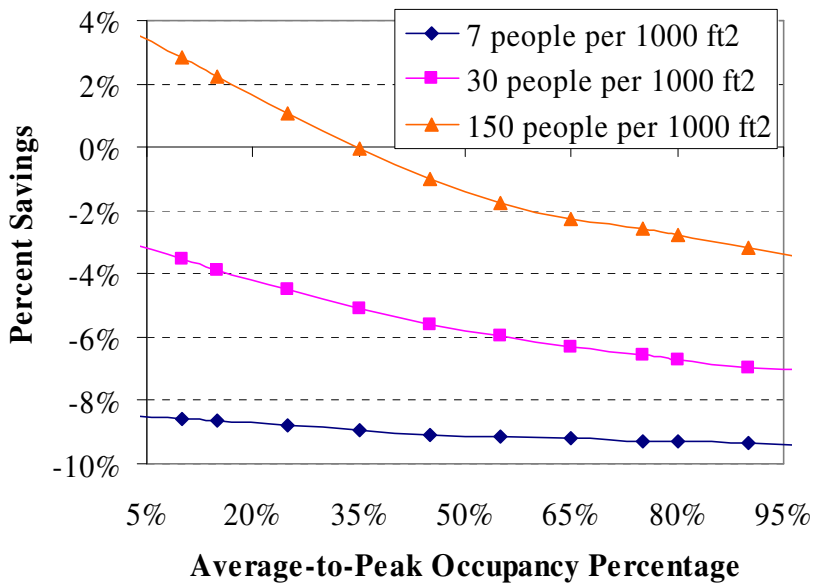

Figure 18. HPHR Percent Savings vs. Average-to-Peak Occupancy Percentage for Office in CZ 15

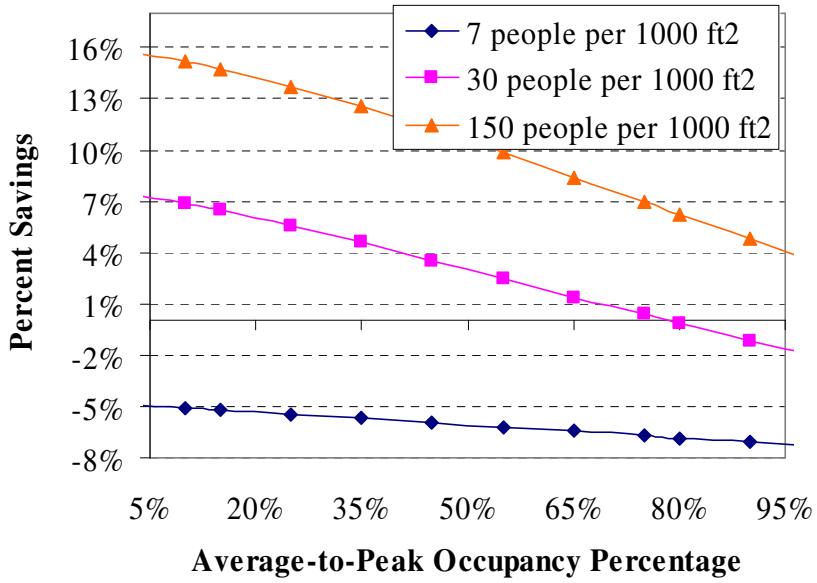

Figure 19. HXHR Percent Savings vs. Average-to-Peak Occupancy Percentage for Office in CZ 15

Impact of Exhaust Fan Efficiency

The heat pump (HPHR) and enthalpy exchanger (HXHR) ventilation strategies both require a fan in the exhaust air stream to overcome additional pressure losses. In some applications, an additional ventilation fan may also be necessary. The default HPHR fan power was based upon measurements from a commercial unit having only an exhaust fan

and is consistant with a fan/motor efficiency of 15% and a static pressure loss for the wheel media or heat exchanger of 0.64 inches of water.

Figure 20 shows the effect of the exhaust/ventilation fan power on the relative savings for the HPHR and HXHR systems for July 19 in CZ 16. A value of 0.2 watts per cfm is representative of a system having only an exhaust fan, but with improved fan/motor efficiency. A value of 1.0 watts per cfm is representative of a system having both an exhaust and ventilation fan with the default fan/motor efficiency. The fan power can make the difference between positive and negative savings for the HXHR and HPHR systems. Although lowering the fan power for the HPHR system does not result in positive savings for this case, it does increase the number of situations (building types / climate zones) where the HPHR system yields positive savings. The lower fan power for the HXHR does not lead to payback periods that are competitive with DCV+EC for the systems considered.

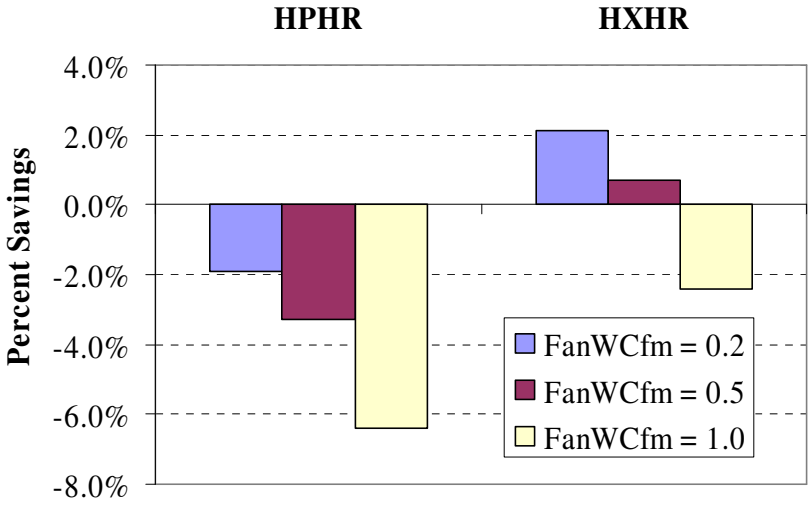

Figure 20. Annual Percent Savings for Different Exhaust/Ventilation Fan Powers – Office, CZ15

Impact of Economizer for HPHR and HXHR Systems

One of the reasons that DCV systems have greater cost savings than HPHR and HXHR systems in California is that these alternative technologies do not incorporate economizers. Although an "economzer mode" for the HPHR and HXHR systems involves turning the units off when the ambient temperature is below the return air temperature, the ventilation flowrate is fixed at the value necessary to satisfy ASHRAE 62-1999. For the DCV systems, the economizer allows the use of 100% outside air and significantly greater "free cooling" can be achieved.

In order to evaluate the penalty associated with the loss of free cooling, a differential enthlapy economizer was implemented in combination with the HPHR and HXHR systems. When the economizer is enabled, the ventilation heat pump or enthalpy exchanger is off and the outside air damper is controlled to meet a mixed air temperature set point of 55 F or is fully open. Two different implementations for the economizer were considered: 1) the ventilation and exhaust air are assumed to flow through the heat pump or enthalpy exchanger in economizer mode, so that the exhaust fan must operate

and 2) the ventilation and exhaust flows are assumed to bypass the heat pump or enthalpy exchanger in economizer, so the exhaust fan is turned off. The first implementation would only require a controllable return damper, whereas the second implementation would require controllable ventilation, exhaust, and return dampers but would require less fan power.

Figure 21 and Figure 22 show example comparisons of the HPHR and HXHR systems with and without a flow-through economizer for a mild California climate (CZ 06) and a hot climate (CZ 15) for the restaurant. For these examples, the exhaust fans operate and the return air damper is closed when the economizer is enabled. These figures also include results for DCV both with and without an economizer.

In the mild climate, the savings are negative for both the HXHR and HPHR technologies indicating that the base case with a differential economzier has lower utility costs. This is due to the extra power associated with running the exhaust fan for the HXHR system and the compressor and exhaust fan for the HPHR system. The use of an economizer does significantly reduce the costs, but savings are still negative. Savings for DCV without the use of an economizer are also negative. For the hot climate, savings associated with both the HPHR and HXHR technologies are positive. The use of an economizer increases the savings, but has a smaller effect than for the mild climate.

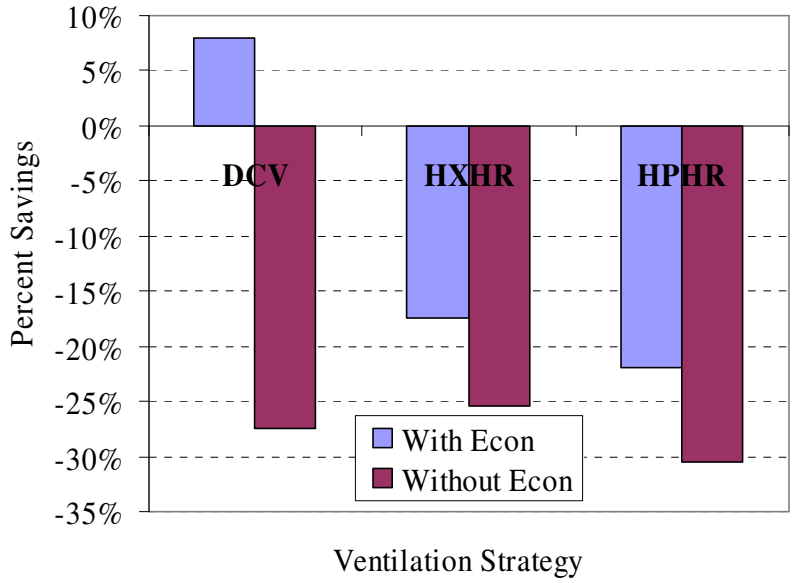

Figure 21. Flow-Through Economizer Savings for the Restaurant in CZ 06

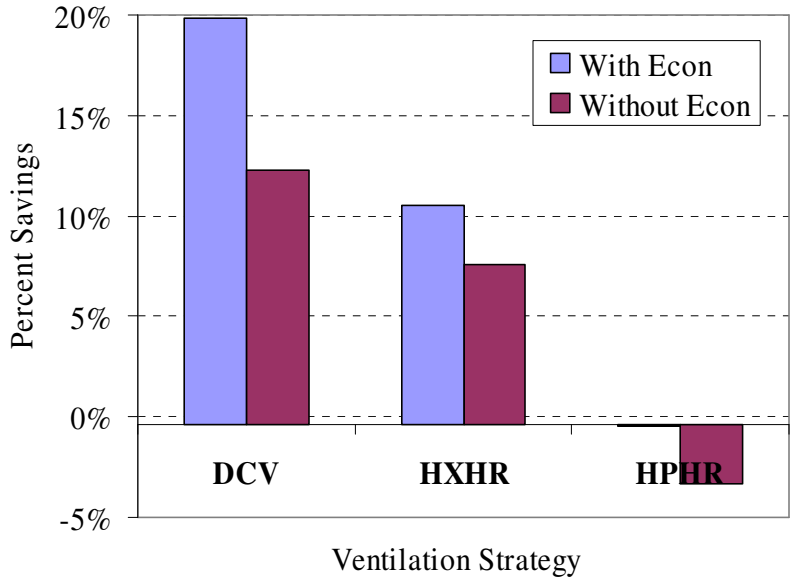

Figure 22. Flow-Through Economizer Savings for the Restaurant in CZ 15

Figure 23 and Figure 24 show example results for the bypass economizer. In this case, the ventilation bypasses the heat pump or enthalpy exchanger and the exhaust fan is off during economizer operation. The performance of the HXHR and HPHR systems improve in both climates for the bypass economizer, but is still not competitive with DCV.

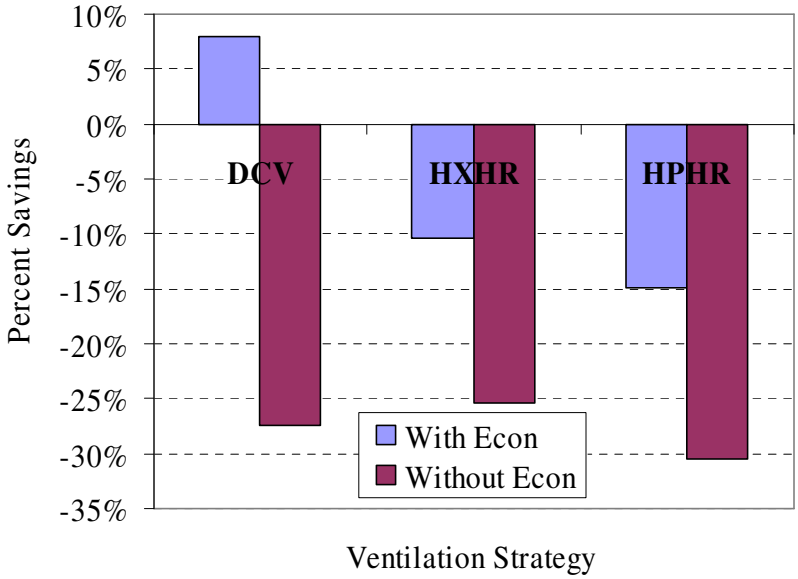

Figure 23. Bypass Economizer Savings for the Restaurant in CZ 06

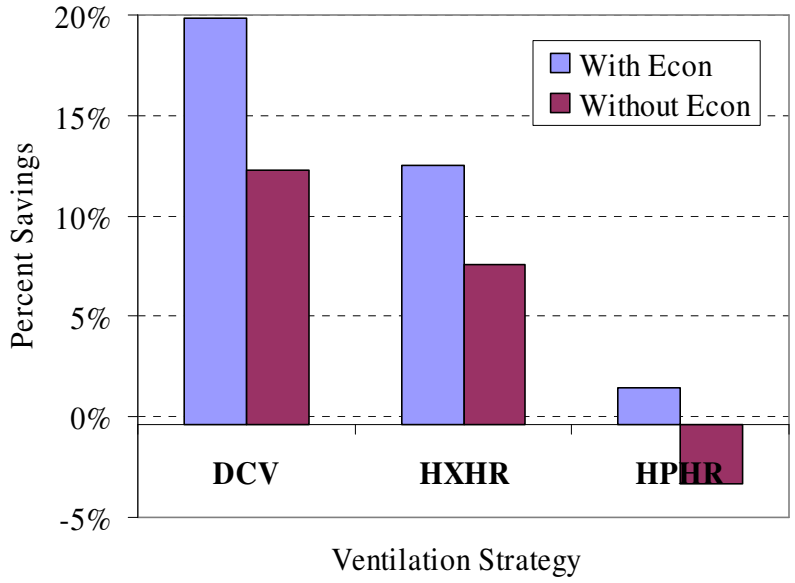

Figure 24. Bypass Economizer Savings for the Restaurant in CZ 15

Zone Humidity Comparisons

One of the advantages of any of the three alternative technologies is lower humidity levels in the zones during the cooling season for humid climates. DCV reduces moisture gains due to ventilation as a result of reduced ventilation air flow. The heat pump heat recovery unit and enthalpy exchanger remove moisture from the ventilation stream as part of the overall energy recovery.

Figure 25, Figure 26 and Figure 27 compare occupied period zone relative humidities for the month of July in Houston for the restaurant, office and auditorium. The results are presented as histograms of relative humidity between 30% and 80%. Relative humidities greater than about 60% are outside of the ASHRAE recommended range of comfort. These zone relative humidities were calculated by controlling the zone temperature to 75 F.

For the office, Figure 25 shows that zone conditions remained within the comfort range for the base case and three alternative ventilation strategies. All three alternative ventilation technologies resulted in reduced humidity levels when compared with the base case. DCV resulted in the lowest zone humidity levels, followed by the enthalpy exchanger and then the ventilation heat pump system.

Figure 26 and Figure 27 show similar trends for the restaurant and auditorium. However, the zone humidity levels were much higher for the strategies having fixed ventilation rates (base case, HPHR, and HXHR) because of the high design occupant densities. Both the base case and the HPHR systems had a significant number of hours with relative humidities greater than 60%. In actual operation, the zone set point would be lowered below 75 F in order to achieve zone humidities within the comfort area. The DCV system had significantly lower humidity ratios than the other technologies for the auditorium because this application has low average occupancies.

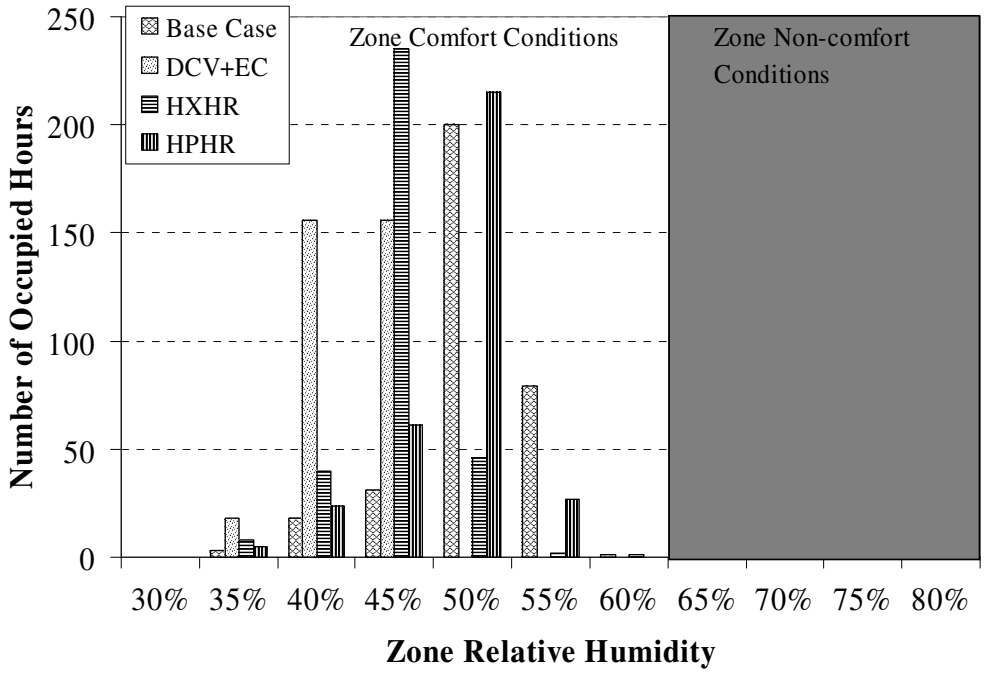

Figure 25. Occupied Hours of Zone Relative Humidity for the Office in Houston

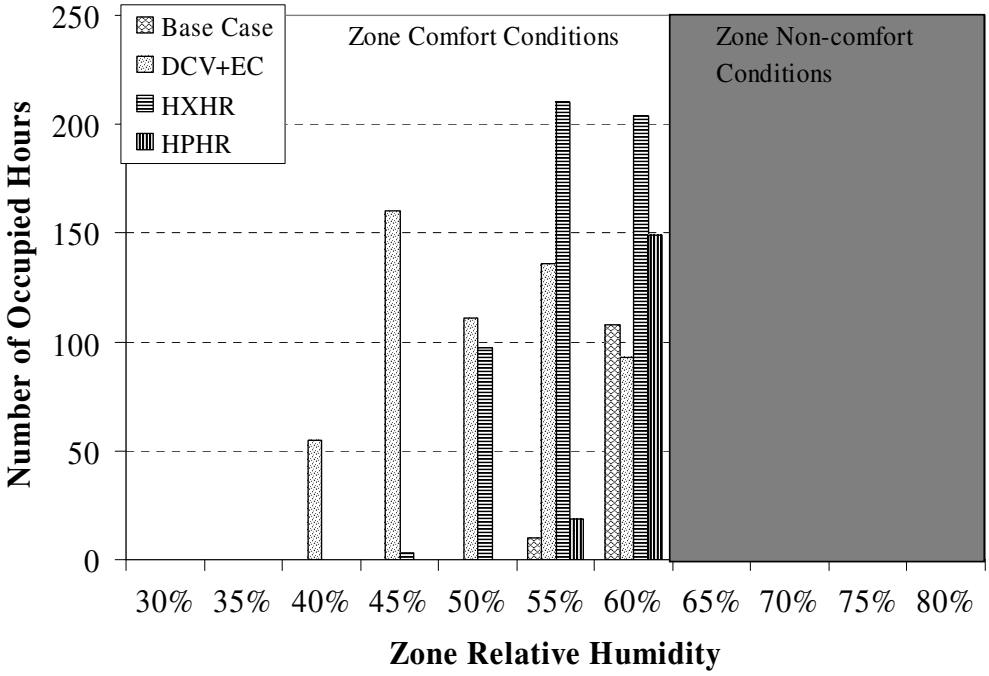

Figure 26. Occupied Hours of Zone Relative Humidity for the Restaurant in Houston

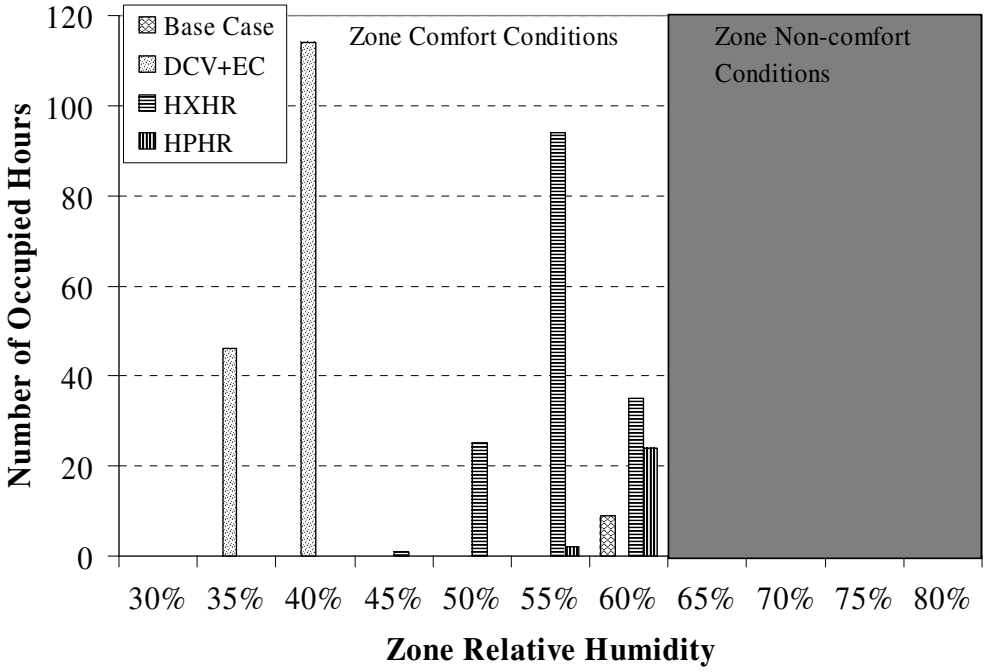

Figure 27. Occupied Hours of Zone Relative Humidity for the Auditorium in Houston

New Building Applications

Additional cost savings are possible for new applications with systems employing enthalpy exchangers or heat pump heat recovery. The use of energy recovery leads to reduced primary equipment loads and an opportunity to downsize the primary RTUs. Operating cost savings may also increase for these systems in new applications compared to retrofit applications due to a decrease in primary RTU on/off cycling resulting from the downsizing.

In order to assess the impact of RTU resizing on savings, four building types in two climate zones were investigated: the office, restaurant, retail store and school auditorium in CACZ 06 and 15. These combinations cover mild and hot climate zones with a large variability in peak occupant density and occupancy schedules relative to the peak occupant density.

A rate of return for each case was calculated for comparisons with the base case and DCV+EC. RTU equipment cost savings were calculated using an installed cost of $1000 per ton of cooling. Reductions in primary heater equipment costs were not considered. For DCV+EC, the RTU can not be downsized for new designs.

Figure 28 through Figure 35 show cumulative rates of return for the different cases as a function of year after the retrofit. The simple payback period occurs at the point where the rate of return becomes positive. Several conclusions can be made from these results, including: 1) rates of return are higher in the hotter climate and for the buildings having higher peak occupancy (e.g, the auditorium versus the office), 2) the HXHR and HPHR systems do not have positive rates of return in the moderate climate, 3) in the hotter climate, the enthalpy exchanger results an immediate rate of return (immediate payback)

due to RTU equipment cost savings, 4) although the rates return for the DCV+EC start out negative (due to the initial investment), they surpass the enthalpy exchanger rates of return within a short time period, and 5) the HPHR system is not competitive with the other technologies.

Overall, the conclusions do not change for new building applications. Demand-controlled ventilation has better overall economics than the other energy recovery technologies for the systems and conditions considered in this study. More detailed results are given in Appendix C.

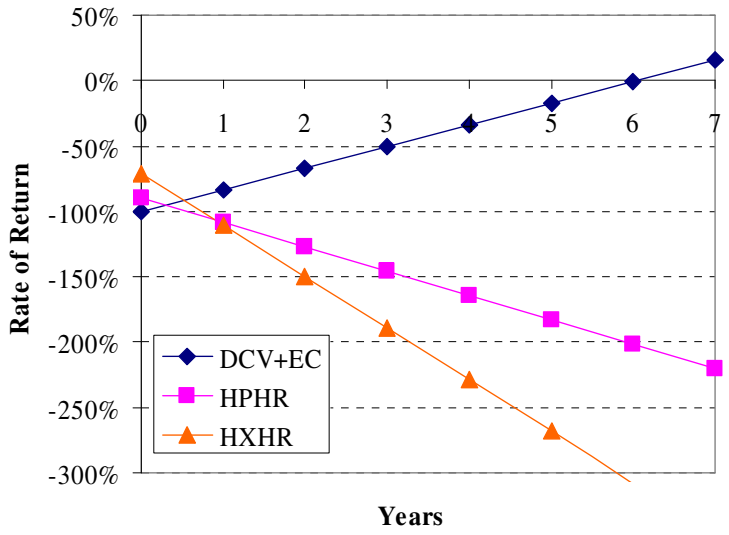

Figure 28. Cumulative Rate of Return for Office in CACZ 06

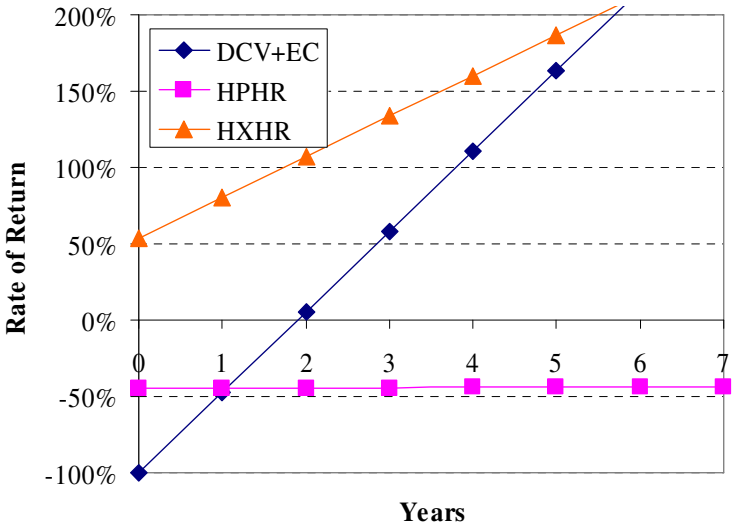

Figure 29. Cumulative Rate of Return for Office in CACZ 15

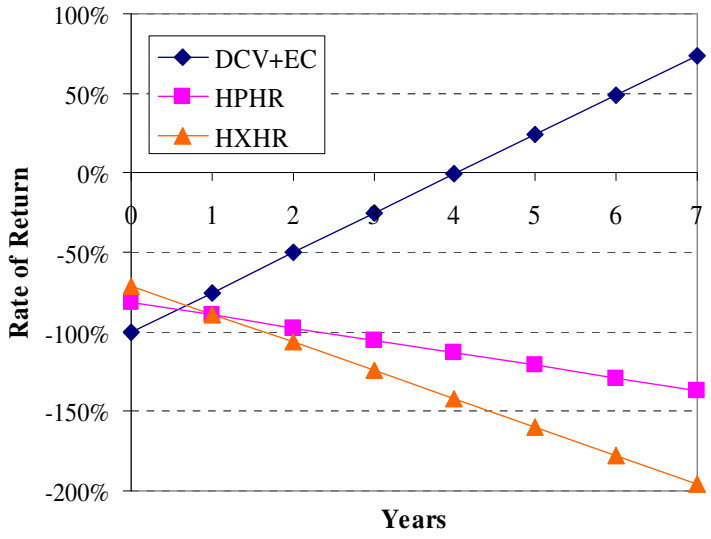

Figure 30. Cumulative Rate of Return for Restaurant in CACZ 06

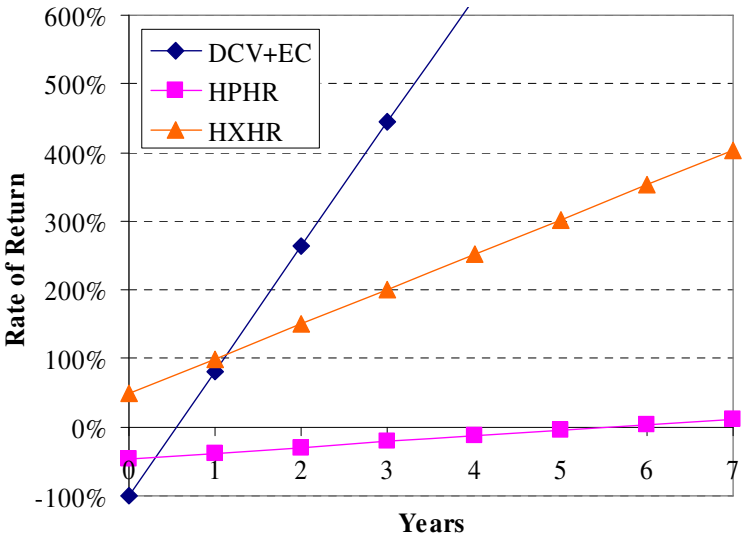

Figure 31. Cumulative Rate of Return for Restaurant in CACZ 15

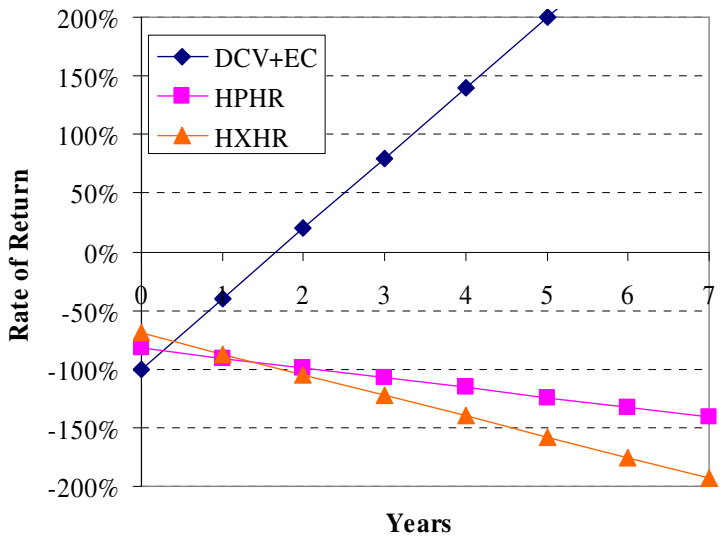

Figure 32. Cumulative Rate of Return for Retail Store in CACZ 06

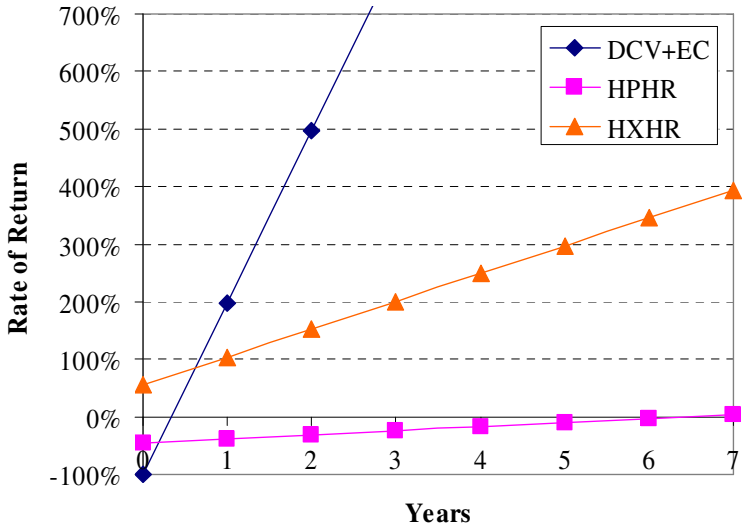

Figure 33. Cumulative Rate of Return for Retail Store in CACZ 15

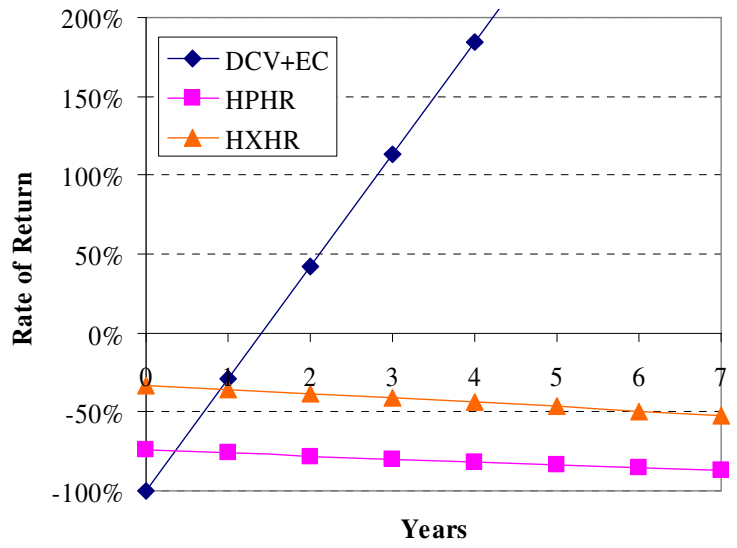

Figure 34. Cumulative Rate of Return for Auditorium in CACZ 06

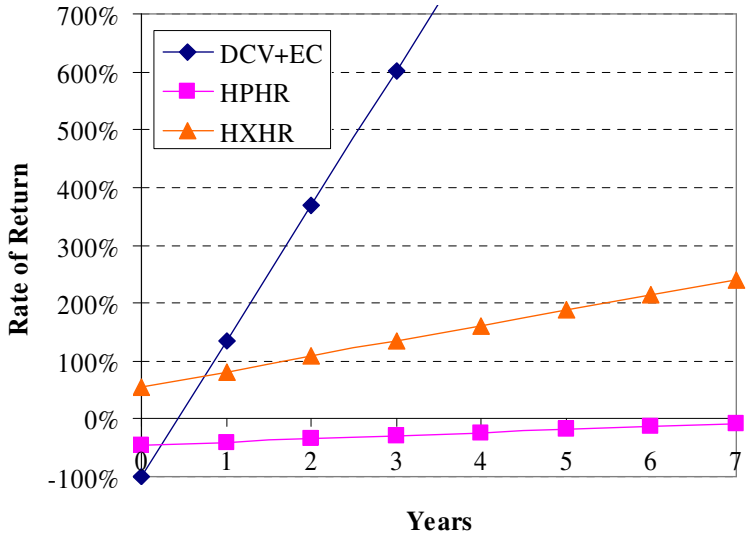

Figure 35. Cumulative Rate of Return for Auditorium in CACZ 15

IV. DCV FIELD TESTING

DCV Field Sites

For evaluation of DCV, field sites were established for three different building types in two different climate zones within California. The building types are: 1) McDonalds PlayPlace® areas, 2) modular school rooms, and 3) Walgreens drug stores. In each case, nearly duplicate test buildings were identified in both coastal and inland climate areas.

This section provides a brief overview of these field sites. A detailed description of the field test sites and the data collection system is included in Deliverable 3.1.1a (2003).

The PlayPlace areas are isolated from the main dining area and have separate packaged rooftop HVAC unit(s). Heating is provided by natural gas burners. Two restaurants sites are located approximately 15 miles apart in the San Francisco Bay area (south of Oakland and north of San Jose). Two other restaurant sites are in the Sacramento area.

The modular schoolrooms are typical of thousands employed throughout California and the United States. They use a single sidewall mounted packaged heat pump system. Two schoolrooms are located in Oakland and two are in Woodland, just east of Sacramento.

The drug stores selected for this study are larger than the other field sites and use five rooftop units that service the store and pharmacy areas. Due to the larger number of HVAC units at the Walgreens sites, only one store in each climate type is being monitored. One store is near Riverside and the other is in Anaheim.

The two alternative control strategies compared were DCV with economizer control (DCV On) and economizer cooling only (DCV Off). With the DCV On strategy, the return air CO_2 set point was 800 ppm_v. When the return air CO_2 concentration was below the set point, the outdoor air ventilation damper was fully closed. Otherwise, the Honeywell controller provided feedback control of the damper position. For the DCV Off mode, a minimum damper position was set so as to provide the required outdoor airflow as specified in ASHRAE Standard 62-1999 (ASHRAE, 1999). The fixed damper position that satisfies the standard was estimated to be 40% for the McDonalds and the modular schools and 20% open for the Walgreens stores. However, field airflow measurements at one McDonalds store indicates that the actual total supply airflow varies significantly with damper position. This impacts the actual amount of ventilation air provided.

The field measurements for HVAC equipment included electric power, integrated electrical energy, digital control signals for the gas valve and supply fan, ambient, return, and mixed air temperature and humidity, supply air temperature, and return air CO_2 concentration.

The power is calculated from voltage and current readings for each unit (fans plus compressor). For the Bradshaw Road and Milpitas sites that have two rooftop units, only direct power measurements from one of the units were available, but they are duplicate systems. Operation of the second rooftop unit was monitored via the digital control signals indicating fan, cooling or heating being on. Since the modular school sites use a single phase electrical power connection, separate monitoring of the total unit and compressor power is performed.

Data were collected every five minutes and downloaded to a server on a daily basis using a cell phone. A website provided direct access to the data. A screening analysis program was used to check for erroneous data and compute hourly averages.

Installation at the field test sites began in late 2000 with installation, checkout and debugging finished by the end of 2001 for the McDonalds and modular schoolroom sites. The Walgreens store installation and debugging continued into 2002.

Comparison Methodologies

The costs for heating associated with the field sites are relatively small compared to the cooling costs and only cooling season results are presented in this report. Heating season results are described by Lawrence and Braun (2003). The cooling season results are presented in this report using the different approaches described below.

Direct side-by-side comparisons – Nearly identical sites were chosen in the northern California climates to allow direct side-by-side comparisons for the same time periods. As a check on the differences between sites, it is important to also compare energy use with both sides operating in the same mode (e.g., DCV On or DCV Off).

Correlated daily energy usage – This approach involves comparison of average daily energy use for heating or cooling at the same site. Total daily energy usage was correlated as a function of average ambient temperature for different time periods when the DCV was on and off. Separate correlations were developed for DCV On and Off and then used to compare energy use for a given daily ambient condition or over a period of time (e.g., cooling or heating season).

Calibrated simulation – Field site information and data were used to develop VSAT simulations for the field sites. The field measurements were then compared with VSAT predictions using short-term data for validation purposes and annual simulations were performed to evaluate savings and economic payback. Lawrence and Braun (2003) present additional comparisons of energy usage based upon hourly models that were derived from the data.

In addition, CO_2 levels in the zone were compared for DCV and fixed ventilation.

Field Results for McDonalds PlayPlace Areas

Side-by-Side Energy Use Comparisons

Variations in the DCV control settings were made at the Milpitas and Castro Valley sites in the San Francisco area to allow side-by-side comparisons. Figure 36 shows daily energy usage for cooling (compressor + fan energy) for a time period where DCV was off for both sites. The Castro Valley site had slightly higher energy consumption (82.8 kW-hr per day) compared to the Milpitas site (80.0 kW-hr per day), a difference of about 3.5%.

Figure 37 shows side-by-side comparisons of daily cooling energy usage for DCV On and DCV Off at the two sites during a three-week period. The strategies were alternated between the two sites, but the savings for DCV On were nearly the same regardless of which sites were on and off. Average measured daily energy savings for DCV On was about 14% for this time period.

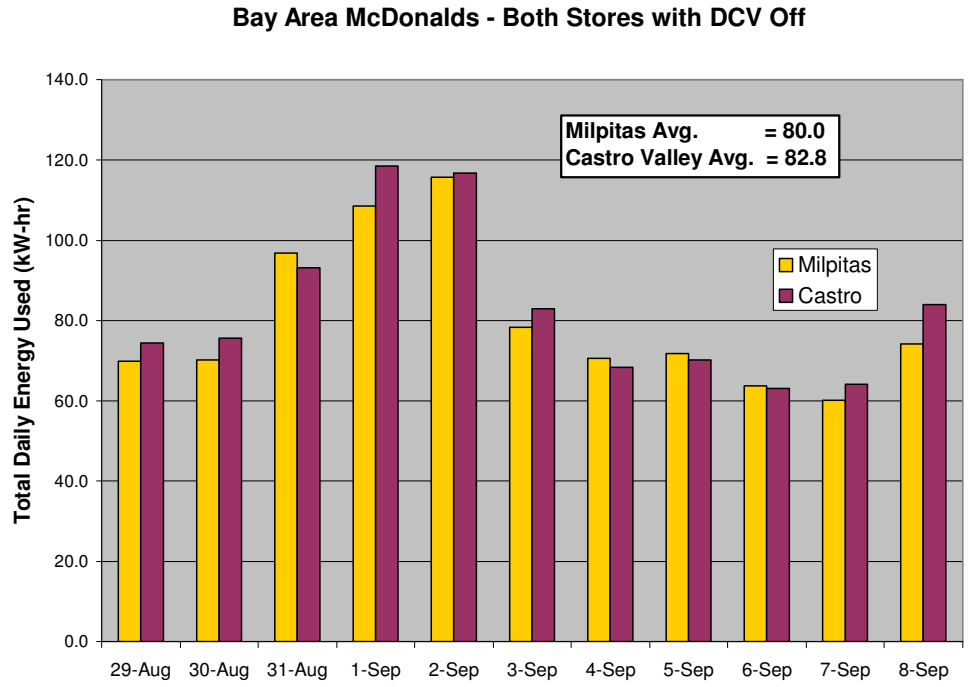

Figure 36. Cooling Energy Use for DCV Off at Bay Area McDonalds

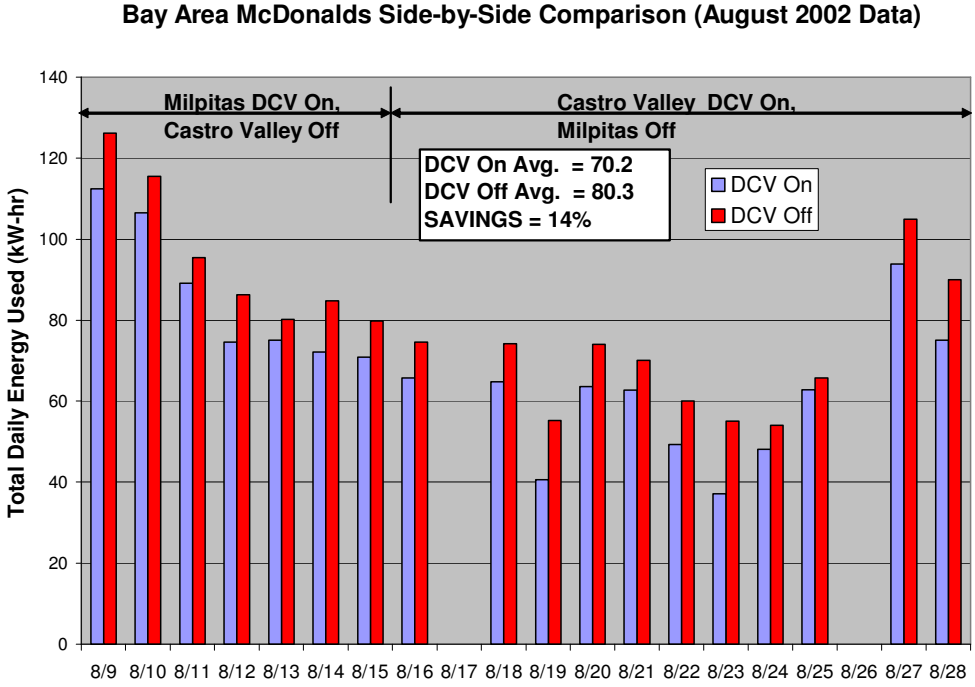

Figure 37. Cooling Energy Use for DCV On and Off at Bay Area McDonalds

Correlated Daily Energy Usage

Figure 38 shows daily energy usage for cooling as a function of daily average ambient temperature for the Milpitas site (bay area) for both DCV On and Off. The daily data correlates relatively well as a linear function of ambient temperature. For a hot day with an average temperature of 80º F, the estimated savings are about 12%. Figure 39 shows similar results for the other bay area site (Castro Valley). In this case, the savings are a little smaller than for the Milpitas site. This may be because this site has a greater occupancy, leading to higher ventilation rates for DCV On as compared with Milpitas.

Figure 40 shows daily energy usage for cooling as a function of daily average ambient temperature for the Bradshaw (Sacramento area) McDonalds for DCV On and Off. For a hot day with an average temperature of 80º F, the estimated savings are about 28%. These savings are considerably larger than those for the Bay area sites. For the same average daily temperature, the daytime temperatures are higher for Sacramento than the bay area leading to larger ventilation loads and greater savings with DCV. Also, the occupancy at the Bradshaw site appears to be lower than for the other McDonalds sites.

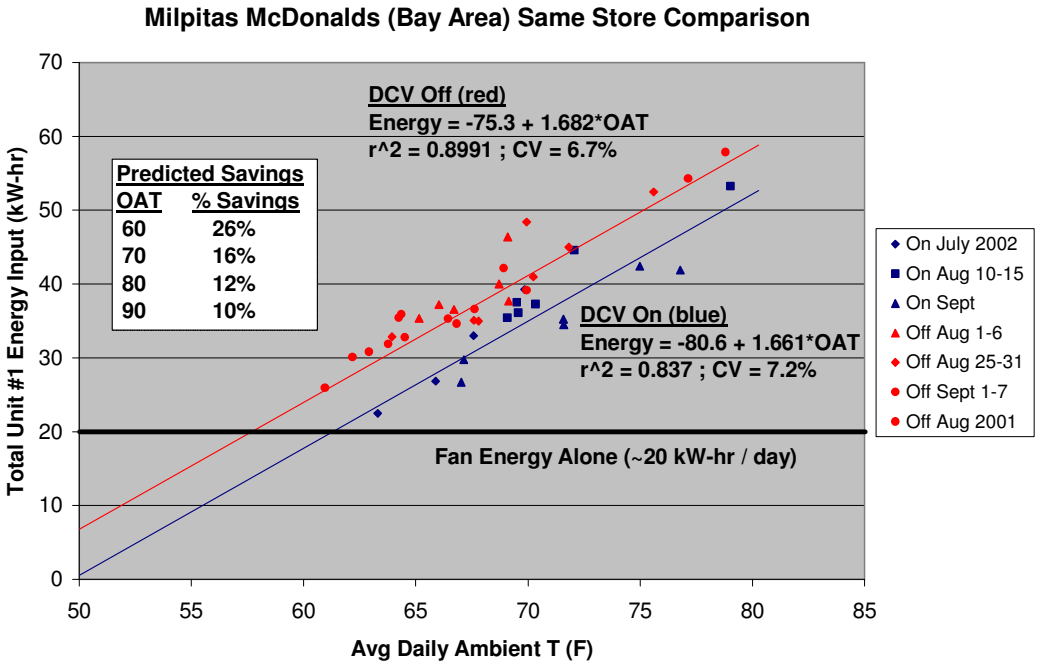

Figure 38. Correlated Daily Cooling Energy Use for DCV On and Off at Milpitas (Bay Area) McDonalds Site

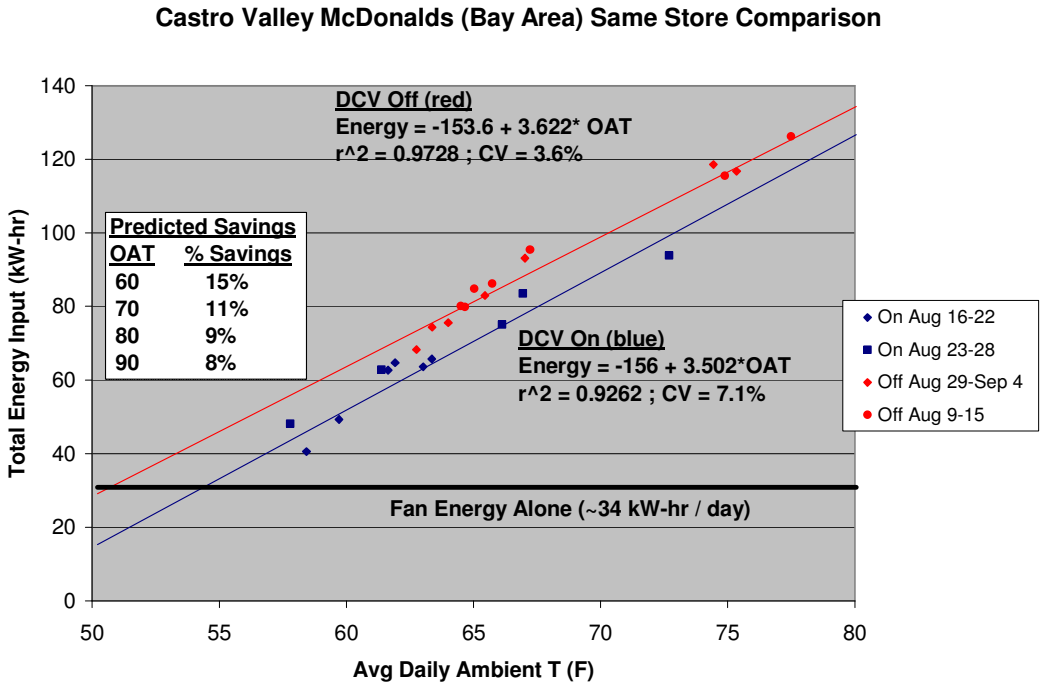

Figure 39. Correlated Daily Cooling Energy Use for DCV On and Off at Castro Valley (Bay Area) McDonalds Site

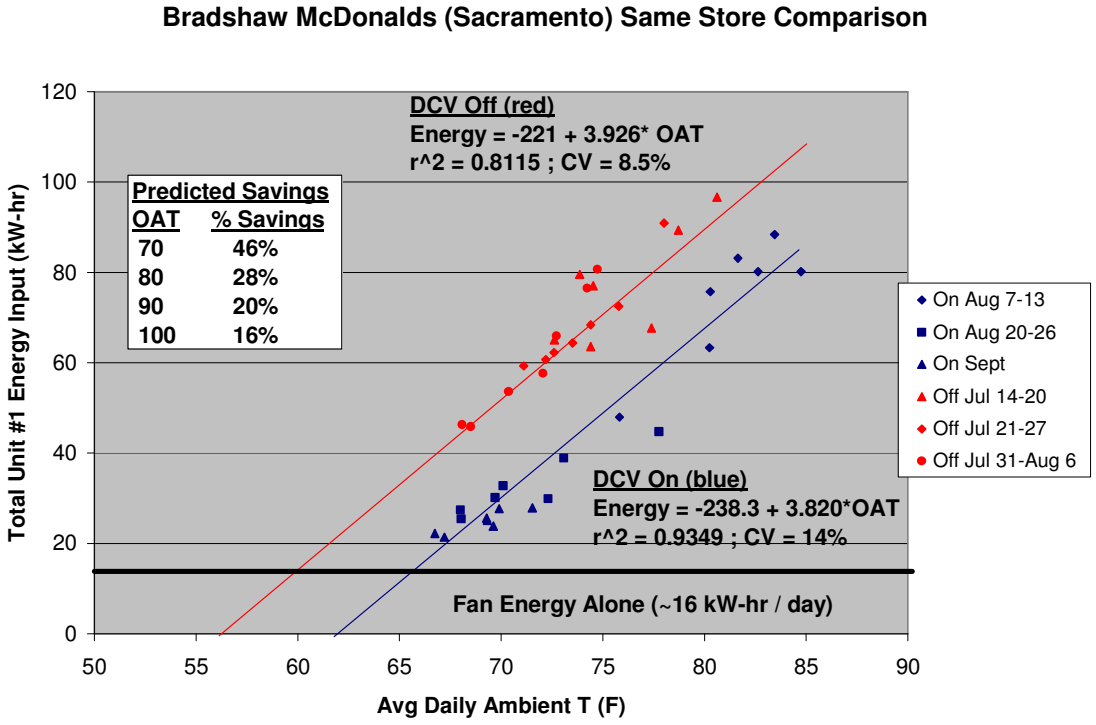

Figure 40. Correlated Daily Cooling Energy Use for DCV On and Off at Bradshaw (Sacramento) McDonalds Site

Table 13 summarizes the energy savings versus daily average ambient air temperature for the three McDonalds sites predicted from the time period with the available field data.

Table 13. Measured Savings Percentages with DCV On Control Strategy at McDonalds PlayPlace Areas

Daily Average Temperature (F)	Bradshaw Road (Sacramento)	Milpitas (Bay Area)	Castro Valley (Bay Area)
60	Not applicable (fan only)	26%	15%
70	46%	16%	11%
80	28%	12%	9%
90	20%	10%	8%

VSAT Comparisons

Site-specific VSAT models were prepared for the McDonalds sites and predicted daily energy consumption was compared with field measurements for same time periods used for Figure 38 to Figure 40. Parameters that describe the buildings and equipment were collected from site visits. An average occupancy profile was estimated from measurements of zone CO_2 concentrations and assumptions about average metabolic rates. Figure 41 to Figure 43 show that the predicted results generally match the measurements. The solid symbols represent the field measurements and the open symbols represent the VSAT predictions for the same dates and weather conditions. Regession correlation lines are also shown for the VSAT data. The field data and VSAT predictions are shown separately for DCV On and DCV Off operating modes for the Milpitas and Castro Valley sites for better clarity. At the Bradshaw site, there is enough separation between the DCV On and DCV Off data points to show them both on the same plot. On any given day, the model may not match the predictions very well due to differences in occupancy or other unmeasured differences. However, the correlations between daily energy usage and ambient temperature are close in most cases. In general, the estimated daily savings are smaller at lower average daily temperatures than for higher averages. On cooler days, economizer cooling is more significant and there is less potential for DCV savings. It was not possible to distinguish this trend from the experimental results due to the limited data and other confounding factors.

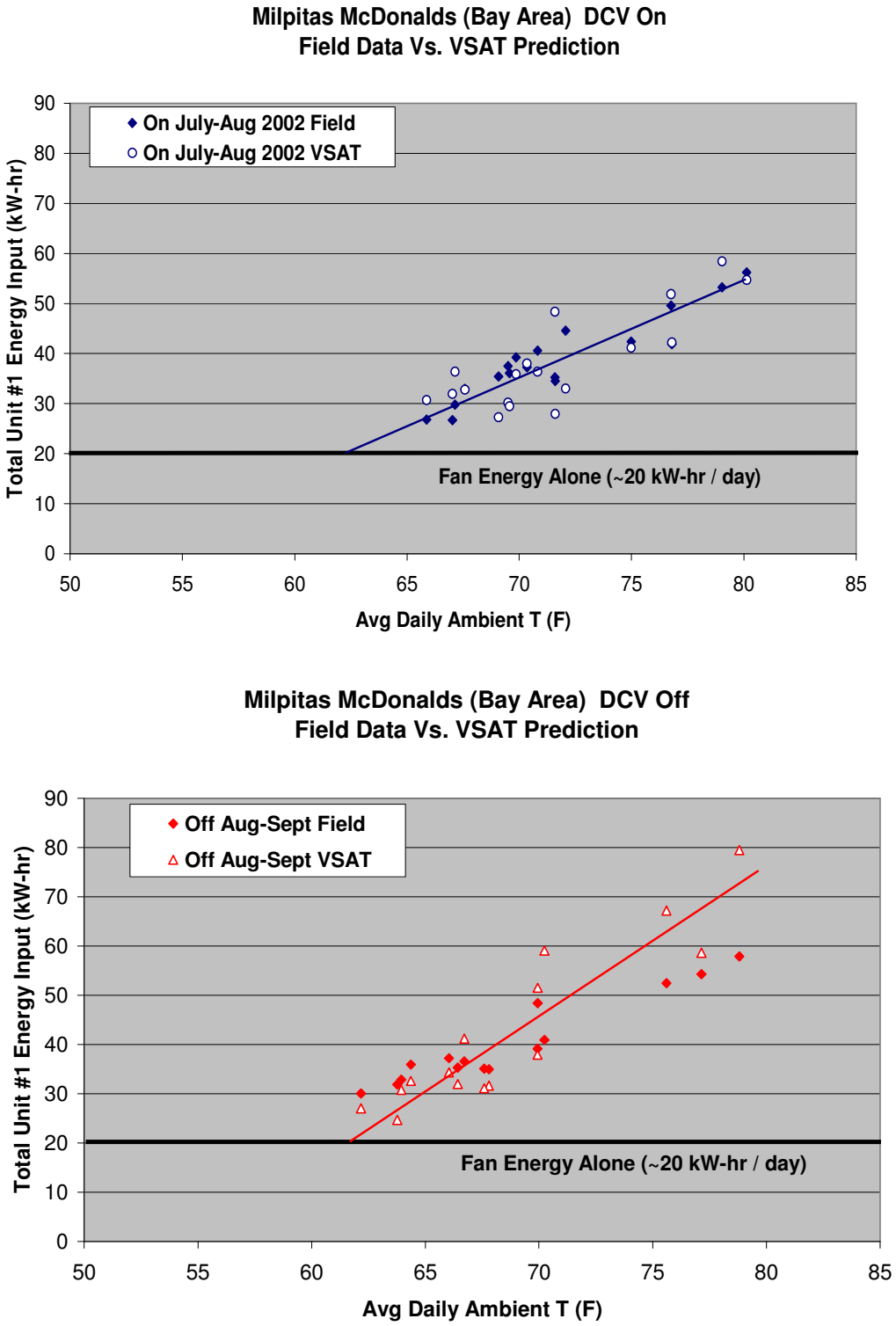

Figure 41. Comparison of Daily Cooling Energy Use at Milpitas (Bay Area) McDonalds Site

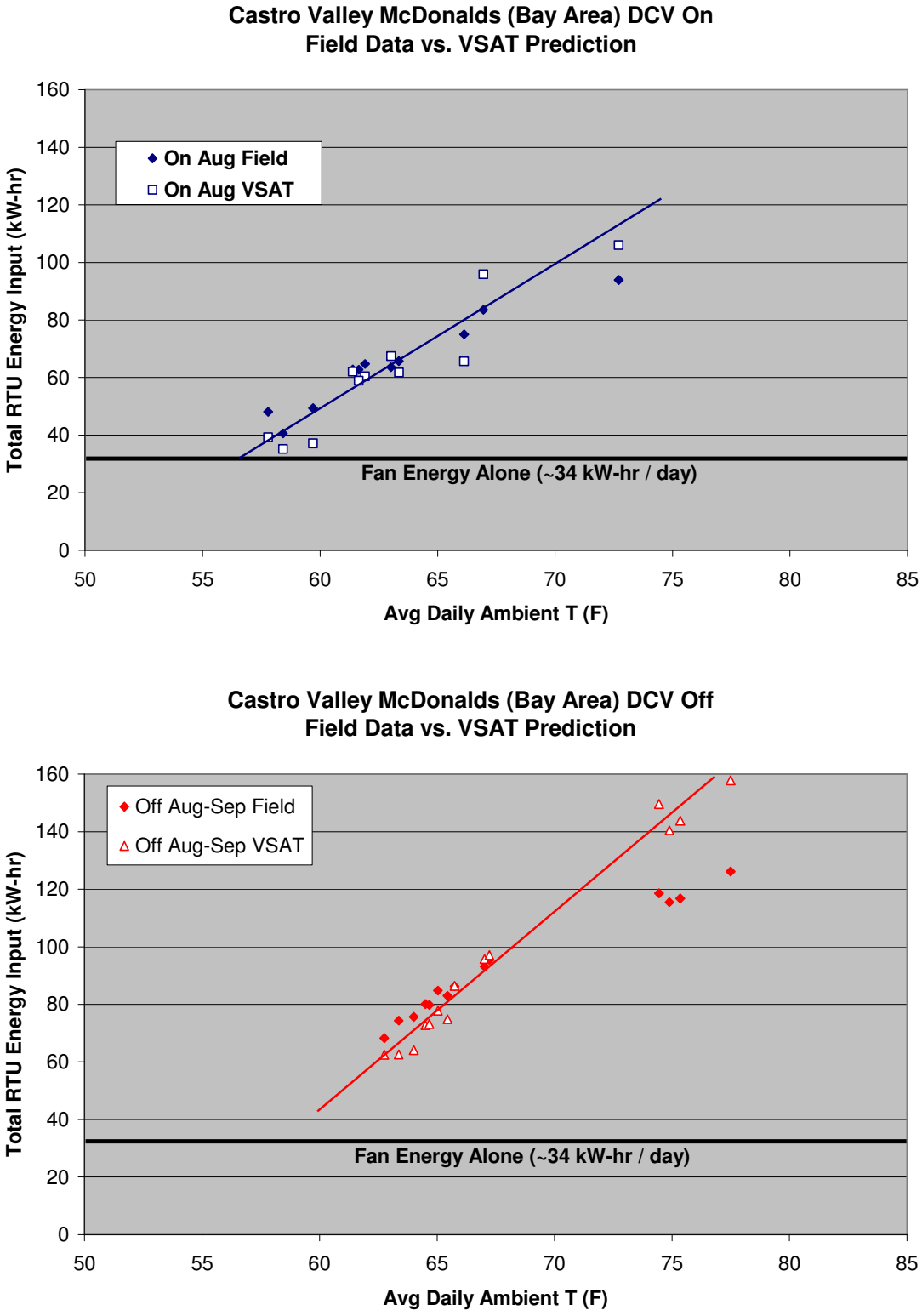

Figure 42. Comparison of Daily Cooling Energy Use at Castro Valley (Bay Area) McDonalds Site

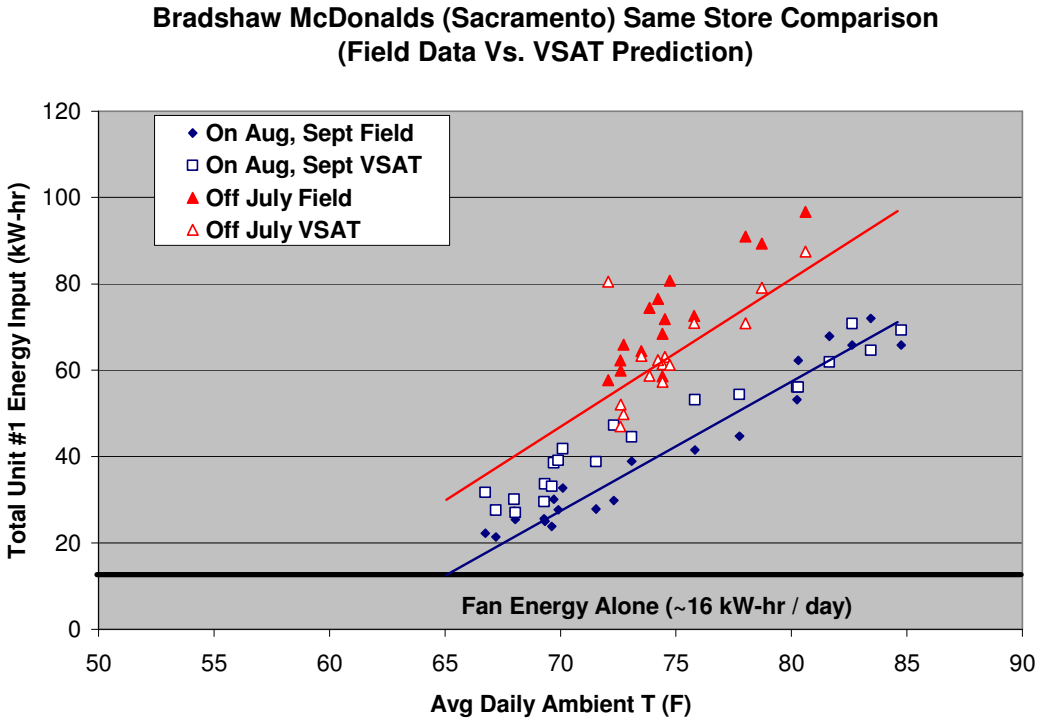

Figure 43. Comparison of Daily Cooling Energy Use at Bradshaw (Sacramento Area) McDonalds Site

Annual Cost Savings and Economic Analyses

The calibrated VSAT simulations for the field sites were used to evaluate annual operating cost savings, simple payback period, and return on investment for a 5-year period. The results are given in Table 14 and are based upon cooling season results only. Some additional cost savings will be realized from the heating season leading to lower payback periods. The payback periods are similar to those determined for the prototypical restaurant considered in the simulation section. Furthermore, the payback period is lower for the inland climate (Bradshaw) than for the coastal climate (Milpitas and Castro Valley). Note that the energy cost savings for the two restaurants in the coastal climate are similar, only differing by about $30. However, the economic payback and return on investment are very different. The Castro Valley site has only one rooftop unit, compared to two at Milpitas, and therefore shows a faster payback period and better return on the smaller initial investment. The field site comparison data in Figure 38 and Figure 39 were for a sampling of the entire cooling season when data were available. From the field site data alone during this sample period, the Milpitas site appears to have a slightly beter savings potential with DCV. However, when looked at on an annual basis and considering the initial cost of equipment for DCV, the Castro Valley site would be a better return on investment.

The rate of return is the interest rate that would provide an equivalent return on an investment; in this case the investment decision is whether to invest in a DCV system. The analysis is based on five years since that is the period for which the calibration of the CO_2 sensors are guaranteed. Many business may balk at considering investing in capital

projects with a 3 or more year payback period, but the rate of return expected for the $900 per rooftop unit over the five year period is impressive for both the Bradsahw and Castro Valley site. A DCV retrofit would not make much economic sense for the Milpitas site. The assumed cost per rooftop unit is $900, as mentioned earlier. This cost is based on assuming the CO_2 sensors are located near the rooftop unit, such as in the return air stream. If the sensors were to be located in the occupied space, an additional cost would occur for running the wiring from the zone up to the rooftop unit.

Table 14. Predicted Cooling Season Savings with DCV On Control Strategy at McDonalds PlayPlace Areas from Calibrated VSAT Simulations

	Bradshaw Road (Sacramento)	Milpitas (Bay Area)	Castro Valley (Bay Area)
Compressor cooling savings (kW-hr)	1581	-4	228
Peak demand savings (kW)	6.1	2.3	2.0
Annual electrical energy cost savings ($)	$503	$277	$312
# RTU's per site	2	2	1
Total initial capital cost for DCV	$1,800	$1,800	$900
Simple payback period (years)	3.6	6.5	2.9
5 Year rate of return on investment in a DCV retrofit (%)	18.8%	-11.2%	34.8%

Indoor CO_2 Concentrations

Table 15 shows comparisons of average return air CO_2 concentrations during occupied periods for DCV On and DCV Off during the 2002 cooling season. The use of DCV results in higher CO_2 concentration levels for these test sites due to lower ventilation rates. This is consistant with the energy savings for DCV at these sites. The largest differences in CO_2 concentrations occur at the Bradshaw McDonalds. Recall that this site also had the largest energy savings for DCV. The Bradshaw site has lower average CO_2 concentrations for DCV Off than the other sites, implying that the occupancy is lower at this location. Lower occupancies relative to design occupancies generally lead to larger energy savings for DCV.

Table 15. Mean CO_2 Levels with DCV On and DCV Off Control Strategies at McDonalds PlayPlace Areas

DCV Control Strategy	Bradshaw Road (Sacramento)	Milpitas (Bay Area)	Castro Valley (Bay Area)
Off	496 ppm	541 ppm	572 ppm
On	575 ppm	613 ppm	615 ppm

Figure 44 through Figure 46 are histograms of the occupied hours that CO_2 concentrations fell within different bands for the Milpitas, Bradshaw, and Castro Valley sites. At the Milpitas and Bradshaw sites, the DCV controller was generally able to keep the return air CO_2 concentration at or below the 800 ppm set point. However, at the Castro Valley site, about 5% of the occupied hours were at CO_2 levels above 900 ppm.

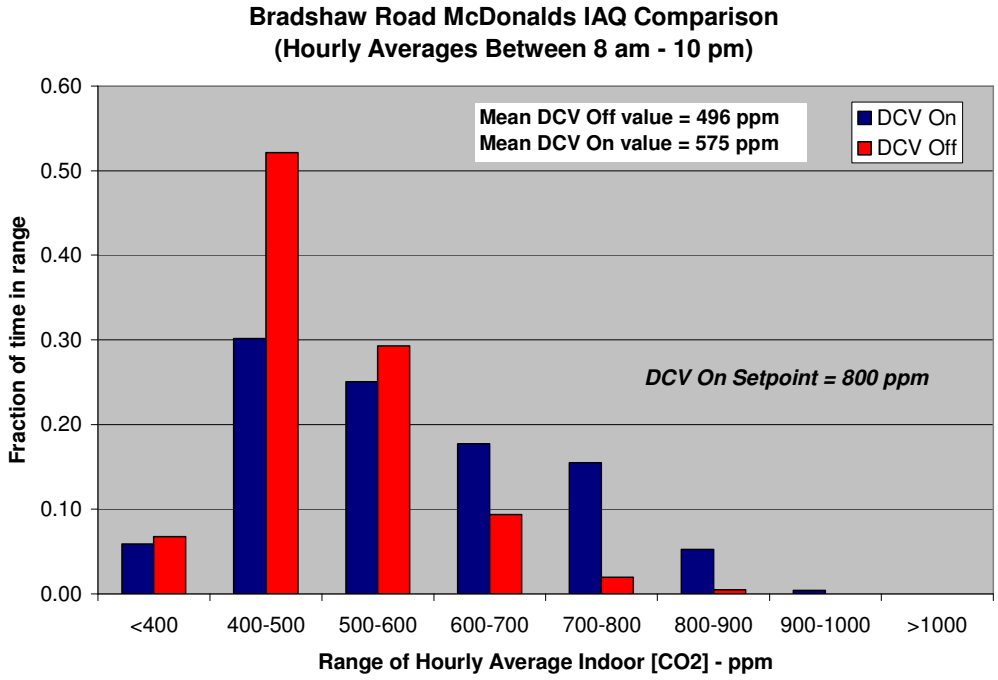

Figure 44. Histogram of Return Air CO_2 Concentrations at Bradshaw (Sacramento) McDonalds PlacePlace for DCV On and Off

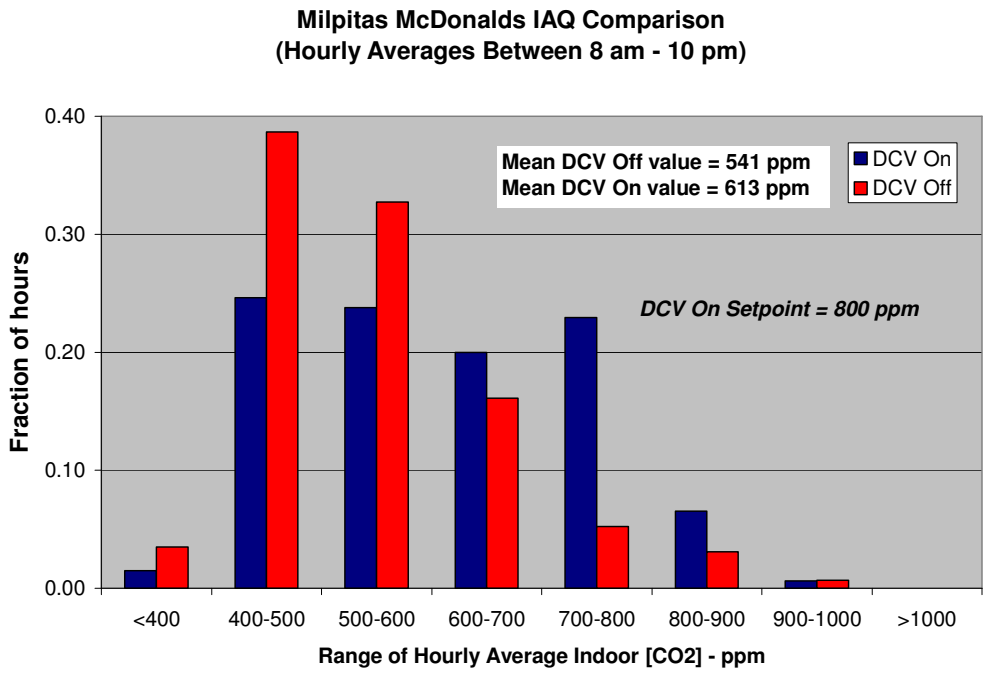

Figure 45. Histogram of Return Air CO_2 Concentrations at Milpitas (Bay Area) McDonalds PlacePlace for DCV On and Off

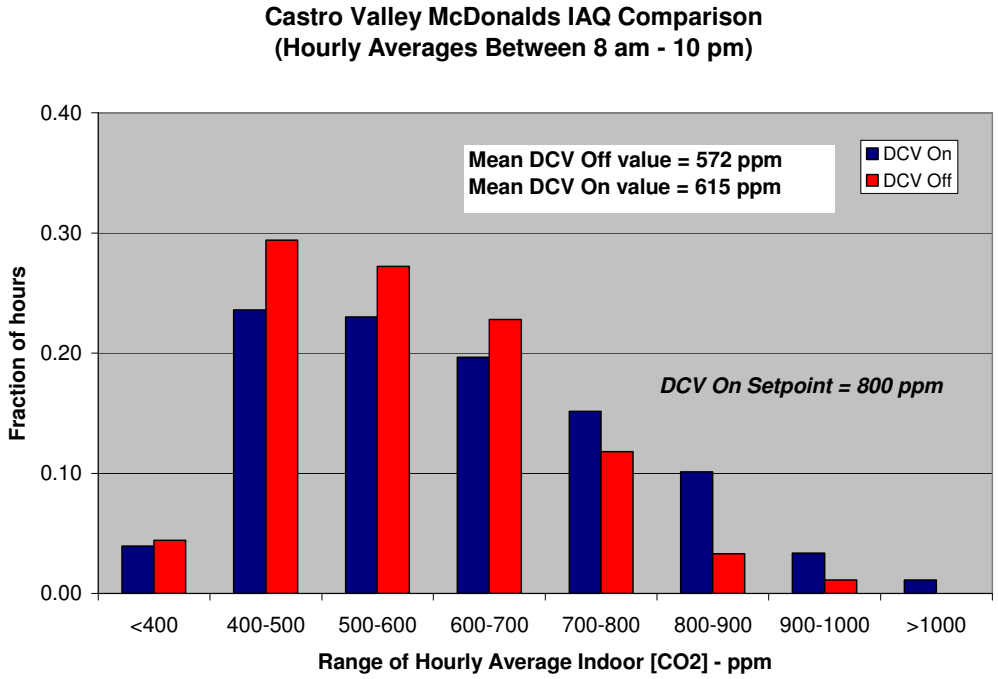

Figure 46. Histogram of Return Air CO_2 Concentrations at Castro Valley (Bay Area) McDonalds PlacePlace for DCV On and Off

Field Results for Modular Schools

Correlated Daily Energy Usage

Figure 47 and Figure 48 show daily energy usage for cooling as a function of daily average ambient temperature for the the Woodland site (Sacramento area) for both DCV On and Off. The average daily cooling energy use is nearly a linear function of ambient temperature. However, there appears to be no real difference in energy usage regardless of the control strategy chosen for the Woodland site. The average damper position for DCV On is essentially the same for both strategies implying that the rooms are fully occupied most of the time when the HVAC system is on and design ventilation air is required to maintain the CO_2 set point for DCV On. These schoolrooms are controlled by programmable thermostats that come on shortly before occupancy and turn off right as school lets out. Therefore, the rooms are most always occupied while the systems are on, which limits the potential for savings with DCV.

For the Woodland Gibson room 1, a special test was performed with the outdoor air damper set to match the amount of ventilation air provided with a unit that has a standard factory issue fixed louver configuration. The amount of ventilation air for this configuration is too small for the occupancy and is approximately 110 cfm or around 3 to 4 cfm per person. Therefore, typical installations for modular schoolrooms probably do not provide adequate indoor air quality. At this lower ventilation air flowrate, the energy usage was nearly the same for both DCV On or DCV Off.

Figure 49 and Figure 50 give similar results for the Oakland schoolrooms. The data do not correlate nearly as well with daily ambient temperature as for the other sites. Although it appears that DCV results in some energy savings, the differences are within the uncertainty of the correlation with ambient temperature.

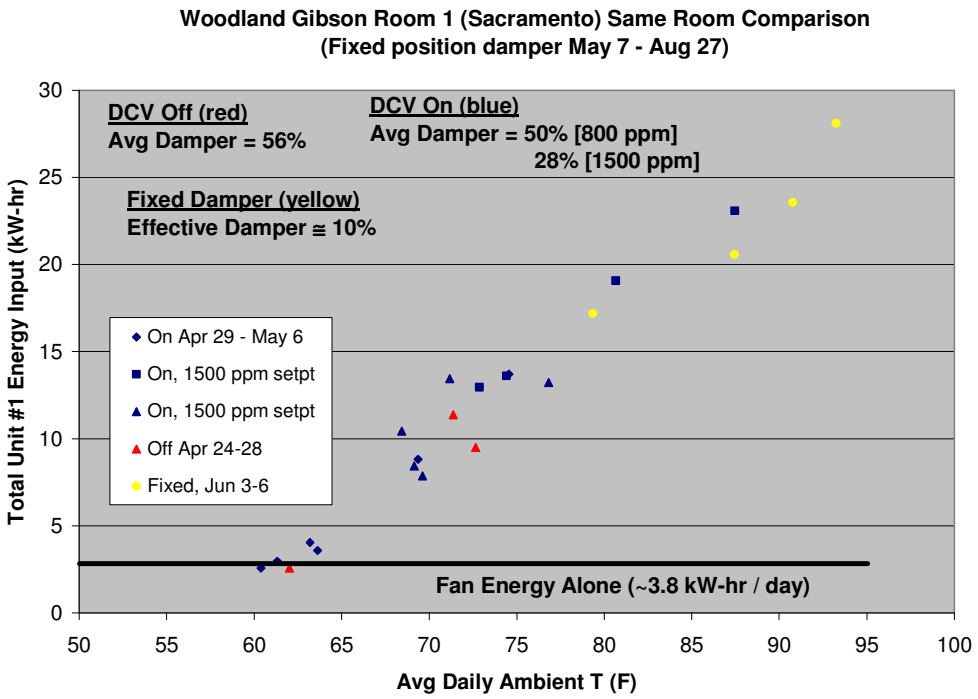

Figure 47. Correlated Daily Cooling Energy Use for DCV On and Off at Woodland (Sacramento) Schoolroom 1

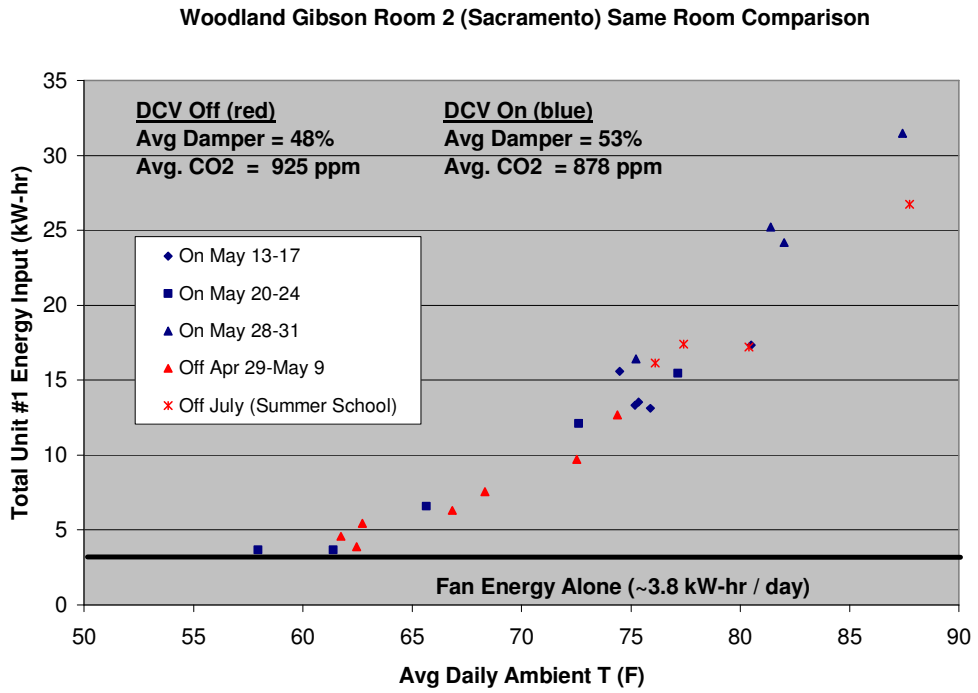

Figure 48. Correlated Daily Cooling Energy Use for DCV On and Off at Woodland (Sacramento) Schoolroom 2

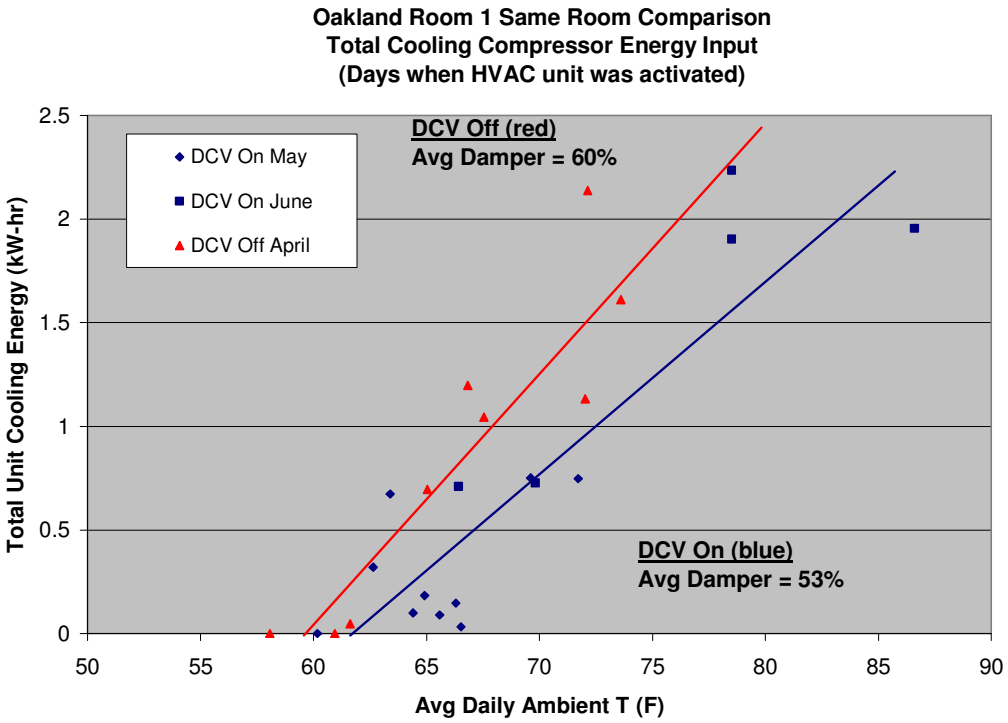

Figure 49. Correlated Daily Cooling Energy Use for DCV On and Off at Oakland Schoolroom 1

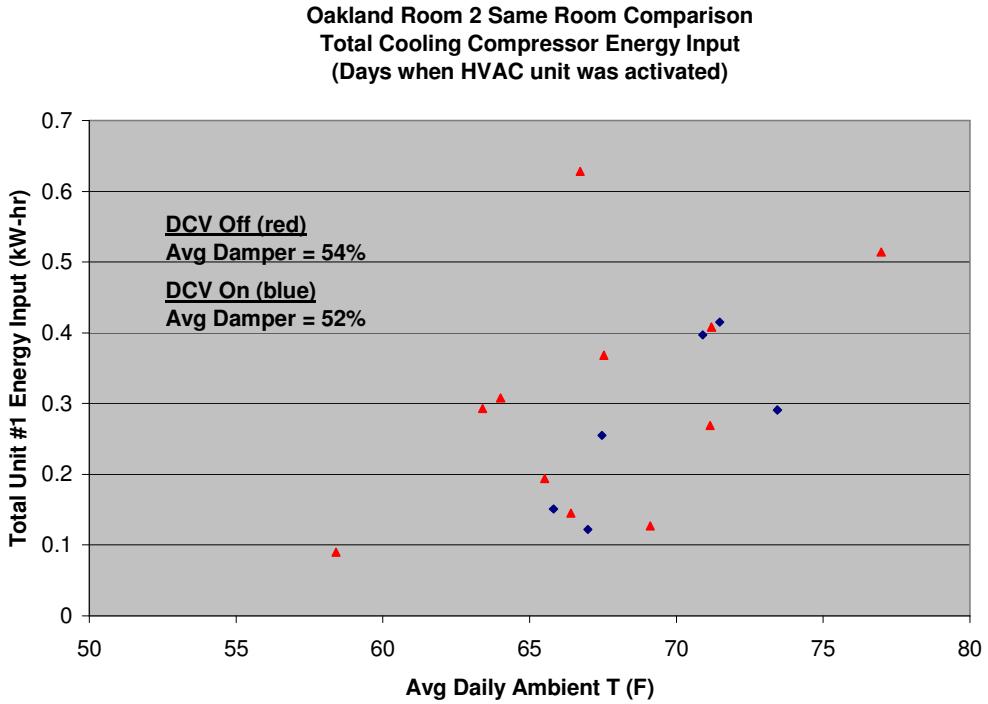

Figure 50. Correlated Daily Cooling Energy Use for DCV On and Off at Oakland Schoolroom 2

Indoor CO_2 Concentrations

Figure 51 is a histogram for return air CO_2 levels at one of the Gibson schoolrooms. Results are included for DCV On, DCV Off with fixed ventilation satisfying ASHRAE Standard 62-1999, and DCV Off with the ventilation airflow at the same level measured at a similar room that has only fixed air inlet louvers. Fixed air inlet louvers are the standard factory configuration for the sidewall mounted HVAC units, unless the economizer option is purchased with a modulating outdoor air damper. Since this is an additional option to the HVAC package, it is probably not installed in most school rooms.

The results in Figure 51 imply that the use of DCV results in better indoor air quality than for fixed ventilation determined according to ASHRAE Standard 62-1999. Possibly the metabolic rates assumed for application of the standard are lower than actually occur for this application. Furthermore, the use of the "Factory Standard" installation results in very high CO_2 concentrations. Over 60% of the occupied hours with the Factory Standard configuration had CO_2 levels that exceeded 1200 ppm. These levels violate California Title 24 requirements.

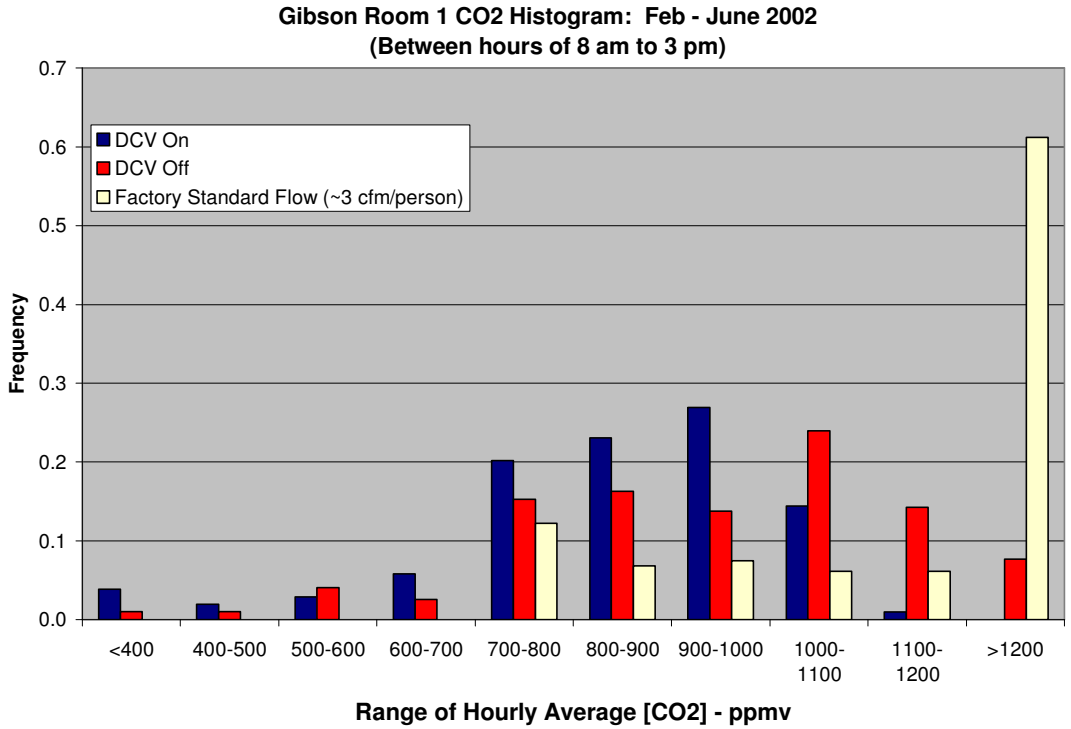

Figure 51. Histogram of Return Air CO_2 Concentrations at Woodland (Sacramento) Gibson Schoolroom 1 for DCV On, DCV Off, and Original Factory Installation

Figure 52 gives a histogram for the second Gibson schoolroom. Compared to room 1, the CO_2 levels are much higher for this room, implying a higher occupancy. However, there is a large number of hours for CO_2 concentrations above 1200 ppm with DCV Off that can't be explained by higher occupancy. This result may be due to problems with the controller. In some of the field sites, the minimum position for the outdoor air damper changes randomly at times and is not always maintained at the 40% set point for DCV Off.

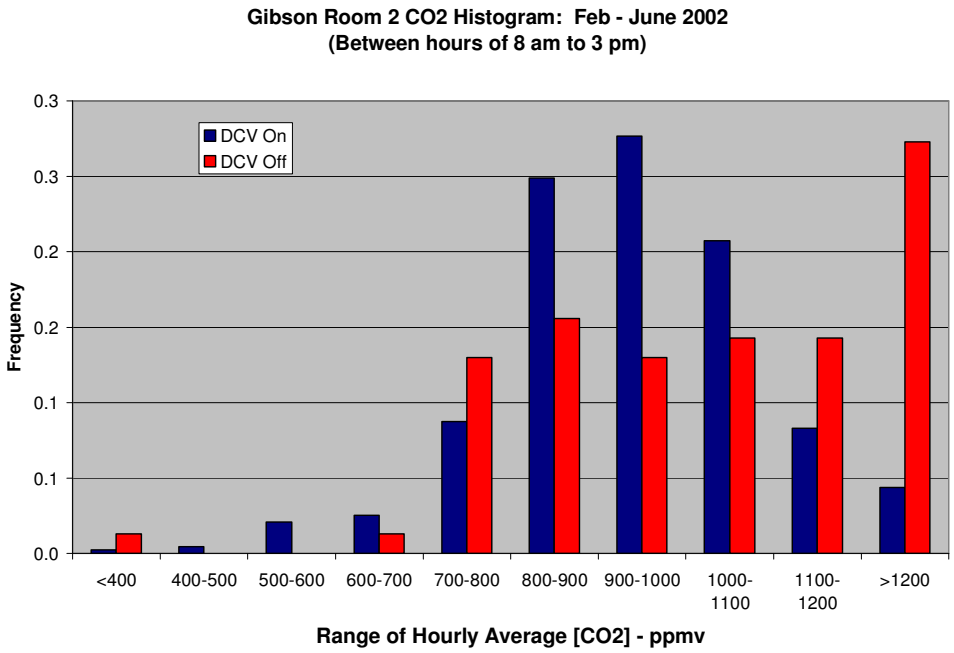

Figure 52. Histogram of Return Air CO_2 Concentrations at Woodland (Sacramento) Gibson Schoolroom 2 for DCV On and DCV Off

Field Results for Walgreens

Insufficient data are currently available to allow direct comparison of the DCV energy usage for cooling at the Walgreen sites. However, limited data for the late fall of 2002 at the Rialto site were used to validate a site-specific VSAT model. Figure 52 shows comparisons between daily measured and predicted energy usage for this site. The predictions of daily energy usage tend to be lower than the actual measurements for both DCV On and Off. However, the trends with respect to ambient temperature are similar. The measured performance is probably poorer than the predictions due to poor maintenance of the equipment at this site. The simulation could be improved through calibration of the equipment models. Figure 52 doesn't demonstrate significant savings for DCV. However, that is because the data are at low daily average ambient temperatures where an economizer operates a signficant portion of the time.

The VSAT simulation model was then used to predict total annual energy savings with a DCV retrofit for the Rialto Walgreens site. This comparison is given in Table 13. The comparison is only for the main retail store area and does not include the separate rooftop unit servicing the pharamacy area. These sites use heat pumps and thus electricity is the only energy source. The economic analysis for the Walgreen site does indeed provide an impressive case for installing DCV for a retail store in this climate. These results are very consistant with simulation results determined for the prototypical retail store in this climate zone. Actual cost savings realized depend on the assumption that the base case utilizes ventilation air flow rates that conform to the ASHRAE standard. For a retrofit installation, the economic benefit analysis also assumes that controllable air dampers, such as provided with an economizer system, are already installed. This was

not the case for both the Walgreens and modular school sites which had to be modified for controllable air dampers as part of this study.

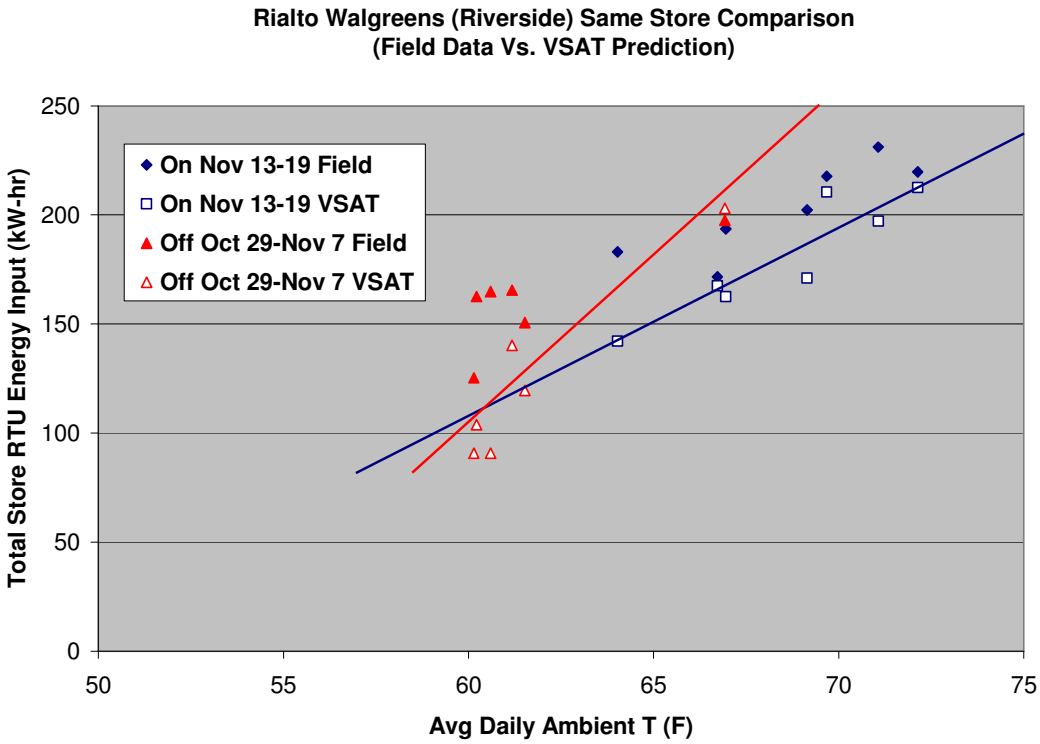

Figure 53. Comparison of Daily Cooling Energy Use at Rialto (LA Area, Inland Climate) Walgreens Site

Table 16. Predicted Annual Energy Savings with DCV On Control Strategy at a Walgreens Site Using VSAT Simulations

	Rialto (Riverside, CA)
Compressor power savings for heating and cooling (kW-hr)	16,391
Peak demand savings (kW)	17.1
Annual electrical energy cost savings ($)	$4,599
# RTU's per site	4
Total initial capital cost for DCV	$3,600
Simple payback period (years)	0.8
5 Year rate of return on investment in a DCV retrofit (%)	>300%

V. HPHR FIELD TESTING

A single field site was established for the heat pump heat recovery unit in order to verify that the equipment operates properly and that field performance is comparable to data obtained from the manufacturer and laboratory tests.

The heat pump was installed at Douglas Elementary School in Woodland, CA, in combination with a Carrier® 6-ton rooftop unit. Air inlet and outlet temperatures were measured using thermistors. Polymer capacitance humidity sensors were used to measure relative humidity at the inlets and outlets of the evaporator. Power consumption of the heat pump was monitored using a direct measure of the supply voltage and current draw from the unit. Two independent current measurements were taken in order to obtain both total and compressor power consumption. A more detailed description of the field site installation and setup is given by Braun and Mercer (2003b).

Figure 54 and Figure 55 show example operating conditions for cooling. Ambient air temperatures were very moderate throughout much of the day on August 2 and the heat pump did not operate very much during the first 4 occupied hours. The fan operated continuously for the entire occupied time to maintain proper ventilation. It's important to note that the fan power is very significant compared to the compressor power. The zone cooling set point for this day was approximately 72 F. The heat pump only operated to precondition the outside air for approximately one hour during the entire 8 hours of occupied cooling mode. Under these conditions, a system having an economizer with no energy recovery would have been would have used less energy and cost less to operate than the system with a heat pump. This is true throughout much of the cooling season in Woodland.

Figure 56 and Figure 57 give temperature and power measurements, respectively, for a much hotter day in Woodland. Ambient temperatures during occupied mode on July 24 were higher when compared to most other days in the data set from 2001 – 2002. For ambient temperatures between 90 F and 105 F, relative humidity varied from 24% to 4%, respectively. Therefore, even though ambient dry bulb temperatures were high, the actual wet bulb temperatures remained moderately low (~ 64 F) throughout the day. The heat pump operated several more hours on July 24 when compared to August 2 because of the higher building load, partly due to the higher ambient temperatures. For cooling mode, ambient wet bulb temperatures must exceed about 75 F and the heat pump must operate for a significant number of hours to enable a overall energy savings (see Braun and Mercer, 2003c).

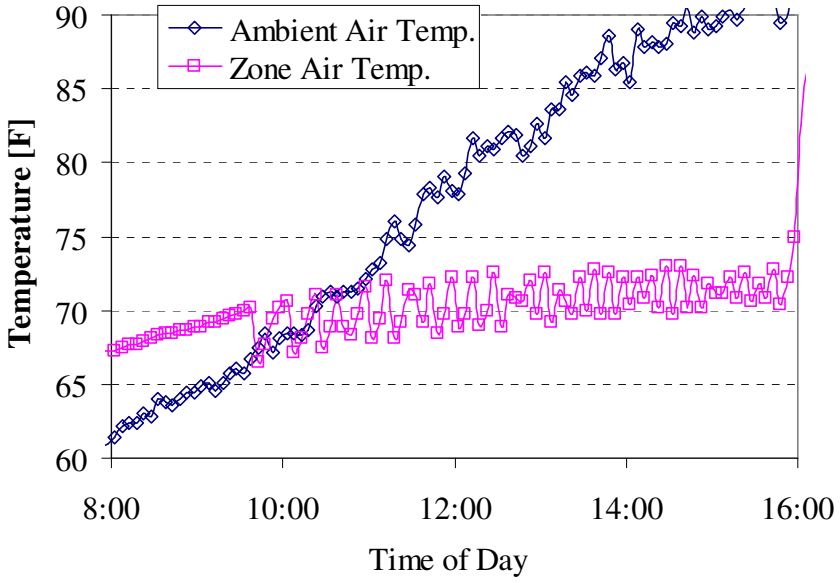

Figure 54. Occupied Daily Temperatures, August 2, 2002

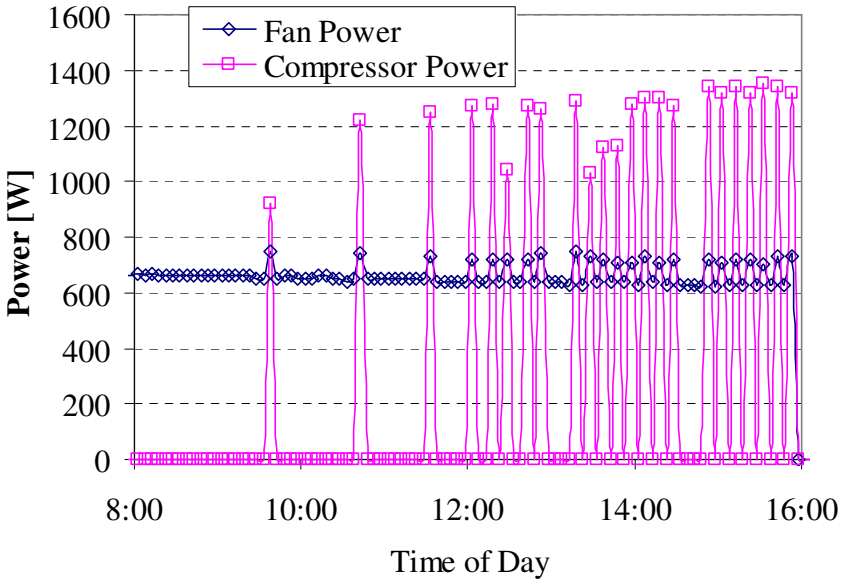

Figure 55. Occupied Daily Power, August 2, 2002

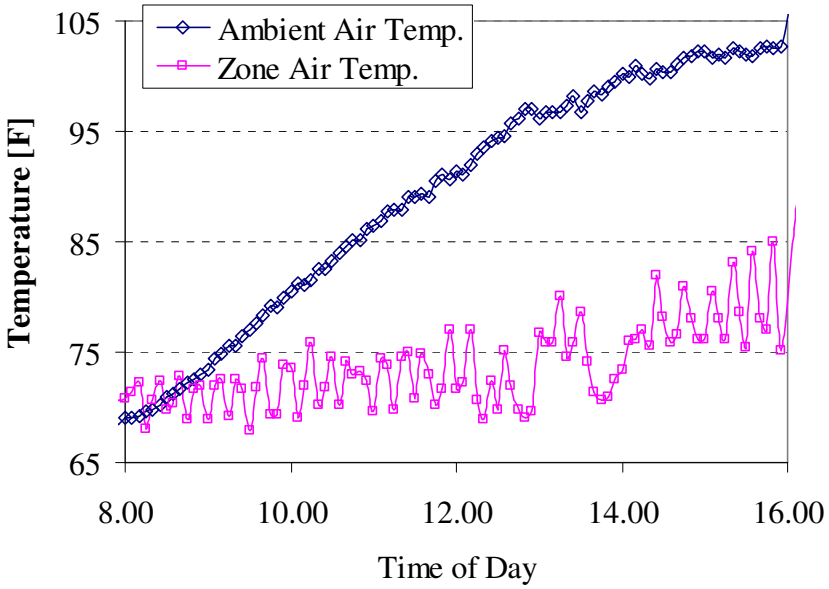

Figure 56. Occupied Daily Temperatures, July 24, 2002

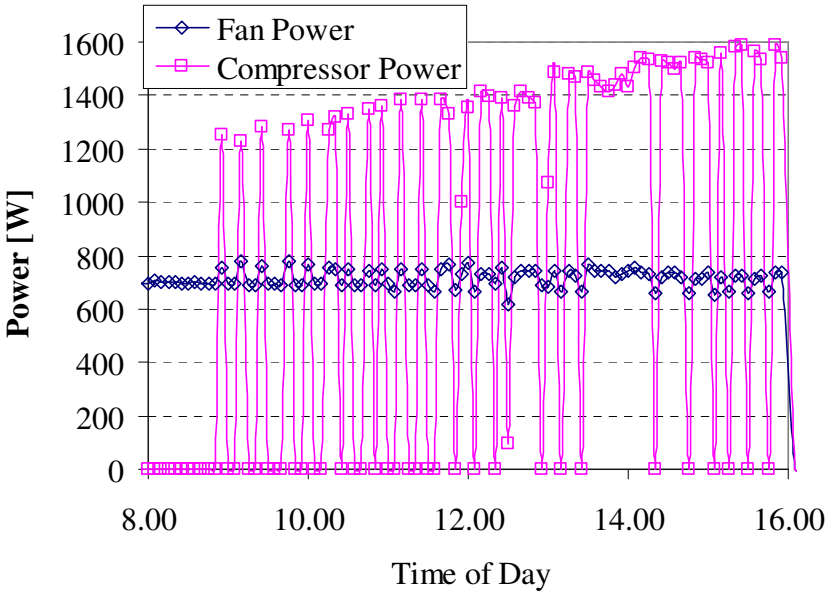

Figure 57. Occupied Daily Power, July 24, 2002

Steady-state operation of the heat pump occurred between 3:15 and 3:45 PM (7 – five-minute increment data points) on July 24. Figure 58 and Figure 59 show capacity and compressor power consumption for these steady-state points compared to model predictions, respectively. At steady-state conditions, the performance of the heat pump in the field is very close to the performance determined in the laboratory and published by the manufacturer. Furthermore, the model implemented within VSAT for the heat pump accurately predicts capacity and compressor power when compared to recorded field data

for steady-state conditions. However, the VSAT model does not include energy losses due to on/off cycling. Therefore, the VSAT predictions tend to be optimistic with respect to energy savings associated with the heat pump heat recovery unit.

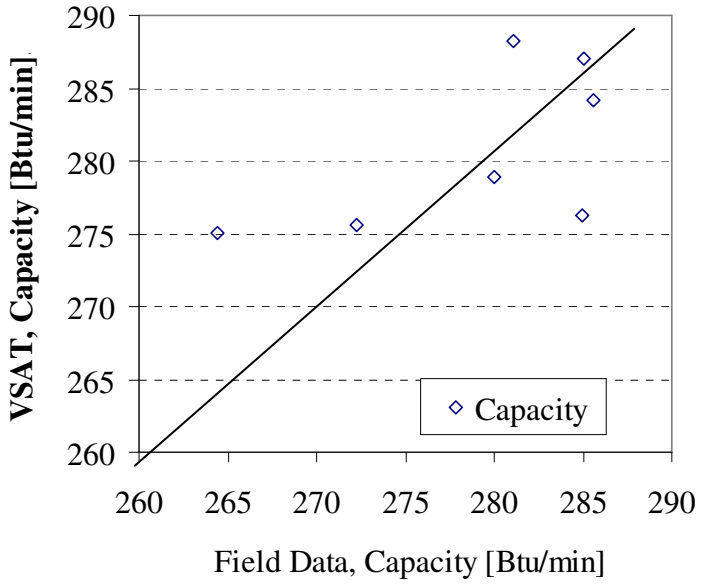

Figure 58. Predicted vs. Recorded Capacity (July 24, 2002)

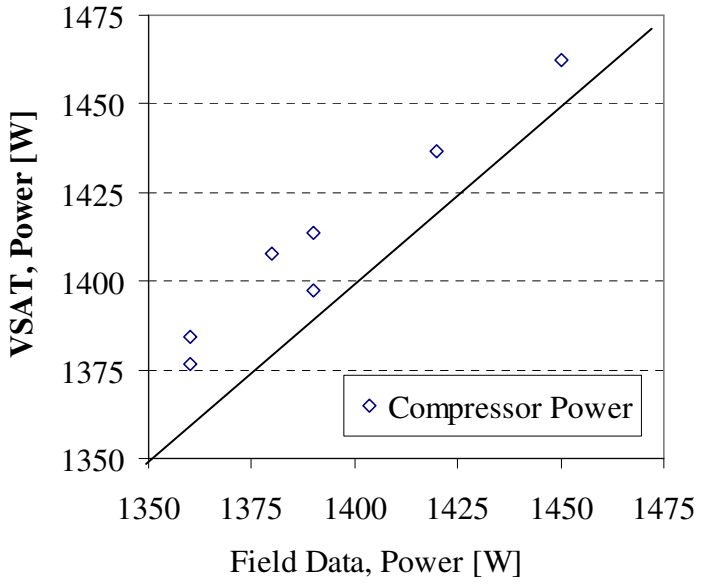

Figure 59. Predicted vs. Recorded Compressor Power (July 24, 2002)

Figure 60 and Figure 61 show example conditions for a day during the heating season in Woodland. The ambient temperature was near freezing early in the morning, but steadily increased up to 55 F by the end of the occupied time. The zone heating set point for this day was approximately 65 F. However, as in cooling season, the zone temperature set points were frequently altered.

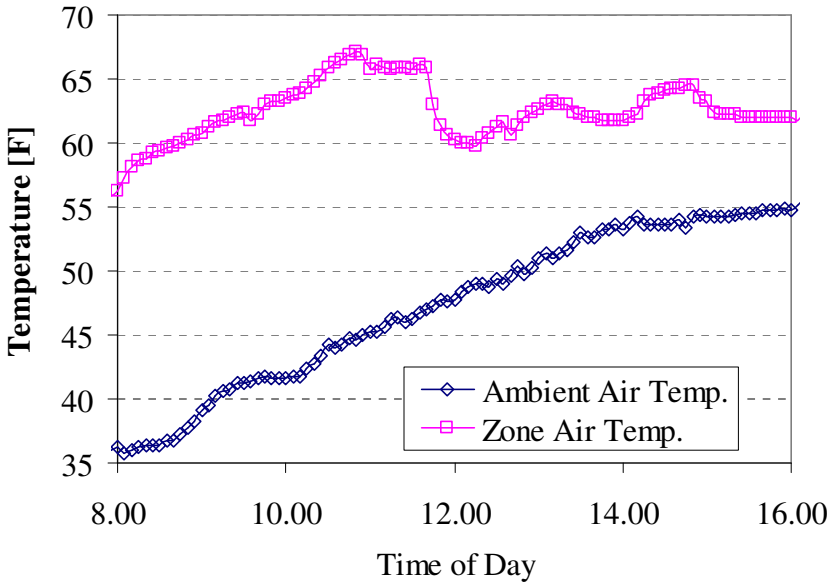

Figure 60. Occupied Daily Temperatures, Jan. 17, 2002

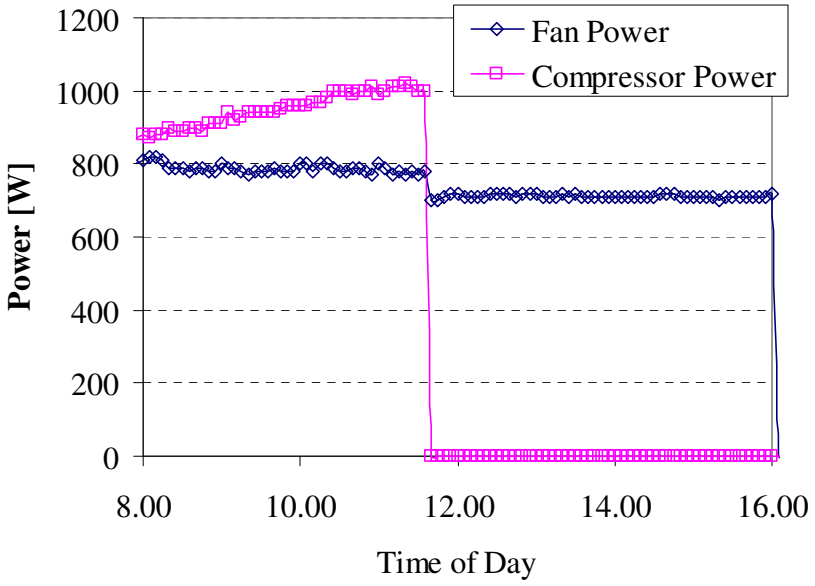

Figure 61. Occupied Daily Power, Jan. 17, 2002

Steady-state operation of the heat pump occurred between 8:00 and approximately 11:30 AM on January 17. For this 3 ½ hour time period, heat pump compressor power increased as ambient temperature increased. A total of 40, five-minute increment steady-state data points were used for comparisons with the VSAT model. Figure 62 and Figure 63 show capacity and compressor power consumption for these steady-state points compared to model predictions, respectively. For steady-state operation, the heat pump component model within VSAT accurately predicts capacity and compressor power compared to recorded field data.

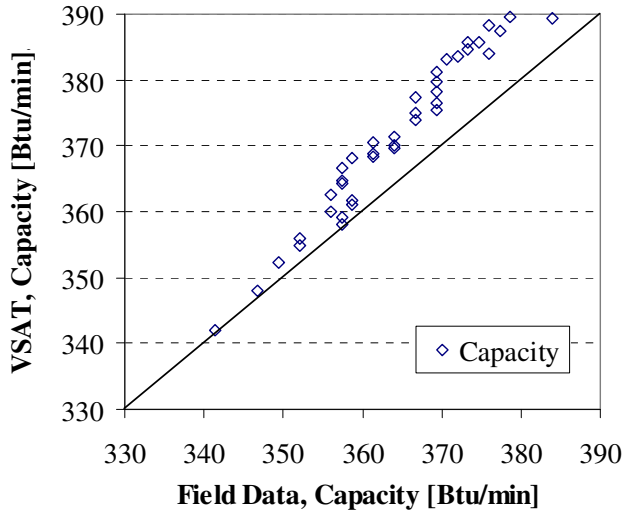

Figure 62. Predicted vs. Recorded Capacity (Jan. 17, 2002)

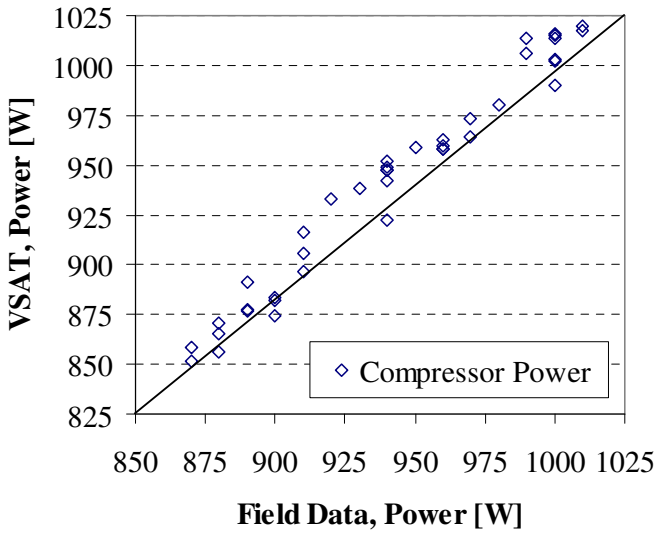

Figure 63. Predicted vs. Recorded Compressor Power (Jan. 17, 2002)

VI. CONCLUSIONS AND RECOMMENDATIONS

Demand-controlled ventilation coupled with an economizer (DCV+EC) was found to give the largest cost savings relative to an economizer only system for a number of different prototypical buildings and systems evaluated in the 16 California climate zones. These results were independent whether DCV is considered for retrofit or new applications. DCV reduces ventilation requirements and loads whenever the economizer is not enabled and the occupancy is less than the peak design value typically used to establish fixed ventilation rates according to ASHRAE Standard 62-1999. Lower ventilation loads lead to lower equipment loads, energy usage and peak electrical demand. The greatest cost savings occur for buildings that have low average occupancy relative to their peak occupancy, such as auditoriums, gyms and retail stores. From a climate perspective, the greatest savings and lowest payback periods occur in extreme climates (either hot or cold). The mild coastal climates have smaller savings and longer payback periods. In most cases, the payback period associated with DCV+EC was less than 2 years.

The heat pump heat recovery (HPHR) system did not provide positive cost savings for many situations investigated for California climates. Heating requirements are relatively low for California climates and therefore overall savings are dictated by cooling season performance. The cooling COP of the HPHR system must be high enough to overcome additional cycling losses from the primary air conditioner compressor, additional fan power associated with the exhaust and/or ventilation fan, additional cooling requirements due to a higher latent removal and a lower operating COP for the primary air conditioner compressor because of a colder mixed air temperature. In addition, the HPHR system is an alternative to an economizer and so economizer savings are also lost when utilizing this system. There are not sufficient hours of ambient temperatures above the breakeven points to yield overall positive savings with the HPHR system compared to a base case system with an economizer for the prototypical buildings in California climates.

The breakeven ambient temperatures for positive savings with the HXHR system are much lower than for the HPHR system because the energy recovery (and reduced ventilation load) does not require additional compressor power. The primary penalty is associated with increased fan power due to an additional exhaust fan. In addition, as with the HPHR system, the HXHR system is an alternative to an economizer. Therefore, economizer savings are also lost when utilizing this system. Although positive savings were realized for a number of different buildings and climate zones, the HXHR system had greater operating costs than the DCV system for all cases considered. Furthermore, the initial cost for an HXHR system is higher than a DCV system and also requires higher maintenance costs. Payback for the enthalpy exchanger was found to be greater than 7 years for most all areas of California, except for some building types in climate zone 15. However, paybacks were calculated assuming a retrofit application. The use of an enthalpy exchanger would lead to a smaller design load for the HVAC equipment which could impact the overall economics.

For humid climates (outside of California), the alternative ventilation strategies provide lower zone humidity levels than a conventional system during the cooling season. Typically, DCV provides the lowest zone humdities, followed by the HXHR system, and then the HPHR system.

The savings and trends determined through simulation for DCV were verified through field testing in a number of sites. Field sites were established for three different building types in two different climate zones within California. The building types are: 1) McDonalds PlayPlace® areas, 2) modular school rooms, and 3) Walgreens drug stores. In each case, nearly duplicate test buildings were identified in both coastal and inland climate areas. For cooling, greater energy and cost savings were achieved at the McDonalds PlayPlaces and Walgreens than for the modular schoolrooms. Primarily, this is because these buildings have more variability in their occupancy than the schoolrooms. The largest energy and cost savings were achieved at the Walgreens in Rialto, followed by the Bradshaw McDonalds PlayPlaces. The Rialto Walgreens appears to have the lowest occupancy and is located in a relatively hot climate with relatively large ventilation loads. The Bradshaw McDonalds PlacePlace appears to have the lowest average occupancy level compared to the other McDonalds PlacePlaces. This site is located in Sacramento and has larger ventilation and total cooling loads than the bay area McDonalds. The payback period for the Rialto Walgreens is less than a year and is between 3 and 6 years for the McDonalds PlayPlaces.

There were no substantial cooling season savings for the modular school rooms. The occupancy for the schools is relatively high with relatively small variability. The school sites are also on timers or controllable thermostats that mean the HVAC units only operate during the normal school day. The schools are also generally unoccupied during the heaviest load portion of the cooling season. Furthermore, the results imply that the average metabolic rate of the students may be higher than the value used in ASHRAE Standard 62-1999 to establish a fixed ventilation rate. In fact, the DCV control resulted in lower CO_2 concentrations than for fixed ventilation rate in the Woodland modular schoolrooms.

The field data confirmed that the steady-state performance of the heat pump in the field is very close to the performance determined in the laboratory and published by the manufacturer for both cooling and heating modes. Furthermore, the model implemented within VSAT for the heat pump accurately predicts capacity and compressor power when compared to recorded field data for steady-state conditions.

For most all locations throughout the state of California, demand-controlled ventilation with an economizer is the recommended ventilation strategy. An enthalpy exchanger is viable in many situations, but DCV was found to have better overall economics for retrofit applications. Heat pump heat recovery is not recommended for California. This technology would make more sense in cold climates where heating costs are more significant. The savings potential for all ventilation strategies is greater in cold climates where heating dominates.

VII. REFERENCES

ASHRAE (1999), *ANSI/ASHRAE Standard 62-1999: Ventilation for Acceptable Indoor Air Quality,* ASHRAE, 1791 Tullie Circle, NE, Atlanta, GA 30329.

Balcomb, J. D. (2002), *Mastering Energy-10: A User Manual for Version 1.5*, National Renewable Energy Laboratory, Golden, CO.

Brandemuehl, M.J. and Braun, James E. (2002), *The Savings Estimator,* Honeywell International Inc., Morristown, NJ., http://thermal.ies.lafayette.in.us/savest

Brandemuehl, M.J. and Braun, James E. (1999), *The Impact of Demand-Controlled and Economizer Ventilation Strategies of Energy Use in Buildings,* ASHRAE Transactions 105 (2): 39-50.

Brandemuehl, M.J., Gabel, S., and Andresen, I. (2000), *HVAC2 Toolkit: Algorithms and Subroutines for Secondary HVAC System Energy Calculations,* ASHRAE, 1791 Tullie Circle, NE, Atlanta, GA 30329.

Braun, J.E., and Mercer, K. (2002), *Laboratory Test Evaluation And Field Installation Of The Energy Recycler® Heat Pump as Deliverable 4.2.4a*, California Energy Commission, Sacramento, CA.

Braun, J.E. and Mercer, K. (2003), *VSAT – Ventilation Strategy Assessment Tool as Deliverables 3.1.2, 3.2.1 and 4.2.2,* California Energy Commission, Sacramento, CA.

Braun, J.E. and Mercer, K. (2003), *Field Data Analysis of the Energy Recycler® Heat Pump as Deliverable 4.2.5a*, California Energy Commission, Sacramento, CA.

Braun, J.E. and Mercer, K. (2003), *Operating Cost Assessments And Comparisons For Demand Controlled Ventilation, Heat Hump Heat Recovery And Enthalpy Exchangers as Deliverable 4.2.3a*, California Energy Commission, Sacramento, CA.

Carpenter, S.C. (1996), *Energy and IAQ Impacts of CO_2-Based Demand-Controlled Ventilation,* ASHRAE Transactions 102 (2): 80-88.

Donnini, G., Haghighat, F., and Hguyen, V. H. (1991), *Ventilation Control of Indoor Air Quality, Thermal Comfort, and Energy Conservation by CO_2 Measurement,* Proceedings of the 12th AIVC Conference Air Movement and Ventilation Control within Buildings: 311-331.

Emmerich, Steven J. and Persily, Andrew K. (2001), *State-of-the-Art Review of CO_2 Demand Controlled Ventilation Technology and Application,* Technical Report NISTIR 6729, National Institute of Standards and Technology, Gaithersburg, MD.

Fehrm, M., Reiners, W., and Ungemach, M. (2002), *Exhaust Air Heat Recovery in Buildings,* International Journal of Refrigeration 25: 439-449.

Gabel, S. D., Janssen, J., Christoffel, J., and Scarborough, S. (1986), *Carbon Dioxide Based Ventilation Control System Demonstration,* Technical Report DE-AC79-84BP15102, U.S. Department of Energy.

Haghighat, F., Zmeureanu, R., and Donnini G. (1993), *Energy Savings in a Building by a Demand Controlled Ventilation System,* Proceedings of the 6th International Conference on Indoor Air Quality and Climate. 5: 51-56.

Huang, Y.J., Akbari, H., Rainer, L., and Ritschard, R.L. (1990), *481 Prototypical Commercial Buildings for Twenty Urban Market Areas (Technical documentation of building loads data base developed for the GRI Cogeneration Market Assessment Model),* LBNL Report 29798, Lawrence Berkeley National Laboratory, Berkeley, CA.

Huang, Y.J., and Franconi, E. (1995), *Commercial Heating and Cooling Load Component Analysis,* LBNL Report 38970, Lawrence Berkeley National Laboratory, Berkeley, CA.

Janssen, J., Hill, T., Woods, J., and Maldonado, E. (1982), *Ventilation for Control of Indoor Air Quality: A Case Study,* Environment International. 8: 487-496.

Knoespel, P., Mitchell, J., and Beckman, W. (1991), *Macroscopic Model of Indoor Air Quality and Automatic Control of Ventilation Airflow,* ASHRAE Transactions 97 (2): 1020-1030.

Lawrence T.M. and Braun, J.E. (2003), *Initial Cooling And Heating Season Field Evaluations For Demand-Controlled Ventilation as Deliverable 3.1.3a and 3.1.4a*, California Energy Commission, Sacramento, CA.

Rengarajan, K., Shirey III, D., and Raustad, D. (1996), *Cost-Effective HVAC Technologies to Meet ASHRAE Standard 62-1989 in Hot and Humid Climates*, ASHRAE Transactions 102 (1): 166-182.

Shirey III, D., and Rengarajan, K. (1996), *Impact of ASHRAE Standard 62-1989 on Small Florida Offices,* ASHRAE Transactions 102 (1): 153-165.

Slayzak, S. J., Pesaran, A. A., and Hancock, C. E. (1998), *Experimental Evaluation of Commercial Desiccant Dehumidifier Wheels*, NREL Technical Report.

Slayzak, S. J., and Ryan, J. P. (1998), *Instrument Uncertainty Effect on Calculation of Absolute Humidity Using Dew Point, Wet Bulb, and Relative Humidity Sensors*, International Solar Energy Conference: 473-479.

Stiesch, G., Klein, S. A., and Mitchell, J. W. (1995), *Performance of Rotary Heat and Mass Exchangers*, International Journal HVAC&R Research 1(4): 308-323.

TRNSYS (2000), *TRNSYS Users Guide: A Transient Simulation Program*, Solar Energy Laboratory, University of Wisconsin-Madison. http://sel.me.wisc.edu/trnsys/Default.htm

Zamboni, M., Berchtold, O., Filleux, C., Fehlmann, J., and Drangsholt, F. (1991), *Demand Controlled Ventilation – An Application of Auditria,* Proceedings of the 12th AIVC Conference Air Movement and Ventilation Control within Buildings: 143-155.

APPENDIX A – PROTOTYPICAL BUILDING DESCRIPTIONS

Seven different types of buildings are considered in VSAT: small office, school class wing, retail store, restaurant dining area, school gymnasium, school library, and school auditorium. Descriptions for these buildings were obtained from prototypical building descriptions of commercial building prototypes developed by Lawrence Berkeley National Laboratory (Huang, et al., 1990 & Huang, et al., 1995). These reports served as the primary sources for prototypical building data. However, additional information was obtained from DOE-2 input files used by the researchers for their studies.

Tables A.1 through A.7 contain information on the geometry, construction materials, and internal gains used in modeling the different buildings. Although not given in these tables, the walls, roofs and floors include inside air and outside air thermal resistances. The window R-value includes the effects of the window construction and inside and outside air resistances. Table A.8 lists the properties of all construction materials and the air resistances. The geometry of each of the buildings is assumed to be rectangular with four sides and is specified with the following parameters: 1) floor area, 2) number of stories, 3) aspect ratio, 4) ratio of exterior perimeter to total perimeter, 5) wall height and 6) ratio of glass area to wall area. The aspect ratio is the ratio of the width to the length of the building. However, exterior perimeter and glass areas are assumed to be equally distributed on all sides of the building, giving equal exposure of exterior walls and windows to incident solar radiation. The four exterior walls face north, south, east, and west.

The user can specify occupancy schedules, but default values are based upon the original LBNL study. In the LBNL study, the occupancy was scaled relative to a daily average maximum occupancy density (people per 1000 ft^2). In VSAT, the user can specify a peak design occupancy density (people per 1000 ft^2) that is used for determining fixed ventilation requirements (no DCV). This same design occupancy density is used as the scaling factor for the hourly occupancy schedules. As a result, the original LBNL occupancy schedules were rescaled using the default peak design occupancy densities.

The heat gains and CO_2 generation per person depend upon the type of building (and associated activity). Design internal gains for lights and equipment also depend upon the building and are scaled according to specified average daily minimum and maximum gain fractions. For all of the buildings, the lights and equipment are at their average maximum values whenever the building is occupied and are at their average minimum values at all other times.

Zone thermostat set points can be set for both occupied and unoccupied periods. The default occupied set points for cooling and heating are 75 F and 70 F, respectively. The default unoccupied set points for cooling (setup) and heating (setback) are 85 F and 60 F, respectively. The lights are assumed to come on one hour before people arrive and stay on one hour after they leave. The occupied and unoccupied set points follow this same schedule.

Table A.1. Office Building Characteristics

Windows		
R-value, hr-ft^2-F/Btu	1.58	
Shading Coefficient	0.75	
Area ratio (window/wall)	0.15	
Exterior Wall Construction		
Layers	1" stone R-5.6 insulation R-0.89 airspace 5/8" gypsum	
Roof Construction		
Layers	Built-up roof (3/8") 4" lightweight concrete R-12.6 insulation R-0.92 airspace ½" acoustic tile	
Floor		
Layers	6" heavyweight concrete Carpet and pad	
Slab perimeter loss factor, Btu/h-ft-F	0.5	
General		
Floor area, ft^2	6600	
Wall height, ft	11	
Internal mass, lb/ft^2	25	
Number of stories	1	
Aspect Ratio	0.67	
Ratio of exterior perimeter to floor perimeter	1.0	
Design equipment gains, W/ft^2	0.5	
Design light gains, W/ft^2	1.7	
Ave. daily min. lights/equip. gain fraction	0.2	
Ave. daily max. lights/equip. gain fraction	0.9	
Sensible people gains, Btu/hr-person	250	
Latent people gains, Btu/hr-person	250	
CO_2 people generation, L/min-person	0.33	
Design occupancy for vent., people/1000 ft^2	7	
Design ventilation, cfm/person	20	
Average weekday peak occucpancy, ft^2/person	470	
Default average weekday occupancy schedule * Values given relative to average peak	Hours 1-7 8 9 10-16 17 18-24	Values 0.0 0.33 0.66 1.0 0.5 0.0
Default average weekend occupancy schedule * Values given relative to average peak	Hours 1-8 9 10-12 12-13 13-24	Values 0.0 0.15 0.2 0.15 0.0
Monthly occupancy scaling * relative to daily occupancy schedule	Month 1-12	Value 1.0

Table A.2. Restaurant Dining Area Characteristics

Windows		
R-value, hr-ft^2-F/Btu	1.53	
Shading Coefficient	0.8	
Area ratio (window/wall)	0.15	
Exterior Wall Construction		
Layers	3" face brick ½" plywood R-4.9 insulation 5/8" gypsum	
Roof Construction		
Layers	Built-up roof (3/8") ¾" plywood R-13.2 insulation R-0.92 airspace ½" acoustic tile	
Floor		
Layers	4" heavyweight concrete Carpet and pad	
Slab perimeter loss factor, Btu/h-ft-F	0.5	
General		
Floor area, ft^2	5250	
Wall height, ft	10	
Internal mass, lb/ft^2	25	
Number of stories	1	
Aspect Ratio	1.0	
Ratio of exterior perimeter to floor perimeter	0.75	
Design equipment gains, W/ft^2	0.0	
Design light gains, W/ft^2	2.0	
Ave. daily min. lights/equip. gain fraction	0.2	
Ave. daily max. lights/equip. gain fraction	1.0	
Sensible people gains, Btu/hr-person	250	
Latent people gains, Btu/hr-person	275	
CO_2 people generation, L/min-person	0.35	
Design occupancy for vent., people/1000 ft^2	30	
Design ventilation, cfm/person	20	
Average weekday peak occucpancy, ft^2/person	50	
Default average weekday occupancy schedule * Values given relative to average peak	Hours 1-6 7-12 13-24	Values 0.0 0.2,0.3,0.1,0.05,0.2,0.5 0.5,0.4,0.2,0.05,0.1,0.4, 0.6,0.5,0.4,0.2,0.1,0.0
Default average weekend occupancy schedule * Values given relative to average peak	Hours 1-6 7-12 13-24	Values 0.0 0.3,0.4,0.5,0.2,0.2,0.3 0.5,0.5,0.5,0.35,0.25, 0.5,0.8,0.8,0.7,0.4,0.2, 0.0
Monthly occupancy scaling * relative to daily occupancy schedule	Month 1-5 6-8 9-12	Value 1.0 0.5 1.0

Table A.3. Retail Store Characteristics

Windows		
R-value, hr-ft^2-F/Btu	1.5	
Shading Coefficient	0.76	
Area ratio (window/wall)	0.15	
Exterior Wall Construction		
Layers	8” lightweight concrete R-4.8 insulation R-0.89 airspace 5/8” gypsum	
Roof Construction		
Layers	Built-up roof (3/8”) 1.25” lightweight concrete R-12 insulation R-0.92 airspace ½” acoustic tile	
Floor		
Layers	4” lightweight concrete Carpet and pad	
Slab perimeter loss factor, Btu/h-ft-F	0.5	
General		
Floor area, ft^2	80,000	
Wall height, ft	15	
Internal mass, lb/ft^2	25	
Number of stories	2	
Aspect Ratio	0.5	
Ratio of exterior perimeter to floor perimeter	1.0	
Design equipment gains, W/ft^2	0.4	
Design light gains, W/ft^2	1.6	
Ave. daily min. lights/equip. gain fraction	0.2	
Ave. daily max. lights/equip. gain fraction	0.9	
Sensible people gains, Btu/hr-person	250	
Latent people gains, Btu/hr-person	250	
CO_2 people generation, L/min-person	0.33	
Design occupancy for vent., people/1000 ft^2	25	
Design ventilation, cfm/person	15	
Average weekday peak occucpancy, ft^2/person	390	
Default average weekday occupancy schedule * Values given relative to average peak	Hours 1-7 8 9 10-20 21 22-24	Values 0.0 0.33 0.66 1.0 0.5 0.0
Default average weekend occupancy schedule * Values given relative to average peak	Hours 1-7 8 9 10-20 21 22-24	Values 0.0 0.33 0.66 1.0 0.5 0.0
Monthly occupancy scaling * relative to daily occupancy schedule	Month 1-12	Value 1.0

Table A.4. School Class Wing Characteristics

Windows		
R-value, hr-ft^2-F/Btu	1.7	
Shading Coefficient	0.73	
Area ratio (window/wall)	0.18	
Exterior Wall Construction		
Layers	8" concrete block R-5.7 insulation 5/8" gypsum	
Roof Construction		
Layers	Built-up roof (3/8") ¾" plywood R-13.3 insulation R-0.92 airspace ½" acoustic tile	
Floor		
Layers	6" heavyweight concrete	
Slab perimeter loss factor, Btu/h-ft-F	0.5	
General		
Floor area, ft^2	9600	
Internal mass, lb/ft^2	25	
Wall height, ft	10	
Number of stories	2	
Aspect Ratio	0.5	
Ratio of exterior perimeter to floor perimeter	0.875	
Design equipment gains, W/ft^2	0.3	
Design light gains, W/ft^2	2.2	
Ave. daily min. lights/equip. gain fraction	0.1	
Ave. daily max. lights/equip. gain fraction	0.95	
Sensible people gains, Btu/hr-person	250	
Latent people gains, Btu/hr-person	200	
CO_2 people generation, L/min-person	0.3	
Design occupancy for vent., people/1000 ft^2	25	
Design ventilation, cfm/person	15	
Average weekday peak occucpancy, ft^2/person	50	
Default average weekday occupancy schedule * Values given relative to average peak	Hours 1-6 7 8-11 12-15 16 17 18 19-21 22-24	Values 0.0 0.1 0.9 0.8 0.45 0.15 0.05 0.33 0.0
Default average weekend occupancy schedule * Values given relative to average peak	Hours 1-9 10-13 14-24	Value 0.0 0.1 0.0
Monthly occupancy scaling * relative to daily occupancy schedule	Month 1-5 6-8 9-12	Value 1.0 0.5 1.0

Table A.5. School Gymnasium Characteristics

Windows		
R-value, hr-ft^2-F/Btu	1.7	
Shading Coefficient	0.73	
Area ratio (window/wall)	0.18	
Exterior Wall Construction		
Layers	8" concrete block R-5.7 insulation 5/8" gypsum	
Roof Construction		
Layers	Built-up roof (3/8") ¾" plywood R-13.3 insulation R-0.92 airspace ½" acoustic tile	
Floor		
Layers	6" heavyweight concrete	
Slab perimeter loss factor, Btu/h-ft-F	0.5	
General		
Floor area, ft^2	7500	
Internal mass, lb/ft^2	25	
Wall height, ft	32	
Number of stories	1	
Aspect Ratio	0.86	
Ratio of exterior perimeter to floor perimeter	0.86	
Design equipment gains, W/ft^2	0.2	
Design light gains, W/ft^2	0.65	
Ave. daily min. lights/equip. gain fraction	0.0	
Ave. daily max. lights/equip. gain fraction	0.9	
Sensible people gains, Btu/hr-person	250	
Latent people gains, Btu/hr-person	550	
CO_2 people generation, L/min-person	0.55	
Design occupancy for vent., people/1000 ft^2	30	
Design ventilation, cfm/person	20	
Average weekday peak occucpancy, ft^2/person	180	
Default average weekday occupancy schedule * Values given relative to average peak	Hours 1-7 8-15 16-24	Value 0.0 1.0 0.0
Default average weekend occupancy schedule * Values given relative to average peak	Hours 1-24	Value 0.0
Monthly occupancy scaling * relative to daily occupancy schedule	Month 1-5 6-8 9-12	Value 1.0 0.1 1.0

Table A.6. School Library Characteristics

Windows		
R-value, hr-ft^2-F/Btu	1.7	
Shading Coefficient	0.73	
Area ratio (window/wall)	0.18	
Exterior Wall Construction		
Layers	8" concrete block R-5.7 insulation 5/8" gypsum	
Roof Construction		
Layers	Built-up roof (3/8") ¾" plywood R-13.3 insulation R-0.92 airspace ½" acoustic tile	
Floor		
Layers	6" heavyweight concrete	
Slab perimeter loss factor, Btu/h-ft-F	0.5	
General		
Floor area, ft^2	1500	
Internal mass, lb/ft^2	25	
Wall height, ft	10	
Number of stories	1	
Aspect Ratio	0.2	
Ratio of exterior perimeter to floor perimeter	0.75	
Design equipment gains, W/ft^2	0.4	
Design light gains, W/ft^2	1.5	
Ave. daily min. lights/equip. gain fraction	0.1	
Ave. daily max. lights/equip. gain fraction	0.95	
Sensible people gains, Btu/hr-person	250	
Latent people gains, Btu/hr-person	250	
CO_2 people generation, L/min-person	0.33	
Design occupancy for vent., people/1000 ft^2	20	
Design ventilation, cfm/person	15	
Average weekday peak occucpancy, ft^2/person	100	
Default average weekday occupancy schedule * Values given relative to average peak	Hours 1-6 7 8-11 12-15 16 17 18 19-21 22-24	Value 0.0 0.1 0.9 0.8 0.45 0.15 0.05 0.33 0.0
Default average weekend occupancy schedule * Values given relative to average peak	Hours 1-9 10-13 14-24	Value 0.0 0.1 0.0
Monthly occupancy scaling * relative to daily occupancy schedule	Month 1-5 6-8 9-12	Value 1.0 0.5 1.0

Table A.7. School Auditorium Characteristics

Windows		
R-value, hr-ft^2-F/Btu	1.7	
Shading Coefficient	0.73	
Area ratio (window/wall)	0.18	
Exterior Wall Construction		
Layers	8" concrete block R-5.7 insulation 5/8" gypsum	
Roof Construction		
Layers	Built-up roof (3/8") ¾" plywood R-13.3 insulation R-0.92 airspace ½" acoustic tile	
Floor		
Layers	6" heavyweight concrete	
Slab perimeter loss factor, Btu/h-ft-F	0.5	
General		
Floor area, ft^2	6000	
Internal mass, lb/ft^2	25	
Wall height, ft	32	
Number of stories	1	
Aspect Ratio	0.64	
Ratio of exterior perimeter to floor perimeter	0.85	
Design equipment gains, W/ft^2	0.2	
Design light gains, W/ft^2	0.8	
Ave. daily min. lights/equip. gain fraction	0.0	
Ave. daily max. lights/equip. gain fraction	0.9	
Sensible people gains, Btu/hr-person	250	
Latent people gains, Btu/hr-person	200	
CO_2 people generation, L/min-person	0.3	
Design occupancy for vent., people/1000 ft^2	150	
Design ventilation, cfm/person	15	
Average weekday peak occucpancy, ft^2/person	100	
Default average weekday occupancy schedule * Values given relative to average peak	Hours 1-9 10-11 12 13-14 15-24	Values 0.0 0.75 0.2 0.75 0.0
Default average weekend occupancy schedule * Values given relative to average peak	Hours 1-24	Value 0.0
Monthly occupancy scaling * relative to daily occupancy schedule	Month 1-5 6-8 9-12	Value 1.0 0.1 1.0

Table A.8. Construction Material Properties

	Conductivity (Btu/h*ft*F)	Density (lb/ft^3)	Specific Heat (Btu/lb*F)
stone	1.0416	140	0.20
light concrete	0.2083	80	0.20
heavy concrete	1.0417	140	0.20
built-up roof	0.0939	70	0.35
face brick	0.7576	130	0.22
acoustic tile	0.033	18	0.32
gypsum	0.0926	50	0.20
	Thermal Resistance ($h*ft^2*F/Btu$)		
3/4" plywood	0.93703		
1/2" plywood	0.62469		
carpet and pad	2.08		
inside air	0.67		
outside air	0.33		

APPENDIX B – BASE CASE ANNUAL SIMULATION RESULTS

The assumed base case utilizes a fixed damper position with a setup/setback control thermostat and a differential enthalpy economizer. Most commercial buildings in California employ an economizer control and therefore, it is not relevant to compare savings to systems that do not have an economizer. Annual results are presented in this section for each of the prototypical building types in all California climate zones. The results include the following quantities:

- Input air conditioner energy (AC compressor and condenser fan), kWh
- Input supply fan energy, kWh
- Peak electric demand, kW
- Input gas, Therm
- Energy consumption cost, $
- Electric demand cost, $
- Total electric cost, $
- Gas consumption cost, $
- Total system operating cost, $

Tables B.1 – B.7 show the annual results for all California climate zones assuming the base case and default building descriptions. Annual AC input power and electric demand for all building types is the lowest for CZ 1. This zone is located in the northwest coastal area of California (see Figure 5). Summer ambient temperatures are relatively moderate in this region and afford a greater opportunity for economizer controls. The highest cooling requirements are for buildings in zones 4, 10, 13 and 15. These zones are located in the south-central area of the state where it is typically very hot and dry during the summer. Not as much opportunity exists for economizer control and as a result, more mechanical cooling is required. Zones in the southwest and north/central east areas of the state require a moderate amount of mechanical cooling. Higher ambient temperatures are found here, however, not in the extreme dry bulb ranges found in the south-central zones. Input gas for furnace operation is relatively low for the entire state of California when compared to other locations across the United States. Climate zones 1, 14 and 16 typically require the most heating during winter months. These locations are further to the north and eastern areas of the state. Zones in the central and western areas of the state require less heating with generally the least amount of heating in zones 6, 7 and 15.

Table B.1. Office Base Case Annual Results

Setup/ Setback with Economizer - Base Case									
location	AC, kwh	Fan, kwh	Elec. Dmd, kW	Gas, Therm	Energy, $	Demand, $	Total Elec., $	Gas, $	Total, $
CACZ01	3497	6328	14	277	652	1583	2235	205	2439
CACZ02	15236	9570	23	322	1683	2788	4470	238	4708
CACZ03	10439	7814	18	119	1231	2231	3462	88	3550
CACZ04	17902	9395	25	169	1841	2841	4681	125	4807
CACZ05	12716	7961	19	100	1371	2306	3677	74	3751
CACZ06	17312	7931	18	17	3848	703	4552	12	4564
CACZ07	20216	8316	21	12	2783	1108	3891	9	3900
CACZ08	22873	9213	24	44	4879	897	5777	31	5808
CACZ09	24499	11365	28	28	5490	1048	6537	20	6557
CACZ10	25879	10710	27	88	5683	1036	6720	62	6782
CACZ11	22613	11314	28	354	2266	3222	5488	262	5749
CACZ12	21107	11480	29	287	2188	3175	5363	213	5576
CACZ13	30116	12567	32	224	2810	3677	6488	166	6653
CACZ14	25515	11151	28	368	5762	1039	6802	260	7062
CACZ15	49615	12966	34	30	9194	1353	10547	22	10569
CACZ16	10483	9099	22	1082	3261	792	4053	766	4819

Table B.2. Restaurant Dining Area Base Case Annual Results

Setup/ Setback with Economizer - Base Case									
location	AC, kwh	Fan, kwh	Elec. Dmd, kW	Gas, Therm	Energy, $	Demand, $	Total Elec., $	Gas, $	Total, $
CACZ01	2329	9693	15	1969	742	1523	2264	1434	3699
CACZ02	17331	19882	27	1697	2410	3204	5614	1245	6859
CACZ03	8879	15802	23	975	1567	2593	4159	717	4877
CACZ04	20949	23008	36	1031	2833	3728	6561	760	7321
CACZ05	10268	16955	24	931	1713	2643	4356	681	5037
CACZ06	16266	14309	24	383	4452	850	5302	271	5573
CACZ07	19990	16418	31	299	3539	1348	4887	224	5111
CACZ08	24522	19509	32	454	6440	1157	7596	321	7918
CACZ09	29125	23927	37	407	7747	1341	9088	288	9376
CACZ10	32998	23997	34	668	8399	1299	9698	473	10171
CACZ11	29835	23269	33	1569	3402	3595	6997	1159	8156
CACZ12	25643	22219	33	1448	3095	3523	6618	1068	7686
CACZ13	41199	26197	38	1127	4277	4257	8534	833	9367
CACZ14	34117	23868	34	1700	8554	1264	9818	1203	11022
CACZ15	72157	28763	44	294	14247	1715	15962	208	16170
CACZ16	12303	19206	25	4031	4683	937	5620	2853	8473

Table B.3. Retail Store Base Case Annual Results

Setup/ Setback with Economizer - Base Case									
location	AC, kwh	Fan, kwh	Elec. Dmd, kW	Gas, Therm	Energy, $	Demand, $	Total Elec., $	Gas, $	Total, $
CACZ01	34215	85859	167	9075	7686	16403	24089	6692	30780
CACZ02	189276	171442	279	8387	23806	32462	56269	6187	62456
CACZ03	109924	130176	238	3763	15699	26149	41849	2784	44633
CACZ04	233357	187506	356	4233	27684	36940	64623	3132	67755
CACZ05	122766	137116	241	2669	16790	26106	42897	1973	44869
CACZ06	196679	117971	235	689	46939	8413	55352	488	55840
CACZ07	233119	136999	297	436	36122	13652	49774	327	50100
CACZ08	273477	159503	308	1164	64737	11239	75976	824	76800
CACZ09	312805	203975	363	889	77227	13231	90458	630	91088
CACZ10	347519	188952	325	2169	80993	12472	93465	1536	95001
CACZ11	310053	196469	328	8661	32999	36398	69398	6407	75805
CACZ12	275714	197827	343	7303	31098	36551	67650	5403	73053
CACZ13	418430	214643	380	5636	40832	42054	82886	4170	87057
CACZ14	346838	199771	338	9049	82937	12583	95520	6406	101926
CACZ15	710167	239280	433	660	137239	16948	154187	467	154654
CACZ16	129851	152802	257	26113	44036	9281	53317	18485	71802

Table B.4. School Library Base Case Annual Results

Setup/ Setback with Economizer - Base Case									
location	AC, kwh	Fan, kwh	Elec. Dmd, kW	Gas, Therm	Energy, $	Demand, $	Total Elec., $	Gas, $	Total, $
CACZ01	612	2379	4	224	190	421	611	165	777
CACZ02	4590	4189	8	203	582	896	1477	150	1627
CACZ03	2595	3251	6	94	384	700	1084	70	1154
CACZ04	5430	4358	9	109	646	947	1593	81	1673
CACZ05	3065	3401	6	57	420	704	1124	42	1166
CACZ06	4591	3723	7	11	1238	238	1476	8	1484
CACZ07	5731	3426	7	6	894	363	1257	5	1262
CACZ08	6751	3904	8	24	1593	302	1895	17	1911
CACZ09	7538	4950	10	18	1869	362	2231	13	2244
CACZ10	8368	4589	9	43	1964	345	2309	30	2339
CACZ11	7749	4760	9	225	819	1038	1857	166	2023
CACZ12	6816	4802	9	190	766	1026	1791	140	1932
CACZ13	10407	4787	10	152	985	1160	2145	112	2258
CACZ14	8758	4772	9	205	2065	356	2421	145	2567
CACZ15	17545	5647	12	13	3361	497	3858	9	3868
CACZ16	3275	3635	7	625	1091	256	1347	442	1789

Table B.5. School Gym Base Case Annual Results

Setup/ Setback with Economizer - Base Case									
location	AC, kwh	Fan, kwh	Elec. Dmd, kW	Gas, Therm	Energy, $	Demand, $	Total Elec., $	Gas, $	Total, $
CACZ01	930	5606	21	2070	419	1647	2066	1517	3584
CACZ02	16170	11538	44	1674	1893	4861	6754	1233	7988
CACZ03	7784	8376	34	1069	1093	3564	4657	789	5446
CACZ04	18736	12324	55	1086	2109	5460	7570	803	8373
CACZ05	9720	9189	35	673	1256	3666	4922	497	5419
CACZ06	15729	10383	36	286	4034	1318	5352	203	5554
CACZ07	20531	9028	46	166	2909	1835	4744	124	4868
CACZ08	24718	10977	50	308	5560	1796	7355	218	7573
CACZ09	28146	14594	58	322	6721	2087	8808	228	9036
CACZ10	30893	13435	53	411	7057	2049	9106	291	9397
CACZ11	29218	14074	54	1723	2897	5890	8787	1275	10062
CACZ12	26250	13696	55	1575	2696	5696	8392	1165	9557
CACZ13	41168	14330	61	1280	3650	6549	10199	947	11146
CACZ14	34363	14297	55	1511	7711	2069	9780	1070	10850
CACZ15	73327	17778	71	173	13455	2723	16178	122	16300
CACZ16	11051	10144	42	3924	3585	1468	5053	2778	7831

Table B.6. School Classroom Wing Base Case Annual Results

Setup/ Setback with Economizer - Base Case									
location	AC, kwh	Fan, kwh	Elec. Dmd, kW	Gas, Therm	Energy, $	Demand, $	Total Elec., $	Gas, $	Total, $
CACZ01	5535	16231	26	382	1388	3007	4395	283	4678
CACZ02	28507	22765	43	470	3392	5131	8522	347	8870
CACZ03	18135	19092	36	136	2443	4349	6793	100	6893
CACZ04	34679	24676	52	193	3911	5760	9671	143	9814
CACZ05	22393	19751	37	88	2721	4381	7101	65	7167
CACZ06	29995	23756	40	6	7857	1453	9310	4	9314
CACZ07	38187	20338	44	3	5683	2247	7929	2	7932
CACZ08	43903	22324	50	34	9754	1754	11508	24	11532
CACZ09	46868	28725	56	13	11201	2072	13273	9	13282
CACZ10	51342	25735	50	90	11557	1931	13488	64	13551
CACZ11	44422	24917	49	579	4532	5665	10197	428	10625
CACZ12	40086	24557	50	448	4259	5618	9877	332	10209
CACZ13	59456	25356	54	348	5486	6400	11886	257	12143
CACZ14	49725	25598	50	614	11410	1917	13327	435	13762
CACZ15	99443	30298	63	22	18675	2625	21300	15	21315
CACZ16	20232	19548	39	2177	6255	1434	7689	1541	9231

Table B.7. School Auditorium Base Case Annual Results

Setup/ Setback with Economizer - Base Case									
location	AC, kwh	Fan, kwh	Elec. Dmd, kW	Gas, Therm	Energy, $	Demand, $	Total Elec., $	Gas, $	Total, $
CACZ01	219	10855	23	3739	713	1808	2521	2715	5236
CACZ02	18264	12109	69	2726	2092	7291	9382	2006	11388
CACZ03	5229	10869	45	2080	1077	4855	5932	1532	7464
CACZ04	20421	12911	93	1900	2274	8308	10582	1404	11986
CACZ05	8800	10854	54	1104	1299	5373	6672	813	7485
CACZ06	14539	10882	54	669	3909	1942	5851	473	6324
CACZ07	19222	10915	76	433	2973	2713	5686	324	6011
CACZ08	27241	11847	80	594	6183	2855	9038	420	9459
CACZ09	33231	15704	97	622	7779	3317	11096	441	11536
CACZ10	36685	15006	86	705	8366	3374	11740	499	12240
CACZ11	33972	15330	85	2699	3317	8954	12271	1994	14265
CACZ12	29786	14327	84	2607	2987	8432	11418	1926	13345
CACZ13	48705	15989	95	2097	4277	10188	14464	1551	16015
CACZ14	42047	16090	91	2392	9283	3420	12704	1693	14397
CACZ15	94136	21104	122	232	17284	4675	21959	164	22124
CACZ16	12381	11086	57	5780	3976	2163	6139	4092	10230

APPENDIX C – NEW BUILDING DESIGN APPLICATION RESULTS

Table C.1. Savings for DCV+EC in New Building Applications

	RTU Size tons	number of DCV units	First Cost $	Annual Cost Savings, $
	Office			
CACZ06	14.54	2	1800	299
CACZ15	23.91	2	1800	948
	Restaurant			
CACZ06	14.80	2	1800	446
CACZ15	29.73	2	1800	3269
	Retail Store			
CACZ06	144.82	7	6300	3775
CACZ15	294.49	14	12600	37612
	Auditorium			
CACZ06	42.54	3	2700	1921
CACZ15	78.77	4	3600	8430

Table C.2. Savings for HXHR in New Building Applications

	RTU Size tons	OA frac.	HXHR Downsize, tons	Downsize Cost Saved, $	Vent. Flow cfm	First Cost $	Annual Cost Savings, $
				Office			
CACZ06	14.01	0.188	0.53	529	921	1842	-726
CACZ15	21.07	0.125	2.85	2846	924	1848	490
				Restaurant			
CACZ06	12.98	0.692	1.82	1821	3144	6287	-1117
CACZ15	20.39	0.439	9.34	9336	3132	6264	3172
				Retail Store			
CACZ06	126.49	0.678	18.33	18333	30000	60000	-10603
CACZ15	201.78	0.424	92.71	92714	29994	59988	29054
				Auditorium			
CACZ06	24.46	0.909	18.08	18079	13497	26994	-730
CACZ15	36.98	0.909	41.79	41795	13514	27028	7177

Table C.3. Savings for HPHR in New Building Applications

	RTU Size	OA frac.	HXHR	Downsize	Vent. Flow	First Cost	Annual Cost
	tons		Downsize, tons	Cost Saved, $	cfm	$	Savings, $
				Office			
CACZ06	14.06	0.187	0.47	474	921	4604	-860
CACZ15	21.36	0.124	2.56	2557	924	4620	6
				Restaurant			
CACZ06	11.92	0.753	2.88	2882	3144	15719	-1240
CACZ15	21.27	0.421	8.46	8458	3134	15668	1297
				Retail Store			
CACZ06	117.82	0.728	27.00	27003	30000	150000	-12700
CACZ15	212.73	0.402	81.77	81766	29998	149991	10454
				Auditorium			
CACZ06	25.10	0.886	17.44	17442	13497	67486	-1256
CACZ15	42.12	0.796	36.65	36650	13480	67402	3653

Table C.4. Cumulative Rate of Return for New Building Applications – DCV+EC

	Cumulative Years							
	0	1	2	3	4	5	6	7
				Office				
CACZ06	-100%	-83.4%	-66.8%	-50.2%	-33.6%	-16.9%	-0.3%	16.3%
CACZ15	-100%	-47.3%	5.3%	58.0%	110.7%	163.3%	216.0%	268.7%
				Restaurant				
CACZ06	-100%	-75.2%	-50.4%	-25.7%	-0.9%	23.9%	48.7%	73.4%
CACZ15	-100%	81.6%	263.2%	444.8%	626.4%	808.1%	989.7%	1171.3%
				Retail Store				
CACZ06	-100%	-40.1%	19.8%	79.8%	139.7%	199.6%	259.5%	319.4%
CACZ15	-100%	198.5%	497.0%	795.5%	1094.0%	1392.5%	1691.0%	1989.6%
				Auditorium				
CACZ06	-100%	-28.9%	42.3%	113.4%	184.6%	255.7%	326.9%	398.0%
CACZ15	-100%	134.2%	368.3%	602.5%	836.7%	1070.8%	1305.0%	1539.2%

Table C.5. Cumulative Rate of Return for New Building Applications - HXHR

	Cumulative Years							
	0	1	2	3	4	5	6	7
	Office							
CACZ06	-71.3%	-110.7%	-150.1%	-189.6%	-229.0%	-268.4%	-307.8%	-347.2%
CACZ15	54.0%	80.5%	107.0%	133.6%	160.1%	186.6%	213.1%	239.6%
	Restaurant							
CACZ06	-71%	-88.8%	-106.6%	-124.3%	-142.1%	-159.9%	-177.6%	-195.4%
CACZ15	49%	99.7%	150.3%	201.0%	251.6%	302.2%	352.9%	403.5%
	Retail Store							
CACZ06	-69%	-87.1%	-104.8%	-122.5%	-140.1%	-157.8%	-175.5%	-193.1%
CACZ15	55%	103.0%	151.4%	199.9%	248.3%	296.7%	345.2%	393.6%
	Auditorium							
CACZ06	-33%	-35.7%	-38.4%	-41.1%	-43.8%	-46.5%	-49.3%	-52.0%
CACZ15	55%	81.2%	107.7%	134.3%	160.8%	187.4%	214.0%	240.5%

Table C.6. Cumulative Rate of Return for New Building Applications – HPHR

	Cumulative Years							
	0	1	2	3	4	5	6	7
	Office							
CACZ06	-89.7%	-108.4%	-127.1%	-145.7%	-164.4%	-183.1%	-201.8%	-220.5%
CACZ15	-44.7%	-44.5%	-44.4%	-44.3%	-44.1%	-44.0%	-43.9%	-43.8%
	Restaurant							
CACZ06	-82%	-89.6%	-97.4%	-105.3%	-113.2%	-121.1%	-129.0%	-136.9%
CACZ15	-46%	-37.7%	-29.5%	-21.2%	-12.9%	-4.6%	3.6%	11.9%
	Retail Store							
CACZ06	-82%	-90.5%	-98.9%	-107.4%	-115.9%	-124.3%	-132.8%	-141.3%
CACZ15	-45%	-38.5%	-31.5%	-24.6%	-17.6%	-10.6%	-3.7%	3.3%
	Auditorium							
CACZ06	-74%	-76.0%	-77.9%	-79.7%	-81.6%	-83.5%	-85.3%	-87.2%
CACZ15	-46%	-40.2%	-34.8%	-29.4%	-23.9%	-18.5%	-13.1%	-7.7%